

Exploring the Secondary Metabolism of Basidiomycota: Unveiling Novel Bioactive and Chemically Diverse Compounds

Der Fakultät für Lebenswissenschaften

der Technischen Universität Carolo-Wilhelmina zu Braunschweig

zur Erlangung des Grades eines

Doktors der Naturwissenschaften

(Dr. rer. nat.)

eingereichte

D i s s e r t a t i o n

Kumulative Arbeit

von Sebastian Pfütze
aus Schönebeck (Elbe), Deutschland

1. Referent:

Prof. Dr. Marc Stadler

2. Referent:

Prof. Dr. Stefan Schulz

eingereicht am:

mündliche Prüfung (Disputation) am:

Vorveröffentlichungen der Dissertation

Teilergebnisse aus dieser Arbeit wurden mit Genehmigung der Fakultät für Lebenswissenschaften, vertreten durch den Mentor der Arbeit, in folgenden Beiträgen vorab veröffentlicht:

List of Publications

Roman numerals within the text correspond to the following publications.

- I. Pathompong P[†], **Pfütze S[†]**, Surup F, Boonpratuang T, Choeyklin R, Matasyoh JC, Decock C, Stadler M, Boonchird C (**2022**) Drimane-type sesquiterpenoids derived from the tropical Basidiomycetes *Perenniporia centrali-africana* and *Cerrena* sp. nov. *Molecules* 27(18):5968.
- II. **Pfütze S**, Khamsim A, Surup F, Decock C, Matasyoh JC, Stadler M (**2023**) Calamene-type sesqui-, mero-, and bis-sesquiterpenoids from cultures of *Heimiomyces* sp., a Basidiomycete collected in Africa. *Journal of Natural Products* 86(2):390–397.
- III. **Pfütze S**, Khamsim A, Surup F, Decock C, Matasyoh JC, Stadler M (**2023**) Heimionones A–E, new sesquiterpenoids produced by *Heimiomyces* sp., a Basidiomycete collected in Africa. *Molecules* 28(9):3723.
- IV. **Pfütze S**, Nedder DL, Surup F, Stadler M (**2023**) 5'-O-methyl-14-hydroxyarmillane, a new armillane-type sesquiterpene from cultures of *Guyanagaster necrorhiza*. *Mycological Progress* 22:70.
- V. **Pfütze S**, Charria-Girón E, Schulzke E, Toshe R, Khonsanit A, Franke R, Surup F, Brönstrup M, Stadler M (**2024**) Depicting the chemical diversity of bioactive meroterpenoids produced by the largest organism on earth. *Angewandte Chemie, International Edition* 63:e202318505.

[†] these authors contributed equally to this work

Tagungsbeiträge

Pfütze S: Chemical Diversity and Bioactivity of Natural Products Isolated from Basidiomycota.
(Talk) Asian Mycological Congress 2023 – AMC in Busan, Republic of Korea, October 10–13

Posterbeiträge

Pfütze S: Chemical diversity of Sesquiterpenoids produced by *Heimiomyces* sp. (Poster)
American Society of Pharmacognosy 2022 – ASP in Charleston, SC, USA, July 23–28

Pfütze S: Chemical diversity of Sesquiterpenoids produced by *Heimiomyces* sp. (Poster)
International Helmholtz Drug Discovery Conference 2023 – HDDC in Braunschweig, Germany,
May 15–16

Pfütze S: Chemical diversity of Sesquiterpenoids produced by *Heimiomyces* sp. (Poster) DZIF
TTU Novel Antibiotics Strategic Meeting 2022 – Braunschweig, Germany, March 30–April 04

Pfütze S: Chemical diversity of Sesquiterpenoids produced by *Heimiomyces* sp. (Poster) PhD
Assembly for HZI and Uds Doctoral Researchers 2023 – Saarbrücken, Germany, May 4–5

Declaration of Contribution to the Publications

The contributions of Sebastian Pfütze (SP) and the co-authors of the listed publications are described below.

- I. PP and SP did the scale-up fermentation, harvesting of the cultures, extraction, chemical profiling of the extracts and preparative isolation of the compounds. SP and FS collaborated on structure elucidation and description of the pure compounds. JCM, CD, TB and RC collected the fungal material. TB and RC did the identification of the fungal material. The manuscript was authored by PP, SP, and FS. Project supervision and final draft oversight were provided by MS and CB.
- II. Under the supervision of SP, the scale-up fermentation, culture harvesting, extraction, chemical profiling of the extracts, and preparative isolation of the compounds were conducted by AK. SP and FS collaborated on the analysis of the chemical profiles, structure elucidation, and description of the pure compounds. Derivatization reactions were carried out by SP under the guidance of FS. Fungal material was collected by JCM and CD. The initial draft of the manuscript was primarily authored by SP and FS, with finalization by project supervisor MS.
- III. Under SP's supervision, AK carried out the scale-up fermentation, culture harvesting, extraction, chemical profiling of the extracts, and preparative isolation of the compounds. SP and FS worked together on analyzing the chemical profiles, elucidating structures, and describing the pure compounds. JCM and CD collected the fungal material. The manuscript was drafted by SP and FS, with finalization by project supervisor MS.
- IV. DLN performed the scale-up fermentation, culture harvesting, extraction, chemical profiling of the extracts, and preparative isolation of the compounds under the guidance of SP. Analyses of the chemical profiles, structure elucidation, and description of the pure compounds were conducted by SP and FS. SP and FS authored the initial draft of the manuscript, while it was finalized by project supervisor MS.

- V. AK conducted the strain identification. ES and RT were responsible for the scale-up fermentation, culture harvesting, extraction, and chemical profiling of the extracts, as well as the preparative isolation of the compounds, while also recording the physicochemical data of the compounds under the supervision of SP. SP and FS conducted the analyses of the chemical profiles, structure elucidation, and description of the pure compounds. SP carried out hydrolysis and GC analysis. ECG performed the untargeted metabolomics analyses and chemoinformatic analyses of the bioactivity data under the supervision of RF. The initial draft of the manuscript was authored by SP, ECG, and FS, and was finalized by project supervisors MS and MB.

Acknowledgements

When I began my long journey with the research group Microbial Drugs (“MWIS”) in 2015, it was unimaginable to me that one day I would be sitting here, writing the final lines of my dissertation, and that I am about to conclude my academic career with a doctorate. Today, I can look back on a wonderful time as a bachelor’s, master’s, and PhD student, during which I not only learned a lot about fungi and natural product chemistry but also made many new friends.

For this reason, I would like to express my deepest gratitude to my supervisor, Prof. Dr. Marc Stadler, who gave me the opportunity to be part of his research group for such a long time. His vast knowledge and expertise in many areas, along with his guidance on my projects and in writing publications, significantly contributed to my successful time at MWIS and to the completion of this thesis. Additionally, he enabled me to attend several great conferences, which, among other things, led to two unforgettable and wonderful trips through the USA and South Korea.

I am also deeply grateful to my thesis committee members, Prof. Wulf Blankenfeldt and Prof. Mark Brönstrup, for their valuable feedback and support throughout this process. Their insightful comments and constructive criticism were instrumental in refining my work.

Another sincere thanks goes to Prof. Dr. Stefan Schulz for being the second referee of this thesis and to Prof. Dr. Ludger Beerhues for taking over the chair during my defense.

I would like to acknowledge the financial support provided by a grant from the Life Science-Stiftung zur Förderung von Wissenschaft und Forschung (LSS) and the Helmholtz Centre for Infection Research (HZI) for providing the resources and facilities necessary for my research.

A special thanks goes to Dr. Frank Surup, who was my first supervisor during my time as a bachelor’s student and continued supervising me during my master’s and PhD studies. His expertise in natural product chemistry and structure elucidation was particularly important to me, as he not only supported me in this regard but also taught me a lot about it.

This brings me to the next person to whom I would like to express special thanks: Dr. Kevin Becker, who was my supervisor for the master's thesis and has also become a good friend. I

have learned a lot from him about natural product chemistry and structure elucidation, which has significantly contributed to my ability to elucidate the structures for my later PhD projects myself.

During my time as a doctoral student, I also had the great fortune to supervise some very diligent bachelor's and master's students, who have contributed a significant portion to the wealth of results and publications that I can present in this thesis. Therefore, I would like to thank Esther Schulzke, Atchara Khamsim, Natalie Kommissarov, Dana Nedder, Jacklyne Chepkemoi, and Rita Toshe.

Among the many friends that I found during my time at MWIS, I am especially grateful to Esteban Charria Girón, who has become like a little brother to me and even invited me to his home in Cali, which resulted in an amazing trip through Colombia. Together we shared the first authorship of my favorite publication (the “hermanos-paper”) that became a central part of my thesis. I really enjoyed the time we spent together, as well as the many funny and scientific conversations that we had in our office. Moreover, in Colombia, I experienced the weather that you are usually accustomed to, which made me appreciate even more the cold and rainy days in the Eintracht stadium that you spent with me.

Some other close friends I want to thank are Adéla Čmoková, Jan-Peer (“JP”) Wennrich, Eric Kuhnert, Ruth Benavente, Yasmina Marin Felix, Natalia Llanos López, Daniela Valencia and Sarunyou Wongkanoun (“Bank”). Besides all the fun we had during our conversations and hang-outs, you were always very supportive and provided a lot of help and input for my work. From these friendships, bonds have developed that will continue beyond our time at MWIS.

Of course, I would also like to thank all my fellow PhD students, lab mates, technicians and other members of MWIS and HZI that I met during my time here. Among them, I would like to highlight Manuela Agudelo Restrepo, Christopher Lambert, Sandra Halecker, Lucile Wendt, Christiane Fritz-Braun, Kathrin Wittstein, Christian Richter, Jörg Wieschhaus, Nadine Wurzler, Artit Khonsanit (“Tony”), Pathompong Paomephan (“Paulie”), Khadijita Hassan, Tian Cheng, Zeljka Rupcic, Marjorie Cedeño, Özge Demir, Güner Ekiz, Winnie Sum Chemutai, Lucky Mulwa, Silke Reinecke, Wera Collisi, Anke Skiba, Karen Harms, Birthe Sandargo, Christel Kakoschke, Hedda Schrey, Soleiman Helaly, Blondelle Matio Kemkuignou, Miriam Große, Stephan Hüttel,

Lillibeth Chaverra-Muñoz, Axel Schulz, Christin Löhner, Steffen Bernecker, Andrew Perreth, Reinhard Sterlinski and Max Niehage.

Finally, the biggest thanks go to the two most important people in my life, my mom, Silke, and my girlfriend, Dori. I don't think I would be where I am today without your support. You have carried me through my studies and my time as a doctoral student, always supported me emotionally with your love, encouraged and rebuilt me in difficult phases and thus played a very big part in making this time so successful in the end.

Content

| | |
|---|----|
| Symbols and Abbreviations | 1 |
| Summary | 3 |
| 1. Introduction..... | 4 |
| 1.1. Historical importance of natural products in drug discovery..... | 4 |
| 1.2. Role and history of fungal secondary metabolites in drug research..... | 5 |
| 1.3. The largest organism on earth and three other Basidiomycota as prolific producers of chemical diverse natural products | 10 |
| 1.4. Current challenges and requirements on natural product and drug discovery..... | 14 |
| 1.5. Aims and outline of the thesis..... | 15 |
| 2. Materials and Methods | 16 |
| 2.1. Fungal material..... | 16 |
| 2.2. Seed cultures | 16 |
| 2.3. Scale-up fermentations | 17 |
| 2.3.1. Fermentation of <i>A. ostoyae</i> (DSM 115711) in solid and liquid media | 17 |
| 2.3.2. Fermentation of <i>G. necrorhiza</i> (CBS 138623) in liquid media | 17 |
| 2.3.3. Fermentation <i>Heimiomyces sp.</i> (MUCL 56078) in liquid and solid media..... | 18 |
| 2.3.4. Fermentation of <i>P. centrali-africana</i> (MUCL 56028) in liquid media | 18 |
| 2.4. Harvest of fungal cultures | 19 |
| 2.4.1. Liquid cultivations..... | 19 |
| 2.4.2. Solid rice cultures | 19 |
| 2.5. Preparative isolation of pure compounds by reversed phase liquid chromatography..... | 20 |
| 2.6. Analytical HPLC-DAD/MS analysis of pure compounds and extracts..... | 21 |
| 2.7. Structure elucidation and chemical characterization of pure compounds..... | 21 |
| 2.7.1. General analytical and spectroscopic methods..... | 21 |
| 2.7.2. Hydrolysis and GC analysis of the fatty acid substituted sesquiterpene aryl esters..... | 22 |
| 2.7.3. Acetylation of 41 | 23 |
| 2.7.4. Mosher's method: Preparation of the (<i>R</i>)- and (<i>S</i>)-MTPA ester derivatives of 49, 51 and 53 | 23 |
| 2.8. Untargeted Metabolomics analyses..... | 23 |
| 2.9. Assessment of biological activities | 24 |
| 2.9.1. Evaluation of antimicrobial activity | 24 |
| 2.9.2. Evaluation of cytotoxicity | 25 |
| 3. Results and Discussion | 25 |

| | |
|---|----|
| 3.1. Secondary metabolites from two closely related members of the <i>Physalacriaceae</i> (Agaricales) | 25 |
| 3.1.1. Chemical diversity of sesquiterpene aryl esters isolated from <i>A. ostoyae</i> (DSM 115711) and <i>G. necrorhiza</i> (CBS 138623) | 26 |
| 3.1.2. Assessment of melleolide production in <i>A. ostoyae</i> under different cultivation conditions using metabolomics techniques | 31 |
| 3.1.3. Bioactivities and insights into the structure-activity relationships of melleolide-type meroterpenoids | 34 |
| 3.2. <i>Heimiomyces</i> sp. (MUCL 56078) as a prolific producer of novel terpenoids | 41 |
| 3.2.1. Metabolic shift and chemical diversity of secondary metabolites produced by <i>Heimiomyces</i> sp. | 41 |
| 3.2.2. Biological evaluation of secondary metabolites produced by <i>Heimiomyces</i> sp. | 48 |
| 3.3. Drimane-type sesquiterpenoids from <i>Perenniporia centrali-africana</i> (MUCL 56028) | 49 |
| 3.3.1. Structures of known and new drimane-type sesquiterpenoids isolated from <i>P. centrali-africana</i> | 49 |
| 3.3.2. Biological evaluation of secondary metabolites produced by <i>P. centrali-africana</i> | 50 |
| 4. Conclusion and Outlook | 51 |
| 5. References | 56 |
| 6. Appendices: Publications of the Dissertation | 65 |

Symbols and Abbreviations

| | |
|------------------|---|
| ATR | attenuated total reflectance |
| BAF | buffered acid broth (medium) |
| CBS | Centraalbureau voor Schimmelcultures, Utrecht, the Netherlands |
| COSY | correlation spectroscopy |
| DAD | diode array detection |
| DSM | strain accession numbers of the German Collection of Microorganism and Cell Cultures, Braunschweig, Germany |
| DMSO | dimethyl sulfoxide |
| ECD | electronic circular dichroism |
| ESI | electrospray ionization |
| EtOAc | ethyl acetate |
| FAME | fatty acid methyl ester |
| FBMN | feature-based molecular network |
| FID | flame ionization detector |
| FPP | farnesyl diphosphate |
| GNPS | global natural products social molecular networking |
| HMBC | heteronuclear multiple-bond spectroscopy |
| HPLC | high performance liquid chromatography |
| HSQC | heteronuclear single-quantum spectroscopy |
| HR | high resolution |
| IC ₅₀ | half-maximum inhibitory concentration |
| IM-MS | ion mobility mass spectrometry |
| IR | infrared |
| LC | liquid chromatography |
| MeCN | acetonitrile |
| MeOH | methanol |
| MES | 2(<i>N</i> -morpholino)-ethanesulfonic acid |
| MF | molecular family |
| MIC | minimum inhibitory concentration |
| MOF | mannitol oat flour (medium) |
| MS | mass spectrometer |

| | |
|------------|--|
| MTPA | (<i>R</i>)-(+)- α -methoxy- α -(trifluoromethyl)phenylacetyl chloride (Mosher's acid) |
| MUCL | strain accession number of the Mycotheque de l'Université catholique de Louvain, Louvain-la-Neuve, Belgium |
| <i>m/z</i> | mass to charge ratio |
| NMR | nuclear magnetic resonance |
| PCA | principal component analysis |
| PKS | polyketide synthase |
| PLC | preparative liquid chromatography |
| ROESY | rotating frame nuclear Overhauser effect spectroscopy |
| RP | reverse phase |
| SAR | structure-activity relationship |
| SPME | solid phase micro extraction |
| TOF | time-of-flight |
| UPLC | ultra-performance liquid chromatography |
| UV-Vis | ultraviolet/visible (light) |
| YM | yeast-malt extract (medium) |
| YMWB | yeast-malt extract, wheat bran (medium) |

Summary

Basidiomycota, the second largest division of the fungal kingdom, exhibit remarkable chemical and biological diversity. They play crucial ecological roles as decomposers, mycorrhizal symbionts, and plant pathogens, highlighting their significance in ecosystems. Additionally, Basidiomycota are well-known to produce a wide array of secondary metabolites, including polyketides, terpenoids, alkaloids, and peptides, contributing to their diverse ecological roles. These compounds possess various biological activities such as antimicrobial, antitumor and antiviral, making Basidiomycota a valuable resource for drug discovery and biotechnological applications.

This thesis comprises the investigations on the secondary metabolism of four different Basidiomycota, including *Armillaria ostoyae*, *Guyanagaster necrorhiza*, *Heimiomyces* sp. and *Perenniporia centrali-africana*. For this purpose, these fungi were cultivated under different growth conditions, mainly liquid and solid fermentation. Extracts that were obtained from these cultivations were separated by preparative high performance liquid chromatography (HPLC) after evaluation of the corresponding analytical HPLC-DAD/MS profiles. The planar structures of the purified compounds were elucidated by 1D and 2D NMR spectroscopy in addition to HR-ESI-MS data. Relative configurations were assigned by analysis of ROESY spectra, while absolute configurations were derived by the synthesis of MTPA esters or from crystal structures and ECD spectra comparison of related known derivatives. This led to the identification of a total of 34 new secondary metabolites and 37 known derivatives from the organisms under investigation. *A. ostoyae* was given a special role in this, because its secondary metabolism was systematically explored by MS-based untargeted metabolomics, providing insights into the diversity of the compound class of the sesquiterpene aryl esters. All isolated compounds were analyzed for their i) antibacterial activities in a serial dilution assay against fungal strains, Gram-positive and Gram-negative bacteria and ii) for their cytotoxicity against different cancer cell lines. These data were utilized not only for assessing bioactivities but also for identifying potential structure-activity relationships (SARs) through comparative analysis, which was especially supported by cheminformatic methods in the case of *A. ostoyae*. In summary, all findings demonstrated the importance of Basidiomycota as a prolific resource for the discovery and production of new bioactive natural products.

1. Introduction

Natural products encompass primary and secondary metabolites synthesized by living organisms, typically plants, microbes, or marine organisms. While primary metabolites are essential for fundamental cellular functions like growth, energy production, and metabolism, secondary metabolites are not directly involved in these processes and rather have specialized functions such as defense, communication, or competition. The important role of natural products across diverse domains like pharmaceuticals, agriculture, cosmetics, nutrition, biotechnology and bioprocessing, underscores their essential value in advancing scientific innovation and addressing multifaceted challenges. However, this study primarily focuses on the isolation and characterization of fungal secondary metabolites to evaluate their antimicrobial and cytotoxic potentials, since historically natural products have been a prolific source of drugs, with many important medications originating from natural sources (Newman and Cragg 2020). These compounds often possess unique chemical scaffolds and biological activities that make them valuable starting points for drug discovery and development. Consequently, natural products have played a crucial role in addressing challenging therapeutic targets, such as infectious diseases, cancer, cardiovascular diseases, neurological disorders, metabolic disorders, inflammatory disorders and more (Koehn and Carter 2005; Newman and Cragg 2020).

1.1. Historical importance of natural products in drug discovery

Before the advent of modern pharmaceuticals, natural products served as the foundation of traditional medicine systems around the world. Indigenous cultures and ancient civilizations relied on plants, fungi, and other natural sources to treat various diseases and maintain health. From this point onwards to modern pharmaceutical research, natural products have remained a rich source of therapeutic agents, significantly contributing to the advancement of medicine. One notable example is the use of willow bark, containing salicylic acid, as a pain reliever, which later inspired the development of aspirin in 1897 (Desborough and Keeling 2017). Another important milestone was the discovery of penicillin G (Figure 1) from *Penicillium rubens* in 1928 (Fleming 1929; Houbraken et al. 2011), which revolutionized medicine by providing the first effective treatment for bacterial infections. This breakthrough marked the onset of the “golden era of antibiotics”, during which scientists isolated and characterized numerous antibiotic compounds from diverse natural sources. Streptomycin, tetracycline, and

erythromycin are among the many antibiotics derived from natural products introduced during this period. These discoveries had a profound impact on public health, drastically reducing the morbidity and mortality associated with infectious diseases (Davies 2006).

However, the golden era of antibiotics eventually gave way to a gap in new findings and the emergence of antibiotic resistance. Despite the initial success of antibiotic discovery, the pace of new antibiotic development slowed in subsequent decades due to various factors, such as decreased investment from pharmaceutical companies, technical challenges in isolating and developing new compounds, regulatory hurdles, limited financial motivation, and emergence of antibiotic-resistant bacteria (Ventola 2015). The latter was especially increased by the overuse and misuse of antibiotics, including inappropriate prescribing practices in primary care, self-medication, and non-prescription use of antibiotics. Additionally, the role of antibiotic use in agriculture, particularly for disease prevention in livestock farming, has been a significant contributing factor (Llor and Bjerrum 2014). Recent reports underscore the persistence of these challenges in the 21st century, with the alarming global increase in antimicrobial resistance contributing to millions of deaths annually (World Health Organization 2014; Antimicrobial Resistance Collaborators 2022).

1.2. Role and history of fungal secondary metabolites in drug research

Fungi exhibit immense biodiversity, comprising millions of species with only a fraction formally described, thriving in various ecological niches. Their complex biochemical pathways yield an astonishing array of secondary metabolites, including alkaloids, polyketides, terpenoids, peptides, and phenolic compounds with diverse biological activities (Bills and Gloer 2016).

The story of fungal antibiotics traces back to the late 19th century, preceding the discovery of the first β -lactam antibiotic, penicillin G (Figure 1), in 1928. In 1893, Bartolomeo Gosio isolated mycophenolic acid (Figure 1) as a purified crystalline compound from *Penicillium brevicompactum*, which exhibited inhibitory effects against the anthrax pathogen *Bacillus anthracis*, and is therefore considered the first antibiotic (Florey et al. 1946; Bentley 2000). However, it was ultimately discarded as a potential antibiotic due to concerns over its toxicity (Bills and Gloer 2016). Following the success of penicillin, researchers turned their attention to other fungal species in pursuit of novel therapeutic agents.

In the 1930s, griseofulvin (Figure 1) was isolated from *Penicillium griseofulvum* and emerged as a potent antifungal drug for the treatment of skin, hair, and nail infections caused by dermatophyte fungi (Oxford et al. 1939). Recently, there has been growing interest in this compound for other applications, as it has demonstrated the ability to disrupt mitosis and cell division in human cancer cells, as well as to inhibit the replication of the hepatitis C virus (Aris et al. 2022). Another class of β -lactam antibiotics was introduced in 1945 with the discovery of cephalosporin C (Figure 1) from cultures of the fungus *Sarocladium strictum*, formerly known as *Cephalosporium acremonium* (Summerbell et al. 2011), by Italian scientist Giuseppe Brotzu. The chemical structure was identified shortly after its initial discovery (Newton and Abraham 1955; Abraham and Newton 1961). While cephalosporin C displayed antibacterial properties, it was not initially pursued for therapeutic use due to its limited potency. However, it paved the way for the development of several generations of derivatives with broad antibacterial activity against both Gram-positive and Gram-negative bacteria (Lin and Kück 2022). In 1971, the breakthrough discovery of the cyclic peptide cyclosporine A (Figure 1), an immunosuppressant derived from the fungus *Tolypocladium inflatum*, revolutionized organ transplantation by effectively preventing organ rejection and improving patient outcomes (Borel et al. 1976). The advent of a new class of antifungal drugs, targeting the synthesis of β -glucan in fungal cell walls (Lima et al. 2019), began in 1974 with the discovery of the cyclic lipopeptide echinocandin B (Figure 1) isolated from *Aspergillus nidulans* var. *echinulatus*, now referred to as *A. spinulosprous* (Benz et al. 1974). Currently available echinocandins include the three semi-synthetic derivatives caspofungin, micafungin, and anidulafungin. A significant milestone in treating cardiovascular disorders was achieved in 1978 when researchers at Merck identified a potent inhibitor of HMG-CoA reductase from *Aspergillus terreus* (Alberts et al. 1980). Initially referred to as mevinolin, it was later officially recognized as lovastatin (Figure 1) by the United States Adopted Name (USAN) authority, leading to the development of statin drugs for lowering cholesterol levels and preventing cardiovascular diseases (Tobert 2003; Toth and Banach 2019).

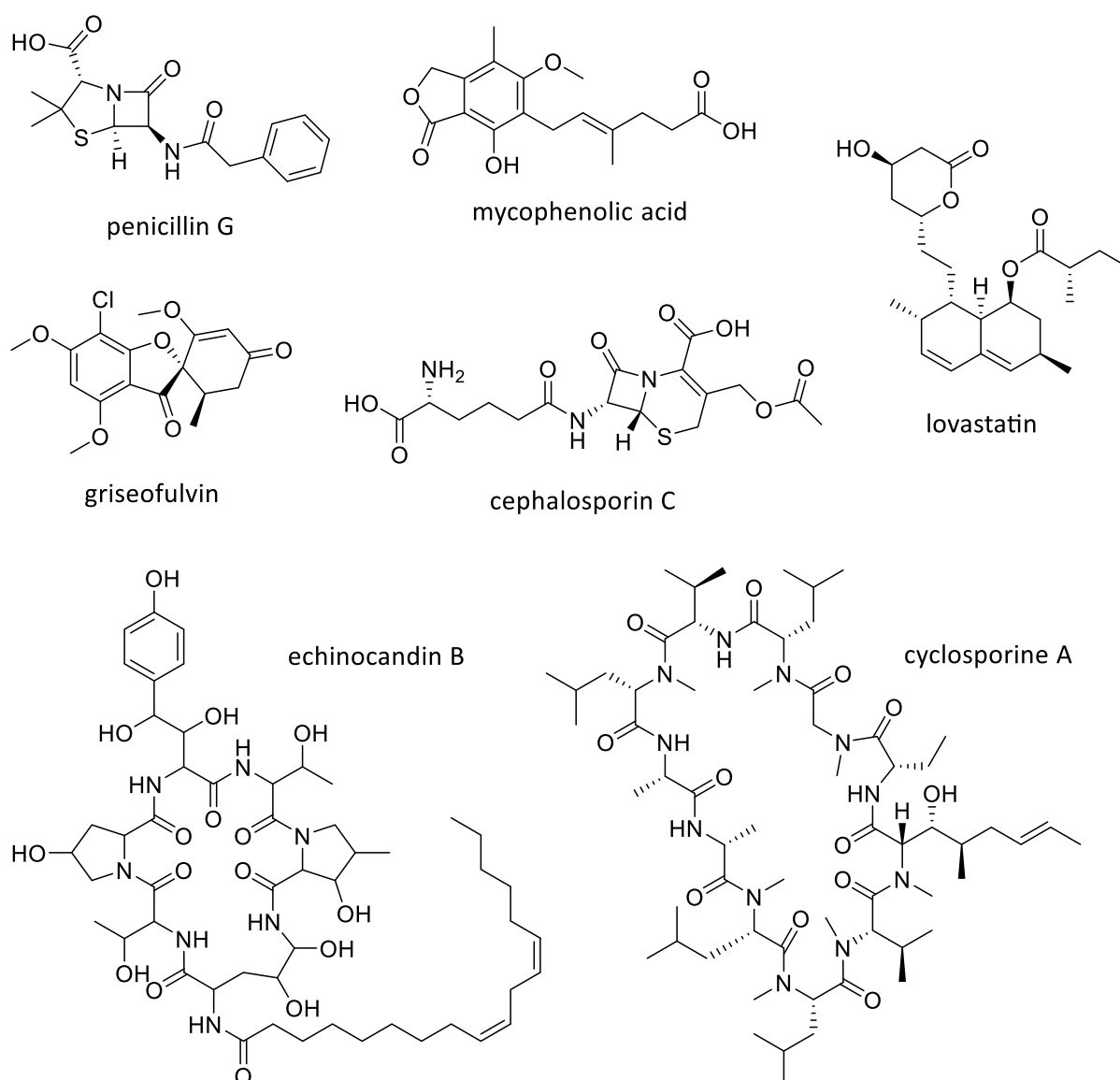


Figure 1. Fungal compounds representing important milestones in natural product and drug research.

Considering that all the previously mentioned compounds were originally isolated from Ascomycota, Basidiomycota seem to have received less attention in research regarding biologically active compounds. However, with their distinctive enzymatic machinery and life cycles, Basidiomycota play a significant role in synthesizing numerous novel and chemically diverse secondary metabolites, presenting potential for the discovery of bioactive substances (Sandargo et al. 2019). Some of these compounds have laid the foundation for developing clinical candidates and, in certain instances, have led to marketed drugs and agrochemicals.

The pleuromutilins stand out as some of the most significant members among these compounds. Pleuromutilin (Figure 2), initially isolated from *Clitopilus passeckerianus*, has been recognized for its potent antibiotic activity against Gram-positive and some Gram-negative pathogens since its discovery in 1947 (Kavanagh 1947; Kavanagh et al. 1951; Paukner and Riedl

2017). However, due to limited concern about antibiotic resistance and challenges in human application, its use was restricted (Novak 2011). Nevertheless, semisynthetic derivatives like tiamulin and valnemulin (Figure 2) found use in veterinary medicine (Poulsen et al. 2001). The highly specific mode of action exhibited by pleuromutilins, which inhibits bacterial protein synthesis and makes resistance development uncommon, has reignited interest in this compound class and spurred the development of retapamulin (Figure 2), the first Basidiomycota-derived antibiotic for human use (Paukner and Riedl 2017).

Another important class of compounds originating from different Basidiomycota species (*Favolaschia*, *Mycena*, *Oudemansiella*, *Strobilurus*, *Xerula*) are the strobilurins (Figure 2), which have led to the development of agricultural β -methoxyacrylate fungicides owing to their ability to inhibit fungal growth and spore germination by targeting mitochondrial cytochromes (Sauter et al. 1999; Stadler and Hoffmeister 2015). While new derivatives continue to be discovered, resistance to strobilurins developed rapidly after their introduction to the market, attributed to their single-target nature, necessitating combination treatments. This approach persists in the case of azoxystrobin (Figure 2) and kresoxim-methyl, which are combined with other antifungal agents (Sandargo et al. 2019).

In the 1950s, a class of illudane-type sesquiterpenes, characterized by a unique cyclopropane ring, was introduced with the discovery of illudins M and S (Figure 2) (Anchel et al. 1950). Produced by species of *Omphalotus* and *Lampteromyces* genera, they were initially explored for their antitumor activities, but their potential as anticancer drugs was hampered by their high toxicity (Sandargo et al. 2019). Consequently, there was a need for analogs with improved therapeutic profiles and enhanced tumor specificity. Semisynthetic approaches led to the development of the illudin S analogue irofulven (Figure 2), also referred to as hydroxymethylacylfulvene (HMAF), currently undergoing cancer drug development (Tanasova and Sturla 2012). While research on new illudane type sesquiterpenes as potential drug candidates is still ongoing (Sandargo et al. 2019), species of the genus *Omphalotus* were also found to produce nematocidal cyclopeptides of the omphalotin type, such as omphalotin A (Figure 2) from *Omphalotus olearius* (Sterner et al. 1997).

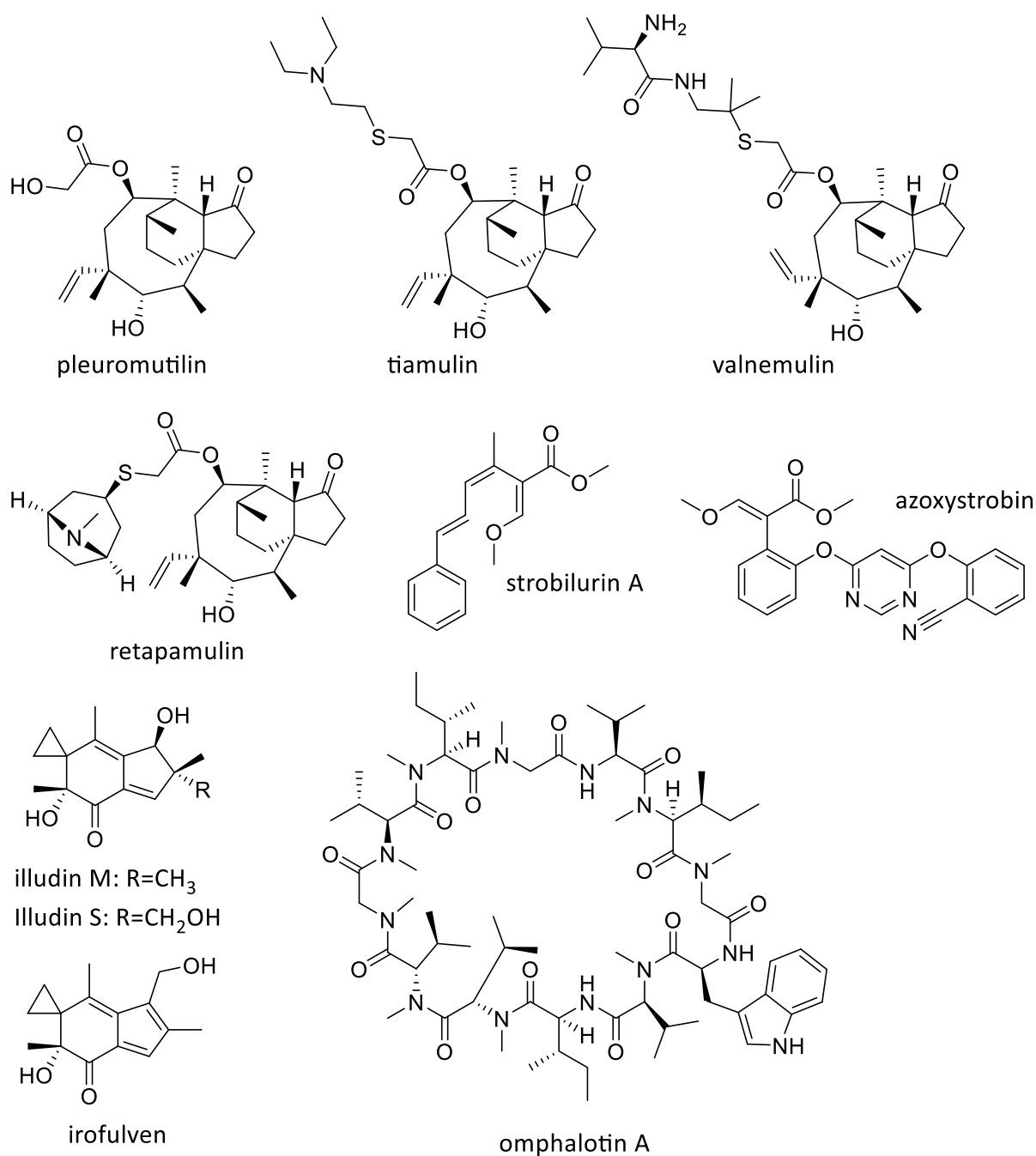


Figure 2. Important compounds from Basidiomycota, which are used as pharmaceuticals and agrochemicals or are drug candidates currently in the developmental stage.

While the previously mentioned compounds are either already on the market as drugs or currently in development as drug candidates, Basidiomycota have yielded numerous other chemically diverse and bioactive substance classes, highlighting their significance as a valuable source for drug and natural product research (Sandargo et al. 2019).

1.3. The largest organism on earth and three other Basidiomycota as prolific producers of chemical diverse natural products

As history has shown, fungi are rich sources of bioactive natural products. Consequently, the main project of this thesis comprises investigations on the secondary metabolism of *Armillaria ostoyae* (DSM 115711), which has been recognized as a prolific producer of secondary metabolites in previous studies. *Armillaria* (Physalacriaceae), commonly referred to as honey mushrooms, is a significant genus of the Basidiomycota distributed worldwide. It is well-known for its broad host range, acting as a plant pathogen by infecting various woody species such as hardwoods, conifers, fruit trees, and grapes and causing butt and root diseases that can lead to extensive forest diebacks (Baumgartner et al. 2011; Coetzee et al. 2018). The so-called *Armillaria* root disease threatens both agronomic and timber plantations, persisting saprotrophically in residual roots after tree clearance and causing recurring infections in subsequent crops. Unfortunately, effective methods to prevent or cure these infections are lacking, resulting in significant yield losses over multiple planting cycles (Baumgartner et al. 2011). This can be attributed by the facultative necrotrophic characteristics of most *Armillaria* species, which exhibit both parasitic and saprophytic phases. Initially, they colonize the cambium of living roots in the parasitic phase and subsequently induce necrotic lesions to feed on the dead tissue in the saprophytic phase (Baumgartner et al. 2011). Additionally, the production of thickened mycelial strands known as rhizomorphs is of particular significance for their pathogenicity, enabling them to efficiently explore extensive areas for nutrients. Thus, *Armillaria bulbosa* and *A. ostoyae* have become some of the largest and oldest organisms on the planet. This was confirmed by genetic studies and extrapolation of their growth speed, which revealed that the mycelium may be several millennia old while covering thousands of square kilometers in certain vast forests of Northeastern North America (Smith et al. 1992; Ferguson et al. 2003).

Another important feature of *Armillaria* is the ability to produce sesquiterpene aryl esters, a class of meroterpenoids known for their chemical diversity and diverse bioactivities. They are considered as meroterpenoids due to the combination of their protoilludene backbone, a sesquiterpenoid, with an orsellinic acid moiety synthesized via a polyketide pathway (Misieki and Hoffmeister 2012). In the literature, these meroterpenoids are often summarized under the term “melleolides”, introduced by Midland et al. in 1982 for a single compound (Midland et al. 1982). The nomenclature has evolved over the years with the discovery of more

derivatives. Mainly, the presence or absence of a double bond and its position within the protoilludene backbone determine this. Compounds with a $\Delta^{2,3}$ double bond in their backbones are denoted as “melleolides”, while the ones featuring a $\Delta^{2,4}$ scaffold are termed “armillyl orsellinates”, and those missing a double bond are known as “armillanes” (Figure 3) (Engels et al. 2021). The second important structural feature to distinguish members of this compound class is the allylic alcohol or aldehyde at position C-1.

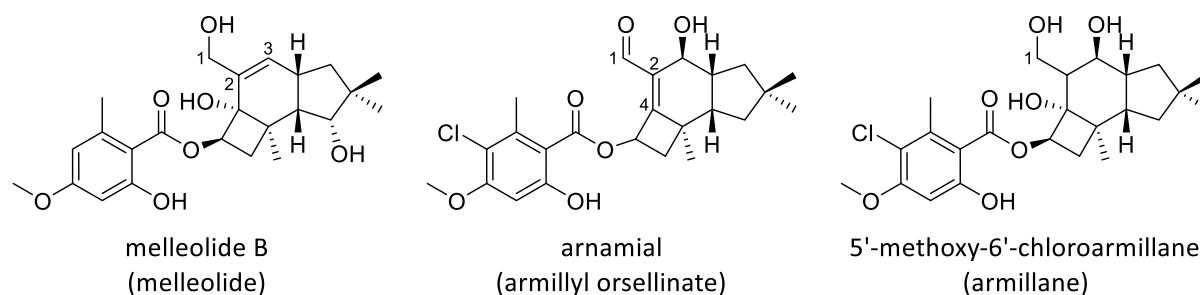


Figure 3. Examples for the classification of sesquiterpene aryl esters according to the presence and position of the double within the protoilludene backbone.

Prior to the investigations shown in this thesis, more than 70 different sesquiterpene aryl esters were described in the literature (Dörfer et al. 2019a). This immense structural diversity is based on a variety of potential modifications that can occur during the biosynthesis of these compounds. Besides the aforementioned double bond and C-1 modification, there are other common possibilities to modify the corresponding core structures, including hydroxylations at C-3, C-4, C-10 and C-13, methyl ether formation at C-5', and chlorination at C-6' (Wick et al. 2016). For this reason, they constitute the largest subclass of protoilludanes, which appear to be solely synthesized by *Armillaria* and related genera (Cadelis et al. 2020). In contrast, the production of orsellinic acid is not limited to Basidiomycota; however, the orsellinic acid polyketide synthases (oaPKS) responsible for its biosynthesis are not evolutionarily related to those found in ascomycetes or bacteria (Gressler et al. 2021). The biosynthesis of the sesquiterpene aryl esters (Figure 4) has been extensively studied and begins with the cyclization of the universal sesquiterpene precursor farnesyl diphosphate (FPP) to the Δ^6 -protoilludene core structure by the sesquiterpene cyclase Mld5 (formerly Pro1) (Engels et al. 2021; Fukaya et al. 2023). Subsequently, various enzymatic modifications occur, encompassing hydroxylation (P450 monooxygenases Mld3 and Mld6), stereochemical inversion at position C-5 (Mld4 and Mld13), transesterification of the polyketide residue, and isomerization of the olefin bond position (Mld7) (Fukaya et al. 2023). Prior to the attachment

of the orsellinic acid moiety, its formation is catalyzed by the non-reducing polyketide synthase (nrPKS) Mld15 (formerly ArmB) (Engels et al. 2021; Fukaya et al. 2023).

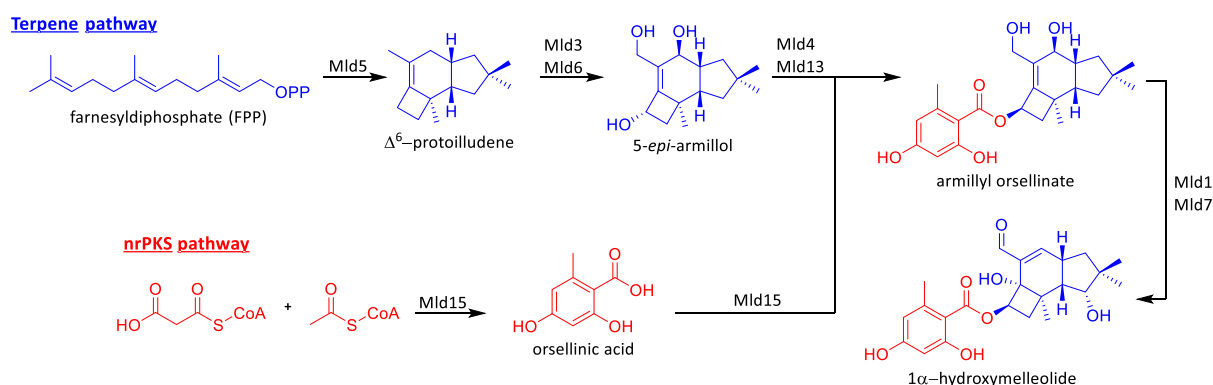


Figure 4. Biosynthetic pathway for the formation of 1 α -hydroxymelleolide as proposed by Fukaya et al. 2023. With the terpene pathway marked blue and the nrPKS pathway red.

The chemical diversity of these compounds is accompanied by numerous bioactivities. These include antibacterial properties, mainly against Gram-positive strains, with the C-4/C-13 hydroxylations and double bond position in the sesquiterpenoid backbone being reported as the main drivers for these effects (Dörfer et al. 2019a). Additionally, sesquiterpene aryl esters show antifungal activities, where the $\Delta^{2,4}$ -double bond of the aldehydes is anticipated to be essential for their antifungal efficacy (Dörfer et al. 2019b). Furthermore, these compounds are known for their cytotoxicity, but there are contradictory reports on the mode of action, whether they induce apoptosis in human cancer cells or cell death is caused by a yet unknown rapid mechanism (Misiek et al. 2009; Bohnert et al. 2014b; Li et al. 2016). In any case, however, it is clear that the cytotoxicity is mainly driven by the presence of an aldehyde at C-1 (Dörfer et al. 2019a).

Up to this point, *Armillaria* was considered to be the only genus producing this type of natural products, but in 2010 *Guyanagaster necrorhiza* was identified as a closely related gasteroid fungus, which was later reclassified under the Armillarioid clade (Henkel et al. 2010; Koch et al. 2017; Kedves et al. 2021). Phylogenetic analysis suggests *Guyanagaster* species diverged from early Armillarioid clade members around 51 million years ago when this lineage emerged in Eurasia (Koch et al. 2017). These findings indicated that *Guyanagaster* species are able to produce melleolide-type meroterpenoids and for this reason the strain *G. necrorhiza* (CBS 138623) was chosen for further investigations.

Tropical rainforests are known to be rich and diverse ecosystems, yet the majority of their biodiversity and natural products remain untapped. A member of such an ecosystem is the strain *Heimiomyces* sp. (MUCL 56078), originating from the Mount Elgon National Reserve in Kenya, whose genus has not been extensively studied for its secondary metabolism until now. A preliminary study revealed the novel heimiomycins A–C and heimiocalamenes C–E (Figure 5), while LC-MS data of the extracts from the liquid cultures indicated the presence of further unknown metabolites, making this strain an interesting candidate for further investigations (Cheng et al. 2020).

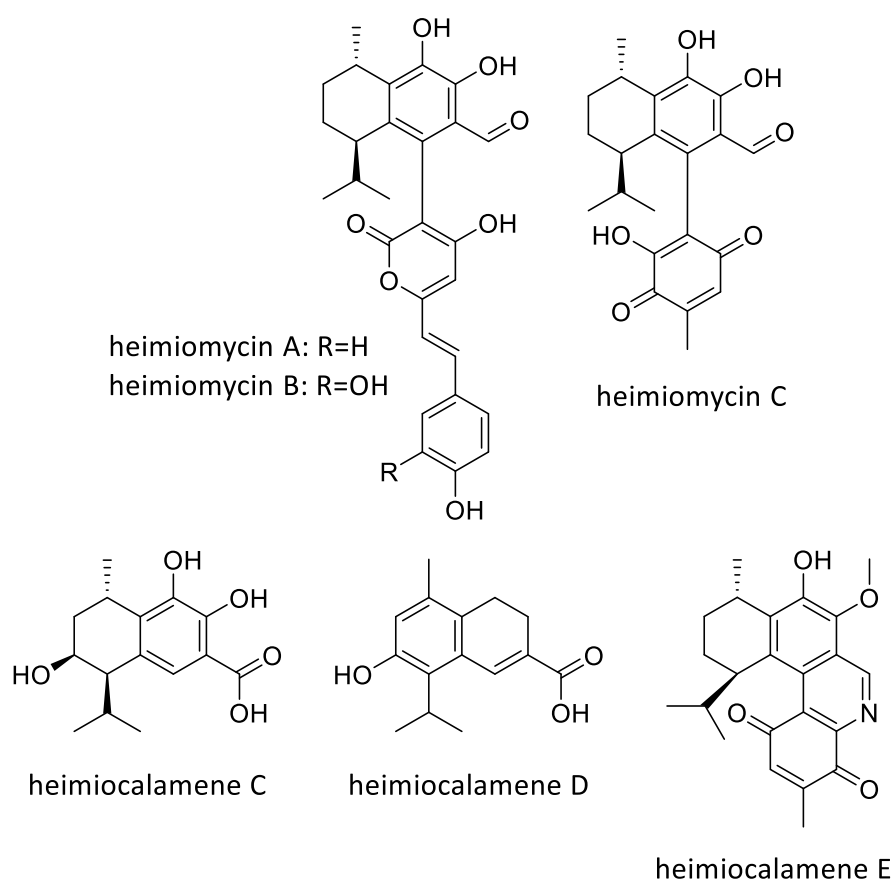


Figure 5. Previously described compounds from liquid cultures of *Heimiomyces* sp. The revised structure of heimiocalamene E is shown.

A third side project involved the exploration of the secondary metabolism of *Perenniporia centrali-africana* (MUCL 56028), but species from this genus have been more extensively studied compared to those of *Guyanagaster* and *Heimiomyces*. For instance, drimane-type sesquiterpenoids such as pereniporin A and B (Figure 6) were isolated from cultures of *P. medullaepanis*, with similar compounds found in *P. maackiae* (Kida et al. 1986; Kwon et al. 2018). Some of them demonstrated antibacterial, cytotoxic, and even phytotoxic effects. Interestingly, lanostane-type triterpenoids, referred to as perenniporiols (Figure 6), were

obtained from cultures of *P. ochroleuca* and *P. maackiae* (Hirotsu et al. 1984; Ino et al. 1984; Guo et al. 2013). Moreover, antioxidant meroterpenoids from *P. medulla-panis* and naphthalenone derivatives (Figure 6), including the antifungal perenniporide A, from a *Perenniporia* sp. were described (Feng et al. 2012; Kim et al. 2019). These results show the capability of *Perenniporia* spp. to produce chemically diverse and potentially bioactive secondary metabolites, reinforcing the endeavor to exploit *P. centrali-africana* for new natural products.

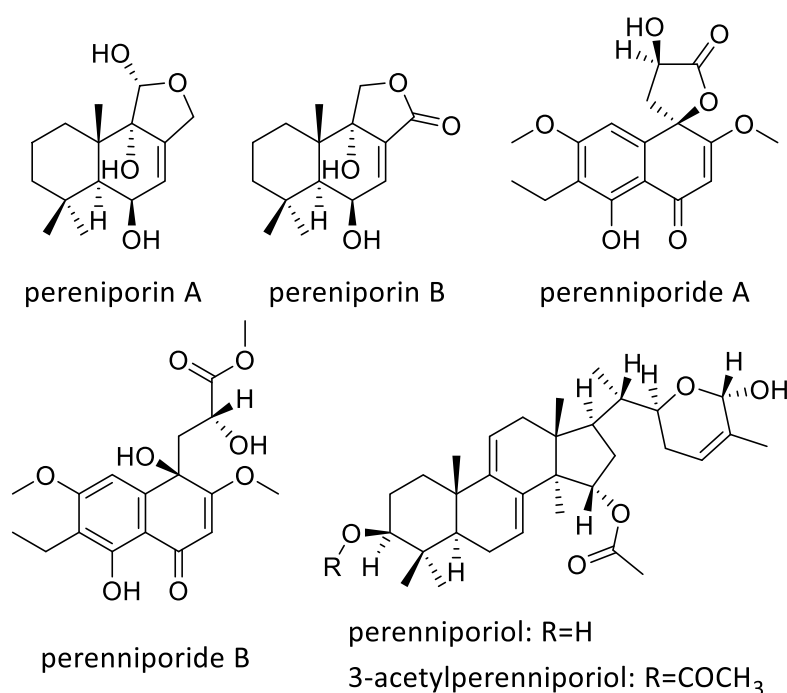


Figure 6. Examples for secondary metabolites isolated from cultures of *Perenniporia* spp.

1.4. Current challenges and requirements on natural product and drug discovery

The occurrence of new infectious diseases, such as those caused by emerging or re-emerging pathogens with increased virulence or drug resistance, presents ongoing challenges for public health (Morens et al. 2004; 2022). Consequently, there is an urgent need for the discovery of novel antibiotics with unique mechanisms of action and efficacy to combat drug-resistant pathogens. While natural products have historically been a rich source of antimicrobial compounds, the pace of antibiotic discovery has slowed in recent decades, with few new classes of antibiotics introduced to the market (von Nussbaum et al. 2006). Fungi are known to produce such bioactive compounds with antibacterial, antifungal, and antiviral activities, thus possessing great potential in addressing emerging infectious diseases. Through systematic screening of fungal secondary metabolites for antibacterial and antifungal

activities, coupled with elucidation of their modes of action, the development of new therapeutics and preventive strategies can be advanced.

As global concerns about environmental sustainability and biodiversity conservation continue to grow, there is an increasing interest in identifying sources of bioactive compounds that address these problems. Fungi offer a promising avenue for sustainable natural product discovery, as they can be cultured in controlled environments and engineered to produce specific metabolites. However, there are challenges associated with optimizing fungal cultivation conditions, scaling up production, and ensuring the sustainable use of fungal resources. Therefore, research aimed at addressing these challenges and developing innovative strategies for exploring fungal biodiversity in a sustainable and environmentally responsible manner is necessary.

Despite advances in genomic and bioinformatic tools, our understanding of fungal secondary metabolism remains incomplete (Keller et al. 2005). Many fungal secondary metabolite biosynthetic gene clusters remain uncharacterized or poorly understood, limiting our ability to predict and access the full diversity of fungal natural products. Consequently, there is a pressing need for integrated approaches that combine genomic, transcriptomic, metabolomic, and biochemical analyses to elucidate the biosynthetic pathways of fungal secondary metabolites and uncover novel bioactive compounds (Brakhage and Schroeckh 2011).

1.5. Aims and outline of the thesis

With regard to the limited availability of new antibiotics, the emergence of new diseases, the endeavor for sustainable sources of bioactive compounds, and the need to better understand the fungal secondary metabolism, natural product and drug discovery face numerous upcoming challenges. For this reason, this thesis focuses on the secondary metabolite production of specific fungal strains, namely *A. ostoyae*, *G. necrorhiza*, *Heimiomyces* sp., and *P. centrali-africana*, aiming to underscore fungi as prolific producers of novel, chemically diverse and bioactive natural products. The fermentation of these Basidiomycota under different cultivation conditions, alongside analytical and preparative chromatographic methods for analyzing and purifying the obtained extracts, as well as the structure elucidation (mainly by HR-ESI-MS and NMR spectroscopy), are described. All isolated compounds,

including new derivatives described in papers I–V and those known from the literature, are presented to discuss their chemical diversity and the influence of the cultivation conditions on secondary metabolite profiles. Particularly, metabolomics investigations on *A. ostoyae* provide further insights into fungal secondary metabolism. Finally, the thesis addresses the antimicrobial and cytotoxic bioactivities of all isolated substances, not only to identify compounds with potential as drug leads but also to detect structure-activity relationships (SARs) to understand their mode of action.

2. Materials and Methods

2.1. Fungal material

The thesis builds upon the investigation of the secondary metabolism of four different Basidiomycota strains (Table 1), all classified within the Agaricomycetes. All strains were maintained on YM 6.3 agar plates.

Table 1. Fungal strains (Basidiomycota) that were investigated for their secondary metabolism.

| Genus | Species | Deposition number | Collector | Origin |
|---------------------|--------------------------|-------------------|--------------------------|---|
| <i>Armillaria</i> | <i>ostoyae</i> | DSM 115711 | M. Stadler | Forsthaus Heldenstein, Edenkoben, Rhineland-Palatinate, Germany |
| <i>Guyanagaster</i> | <i>necrorhiza</i> | CBS 138623 | | |
| <i>Heimiomyces</i> | sp. | MUCL 56078 | C. Decock, J.C. Matasyoh | Mount Elgon National Reserve, Kenya |
| <i>Perenniporia</i> | <i>centrali-africana</i> | MUCL 56028 | C. Decock, J.C. Matasyoh | Mount Elgon National Reserve, Kenya |

2.2. Seed cultures

Seed cultures of all strains under investigation were inoculated by placing three mycelium plugs, each with dimensions of 50 mm², from well-grown YM 6.3 agar plates into a 500 ml Erlenmeyer flask containing 200 ml of YM 6.3 medium (consisting of 10 g/L malt extract, 4 g/L D-glucose, 4 g/L yeast extract, pH 6.3). Incubation took place at 23 °C and 140 min⁻¹ on a rotary shaker. Subsequently, the culture broth underwent homogenization using an Ultra-Turrax®

(T25 easy clean digital, IKA, Staufen im Breisgau, Germany), equipped with an S 25 N – 25 F dispersing tool, operating at 8000 min⁻¹ for 10–20 seconds.

2.3. Scale-up fermentations

2.3.1. Fermentation of *A. ostoyae* (DSM 115711) in solid and liquid media

To inoculate the first cultivation on rice medium, 6 mL of the homogenized seed culture was transferred into two 500 mL Erlenmeyer-shaped culture flasks, each containing solid rice medium (consisting of 1 g/L yeast extract, 0.5 g/L sodium tartrate, 0.5 g/L K₂HPO₄, with 100 mL of the solution added to 28 g of brown rice). Following inoculation, the medium was gently loosened with a sterilized spatula to enhance oxygen accessibility and ensure homogenous distribution of the inoculum. The cultures were then maintained at 23 °C for incubation and harvested after 72 days. A second fermentation involving three rice cultures was conducted under identical conditions but with a different cultivation time (50 days in total).

For the first liquid cultivation, a homogenized seed culture (3 mL per flask) was used to inoculate 21 Erlenmeyer-shaped culture flasks, each with a capacity of 500 mL. These flasks contained 200 mL of YMWB medium, composed of 10 g/L malt extract, 5 g/L wheat bran, 4 g/L D-glucose, 4 g/L yeast extract, adjusted to pH 6.3. Subsequent incubation took place on a rotary shaker at 23 °C and 140 min⁻¹. Glucose consumption was monitored using Medi-Test Glucose strips (Macherey-Nagel, Düren, Germany). After 10 days, when the glucose was depleted as indicated by negative test results, the fermentation process was terminated. A second liquid fermentation was conducted under identical conditions but with a cultivation time of 11 days.

2.3.2. Fermentation of *G. necrorhiza* (CBS 138623) in liquid media

Forty 500 mL Erlenmeyer-shaped culture flasks were each filled with 200 mL of YM 6.3 medium and inoculated with three mycelium pieces, each measuring 50 mm², from well-grown YM 6.3 agar plates. These flasks were then placed on a rotary shaker and incubated at 23°C and 140 min⁻¹. Glucose consumption was monitored using Medi-Test Glucose test strips (Macherey-Nagel). After 24 days of incubation, glucose was no longer detectable in the culture broth, prompting harvesting of the cultures two days later, totaling 26 days of incubation.

2.3.3. Fermentation *Heimiomyces sp.* (MUCL 56078) in liquid and solid media

To inoculate the liquid cultures, 3 mL of the homogenized culture broth was transferred into each of the 15 500 mL Erlenmeyer-shaped culture flasks containing 200 mL of YM 6.3 medium. Subsequently, incubation was conducted at 23°C and 140 min⁻¹ on a rotary shaker. Glucose consumption was monitored using Medi-Test Glucose test strips (Macherey-Nagel), and the fermentation process was terminated two days after the culture broth tested negative for glucose.

A second series of liquid cultivations was conducted by transferring 3 mL of homogenized seed culture per flask into 21 500 mL Erlenmeyer-shaped culture flasks filled with 200 ml of YM 6.3 medium. Additionally, five more 500 mL Erlenmeyer-shaped culture flasks containing 200 ml of MOF medium (75 g/L mannitol, 16.2 g/L MES, 15 g/L oat flour, 5 g/L yeast extract, 4 g/L L-glutamic acid, pH 6.0) were prepared. Incubation was carried out at 23 °C and 140 min⁻¹ on a rotary shaker, with glucose consumption monitored using Medi-Test Glucose strips (Macherey-Nagel). The fermentation continued until two days after glucose depletion from the culture broth (33 days for YM 6.3 cultures and 27 days for MOF cultures).

For the solid cultures, 8 mL of the inoculum was introduced into four 500 mL Erlenmeyer-shaped culture flasks filled with solid rice medium. Subsequently, the medium was gently loosened with a spatula to enhance oxygen accessibility and ensure even dispersion of the inoculum. Incubation took place at 23 °C in an incubator, and after 72 days, the fermentation process was terminated. Following this, a second fermentation was conducted with six solid rice cultures under the same conditions.

2.3.4. Fermentation of *P. centrali-africana* (MUCL 56028) in liquid media

The homogenized seed culture was used to inoculate 25 500 mL Erlenmeyer-shaped culture flasks, each containing 200 mL of BAF medium. Each flask received 3 mL of the homogenized seed culture. The incubation was conducted on a rotary shaker at 23 °C and 140 min⁻¹. Glucose consumption was monitored at regular intervals (every five days) using Medi-Test strips (Macherey Nagel). After a 20-day incubation period, the liquid BAF cultures were harvested. A second BAF cultivation was carried out using identical conditions as described previously.

For the cultivation on rice medium, three 500 mL Erlenmeyer-shaped culture flasks were each filled with solid rice medium. Subsequently, the homogenized seed culture (6 mL per flask) was transferred into these flasks for inoculation. After inoculation, the medium was loosened using a sterilized spatula to promote oxygen accessibility and ensure homogenous distribution of the inoculum. Following these steps, the cultures were maintained at 23 °C for incubation. The rice standing cultures were harvested after 28 days of incubation.

2.4. Harvest of fungal cultures

2.4.1. Liquid cultivations

The separation of mycelium and supernatant was achieved through vacuum filtration or centrifugation at 5100 min⁻¹ for 15 min using a laboratory centrifuge (model 4-16KS, Sigma Laborzentrifugen GmbH, Osterode am Harz, Germany). The mycelium was then treated with acetone and subjected to extraction in an ultrasonic bath for 30 min, repeated twice. Filtration was used to separate the mycelium from the liquid phase, followed by the evaporation of the organic solvent (40 °C) using a rotary evaporator. The remaining aqueous phase was diluted with H₂O and subjected to extraction with EtOAc, followed by the evaporation (40 °C) of the resulting organic phase. The supernatant was extracted with EtOAc (1:1) in a separatory funnel, repeated twice. After removing the aqueous phase, the organic phase was retained and evaporated to dryness (40 °C). Information about the yields can be found in Table 2. Finally, extracts underwent preliminary cleaning using the SPME StrataTM-X 33 µm Polymeric RP cartridge (Phenomenex) to remove debris and strong nonpolar or hydrophobic compounds such as fatty acids.

2.4.2. Solid rice cultures

At first, both the medium and mycelium underwent treatment with acetone and were loosened with a spatula to facilitate mixing with the organic solvent. Ultrasonication for 30 min supported the subsequent extraction process. Separation of the solid and liquid phases was achieved through filtration, followed by another extraction of the solid phase. The organic solvent was then evaporated at 40 °C using a rotary evaporator. The remaining aqueous phase underwent extraction with EtOAc (1:1) in a separatory funnel, twice, and the resulting organic phase was evaporated to dryness (40 °C). For pre-separation, the extract was dissolved in 5 mL of MeOH, followed by the addition of 50 mL of a 1:1 mixture of heptane and MeOH/H₂O (1:1).

After extraction in a separatory funnel, the heptane and aqueous phases were collected separately and evaporated to dryness at 40 °C. Information about the yields can be found in Table 2.

Table 2. Amounts of extracts isolated from liquid and solid cultures of the fungal strains investigated for their secondary metabolism.

| strain | medium | origin | amount [mg] |
|-----------------------------|-----------|-------------|-------------|
| <i>A. ostoyae</i> | 1. solid | aq. phase | 1090 |
| | rice | hept. phase | 321 |
| | 2. solid | aq. phase | 1514 |
| | rice | hept. phase | 225 |
| | 1. liquid | mycelium | 944 |
| | YMWB | supernatant | 664 |
| | 2. liquid | mycelium | 343 |
| | YMWB | supernatant | 120 |
| <i>G. necrorhiza</i> | 1. liquid | mycelium | 126 |
| | YM 6.3 | supernatant | 360 |
| <i>Heimiomyces</i> sp. | 1. liquid | mycelium | 607 |
| | YM 6.3 | supernatant | 251 |
| | 2. liquid | mycelium | 567 |
| | YM 6.3 | supernatant | 651 |
| | 3. liquid | mycelium | 211 |
| | MOF | supernatant | 339 |
| | 1. solid | aq. phase | 476 |
| | rice | hept. phase | 206 |
| | 2. solid | aq. phase | 1071 |
| | rice | hept. phase | - |
| <i>P. centrali-africana</i> | 1. liquid | mycelium | 600 |
| | BAF | supernatant | 720 |
| | 2. liquid | mycelium | 207 |
| | BAF | supernatant | 252 |
| | 1. solid | aq. phase | 140 |
| | rice | hept. phase | 176 |

2.5. Preparative isolation of pure compounds by reversed phase liquid chromatography

After evaluating the data obtained from analytical LC-MS, the extracts underwent separation via RP HPLC utilizing a PLC 2250 purification system (Gilson, Middleton, WI, USA). Three types of columns were employed as the stationary phase: a Gemini LC column (250 × 50 mm, 110 Å, 10 µm, Phenomenex, Aschaffenburg, Germany), a Synergi™ Polar RP column (250 × 50 mm,

80 Å, 10 µm; Phenomenex) or a Nucleodur C18 column (150 × 40 mm, 10 µm, Macherey-Nagel). Flow rates ranged from 40 to 60 mL/min according to the type of the column. Based on the loading capacity of the columns, the extracts were divided into multiple fractions. The mobile phase for all separations consisted of solvent A: Milli-Q H₂O + 0.1% formic acid and solvent B: MeCN + 0.1% formic acid. Further details regarding UV detection, gradient specifications, and additional purification steps for the fractions can be found in papers I–V.

2.6. Analytical HPLC-DAD/MS analysis of pure compounds and extracts

To obtain ESI-MS spectra, the extracts were dissolved in acetone to a concentration of 10 mg/mL, while pure compounds were dissolved to achieve a concentration of 1 mg/mL. Ultrasonication at 40 °C for 10 min aided in the solvation of the extracts. Sample analysis was conducted using an analytical HPLC system (Dionex UltiMate 3000 series) coupled to an ion trap mass spectrometer (amazon speed by Bruker). Each sample, comprising 2 µL, was injected and separated using an ACQUITY-UPLC BEH C18 column (50 × 2.1 mm; particle size: 1.7 µm) by Waters (Milford, MA, USA). HPLC-grade H₂O and MeCN were utilized as the mobile phase, with a flow rate of 600 µL/min. The gradient started with 5% MeCN, followed by a linear increase to 100% MeCN over 20 min, maintaining 100% MeCN for 5 min. Chromatographic data analysis was performed using the Bruker analysis software (Data Analysis 4.4).

2.7. Structure elucidation and chemical characterization of pure compounds

2.7.1. General analytical and spectroscopic methods

NMR spectroscopy, combined with high-resolution electrospray ionization mass spectrometry (HR-ESI-MS), was employed to elucidate the structures of pure compounds.

All samples were dissolved in MeOH or acetone to yield a concentration of 1 mg/mL. HR-ESI-MS mass spectra were obtained using the Agilent 1200 series HPLC-UV system (Santa Clara, CA, USA) coupled with an ESI-TOF-MS (Bruker maXis). Measurements were conducted using a 2.1 × 50 mm, 1.7 µm, C18 Acquity UPLC BEH column (Waters). MilliQ H₂O with 0.1% formic acid was used as solvent A, while MeCN with 0.1% formic acid served as solvent B. The gradient method involved starting at 5% B for 0.5 min, increasing to 100% B over 19.5 min, and maintaining 100% B for 5 min, with a flow rate of 0.6 mL/min and DAD detection at 200–600 nm.

Depending on their solubility and stability, compounds were dissolved in deuterated acetone, MeOH, or DMSO before being transferred to NMR tubes. Subsequently, one-dimensional ^1H and ^{13}C , as well as two-dimensional correlation (COSY, ROESY, HSQC and HMBC) NMR spectra, were measured. This was conducted using either a Bruker Avance III 500 MHz spectrometer equipped with a BBFO (plus) SmartProbe (^1H 500 MHz, ^{13}C 125 MHz) or a Bruker Avance III 700 MHz spectrometer equipped with a 5 mm TCI cryoprobe (^1H 700 MHz, ^{13}C 175 MHz) (Bremen, Germany). Chemical shifts in the NMR data were referenced to selected chemical shifts of acetone- d_6 (^1H : 2.05 ppm, ^{13}C : 29.9 ppm).

Chemical characterization and elucidation of absolute configurations were supported by various methods. Optical rotation measurements were conducted using the PerkinElmer 241 polarimeter, while UV spectra were recorded using a Shimadzu UV-Vis spectrophotometer UV-2450 (Duisburg, Germany). Additionally, ECD spectra were obtained using a J-815 spectropolarimeter (Jasco, Pfungstadt, Germany).

Further details regarding the structure elucidation of the published compounds, supported by Dr. Frank Surup, can be found in papers I–V.

2.7.2. Hydrolysis and GC analysis of the fatty acid substituted sesquiterpene aryl esters

To determine the locations of the double bonds within the fatty acid side chain, compounds carrying a fatty acid side chain underwent degradation to produce their corresponding fatty acid methyl esters (FAMES). Hydrolysis of 0.2 mg of each compound was initiated by incubation with a mixture of MeOH:NaOH (15%) in a 1:1 ratio for 1 h at 100°C, resulting in the formation of the corresponding fatty acid (FA). Subsequently, the fatty acids were derivatized by incubation in MeOH:HCl (37% w/v) in a 5:1 ratio for 10 min at 80°C, leading to the formation of the FAMES. Extraction of the samples followed the method described by Abraham and Hesse (2003). An Agilent 6890N gas chromatograph with flame ionization detector (FID), equipped with a Macherey Nagel Optima 5 column (composed of 5% phenyl and 95% dimethylpolysiloxane; 50 m length, 0.32 mm inner diameter, and 0.25 μm film thickness), was used for the separation of the FAMES along with internal standards. The identification of double bond positions relied on comparing retention times with those of reference compounds, employing a retention time locking approach.

2.7.3. Acetylation of 41

Acetylation was conducted following the method outlined by Duncan et al. (2001). At first, 16 mg of **41** was dissolved in 4.8 mL pyridine, followed by the addition of 2.4 mL of acetic anhydride (resulting in a 2:1 mixture). The reaction solution was kept at room temperature for 3–4 h. Subsequently, the reagents were removed by evaporation (40 °C) using a rotary evaporator. The resulting product was dissolved in acetone and subjected to analysis by LC-MS. To address side product formation, purification was carried out via RP HPLC employing a PLC 2050 Purification System (Gilson). The sample was purified using the XBridge Prep C18 column (19 × 250 mm, 5 µm; Waters) with solvent A: MilliQ H₂O + 0.1% formic acid and solvent B: MeCN + 0.1% formic acid, at a flow rate of 20 mL/min. The gradient commenced with 70% B for 5 min, increasing to 90% B over 35 min, then to 100% B in 5 min, maintaining 100% B for an additional 5 min. The fraction collected between 20.5 and 21.5 min yielded 3.3 mg of compound **41b**.

2.7.4. Mosher's method: Preparation of the (*R*)- and (*S*)-MTPA ester derivatives of 49, 51 and 53

Each compound (0.5 mg) was dissolved in 300 µL of deuterated pyridine. Subsequently, 2 µL of (*R*)-(-)- α -methoxy- α -(trifluoromethyl)phenylacetyl chloride was added to the solution, and the mixture was kept at room temperature for 15 min. The progress of the reaction was monitored using analytical HPLC-DAD/MS. If the compounds were not completely converted into the corresponding Mosher ester, an additional 2 µL of *R*-MTPA was added. After Mosher esterification, the samples were transferred into 3.0 mm NMR tubes. Subsequently, ¹H NMR, ¹H,¹H-COSY NMR, ¹H,¹³C-HSQC NMR, and ¹H,¹³C-HMBC NMR spectra were measured. The identical procedure was replicated with an additional 0.5 mg of each compound using (*S*)-(+)- α -methoxy- α -(trifluoromethyl)phenylacetyl chloride. Evaluation of the resulting $\Delta\delta^{SR}$ values followed the method outlined by Hoyer et al. (2007).

2.8. Untargeted Metabolomics analyses

A. ostoyae (DSM 115711) was cultured in two distinct liquid media (YM 6.3 and Q6 ½) and solid rice medium. Liquid cultures were harvested three days after glucose depletion, while solid cultures were harvested 15 days post-inoculation, following established protocols for cultivating Basidiomycota (Pfütze et al. 2023a; Pfütze et al. 2023c). Subsequently, both the

supernatant and mycelia underwent extraction using EtOAc, and the resulting extracts were analyzed at a concentration of 450 µg/mL using an ultrahigh performance liquid chromatography system (Dionex Ultimate3000RS, Thermo Scientific, Dreieich, Germany) equipped with a C18 column (Kinetex 1.7 µm, 2.1 × 150 mm, 100 Å; Phenomenex). The injection volume of the samples was set at 2 µL. The mobile phase, consisting of A (Milli-Q H₂O + 0.1% formic acid) and B (MeCN + 0.1% formic acid), operated at a constant flow rate of 0.3 mL/min. The gradient started with 1% B for 0.5 min, followed by a linear increase to 5% B in 1 min, then to 100% B over 19 min, and was maintained at this level for 5 min. Throughout the analysis, the column temperature was kept at 40 °C, and UV-Vis data were collected using a DAD within the range of 190–600 nm.

MS spectra were acquired using a trapped ion mobility quadrupole time-of-flight mass spectrometer (timsTOF Pro, Bruker Daltonics, Bremen, Germany) following the instrumental settings and conditions described by Cedeño-Sanchez et al. (2023). For untargeted profiling of the extracts, ESI mass spectra were obtained in positive ion mode. Raw data underwent pre-processing using MetaboScape® 2022 (Bruker Daltonics) within the retention time range of 1.0 to 25 min. Features detected in the blank were excluded. The remaining features were dereplicated based on their accurate molecular weight and MS/MS spectra against compounds reported from the genus *Armillaria* in the Natural Product Atlas (NP Atlas) database (van Santen et al. 2019). MetaboScape® facilitated automatic *in silico* MS/MS matching using the MetFrag algorithm, relying on the InChI encoded structures, to accomplish this goal in the absence of MS/MS reference data (Ruttkies et al. 2016).

Molecular networks were established using the Feature-Based Molecular Networking (FBMN) workflow (Nothias et al. 2020) on the GNPS platform (Wang et al. 2016), based on the pre-processed feature table from MetaboScape®, following the methodology outlined by Charria-Girón et al. (2023b). Visualization of these molecular networks was conducted using the Cytoscape software (Shannon et al. 2003).

2.9. Assessment of biological activities

2.9.1. Evaluation of antimicrobial activity

In 96-well microtiter plates, serial dilution assays were conducted to determine minimum inhibitory concentrations (MICs) against various yeasts, filamentous fungi, and bacteria,

following the protocol outlined by Harms et al. (2021). Selected compounds were tested against a spectrum of microorganisms including *Schizosaccharomyces pombe* (DSM 70572), *Candida albicans* (DSM 1665), *Wickerhamomyces anomalus* (DSM 6766), *Mucor hiemalis* (DSM 2656), *Rhodotorula glutinis* (DSM 10134), *Escherichia coli* (DSM 1116), *Pseudomonas aeruginosa* (DSM PA14), *Chromobacterium violaceum* (DSM 30191), *Bacillus subtilis* (DSM 10), *Staphylococcus aureus* (DSM 346), and *Mycobacterium smegmatis* (ATCC 700084).

Acetone was used to prepare stock solutions of all compounds at a concentration of 1 mg/mL, which were then employed in the serial dilution assay. Positive controls for bacteria included the antimicrobials [O] Oxytetracycline, [G] Gentamycin, and [K] Kanamycin, while [N] Nystatin was used for filamentous fungi and yeast. Acetone (20 µL) was employed as a negative control to demonstrate the absence of inhibitory effects.

2.9.2. Evaluation of cytotoxicity

In vitro cytotoxicity assays were conducted in 96-well plates following the procedure outlined by Harms et al. (2021). Compounds were evaluated against the mouse fibroblast cell line L929 and the cervix carcinoma cell line KB3.1. The most active derivatives were subsequently assessed against additional cancer cell lines, including the breast cancer cell line MCF-7, the lung cancer cell line A549, the ovary cancer cell line SKOV-3, the prostate cancer cell line PC-3, and the epidermal cancer cell line A431.

Stock solutions of all compounds were prepared in acetone at a concentration of 1 mg/mL and were utilized for the cytotoxicity assay. Epothilone B served as the positive control. Acetone (20 µL) was used as the negative control, showing no inhibitory effects.

3. Results and Discussion

3.1. Secondary metabolites from two closely related members of the *Physalacriaceae* (Agaricales)

The primary objective of this work was to investigate the secondary metabolism of fungi belonging to the genus *Armillaria*, which are particularly known for their production of sesquiterpene aryl esters, a class of chemically diverse and biologically active meroterpenoids. Through prior screenings of different *Armillaria* species, *A. ostoyae* (DSM 115711) emerged as

the most productive and promising strain. Consequently, our research focused predominantly on this strain to elucidate the secondary metabolism within this genus.

Furthermore, as part of a secondary investigation, we explored the secondary metabolism of *G. necrorhiza* (CBS 138623), resulting in a surprising discovery. We observed, for the first time, the production of melleolide-type meroterpenoids outside the genus *Armillaria*.

3.1.1. Chemical diversity of sesquiterpene aryl esters isolated from *A. ostoyae* (DSM 115711) and *G. necrorhiza* (CBS 138623)

After cultivating *A. ostoyae* in both liquid (YMWB) and solid rice media, a thorough analysis using HR-ESI-MS revealed the presence of numerous melleolides, characterized by their distinctive UV/Vis absorption peaks at λ_{max} 220, 260, and 300 nm. Surprisingly, among the identified compounds were congeners with higher molecular weights (>800 Da) yet exhibiting similar UV/Vis spectra to the typical melleolide-type compounds (382–490 Da). Consequently, the extracts underwent fractionation via preparative HPLC, leading to the isolation of seventeen new derivatives (**1–17**; Figures 7–9), along with previously documented melleolides **18–38** (Figures 10 and 11).

The absolute configuration of all melleolide-type metabolites adheres to the one established through X-ray analysis of melleolide, armillarin, 4-*O*-methylmelleolide, melledonal C, melleolide L, and armillarivin (Midland et al. 1982; Yang et al. 1984; Donnelly et al. 1985; Arnone et al. 1988; Momose et al. 2000; Schwartz et al. 2013). This was further supported by electronic circular dichroism (ECD) comparison, as detailed in paper V, with structurally related derivatives for the newly described compounds in this study.

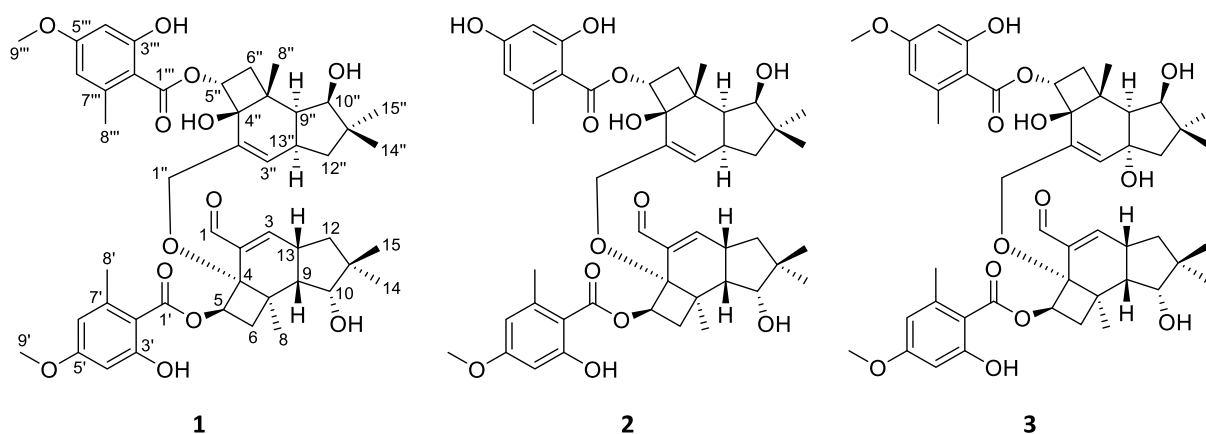


Figure 7. Sesquiterpene aryl ester dimers isolated from cultures of *A. ostoyae*. **1**: bismelleolide BH; **2**: bismelleolide EH; **3**: bismelleolide CH.

While the secondary metabolism of *Armillaria* spp. has been extensively studied, melleolide dimers had not been previously documented (Dörfer et al. 2019).

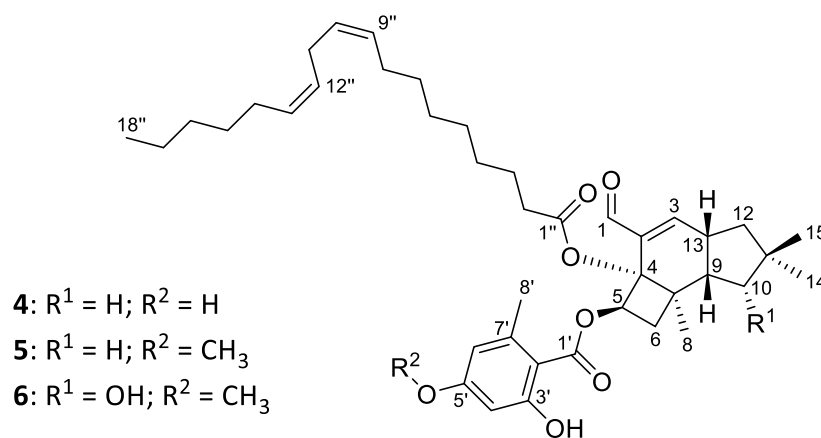


Figure 8. Fatty acid substituted sesquiterpene aryl esters isolated from cultures of *A. ostoyae*. **4:** melleolide linoleate; **5:** armillarine linoleate; **6:** melleolide H linoleate.

Among compounds of this class, it is quite rare to find a linoleic acid side chain esterified to the protoilludene core structure of sesquiterpene aryl esters (Dörfer et al. 2019). Armillatin is currently the only other known congener that exhibits this unique feature (Yang et al. 1991).

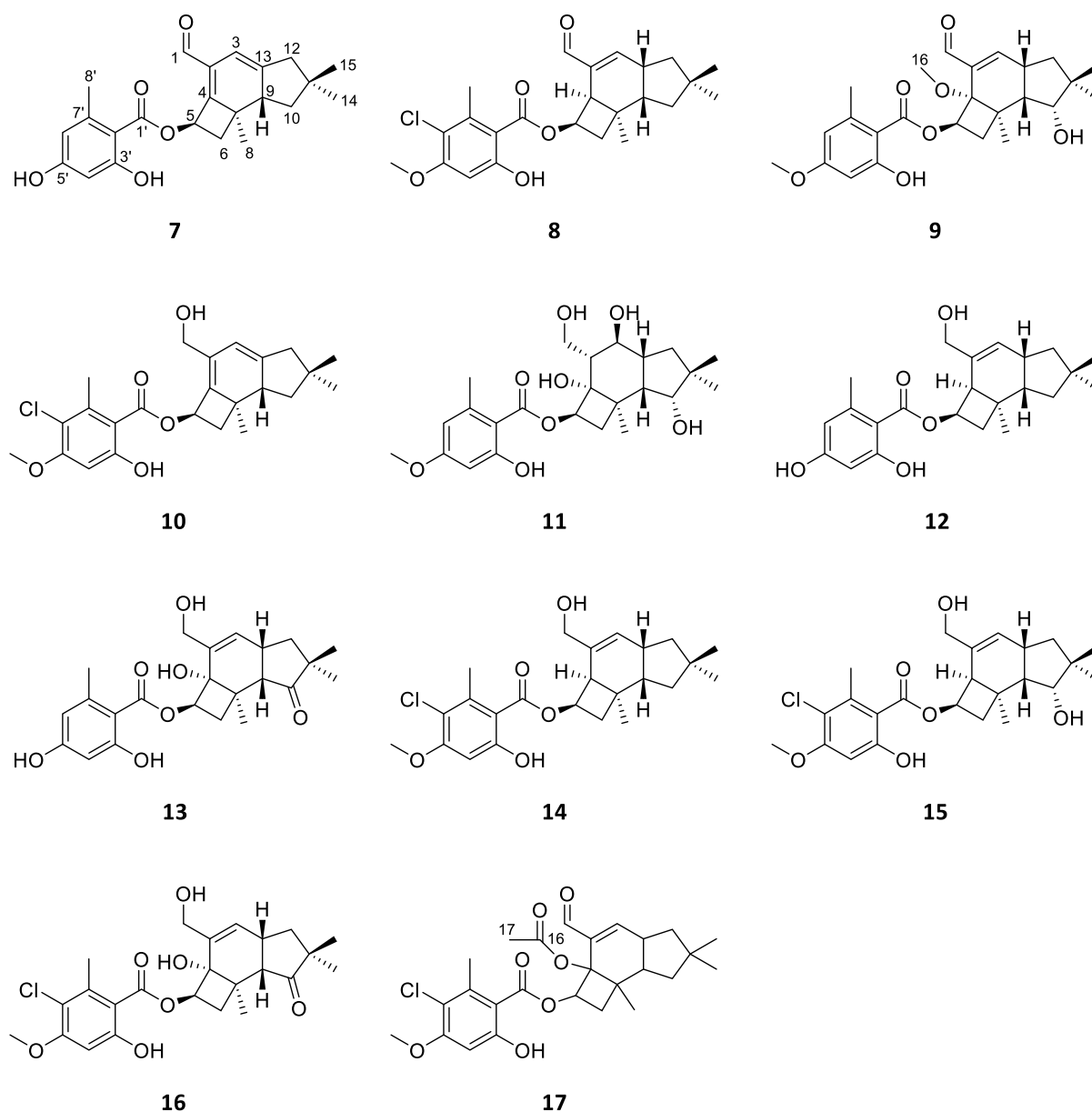


Figure 9. New sesquiterpene aryl esters isolated from cultures of *A. ostoyae*. **7:** 5'-*O*-desmethyllumillaribin; **8:** 4-dehydroxyarmillaridin; **9:** 4-methoxymelleolide H; **10:** 1-hydroxyarmillaricin; **11:** 10-hydroxy-5'-*O*-methyllumillane; **12:** 4-dehydroxymelleolide F; **13:** 10-ketomelleolide E; **14:** 4,10-dehydroxymelleolide I; **15:** 4-dehydroxymelleolide I; **16:** 10-ketomelleolide I; **17:** 4-acetyllumillaridin.

The sesquiterpene aryl esters have been extensively studied, with over 70 congeners previously described (Dörfer et al. 2019). Despite this wealth of prior knowledge, investigations into the secondary metabolism of *A. ostoyae* (DSM 115711) have revealed a remarkable number of new derivatives within this class. Compounds **1-17** represent new structural variations that further enrich the spectrum of derivatives within this intriguing chemical family, highlighting the complexity and diversity inherent in the chemistry of this compound class.

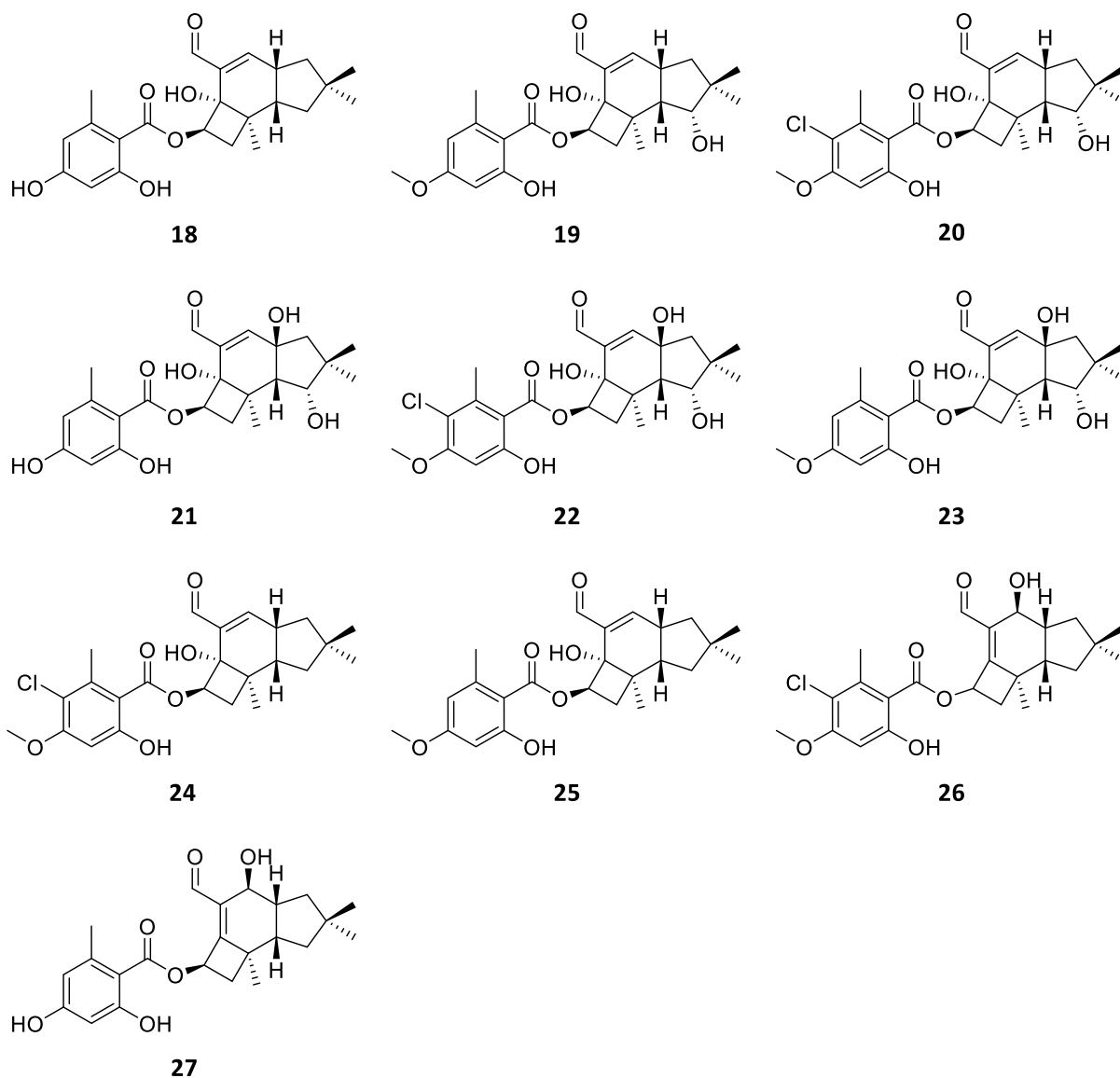


Figure 10. Known aldehydes (C-1) of sesquiterpene aryl esters isolated from *A. ostoyae* (DSM 115711). **18:** melleolide; **19-20:** melleolides H and J; **21-22:** melledonals A and C; **23:** 5'-*O*-methylnelledonal; **24:** armillaridin, **25:** armillarin; **26:** arnamial; **27:** dehydroarmillylorsellinate.

Furthermore, the isolation of 21 known sesquiterpene aryl esters (Figure 10 and 11), alongside the new derivatives, represents only a fraction of the vast array of substances this organism is capable of producing. This has sparked interest in studying its entire metabolome.

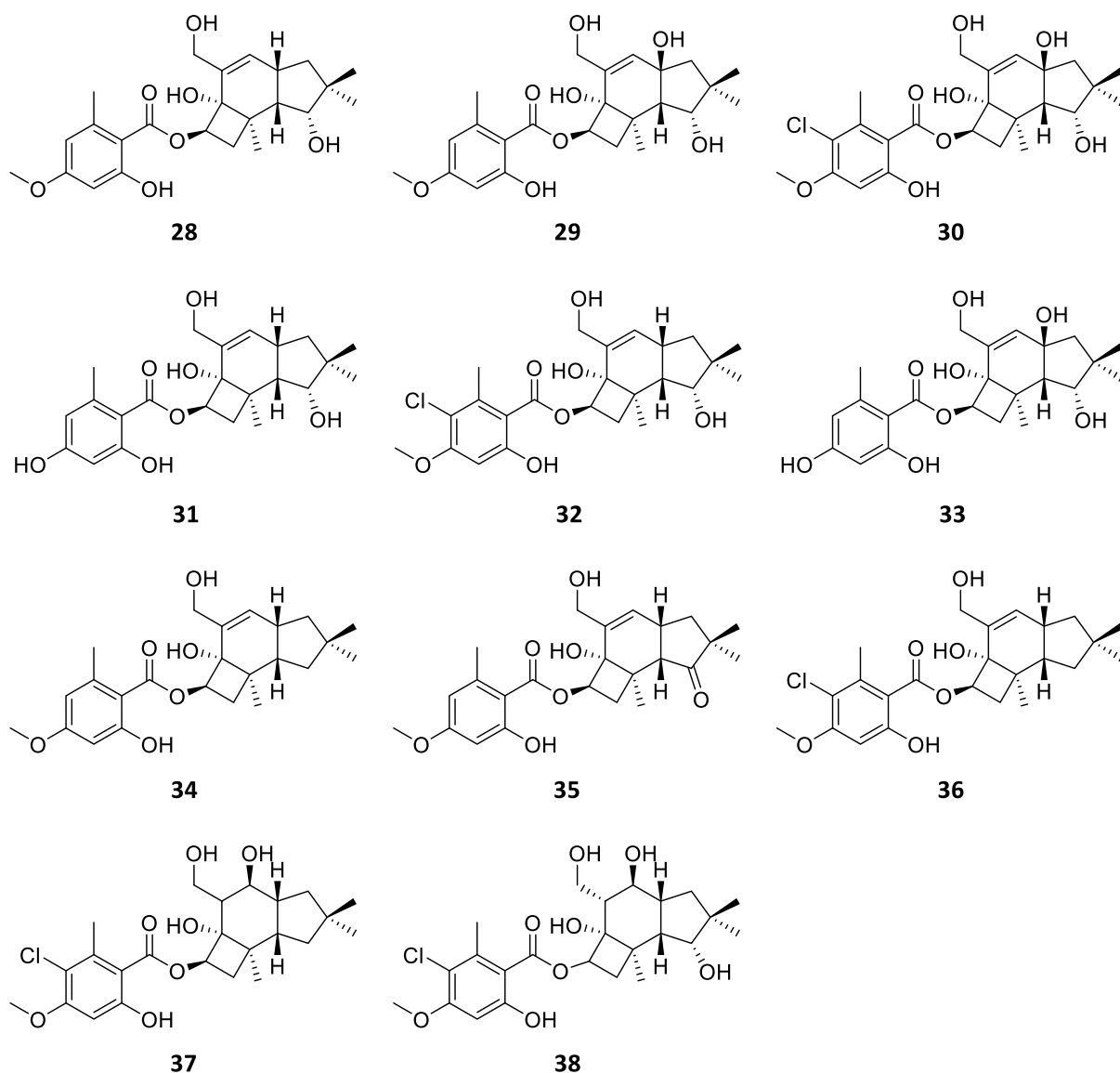


Figure 11. Known alcohols (C-1) of sesquiterpene aryl esters isolated from *A. ostoyae* (DSM 115711). **28-32**: melleolides B-E and I; **33**: melledonol; **34**: 10-dehydroxy-melleolide B; **35**: 10-oxo-melleolide B; **36**: A52a; **37**: 5'-methoxy-6'-chloroarmillane; **38**: 10-hydroxy-5'-methoxy-6'-chloroarmillane.

The cultivation of *G. necrorhiza* (CBS 138623) in liquid YM 6.3 medium, followed by the extraction of its mycelium and culture broth and preparative HPLC purification, resulted in the isolation and characterization of a new armillane-type meroterpenoid called 5'-*O*-methyl-14-hydroxyarmillane (**39**), along with three known congeners (**28**, **34** and **40**; Figure 11 and 12).

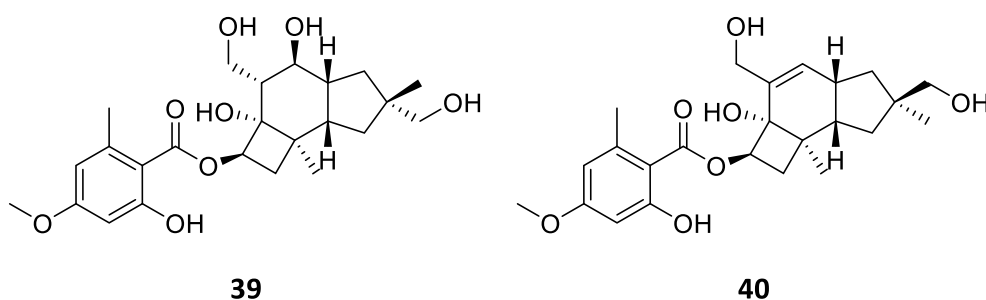


Figure 12. Sesquiterpene aryl esters of the protoilludene type extracted from liquid YM 6.3 cultures of *G. necrorhiza* cultures: **39**: 5'-O-methyl- 14-hydroxyarmillane; **40**: melleolide G.

The isolation and identification of these secondary metabolites from cultures of *G. necrorhiza* represented the first time that members of this compound class were detected in a genus outside *Armillaria*. These findings underscore a strong association between *Armillaria* and *Guyanagaster*, implying the possibility of discovering more congeners, including new derivatives, through further investigations into the secondary metabolism of *Guyanagaster* species.

3.1.2. Assessment of melleolide production in *A. ostoyae* under different cultivation conditions using metabolomics techniques

The compounds **1–38** isolated from liquid and solid cultures of *A. ostoyae* represent over 40% of the entire class of sesquiterpene aryl esters documented to date. To further explore the extensive range of chemical variations within the secondary metabolism of this species, we employed untargeted metabolomics based on mass spectrometry. Consequently, we analyzed the extracts obtained from liquid and solid cultivation using ultrahigh performance liquid chromatography coupled with diode array detection and ion mobility tandem mass spectrometry (UHPLC-DAD-IM-MS/MS).

To comprehensively understand the metabolomes present in each extract, we conducted a principal component analysis (PCA), enabling visualization of sample similarities in a two-dimensional scores plot (Figure 13). The PCA revealed three distinct clusters: the first comprised extracts from the solid rice cultures, while the second cluster encompassed both extracts derived from the supernatant and mycelia of the YM 6.3 liquid cultures. Similarly, the third cluster consisted of the supernatant and mycelial extracts of the Q6 ½ liquid cultures. It became evident that the varied cultivation and extraction procedures resulted in distinct metabolomes (Figure 13). Subsequently, the production of melleolide-type metabolites was analyzed through Feature Based Molecular Networking (FBMN).

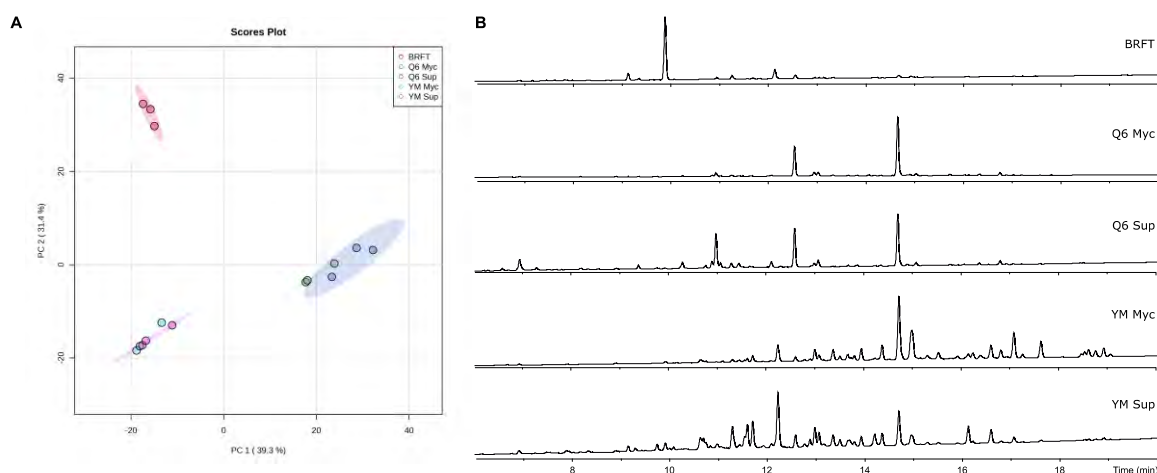


Figure 13. A) PCA scores plot illustrating the secondary metabolomes of *A. ostoyae* derived from analyses of extracts that were obtained from cultivations in different media (YM 6.3, Q6 ½, and solid rice medium (BRFT), $n=3$, with a 95 % confidence interval of normalized m/z intensities derived from the features detected at the MS1 level, positive ionization mode). B) HPLC-UV/Vis chromatograms of the extracts recorded at 210 nm (Pfütze et al. 2024).

The MS/MS data analysis of the isolated melleolide-type meroterpenoids revealed a distinctive fragmentation pattern (Figure 14), primarily characterized by the loss of the substituted orsellinic acid moiety, which displayed a distinctive set of neutral losses typical for this compound class. Thus, differences in compounds, such as chloride substitution, *O*-methylation, fatty acid side chains or dimerization, can be identified through mass differences in fragment ions. However, while MS/MS experiments enable the deduction of the presence of the substitution patterns commonly observed in melleolide-type meroterpenoids, they do not specify the modification position.

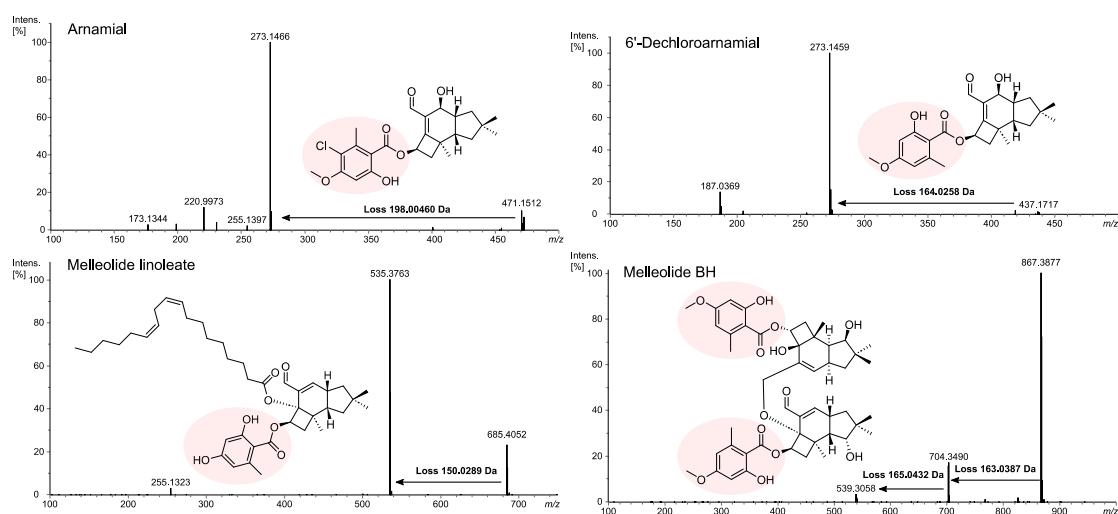


Figure 14. MS/MS spectra of melleolide BH, arnamial, 6'-dechloroarnamial, and melleolide linoleate for reference (Pfütze et al. 2024).

FBMN analyses of the data obtained from the various extracts using the MetaboScape® software resulted in a feature table, which underwent dereplication, leading to the detection of 2227 features at the MS2 level. These were then categorized into 156 molecular families (MFs), each comprising at least two clustered nodes, alongside 1339 singletons (Figure 15A). Among these, 22 MFs comprising 277 features were assigned to the compound class of the melleolide-type meroterpenoids. The two predominant MFs consisted of melleolide B, 5'-methoxyarmillarizin, 4'-methoxymelleolide H, 4-dehydroxymelleolide I, 10-hydroxy-5'-O-methylarmillane, and bismelleolide EH, respectively. Surprisingly, the bismelleolide EH cluster emerged as the second largest MF, while the structurally closely related bismelleolides BH and CH were grouped in another smaller MF. Such structurally similar metabolites that display differing MS/MS spectra due to minor chemical alterations often represent major challenges for metabolomics analyses, and therefore thorough investigations and access to pure standards are crucial for a complete understanding of this phenomenon (Charria-Girón et al. 2023a). Conversely, the MF corresponding to melleolide linoleate indicated a lower quantity of compounds with a substituted fatty acid chain compared to dimeric sesquiterpene aryl esters. Through hierarchical clustering and heatmap analysis of compounds **1–5**, **6–9**, **11–16** (Figure 15B), distinct metabolic profiles were observed among the extracts. Certain compounds showed elevated levels in specific extracts, revealing differences in metabolite abundance between mycelial and supernatant extracts, as well as between different cultivation conditions. Overall, the findings highlight the complex metabolic responses of *A. ostoyae* to varying environmental conditions.

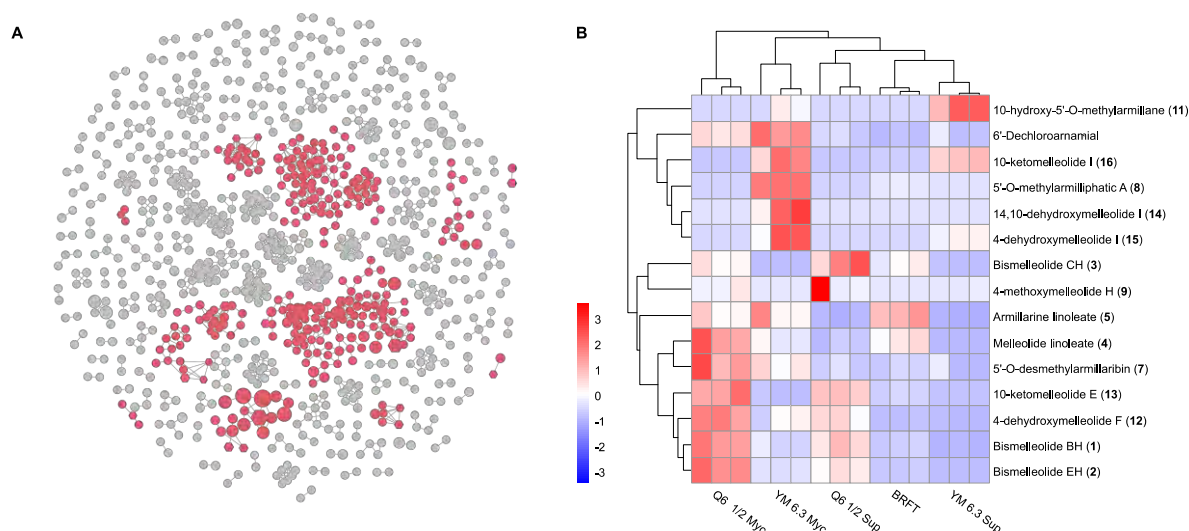


Figure 15. A) Feature-based molecular network (FBMN), wherein melleolide molecular families were annotated by comparing their MS/MS spectra with the metabolites isolated during this study. In the network representation, hexagons in red denote melleolide derivatives, while gray hexagons represent unknown features; the size of each node corresponds to the abundance of the compound. **B)** Heatmap illustrating hierarchical clustering of compounds **1–5**, **6–9**, **11–16**, and 6'-dechloroarnamial annotated in the FBMN. It portrays the abundance of compounds and crude extracts derived from different media, with each extract represented by three columns for three biological replicates. Abundance levels are color-coded from red (high abundance) to dark blue (low abundance), indicating scaled abundance. The heatmap together with the dendrograms was generated utilizing the R package pheatmap (Pfütze et al. 2024).

3.1.3. Bioactivities and insights into the structure-activity relationships of melleolide-type meroterpenoids

Over the years, many melleolide-type meroterpenoids reported in the literature have undergone assessment for their antimicrobial and cytotoxic properties. However, numerous nonsystematic assays conducted on different strains and cell lines have resulted in a multitude of assumptions and hypotheses regarding potential structure-activity relationships. Therefore, an initial attempt was made to examine a wide range of these chemically diverse secondary metabolites under controlled laboratory conditions, aiming to identify the structural elements responsible for the observed effects.

Previous assessments of antibacterial activity testing suggested that hydroxylations at positions C-4, C-10, and C-13 enhance the inhibition of bacterial growth, particularly against Gram-positive bacteria (Dörfer et al. 2019). Based on these assumptions, compounds **1**, **4–9** and **11–38** (Figure 16) were tested for their antibacterial potential against *E. coli*, *P. aeruginosa*, *C. violaceum*, *B. subtilis*, *S. aureus*, and *M. smegmatis*. The complete data set of MIC values can be found in paper V.

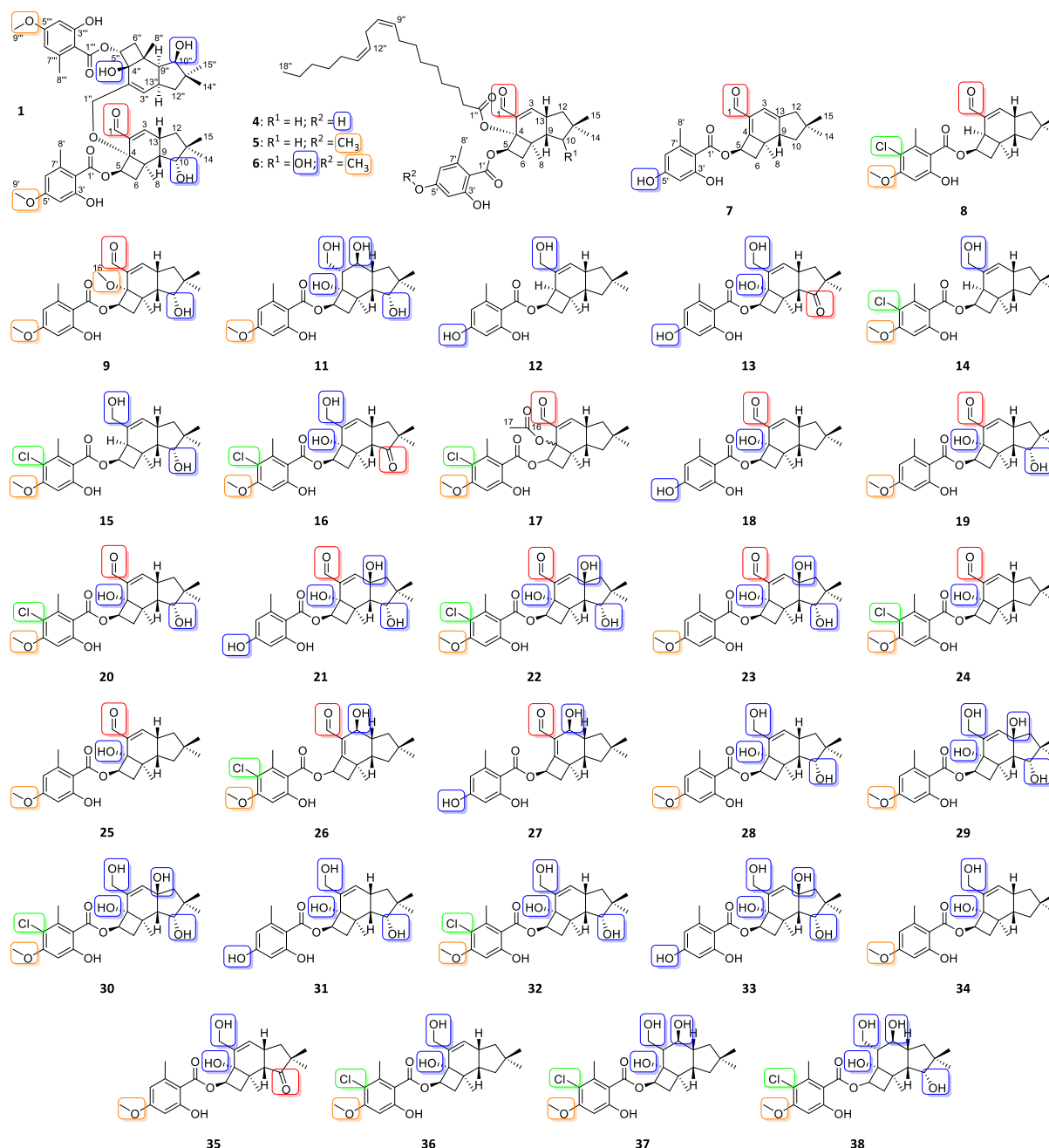


Figure 16. Overview of all sesquiterpene aryl esters examined for their biological effects, highlighting key structural modifications (blue: hydroxylation; red: ketone; green: chlorination; orange: methoxy). **1:** bismelleolide BH; **4:** melleolide linoleate; **5:** armillarine linoleate; **6:** melleolide H linoleate; **7:** 5'-O-desmethyarmillaribin; **8:** 4-dehydroxyarmillaridin; **9:** 4-methoxymelleolide H; **11:** 10-hydroxy-5'-O-methylarmillane; **12:** 4-dehydroxymelleolide F; **13:** 10-ketomelleolide E; **14:** 4,10-dehydroxymelleolide I; **15:** 4-dehydroxymelleolide I; **16:** 10-ketomelleolide I; **17:** 4-acetyarmillaridin; **18:** melleolide; **19-20:** melleolides H-J; **21-22:** melledonals A and C; **23:** 5'-O-methylmelledonal; **24:** armillaridin; **25:** armillarin; **26:** arnamial; **27:** dehydroarmillylorsellinate; **28-32:** melleolides B-E and I; **33:** melledonol; **34:** 10-dehydroxy-melleolide B; **35:** 10-oxo-melleolide B; **36:** A52a; **37:** 5'-methoxy-6'-chloroarmillane; **38:** 10-hydroxy-5'-methoxy-6'-chloroarmillane (Pfütze et al. 2024).

However, our findings yielded a contrasting outcome, with 5'-O-desmethyarmillaribin (**7**), 4-dehydroxymelleolide F (**12**), arnamial (**26**), and A52a (**36**) demonstrating the highest antibacterial activity (4.2 µg/mL against *B. subtilis* and *S. aureus*), despite only compound **36**

featuring a hydroxylation at C-4 (Figure 16). The absence of inhibition against Gram-negative bacteria confirms the prevailing understanding that this compound class predominantly affects Gram-positive bacteria. Furthermore, despite comparing bioactivity and chemical data, we were unable to identify specific structural features responsible for the antibacterial effects.

Previous studies have emphasized the crucial role of the $\Delta^{2,4}$ double bond in the protoilludene moiety for antifungal activities against specific fungal strains, while $\Delta^{2,3}$ -melleolides were reported to be inactive (Bohnert et al. 2014). Consistent with this theory, compounds **1**, **4–9** and **11–38** (Figure 16) were assessed against *S. pombe*, *W. anomalus*, *M. hiemalis*, and *R. glutinis*. The complete data set of MIC values can be found in paper V. In order to identify specific trends in the observed antifungal effects, the compounds underwent clustering based on their MIC values (minimal inhibitory concentration values, $\mu\text{g/mL}$) using a hierarchical clustering method. Through this approach, three primary clusters emerged, each demonstrating distinct characteristics: non, selective, and broad-spectrum antifungal compounds (Figure 17).

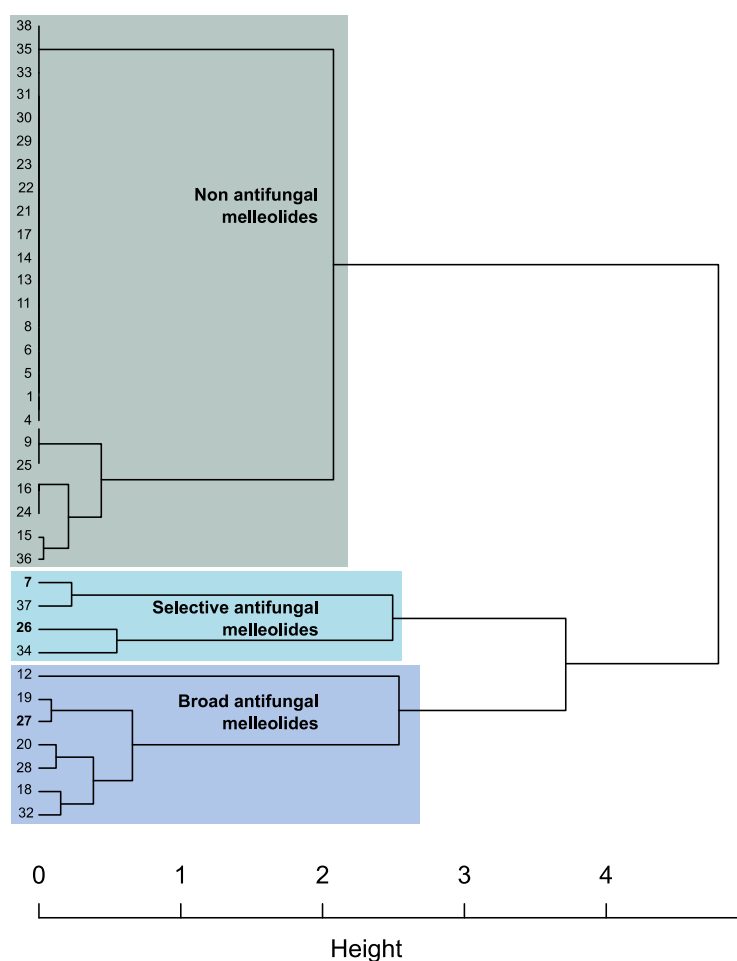


Figure 17. Examination of the antifungal potential of melleolide-type meroterpenoids against *S. pombe*, *W. anomalus*, *M. hiemalis*, and *R. glutinis*: Dendrogram, obtained from hierarchical clustering of the antifungal activities of the tested melleolide-type meroterpenoids. Three major clusters are highlighted with colored boxes, and numbers of compounds featuring a $\Delta^{2,4}$ double bond in the protoilludene moiety are underscored (Pfütze et al. 2024).

Among the 35 compounds assessed, 11 displayed notable antifungal properties. Interestingly, only **7**, **26**, and **27** feature a $\Delta^{2,4}$ double bond in the protoilludene framework. Moreover, **19** and **34** contain a $\Delta^{2,3}$ double bond in the protoilludene backbone, while **37** lacks a terpene double bond. Remarkably, all these compounds demonstrated noteworthy antifungal activity, indicating that the presence of a $\Delta^{2,4}$ double bond is not essential for inhibiting fungal growth (Figure 18).

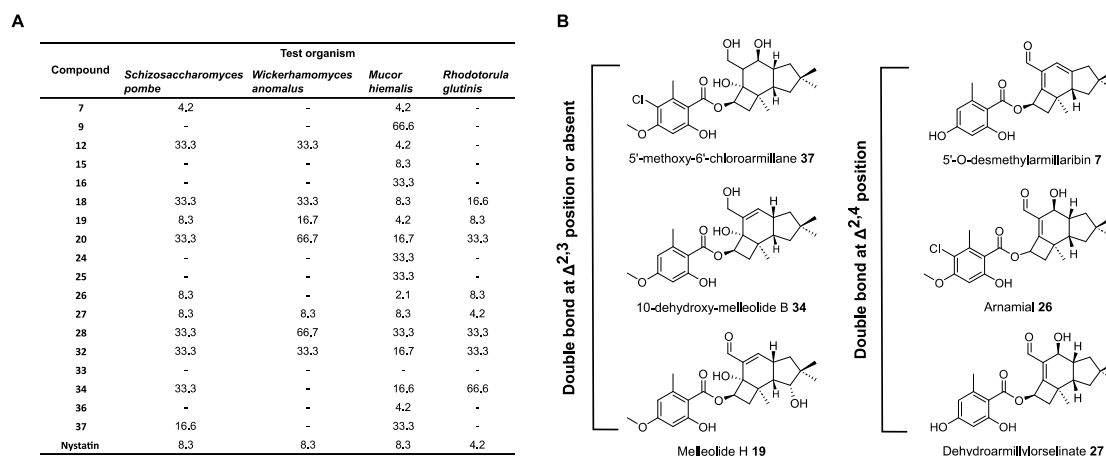


Figure 18. A) Minimum inhibitory concentration (MIC) values ($\mu\text{g/mL}$) against the selected fungal strains. Compounds lacking activity are excluded here, but the full dataset can be found in paper V. **B)** Chemical structures of melleolide-type meroterpenoids with notable antifungal activity are presented. Compounds featuring a $\Delta^{2,3}$ double bond or no terpene double bond in the protoilludene moiety are depicted on the left, while those with a $\Delta^{2,4}$ double bond in the terpene backbone are depicted on the right (Pfütze et al. 2024).

Regarding the cytotoxicity of sesquiterpene aryl esters, it has been suggested that the position of the double bond in the protoilludene backbone does not significantly affect their activity. Instead, the presence of an aldehyde at C-1 has been identified as a crucial characteristic contributing to increased cytotoxicity (Bohnert et al. 2011; Bohnert et al. 2014). Based on these hypotheses, we evaluated the cytotoxic effects of compounds **1**, **4–9** and **11–38** (Figure 16) against L929 (mouse fibroblast) and KB3.1 (cervix carcinoma) cell lines. Furthermore, compounds showing the most potent cytotoxic properties against the L929 and KB3.1 cell lines were subjected to further evaluation against five additional mammalian cell lines. The complete data set of IC_{50} values can be found in paper V.

Hierarchical clustering based on the IC_{50} values (μM) revealed two major clusters (Figure 19): non cytotoxic and cytotoxic compounds. Among the cytotoxic compounds, a total of 12 exhibited notable cytotoxicity and clustered together. Within this clade, all compounds, except for **12**, feature an aldehyde at position C-1, confirming its crucial role for the cytotoxicity (Figure 20C).

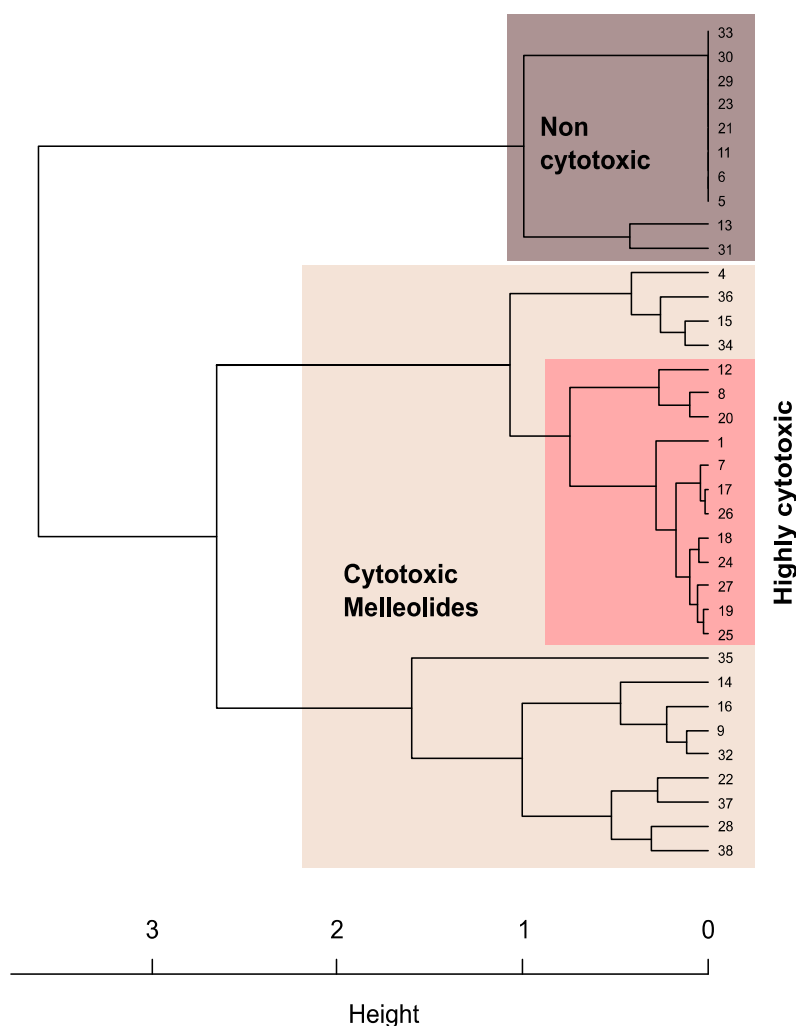


Figure 19. Examination of the cytotoxic characteristics against L929 mouse fibroblast and KB3.1 cervix carcinoma cell lines displayed by melleolide-type meroterpenoids: Dendrogram, a product of hierarchical clustering, showcases the cytotoxic effects of the assessed melleolide-type meroterpenoids. Major groups are indicated by colored boxes (Pfütze et al. 2024).

Additionally, we conducted a comparative analysis of this specific clade with the dendrogram generated from hierarchical clustering of the corresponding chemical structures (Figure 20A and B), revealing the effects of certain chemical modifications on the cytotoxicity of the tested compounds. Another significant correlation between chemical structure and cytotoxicity emerged from the complete loss of activity observed in sesquiterpene aryl esters featuring a hydroxylation at position C-13. Notably, compounds like **19** and **20** were among the most cytotoxic in this study, whereas their counterparts with a hydroxylation at C-13, such as **23** and **22**, exhibit no cytotoxic effects. Similarly, compounds like **21**, **30**, and **33**, sharing the same hydroxylation pattern at positions C-10 and C-13, also demonstrated no cytotoxic activity.

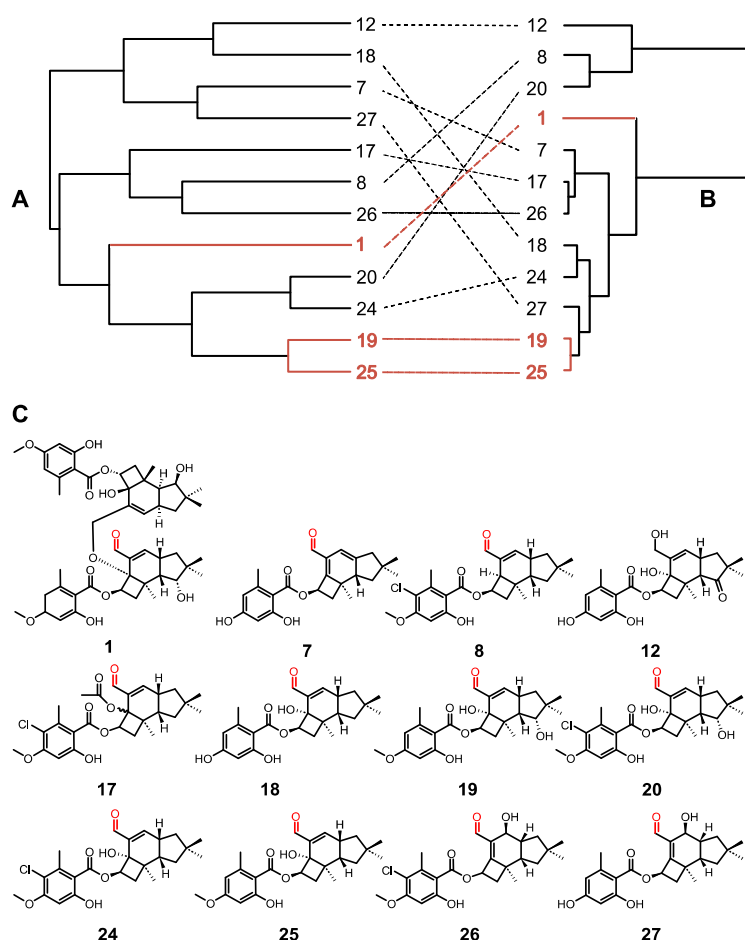


Figure 20. Examination of the cytotoxic characteristics against L929 mouse fibroblast and KB3.1 cervix carcinoma cell lines displayed by melleolide-type meroterpenoids: **A)** Comparison between dendrograms resulting from hierarchical clustering of chemical structures of compounds demonstrating significant cytotoxicity using circular fingerprints and Tanimoto similarity and **B)** corresponding cytotoxic activities; with common clades highlighted in dark orange. **C)** Melleolide-type meroterpenoids showing the highest cytotoxic effects against cell lines L929 and KB3.1, with aldehyde group in the protoilludene moiety highlighted in red (Pfütze et al. 2024).

Except for **28** and **34**, which were already been tested as part of the studies on the secondary metabolism of *A. ostoyae*, the potential bioactivities of **39** and **40** were evaluated in the investigations concerning *G. necrorhiza*. The complete data set of IC₅₀ values can be found in paper IV. The weak or absent cytotoxic effects observed for both compounds could be attributed to the hydroxylation at C-1, as derivatives featuring an aldehyde group at this position are known to possess higher cytotoxic potential (Dörfer et al. 2019). Since both compounds are only hydroxylated at position C-4, while lacking hydroxylations at C-10 and C-13, this may explain the lack of activity against Gram-positive bacteria. Furthermore, no activity against Gram-negative bacteria and fungi was observed.

3.2. *Heimiomyces* sp. (MUCL 56078) as a prolific producer of novel terpenoids

Previous research on *Heimiomyces* sp. (MUCL 56078) resulted in the isolation and description of several new compounds (**56-61**) (Cheng et al. 2020). However, analysis of LC-MS data from the extracts revealed numerous unidentified compounds, indicating the complexity of the fungal metabolome and the potential for further exploration to elucidate novel bioactive molecules. In a follow-up study, cultivations in both liquid and solid media led to the observation of even more unidentified compound peaks in the LC-MS data. These compounds exhibited unknown masses, UV spectra, and retention times, prompting the purification of the extracts to characterize pure compounds.

3.2.1. Metabolic shift and chemical diversity of secondary metabolites produced by *Heimiomyces* sp.

After cultivating *Heimiomyces* sp. on solid rice medium and purifying the obtained extracts, we isolated new meroterpenoids (Figure 21), including bis-heimiomycins A–D (**41–44**) and heimiomycins D and E (**45** and **46**).

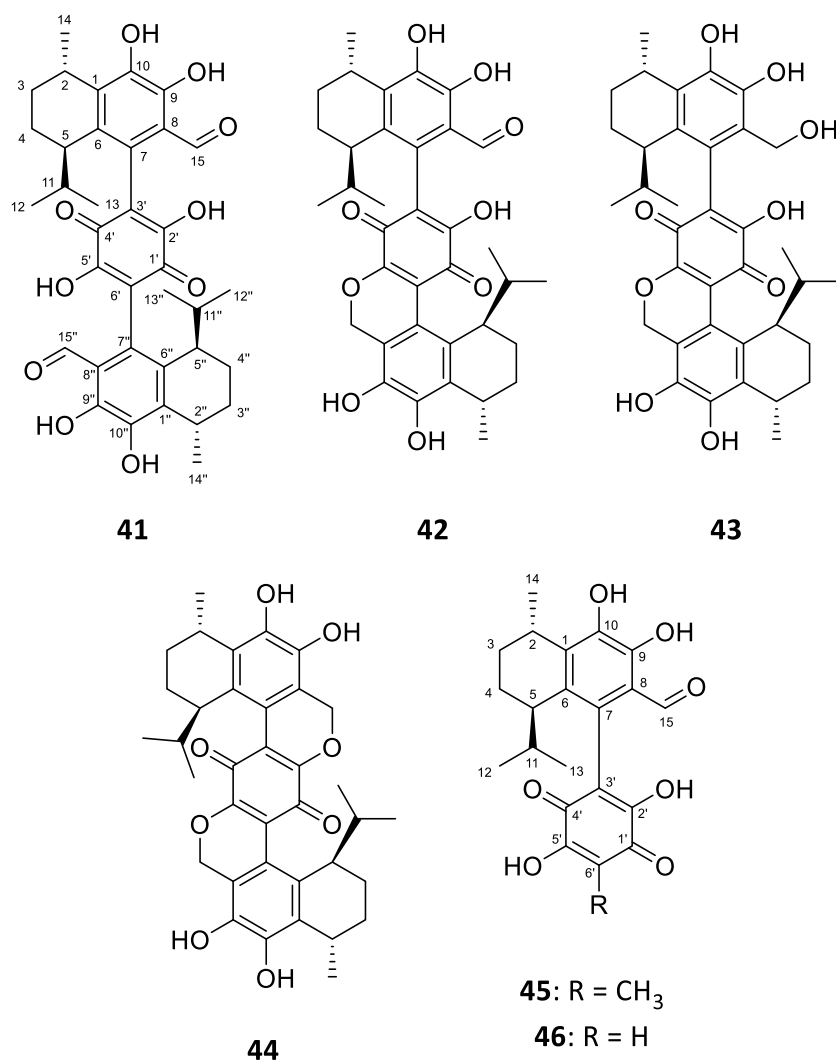
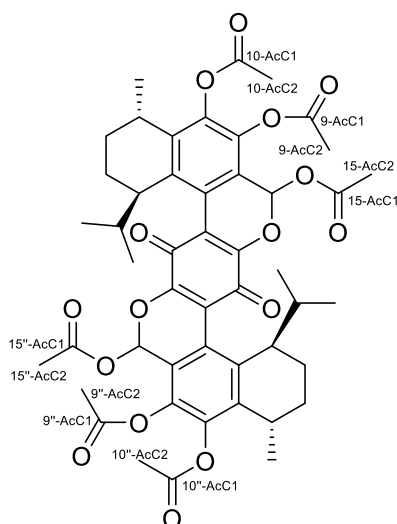


Figure 21. New meroterpenoids isolated from solid rice cultures of *Heimiomyces* sp. **41–44**: bis-heimiomyces A–D; **45–46**: heimiomyces D and E.

The structural elucidation of **41–46** was accompanied by a number of challenges. In the case of **41**, only the C-2'/C-5' dihydroxy-quinone moiety was evident in the ¹³C spectrum, while signals for carbons C-1'/C-3'/C-4'/C-6' were absent. Suspecting rapid tautomerism causing the missing resonances, we subjected **41** to acetylation with acetic anhydride in pyridine, derivatizing positions C-15/C-15'', 2'-OH/5'-OH, 9-OH/9''-OH, and 10-OH/10''-OH. Analysis of the resulting product **41b** (Figure 22) via 1D and 2D NMR confirmed peracetylation and ring closure at C-15/C-15'' of **41**. Details on the evaluation of the NMR spectra can be found in paper II.

**41b****Figure 22.** Product of acetylation of compound **41**.

Additionally, minor isomers were detected in the LC-MS and NMR data of compounds **41** and **42**. After purification via preparative HPLC, analytical HPLC results for compound **41** revealed two peaks with identical molecular masses (Figure 23), occurring in a ratio of 9:1. This ratio spontaneously adjusted, likely due to interconversion between two forms of the compound. Similarly, the LC-MS data for compound **42** showed two peaks exhibiting identical molecular masses (Figure 24). This phenomenon was also evident in the ¹H and ¹³C spectra of both **41** and **42**, where weak signals of the minor isomers were present. Two potential explanations for the presence of these minor isomers are considered: firstly, the quinone substructure of **41–46** might adopt a *para*- or *ortho*-orientation, both exhibiting similar characteristics; secondly, atropisomerism within the molecules could result in different stereoisomers.

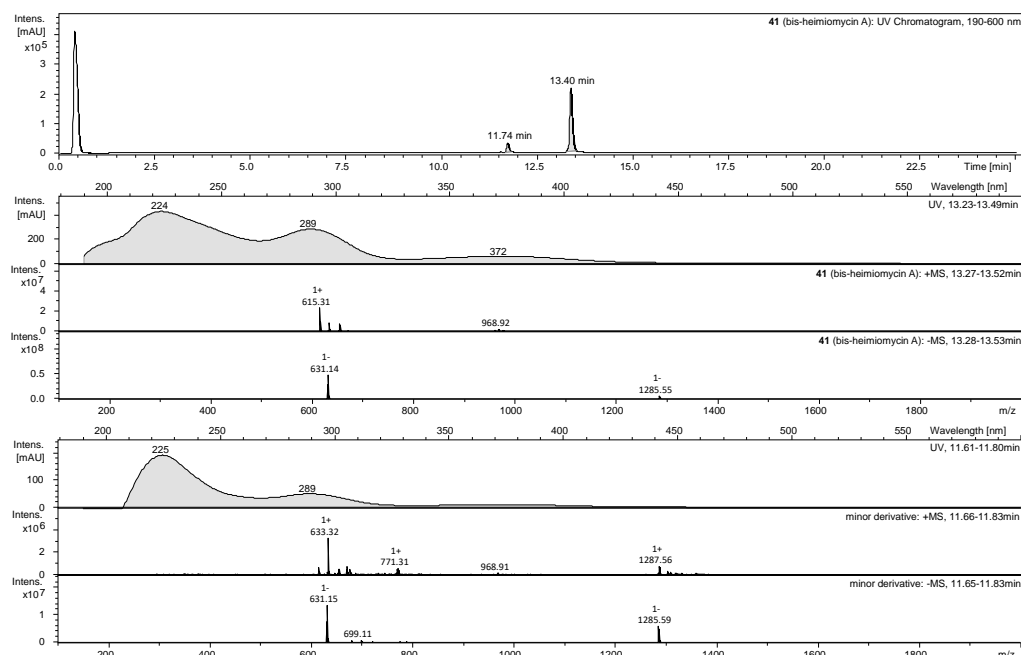


Figure 23. HPLC-UV/vis chromatogram at 190-600 nm, DAD, and ESI-MS (+/-) traces of compound **41**.

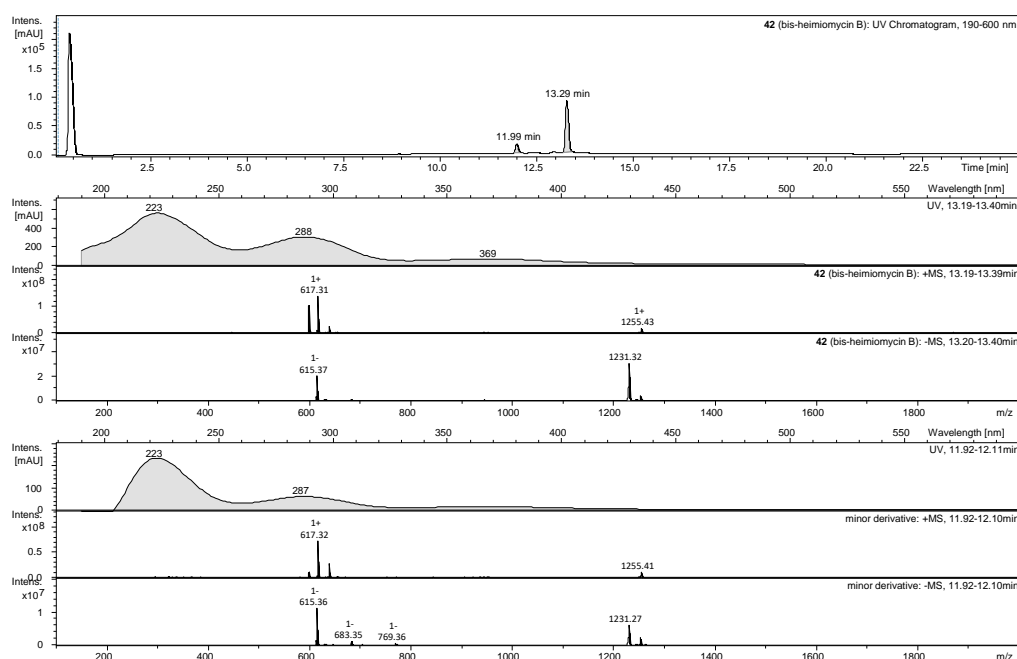


Figure 24. HPLC-UV/vis chromatogram at 190-600 nm, DAD, and ESI-MS (+/-) traces of compound **42**.

Compounds **41–46** were identified as having a *para*-quinone substructure by comparing their UV spectra and ^{13}C data with structurally similar *para*- and *ortho*-quinones previously reported in the literature (Berger and Rieker 1974). Notably, they exhibited absorption maxima at lower wavelengths (strongest intensity at $\lambda_{\text{max}} = 240\text{--}300$ nm and medium intensity at $\lambda_{\text{max}} = 285\text{--}440$ nm), characteristic of *para*-quinones, while lacking the absorption maximum at $500\text{--}580$ nm associated with *ortho*-quinones. However, UV spectra of **41b** and **44** showed slight deviations from the other compounds. In aiding the structural identification of the *para*-

quinone, the IR spectra of compounds **41b** and **44** (Figures 25 and 26) were measured and compared with those of similar quinones described in the literature, as *ortho*-quinones typically lack a distinctive and well-separated carbonyl band around 1680–1700 cm^{-1} (Berger and Rieker 1974).

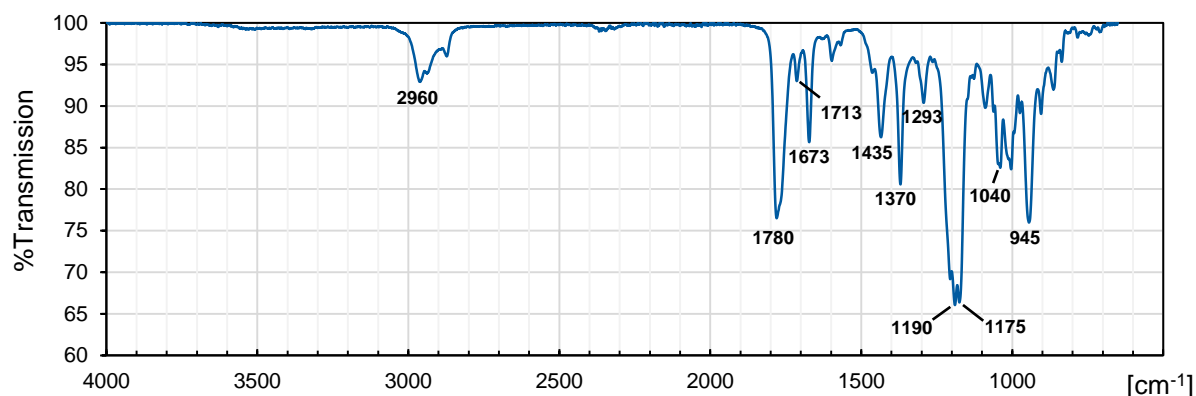


Figure 25. IR spectrum (ATR) of compound **41b** from 4000 to 650 cm^{-1} .

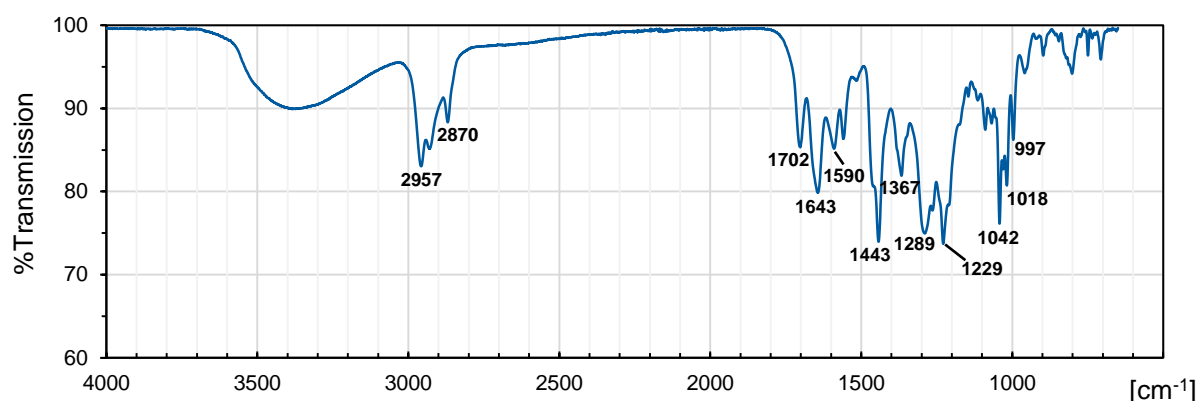


Figure 26. IR spectrum (ATR) of compound **44** from 4000 to 650 cm^{-1} .

Compounds **41–46** may experience hindered rotation around the C-3'/C-7 and C-6'/C-7'' bonds. While bis-heimiomycin A (**41**) and heimiomycins D and E (**45** and **46**) are prone to tautomerism within the *p*-benzoquinone substructure, preventing atropisomerism, compounds **42–44** did not exhibit any ECD data effects indicative of atropisomers. The rapid conversion of potential atropisomers could be attributed to the low rotational barriers of the C-7/C-3' and C-6'/C-7'' bonds. Bott et al. (1980) determined an effective radius of only 1.53 pm and a rotational barrier of 27.1 kJ/mol for the hydroxy group, suggesting that the keto and hydroxy substituents are small enough to permit rotation of the C-7/C-3' and C-6'/C-7'' bonds.

The chemical diversity of the heimiomycins may arise from the combination of calamene-type sesquiterpenoid precursors with various oxidized constituents. For compounds **41–44**, the resultant intermediate potentially undergoes another coupling reaction with a second

calamene-type sesquiterpenoid precursor. These processes could follow either a radical mechanism, reminiscent of the biosynthesis of the bibenzoquinone oosporein (Feng et al. 2015), or an electrophilic aromatic substitution mechanism. Both pathways are predicted to preserve the configurations of carbon centers C-2 and C-5 without alteration. However, the linkage of two sesquiterpenoids via a *p*-benzoquinone is an unusual characteristic in natural products (Zhao et al. 2020). To date, only a handful of similar compounds, such as popolohuanones F–H and nakijiquinone E (Takahashi et al. 2009; Utkina et al. 2010; Li et al. 2018), have been documented in literature.

Surprisingly a metabolic shift was observed after changing the cultivation conditions from solid to liquid media, resulting in the isolation of the new heimiocalamene A (**47**) from MOF cultures and heimiocalamene B (**48**) together with novel heimionones A–E (**49–53**) from YM 6.3 cultures (Figure 27).

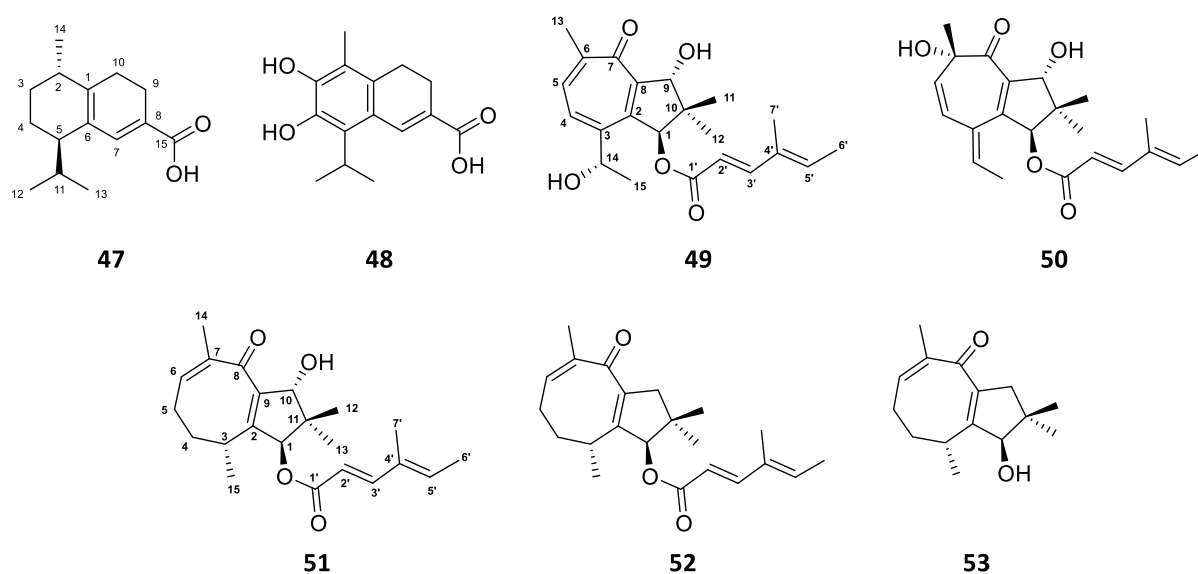


Figure 27. Chemical structures of compounds isolated from liquid MOF and YM 6.3 cultures of *Heimiomyces* sp. **47–48**: heimiocalamene A and B; **49–53**: heimionones A–E.

To determine the absolute configuration of compounds **49–53**, Mosher's method was applied to **49**, **51** and **53** by derivatization to the corresponding *S*- and *R*-MTPA esters at position C-10. Analyses of the $\Delta\delta^{SR}$ chemical shift pattern, as depicted in Figure 28, revealed an *R*-configuration at C-10, enabling the identification of the absolute configuration of the other stereo centers by evaluation of the ROESY NMR spectra. Due to structural similarity and a common biological origin, the results were applied to compounds **50** and **52** as well.

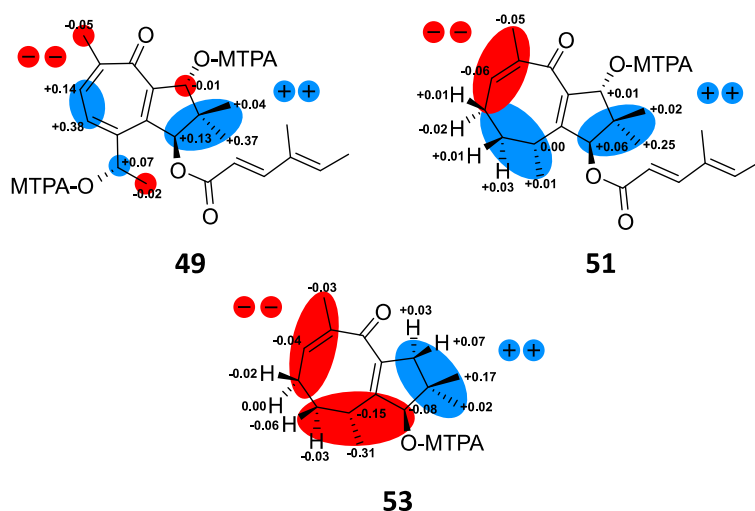


Figure 28. The $\Delta\delta^{SR}$ values derived from the (S)/(R)- MTPA esters obtained from heimionone A (**49**), heimionone C (**51**) and heimionone E (**53**) to determine the absolute configurations (Pfütze et al. 2023b)

While the bicyclo [5.3.0] decane scaffold found in **49** and **50** is present in various sesquiterpenoid types, such as daucane, isodaucane, aromadendrane, lactarane, africane, gualane, nor-guaiane, and pseudoguaiane, the methyl pattern in **49** and **50**, featuring germinal demethylation of C-10, sets them apart (Foley and Maguire 2010). Consequently, the carbon backbone of **49** and **50** introduces a novel scaffold. However, similar structures like nardoguaianone E-I have been previously documented, isolated from *Nardostachys chinensis* (Takaya et al. 2000). In contrast, compounds **51–53** were classified as asteriscanes due to their distinctive four methyl groups on the five-eight-membered ring system (Qin et al. 2019). Notably, asteriscane-type sesquiterpenoids have also been discovered in the soft coral *Sinularia capillosa* (Chen et al. 2013).

In the end, only three known compounds, hispidin (**54**), hypholomin B (**55**), and heimiomycin B (**57**), were found in both liquid and solid media (Figure 29) (Edwards et al. 1961; Fiasson et al. 1977; Cheng et al. 2020). Additionally, the previously described heimiomycin A (**56**) was observed only from liquid cultures of *Heimiomyces* sp. (Figure 29) (Cheng et al. 2020).

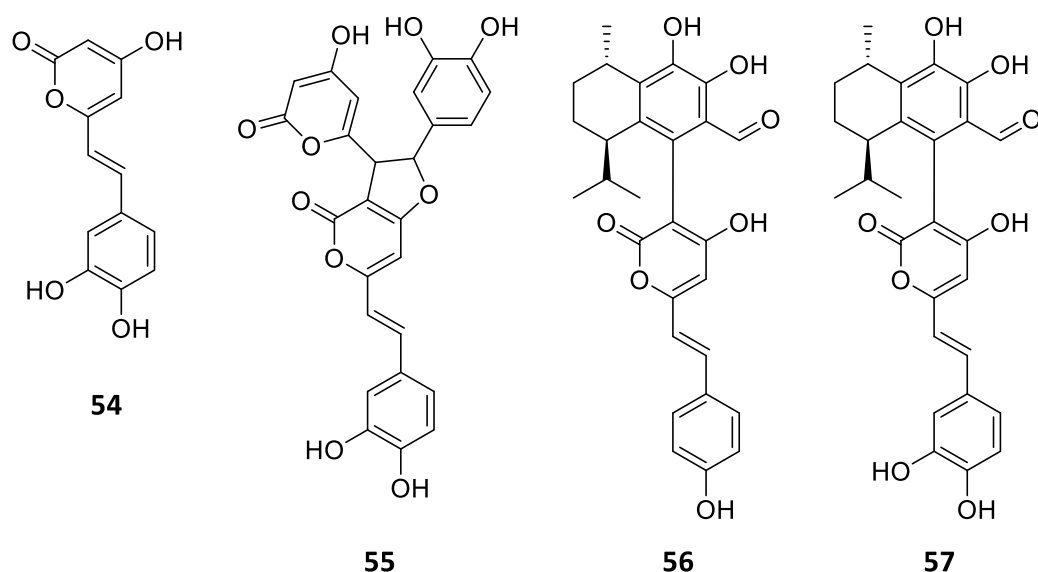


Figure 29. Known compounds isolated from *Heimiomyces* sp. after liquid and solid cultivation. **54**: hispidin; **55**: hypholomin B; **56–57**: heimiomycins A–B.

The altered secondary metabolite profile of *Heimiomyces* sp., resulting from the shift from solid to liquid media, highlights its adaptability. Alongside the compounds previously described by Cheng et al. (2020) from liquid cultures of the same species (Figure 5), this strain has already demonstrated considerable chemical diversity. Moreover, the presence of additional, yet unidentified minor peaks detected in the UV/Vis and MS spectra of its extracts suggests the possibility of discovering further novel secondary metabolites. By inducing larger-scale production through further adjustments in cultivation conditions, similar to those that prompted the initial changes, the potential for uncovering even more intriguing compounds is heightened.

3.2.2. Biological evaluation of secondary metabolites produced by *Heimiomyces* sp.

The antimicrobial activities of all isolated compounds were assessed using a serial dilution assay against both Gram-positive and Gram-negative bacteria, as well as fungal strains; however, most exhibited little to no activity. Additionally, their cytotoxicity was evaluated against KB3.1 and L929 cell lines, with similar results. Heimiomycin D (**45**) demonstrated the strongest cytotoxic effects, with an IC_{50} of 6.3 μ M, against KB3.1. Subsequent testing against other cell lines, including MCF-7, SKOV-3, and A431, revealed significant effects. The complete data sets of MIC and IC_{50} values can be found in paper II and III. Considering the reported diverse biological activities of quinone derivatives, attributed to their reactivity towards nucleophilic attacks and electron reductions, compounds **41–46** emerge as promising

candidates for further testing across various targets, including antiviral or antioxidant studies (El-Najjar et al. 2011; Zhang et al. 2021).

3.3. Drimane-type sesquiterpenoids from *Perenniporia centrali-africana* (MUCL 56028)

3.3.1. Structures of known and new drimane-type sesquiterpenoids isolated from *P. centrali-africana*

The extracts obtained from liquid cultures of *P. centrali-africana* (MUCL 56028) underwent chromatographic purification and resulted in the discovery of three new compounds, which share similarities with the pereniporin core structure previously documented by Kwon et al. (2018). Alongside the new drimane-type sesquiterpenoids **58–60** (Figure 30), known derivatives **61–66** (Figure 31) were isolated and identified (Kida et al. 1986; Clarkson Eliya V; Hansen, Steen Honoré; Smith, Peter J; Jaroszewski, Jerzy W 2007; Madikane et al. 2007; He et al. 2015; Kwon et al. 2018).

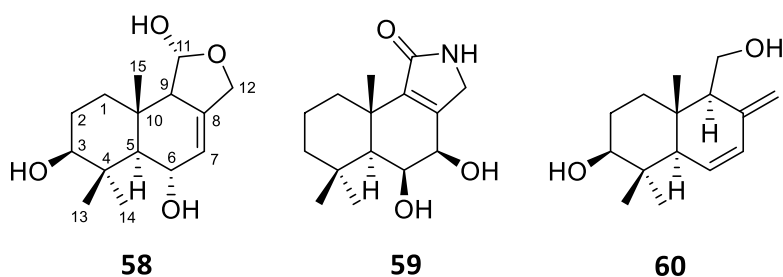


Figure 30. New drimane-type sesquiterpenoids isolated from cultures of *P. centrali-africana*. **58**: 3β-hydroxy-9-dehydroxy-pereniporin A; **59**: 6,7-dihydroxy-12-deoxy-dysidealactam; **60**: 6,7-dehydro-isodrimenediol.

Furthermore, previously reported cryptoporic acids B, H, and I (**67–69**, Figure 31) were exclusively isolated from extracts of the rice standing cultures (Hashimoto et al. 1987; Hirotsu et al. 1991).

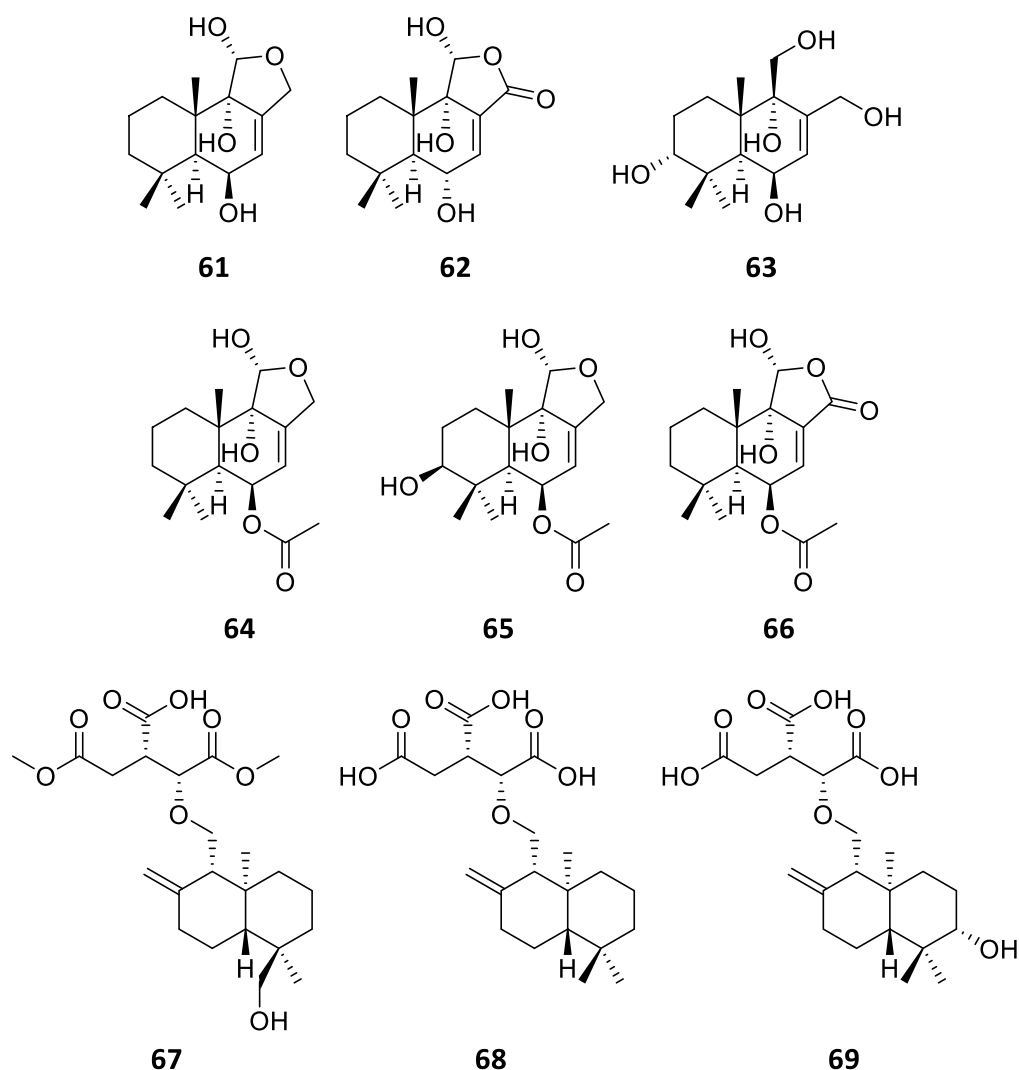


Figure 31. Known drimane-type sesquiterpenoids isolated from cultures of *P. centrali-africana*. **61**: pereniporin A; **62**: 6 α ,9 α ,11 α -trihydroxycinnamolide; **63**: sulphureuine H; **64**: 6-O-acetylpereniporin A; **65**: 3 β -hydroxy-6-O-acetylpereniporin A; **66**: 11 α -hydroxycinnamosmolide; **67–69**: cryptoporic acids B, H and I.

3.3.2. Biological evaluation of secondary metabolites produced by *P. centrali-africana*

Compounds **58**, **61**, **62**, **64** and **65** underwent antimicrobial activity assessment through serial dilution assays against various yeasts, filamentous fungi, and bacteria; however, no antimicrobial effects were observed. Additionally, their cytotoxicity was evaluated, revealing that only compound **64** demonstrated activity against all tested cell lines. Compound **61** yielded negative results in this assay, suggesting that the 6-O-acetylation induces cytotoxicity. Interestingly, this effect was not observed for compound **65**, which features hydroxylation at C-3, indicating a potentially opposing impact on cytotoxicity. The complete data sets of MIC and IC₅₀ values can be found in paper I.

4. Conclusion and Outlook

The emergence of new infectious diseases and the decline in antibiotic discovery underscore the urgent need for novel therapeutics. Fungi offer a promising avenue for the development of bioactive compounds, but challenges in fungal cultivation and understanding of fungal secondary metabolism persist. Consequently, integrated approaches are required to unlock their full potential and address global health and environmental concerns. In particular, Basidiomycota, with their biodiversity and diverse secondary metabolite profiles, offer a rich resource for the discovery of novel bioactive compounds that hold promise in addressing these challenges (Sandargo et al. 2019).

With over 70 previously documented melleolide-type monomers, *Armillaria* has emerged as a prolific genus within the Basidiomycota (Dörfer et al. 2019). Investigations into the secondary metabolism of *A. ostoyae* (DSM 115711) further expanded its chemical diversity after the isolation of the novel dimeric (**1–3**) and fatty acid side chain-carrying (**4–6**) sesquiterpene aryl esters. Prior to this study, the dimerization of two melleolide-type meroterpenoids or the esterification of a linoleic acid side chain had not been documented (Dörfer et al. 2019). Combined with the discovery of the 11 new (**7–17**) and 21 previously known (**18–38**) derivatives, these compounds collectively constitute nearly half of all known melleolide-type meroterpenoids identified to date. Metabolomics analyses unveiled an even greater diversity within this compound class, identifying a total of 22 molecular families with 277 features, significantly exceeding the range of known sesquiterpene aryl ester derivatives. This includes the presence of a large number of yet unidentified melleolide-type dimers as suggested by the MS/MS analysis. Consequently, these results indicate that the potential of this substance class has not yet been exhausted and more derivatives are waiting to be discovered. For instance, this can be achieved by adapting the cultivation conditions, supported by approaches like the heatmap and principal component analysis, which enhance the understanding of the media-dependent production of different melleolide-type meroterpenoids.

Since the discovery of the first melleolide by Midland et al. (1982), numerous research groups studied their biological activities over the years (Dörfer et al. 2019). A common challenge associated with these investigations is the lack of a comprehensive examination, as experiments were conducted using different test organisms and laboratory conditions. This

complicates the comparison of data and hinders the derivation of potential SARs. To address this, thirty-five melleolide-type meroterpenoids were simultaneously assessed for their biological properties in antimicrobial and cytotoxicity assays under controlled laboratory conditions, aiming to explore their SARs by the employment of cheminformatic methodologies. As a result, some previous statements were disproved, while others were confirmed. For instance, it was suggested that hydroxylations at positions C-4, C-10, and C-13 enhance the inhibition of bacterial growth, particularly against Gram-positive bacteria (Dörfer et al. 2019). However, testing compounds against various bacterial strains revealed unexpected outcomes, with certain compounds exhibiting high antibacterial activity despite lacking specific hydroxylation patterns traditionally associated with efficacy. Notably, the observed lack of inhibition against Gram-negative bacteria reaffirms the predominance of this compound class's activity against Gram-positive strains, while further analyses failed to identify specific structural features responsible for antibacterial effects. Furthermore, previous research highlighted the importance of the $\Delta^{2,4}$ double bond in the protoilludene moiety for antifungal activity (Bohnert et al. 2014). In contrast to this, our data obtained from evaluations of antifungal activities against *S. pombe*, *W. anomalus*, *M. hiemalis*, and *R. glutinis* showed no significant difference in activity regardless of the presence or absence of this double bond, suggesting that it is not universally essential for inhibiting fungal growth.

Regarding cytotoxicity, the presence of an aldehyde at C-1 has been identified as crucial for heightened cytotoxicity (Bohnert et al. 2011; Bohnert et al. 2014). We confirmed this assumption by hierarchical clustering based on the obtained IC₅₀ values from tests against several cell lines, as compounds showing significant cytotoxicity predominantly feature an aldehyde at C-1. However, our cheminformatics data also showed that a number of other chemical modifications can interact and influence cytotoxicity, leaving some questions unanswered. One example of this is the hydroxylation at C-10 in combination with chlorine substitution in the orsellinic acid moiety, whose presence or absence can influence the bioactivity of these compounds. Nevertheless, one of the clearest associations between chemical structure and cytotoxicity arises from the absence of activity observed in melleolide-type meroterpenoids with hydroxylations at position C-13 and C-10. As the cytotoxicity of many antimicrobial sesquiterpene aryl esters limits their potential to become a drugs, this finding could help to address this limitation.

Our comprehensive study on this unique class of fungal meroterpenoids is the first of its kind, offering insights into their structural diversity and providing a methodology to integrate and analyze extensive chemical and biological data. Future research should expand this methodology to assess additional species within the genus to gain a broader understanding of metabolite production and facilitate targeted searches for bioactive melleolide-type meroterpenoids. Additionally, the isolation and testing of further derivatives supported by cheminformatics approaches could help unravel the SARs of these metabolites, aiding medicinal chemistry endeavors. Furthermore, untargeted metabolomics may shed light on the ecological role of sesquiterpene aryl esters in nature and contribute to chemotaxonomic studies of the genus *Armillaria*.

Interestingly, we isolated four protoilludene-type sesquiterpene aryl esters from submerged cultures of *G. necrorhiza* (CBS 138623), including a new derivative (**39**), along with three known congeners (**28**, **34** and **40**). Our discovery marks the first instance of isolating members of this compound class from a genus other than *Armillaria*, not only reinforcing the close relationship between *Armillaria* and *Guyanagaster*, but also suggesting the potential for uncovering more novel derivatives. Further investigations on their secondary metabolism could involve a change of the cultivation conditions or the exploration of different specimens.

As stated by Sandargo et al. (2019), the secondary metabolism of many genera and species of the Basidiomycota remains unexplored, particularly in species endemic in tropical regions, likely due to limitations in mycology capacities. For this reason, we also focused our work on the largely untapped genus *Heimiomyces*. Fermentation of *Heimiomyces* sp. (MUCL 56078), collected from Mount Elgon National Reserve in Kenya, resulted in the discovery of novel meroterpenoids (**41–46**) from solid rice cultures and new calamene-type sesquiterpenoids, along with the uncommon bicyclo [5.3.0] decanes and [6.3.0] undecanes (**47–53**) from liquid cultures. The metabolic switch not only demonstrates the generally diverse secondary metabolism of this strain but also underscores the significant role of cultivation conditions in exploring its potential. Particularly noteworthy is the large number of unidentified minor peaks detected in the UV/Vis and MS spectra of extracts derived from *Heimiomyces* sp., indicating the need for further investigations into its secondary metabolism, especially through cultivation in various media types. In contrast to our investigations on the melleolide-type meroterpenoids, the compounds obtained from *Heimiomyces* sp. proved to be largely

inactive in our bioactivity screening and therefore do not show potential as drug candidates at this time. However, due to their chemical properties, compounds with quinone substructures have been shown to exhibit diverse biological activities, such as antioxidant, antiviral and anti-Alzheimer effects (El-Najjar et al. 2011; Zhang et al. 2021). For this reason, **41–46** that were tested negative in the antimicrobial and cytotoxicity assays should be reconsidered for other targets in further investigations.

Another tropical Basidiomycete from the Mount Elgon National Reserve that became the focus of our research is *P. centrali-africana* (MUCL 56028). Investigations into its secondary metabolism led to the discovery of three new drimane-type sesquiterpenoids (**58–60**), further enriching the large number of known derivatives from this compound class (Huang and Valiante 2022). Although various reports document the antimicrobial and cytotoxic activities of drimane-type sesquiterpenoids (Jansen and de Groot 2004; Du et al. 2022), we did not observe these effects for the substances isolated in this study. Nonetheless, certain members of this compound class have exhibited phytotoxic, antiviral, anti-inflammatory, or insecticidal activities (Jansen and de Groot 2004; Du et al. 2022). Therefore, compounds **58–69** should also be considered for further testing against different targets.

In summary, this thesis undertook a comprehensive exploration of fungal secondary metabolites from four Basidiomycota strains. Through systematic fermentation, extraction, purification, and structural elucidation processes, numerous novel compounds were isolated and characterized, shedding light on the vast chemical diversity of fungal secondary metabolism. By assessing the antimicrobial and cytotoxic activities of these compounds, this research not only contributes to the pool of potential drug leads but also unveils valuable insights into structure-activity relationships, crucial for understanding their modes of action. This knowledge represents a significant step towards the development of new therapeutics to combat drug-resistant pathogens and address the challenges posed by emerging infectious diseases. Furthermore, the emphasis on metabolomics investigations provides deeper insights into fungal secondary metabolism, paving the way for uncovering novel bioactive compounds and unlocking the full potential of fungal natural products. Moreover, this contributes to ensuring that fungi will continue to be used as a sustainable source for the production of bioactive secondary metabolites. In conclusion, this work highlights the important role of fungi as prolific producers of novel, chemically diverse, and bioactive natural products. Additionally,

the methods described herein can be transferred to other organisms and contribute to the advancement of natural product and drug discovery.

5. References

- Abraham EP, Newton GG (1961) The structure of cephalosporin C. *Biochemical Journal* 79:377–393.
- Abraham W-R, Hesse C (2003) Isotope fractionations in the biosynthesis of cell components by different fungi: a basis for environmental carbon flux studies. *FEMS Microbiology Ecology* 46:121–128.
- Alberts AW, Chen J, Kuron G, Hunt V, Huff J, Hoffman C, Rothrock J, Lopez M, Joshua H, Harris E, Patchett A, Monaghan R, Currie S, Stapley E, Albers-Schonberg G, Hensens O, Hirshfield J, Hoogsteen K, Liesch J, Springer J (1980) Mevinolin: a highly potent competitive inhibitor of hydroxymethylglutaryl-coenzyme A reductase and a cholesterol-lowering agent. *Proceedings of the National Academy of Sciences of the United States of America* 77:3957–3961.
- Anchel M, Hervey A, Robbins WJ (1950) Antibiotic substances from Basidiomycetes. VII. *Clitocybe illudens*. *Proceedings of the National Academy of Sciences of the United States of America* 36:300–305.
- Antimicrobial Resistance Collaborators (2022) Global burden of bacterial antimicrobial resistance in 2019: a systematic analysis. *Lancet (London, England)* 399:629–655.
- Aris P, Wei Y, Mohamadzadeh M, Xia X (2022) Griseofulvin: An updated overview of old and current knowledge. *Molecules* 27(20):7034.
- Arnone A, Cardillo R, Nasini G, Meille SV (1988) Secondary mould metabolites. Part 19. Structure elucidation and absolute configuration of melledonals B and C, novel antibacterial sesquiterpenoids from *Armillaria mellea*. X-Ray molecular structure of melledonal C. *Journal of the Chemical Society, Perkin Transactions 1* 503–510.
- Baumgartner K, Coetzee MPA, Hoffmeister D (2011) Secrets of the subterranean pathosystem of *Armillaria*. *Molecular Plant Pathology* 12:515–534.
- Bentley R (2000) Mycophenolic acid: A one hundred year odyssey from antibiotic to immunosuppressant. *Chemical Reviews* 100:3801–3826.
- Benz F, Knüsel F, Nüesch J, Treichler H, Voser W, Nyfeler R, Keller-Schierlein W (1974) Stoffwechselprodukte von Mikroorganismen 143. Mitteilung. Echinocandin B, ein neuartiges Polypeptid-Antibioticum aus *Aspergillus nidulans* var. *echinulatus*: Isolierung und Bausteine. *Helvetica Chimica Acta* 57:2459–2477.
- Berger S, Rieker A (1974) Identification and determination of quinones. In: *Quinonoid Compounds. PATAI'S Chemistry of Functional Groups* pp 163–229.
- Bills GF and Gloer JB (2016) Biologically active secondary metabolites from the fungi. *Microbiology Spectrum* 4:1087–1119.
- Bohnert M, Miethbauer S, Dahse H-M, Ziemen J, Nett M, Hoffmeister D (2011) In vitro cytotoxicity of melleolide antibiotics: structural and mechanistic aspects. *Bioorganic & Medicinal Chemistry Letters* 21:2003–2006.

- Bohnert M, Nützmann H-W, Schroeckh V, Horn F, Dahse H-M, Brakhage AA, Hoffmeister D (2014a) Cytotoxic and antifungal activities of melleolide antibiotics follow dissimilar structure-activity relationships. *Phytochemistry* 105:101–108.
- Bohnert M, Scherer O, Wiechmann K, König S, Dahse H-M, Hoffmeister D, Werz O (2014b) Melleolides induce rapid cell death in human primary monocytes and cancer cells. *Bioorganic & Medicinal Chemistry* 22:3856–3861.
- Borel JF, Feurer C, Gubler HU, Stähelin H (1976) Biological effects of cyclosporin A: a new antilymphocytic agent. *Agents Actions* 6:468–475.
- Bott G, Field LD, Sternhell S (1980) Steric effects. A study of a rationally designed system. *Journal of the American Chemical Society* 102:5618–5626.
- Brakhage AA, Schroeckh V (2011) Fungal secondary metabolites - strategies to activate silent gene clusters. *Fungal Genetics and Biology* 48:15–22.
- Cadelis MM, Copp BR, Wiles S (2020) A review of fungal protoilludane sesquiterpenoid natural products. *Antibiotics* 9(12):928.
- Cedeño-Sánchez M, Charria-Girón E, Lambert C, Luangsa-ard JJ, Decock C, Franke R, Brönstrup M, Stadler M (2023) Segregation of the genus *Parahypoxylon* (Hypoxylaceae, Xylariales) from *Hypoxylon* by a polyphasic taxonomic approach. *MycKeys* 95:131–162
- Charria-Girón E, Marin-Felix Y, Beutling U, Franke R, Brönstrup M, Vasco-Palacios AM, Caicedo NH, Surup F (2023a) Metabolomics insights into the polyketide-lactones produced by *Diaporthe caliensis* sp. nov., an endophyte of the medicinal plant *Otoba gracilipes*. *Microbiology Spectrum* 11:e0274323. (<https://doi.org/10.1128/spectrum.02743-23>)
- Charria-Girón E, Stchigel AM, Čmoková A, Kolařík M, Surup F, Marin-Felix Y (2023b) *Amesia hispanica* sp. nov., producer of the antifungal class of antibiotics dactylfungins. *Journal of Fungi* 9(4):463.
- Chen D, Chen W, Liu D, van Ofwegen L, Proksch P, Lin W (2013) Asteriscane-type sesquiterpenoids from the soft coral *Sinularia capillosa*. *Journal of Natural Products* 76:1753–1763.
- Cheng T, Chepkirui C, Decock C, Matasyoh JC, Stadler M (2020) Heimiomycins A–C and calamenens from the African Basidiomycete *Heimiomyces* sp. *Journal of Natural Products* 83:2501–2507.
- Clarkson Eliya V; Hansen, Steen Honoré; Smith, Peter J; Jaroszewski, Jerzy W CM (2007) HPLC-SPE-NMR characterization of sesquiterpenes in an antimycobacterial fraction from *Warburgia salutaris*. *Planta Medica* 73:578–584.
- Coetzee MPA, Wingfield BD, Wingfield MJ (2018) *Armillaria* root-rot pathogens: species boundaries and global distribution. *Pathogens* 7(4):83.
- Davies J (2006) Where have all the antibiotics gone? *Canadian Journal of Infectious Diseases and Medical Microbiology* 17:287–290.
- Desborough MJR, Keeling DM (2017) The aspirin story - from willow to wonder drug. *British Journal of Haematology* 177:674–683.

- Donnelly DMX, Abe F, Coveney D, Fukuda N, O'Reilly J, Polonsky J, Prangé T (1985) Antibacterial sesquiterpene aryl esters from *Armillaria mellea*. *Journal of Natural Products* 48:10–16.
- Dörfer M, Gressler M, Hoffmeister D (2019a) Diversity and bioactivity of *Armillaria* sesquiterpene aryl ester natural products. *Mycological Progress* 18:1027–1037.
- Dörfer M, Heine D, König S, Gore S, Werz O, Hertweck C, Gressler M, Hoffmeister D (2019b) Melleolides impact fungal translation via elongation factor 2. *Organic and Biomolecular Chemistry* 17:4906–4916.
- Du W, Yang Q, Xu H, Dong L (2022) Drimane-type sesquiterpenoids from fungi. *Chinese Journal of Natural Medicines* 20:737–748.
- Duncan SJ, Gruschow S, Williams DH, McNicholas C, Purewal R, Hajek M, Gerlitz M, Martin S, Wrigley SK, Moore M (2001) Isolation and structure elucidation of chlorofusin, a novel p53-MDM2 antagonist from a *Fusarium* sp. *Journal of the American Chemical Society* 123(49):554–560.
- Edwards RL, Lewis DG, Wilson D V (1961) 983. Constituents of the higher fungi. Part I. Hispidin, a new 4-hydroxy-6-styryl-2-pyrone from *Polyporus hispidus* (Bull.) Fr. *Journal of the Chemical Society* 4995–5002.
- El-Najjar N, Gali-Muhtasib H, Ketola RA, Vuorela P, Urtti A, Vuorela H (2011) The chemical and biological activities of quinones: overview and implications in analytical detection. *Phytochemistry Reviews* 10(3):353.
- Engels B, Heinig U, McElroy C, Meusinger R, Grothe T, Stadler M, Jennewein S (2021) Isolation of a gene cluster from *Armillaria gallica* for the synthesis of armillyl orsellinates-type sesquiterpenoids. *Applied Microbiology and Biotechnology* 105:211–224.
- Feng P, Shang Y, Cen K, Wang C (2015) Fungal biosynthesis of the bibenzoquinone oosporein to evade insect immunity. *Proceedings of the National Academy of Sciences of the United States of America* 112:11365–11370.
- Feng Y, Wang L, Niu S, Li L, Si Y, Liu X, Che Y (2012) Naphthalenones from a *Perenniporia* sp. inhabiting the larva of a phytophagous weevil, *Euops chinesis*. *Journal of Natural Products* 75:1339–1345.
- Ferguson BA, Dreisbach TA, Parks CG, Filip GM, Schmitt CL (2003) Coarse-scale population structure of pathogenic *Armillaria* species in a mixed-conifer forest in the Blue Mountains of northeast Oregon. *Canadian Journal of Forest Research* 33:612–623.
- Fiasson J-L, Gluchoff-Fiasson K, Steglich W (1977) Über die Farb- und Fluoreszenzstoffe des Grünblättrigen Schwefelkopfes (*Hypholoma fasciculare*, Agaricales). *Chemische Berichte* 110:1047–1057.
- Fleming A (1929) On the antibacterial action of cultures of a *Penicillium*, with special reference to their use in the isolation of *B. influenzae*. *British Journal of Experimental Pathology* 10:226–236.
- Florey HW, Jennings MA, Gilliver K, Sanders AG (1946) Mycophenolic acid an antibiotic from *Penicillium brevicompactum* Dierckx. *Lancet* 247:46–49.

- Foley DA, Maguire AR (2010) Synthetic approaches to bicyclo[5.3.0]decane sesquiterpenes. *Tetrahedron* 66:1131–1175.
- Fukaya M, Nagamine S, Ozaki T, Liu Y, Ozeki M, Matsuyama T, Miyamoto K, Kawagishi H, Uchiyama M, Oikawa H, Minami A (2023) Total biosynthesis of melleolides from Basidiomycota fungi: Mechanistic analysis of the multi-functional GMC oxidase Mld7. *Angewandte Chemie International Edition* 62:e202308881 (<https://doi.org/10.1002/anie.202308881>).
- Gressler M, Löhr NA, Schäfer T, Lawrinowitz S, Seibold PS, Hoffmeister D (2021) Mind the mushroom: natural product biosynthetic genes and enzymes of Basidiomycota. *Natural Product Reports* 38:702–722.
- Guo H, Si J, Li Z-H, Feng T, Dong Z-J, Dai Y-C, Liu J-K (2013) Two new triterpenoids from the fungus *Perenniporia maackiae*. *Journal of Asian Natural Product Research* 15:253–257.
- Harms K, Surup F, Stadler M, Stchigel AM, Marin-Felix Y (2021) Morinagadepsin, a depsipeptide from the fungus *Morinagamyces vermicularis* gen. et comb. nov. *Microorganisms* 9(6):1191.
- Hashimoto T, Tori M, Mizuno Y, Asakawa Y (1987) Cryptoporic acids A and B, novel bitter drimane sesquiterpenoid ethers of isocitric acid, from the fungus *Cryptoporus volvatus*. *Tetrahedron Letters* 28:6303–6304.
- He J-B, Tao J, Miao X-S, Bu W, Zhang S, Dong Z-J, Li Z-H, Feng T, Liu J-K (2015) Seven new drimane-type sesquiterpenoids from cultures of fungus *Laetiporus sulphureus*. *Fitoterapia* 102:1–6.
- Henkel TW, Smith ME, Aime MC (2010) *Guyanagaster*, a new wood-decaying sequestrate fungal genus related to *Armillaria* (Physalacriaceae, Agaricales, Basidiomycota). *American Journal of Botany* 97:1474–1484.
- Hirotsu M, Furuya T, Shiro M (1991) Cryptoporic acids H and I, drimane sesquiterpenes from *Ganoderma neo-japonicum* and *Cryptoporus volvatus*. *Phytochemistry* 30:1555–1559.
- Hirotsu M, Ino C, Furuya T, Shiro M (1984) Perenniporiol derivatives, six triterpenoids from the cultured mycelia of *Perenniporia ochroleuca*. *Phytochemistry* 23(5):1129–1134.
- Houbraken J, Frisvad JC, Samson RA (2011) Fleming's penicillin producing strain is not *Penicillium chrysogenum* but *P. rubens*. *IMA Fungus* 2:87–95.
- Hoye TR, Jeffrey CS, Shao F (2007) Mosher ester analysis for the determination of absolute configuration of stereogenic (chiral) carbinol carbons. *Nature Protocols* 2:2451–2458.
- Huang Y, Valiante V (2022) Chemical diversity and biosynthesis of drimane-type sesquiterpenes in the fungal kingdom. *Chembiochem* 23(17):e202200173.
- Ino C, Hirotsu M, Furuya T (1984) Two perenniporiol derivatives, lanostane-type triterpenoids, from the cultured mycelia of *Perenniporia ochroleuca*. *Phytochemistry* 23:2885–2888.
- Jansen BJM, de Groot A (2004) Occurrence, biological activity and synthesis of drimane sesquiterpenoids. *Natural Product Reports* 21:449–477.

- Kavanagh F (1947) Chemical determination of pleurotin, an antibacterial substance from *Pleurotus griseus*. Archives of Biochemistry and Biophysics 15:95–98.
- Kavanagh F, Hervey A, Robbins WJ (1951) Antibiotic substances from Basidiomycetes: VIII. *Pleurotus multilus* (Fr.) sacc. and *Pleurotus passeckerianus* pilat. Proceedings of the National Academy of Sciences of the United States of America 37:570–574.
- Kedves O, Shahab D, Champramary S, Chen L, Indic B, Bóka B, Nagy VD, Vágvölgyi C, Kredics L, Sipos G (2021) Epidemiology, biotic interactions and biological control of Armillarioids in the northern hemisphere. Pathogens 10(1):76.
- Keller NP, Turner G, Bennett JW (2005) Fungal secondary metabolism - from biochemistry to genomics. Nature Reviews Microbiology 3:937–947.
- Kida T, Shibai H, Seto H (1986) Structure of new antibiotics, pereniporins A and B, from a basidiomycete. Journal of Antibiotics (Tokyo) 39(4):613–615.
- Kim J-Y, Woo E-E, Ha LS, Ki D-W, Lee I-K, Yun B-S (2019) Three new meroterpenoids from culture broth of *Perenniporia medulla-panis* and their antioxidant activities. Journal of Antibiotics (Tokyo) 72:625–628.
- Koch RA, Wilson AW, Séné O, Henkel TW, Aime MC (2017) Resolved phylogeny and biogeography of the root pathogen *Armillaria* and its gasteroid relative, *Guyanagaster*. BMC Evolutionary Biology 17(1):33.
- Koehn FE, Carter GT (2005) The evolving role of natural products in drug discovery. Nature Reviews Drug Discovery 4:206–220.
- Kwon J, Lee H, Seo YH, Yun J, Lee J, Kwon HC, Guo Y, Kang JS, Kim J-J, Lee D (2018) Cytotoxic drimane sesquiterpenoids isolated from *Perenniporia maackiae*. Journal of Natural Products 81:1444–1450.
- Li J, Wu W, Yang F, Liu L, Wang S-P, Jiao W-H, Xu S-H, Lin H-W (2018) Popolohuanones G - I, dimeric sesquiterpene quinones with IL-6 inhibitory activity from the marine sponge *Dactylospongia elegans*. Chemistry & Biodiversity 15(6):e1800078. (<https://doi.org/10.1002/cbdv.201800078>)
- Li Z, Wang Y, Jiang B, Li W, Zheng L, Yang X, Bao Y, Sun L, Huang Y, Li Y (2016) Structure, cytotoxic activity and mechanism of protoilludane sesquiterpene aryl esters from the mycelium of *Armillaria mellea*. Journal of Ethnopharmacology 184:119–127.
- Lima SL, Colombo AL, de Almeida Junior JN (2019) Fungal cell wall: Emerging antifungals and drug resistance. Frontiers in Microbiology 10:2573.
- Lin X, Kück U (2022) Cephalosporins as key lead generation beta-lactam antibiotics. Applied Microbiology and Biotechnology 106:8007–8020.
- Llor C, Bjerrum L (2014) Antimicrobial resistance: risk associated with antibiotic overuse and initiatives to reduce the problem. Therapeutic Advances in Drug Safety 5:229–241.

- Madikane VE, Bhakta S, Russell AJ, Campbell WE, Claridge TDW, Elisha BG, Davies SG, Smith P, Sim E (2007) Inhibition of mycobacterial arylamine N-acetyltransferase contributes to anti-mycobacterial activity of *Warburgia salutaris*. *Bioorganic & Medicinal Chemistry* 15:3579–3586.
- Midland SL, Izac RR, Wing RM, Zaki AI, Munnecke DE, Sims JJ (1982) Melleolide, a new antibiotic from *Armillaria mellea*. *Tetrahedron Letters* 23:2515–2518.
- Misiek M, Hoffmeister D (2012) Sesquiterpene aryl ester natural products in North American *Armillaria* species. *Mycological Progress* 11:7–15.
- Misiek M, Williams J, Schmich K, Hüttel W, Merfort I, Salomon CE, Aldrich CC, Hoffmeister D (2009) Structure and cytotoxicity of arnamial and related fungal sesquiterpene aryl esters. *Journal of Natural Products* 72:1888–1891.
- Momose I, Sekizawa R, Hosokawa N, Iinuma H, Matsui S, Nakamura H, Naganawa H, Hamada M, Takeuchi T (2000) Melleolides K, L and M, new melleolides from *Armillariella mellea*. *Journal of Antibiotics* (Tokyo) 53:137–143.
- Morens DM, Folkers GK, Fauci AS (2004) The challenge of emerging and re-emerging infectious diseases. *Nature* 430:242–249.
- Newman DJ, Cragg GM (2020) Natural products as sources of new drugs over the nearly four decades from 01/1981 to 09/2019. *Journal of Natural Products* 83:770–803.
- Newton GGF, Abraham EP (1955) Cephalosporin C, a new antibiotic containing sulphur and D- α -aminoadipic acid. *Nature* 175:548.
- Nothias L-F, Petras D, Schmid R, Dührkop K, Rainer J, Sarvepalli A, Protsyuk I, Ernst M, Tsugawa H, Fleischauer M, Aicheler F, Aksenov AA, Alka O, Allard P-M, Barsch A, Cachet X, Caraballo-Rodriguez AM, Da Silva RR, Dang T, Garg N, Gauglitz JM, Gurevich A, Isaac G, Jarmusch AK, Kameník Z, Kang K Bin, Kessler N, Koester I, Korf A, Le Gouellec A, Ludwig M, Martin H. C, McCall L-I, McSayles J, Meyer SW, Mohimani H, Morsy M, Moyne O, Neumann S, Neuweiger H, Nguyen NH, Nothias-Esposito M, Paolini J, Phelan V V, Pluskal T, Quinn RA, Rogers S, Shrestha B, Tripathi A, van der Hooft JJJ, Vargas F, Weldon KC, Witting M, Yang H, Zhang Z, Zubeil F, Kohlbacher O, Böcker S, Alexandrov T, Bandeira N, Wang M, Dorrestein PC (2020) Feature-based molecular networking in the GNPS analysis environment. *Nature Methods* 17:905–908.
- Novak R (2011) Are pleuromutilin antibiotics finally fit for human use? *Annals of the New York Academy of Sciences* 1241:71–81.
- Oxford AE, Raistrick H, Simonart P (1939) Studies in the biochemistry of micro-organisms: Griseofulvin, C(17)H(17)O(6)Cl, a metabolic product of *Penicillium griseo-fulvum* Dierckx. *Biochemical Journal* 33:240–248.
- Paukner S, Riedl R (2017) Pleuromutilins: potent drugs for resistant bugs-mode of action and resistance. *Cold Spring Harbor Perspectives in Medicine* 7(1):a027110 (<https://doi.org/10.1101/cshperspect.a027110>).
- Pfütze S, Charria-Girón E, Schulzke E, Toshe R, Khonsanit A, Franke R, Surup F, Brönstrup M, Stadler M (2024) Depicting the chemical diversity of bioactive meroterpenoids produced by the largest

- organism on earth. *Angewandte Chemie International Edition* 63:e202318505 (<https://doi.org/https://doi.org/10.1002/anie.202318505>).
- Pfütze S, Khamsim A, Surup F, Decock C, Matasyoh JC, Stadler M (**2023a**) Calamene-type sesqui-, mero-, and bis-sesquiterpenoids from cultures of *Heimiomyces* sp., a Basidiomycete collected in Africa. *Journal of Natural Products* 86:390–397.
- Pfütze S, Khamsim A, Surup F, Decock C, Matasyoh JC, Stadler M (**2023b**) Heimionones A-E, new sesquiterpenoids produced by *Heimiomyces* sp., a Basidiomycete collected in Africa. *Molecules* 28(9):3723.
- Pfütze S, Nedder DL, Surup F, Stadler M (**2023c**) 5'-O-methyl-14-hydroxyarmillane, a new armillane-type sesquiterpene from cultures of *Guyanagaster necrorhiza*. *Mycological Progress* 22:70.
- Poulsen SM, Karlsson M, Johansson LB, Vester B (**2001**) The pleuromutilin drugs tiamulin and valnemulin bind to the RNA at the peptidyl transferase centre on the ribosome. *Molecular Microbiology* 41:1091–1099.
- Qin G-F, Liang H-B, Liu W-X, Zhu F, Li P-L, Li G-Q, Yao J-C (**2019**) Bicyclo [6.3.0] undecane sesquiterpenoids: Structures, biological activities, and syntheses. *Molecules* 24(21):3912.
- Ruttkies C, Schymanski EL, Wolf S, Hollender J, Neumann S (**2016**) MetFrag relaunched: incorporating strategies beyond *in silico* fragmentation. *Journal of Cheminformatics* 8:3.
- Sandargo B, Chepkirui C, Cheng T, Chaverra-Muñoz L, Thongbai B, Stadler M, Hüttel S (**2019**) Biological and chemical diversity go hand in hand: Basidiomycota as source of new pharmaceuticals and agrochemicals. *Biotechnology Advances* 37(6):107344.
- Sauter H, Steglich W, Anke T (**1999**) Strobilurins: Evolution of a new class of active substances. *Angewandte Chemie International Edition* 38:1328–1349.
- Schwartz BD, Matoušová E, White R, Banwell MG, Willis AC (**2013**) A chemoenzymatic total synthesis of the protoilludane aryl ester (+)-armillarivin. *Organic Letters* 15:1934–1937.
- Shannon P, Markiel A, Ozier O, Baliga NS, Wang JT, Ramage D, Amin N, Schwikowski B, Ideker T (**2003**) Cytoscape: a software environment for integrated models of biomolecular interaction networks. *Genome Research* 13:2498–2504.
- Smith ML, Bruhn JN, Anderson JB (**1992**) The fungus *Armillaria bulbosa* is among the largest and oldest living organisms. *Nature* 356:428–431.
- Stadler M, Hoffmeister D (**2015**) Fungal natural products - the mushroom perspective. *Frontiers in Microbiology* 6:127.
- Sterner O, Etzel W, Mayer A, Anke H (**1997**) Omphalotin, a new cyclic peptide with potent nematocidal activity from *Omphalotus olearius* II. Isolation and structure determination. *Natural Product Letters* 10:33–38.
- Summerbell RC, Gueidan C, Schroers H-J, de Hoog GS, Starink M, Rosete YA, Guarro J, Scott JA (**2011**) *Acremonium* phylogenetic overview and revision of *Gliomastix*, *Sarocladium*, and *Trichothecium*. *Studies in Mycology* 68:139–162.

- Takahashi Y, Kubota T, Kobayashi J (2009) Nakijiquinones E and F, new dimeric sesquiterpenoid quinones from marine sponge. *Bioorganic & Medicinal Chemistry* 17:2185–2188.
- Takaya Y, Akasaka M, Takeuji Y, Tanitsu M, Niwa M, Oshima Y (2000) Novel guaianoids, nardoguaianone E–I, from *Nardostachys chinensis* roots. *Tetrahedron* 56:7679–7683.
- Tanasova M, Sturla SJ (2012) Chemistry and biology of acylfulvenes: Sesquiterpene-derived antitumor agents. *Chemical Reviews* 112:3578–3610.
- Tobert JA (2003) Lovastatin and beyond: the history of the HMG-CoA reductase inhibitors. *Nature Reviews Drug Discovery* 2:517–526.
- Toth PP, Banach M (2019) Statins: Then and now. *Methodist DeBakey Cardiovascular Journal* 15:23–31.
- Utkina NK, Denisenko VA, Krasokhin VB (2010) Sesquiterpenoid aminoquinones from the marine sponge *Dysidea* sp. *Journal of Natural Products* 73:788–791.
- van Santen JA, Jacob G, Singh AL, Aniebok V, Balunas MJ, Bunsko D, Neto FC, Castaño-Espriu L, Chang C, Clark TN, Cleary Little JL, Delgadillo DA, Dorrestein PC, Duncan KR, Egan JM, Galey MM, Haeckl FPJ, Hua A, Hughes AH, Iskakova D, Khadilkar A, Lee J-H, Lee S, LeGrow N, Liu DY, Macho JM, McCaughey CS, Medema MH, Neupane RP, O'Donnell TJ, Paula JS, Sanchez LM, Shaikh AF, Soldatou S, Terlouw BR, Tran TA, Valentine M, van der Hooft JJ, Vo DA, Wang M, Wilson D, Zink KE, Linington RG (2019) The natural products atlas: An open access knowledge base for microbial natural products discovery. *ACS Central Science* 5:1824–1833.
- Ventola CL (2015) The antibiotic resistance crisis: part 1: causes and threats. *Pharmacy and Therapeutics* 40(4):277–283.
- von Nussbaum F, Brands M, Hinzen B, Weigand S, Häbich D (2006) Antibacterial natural products in medicinal chemistry - exodus or revival? *Angewandte Chemie International Edition* 45:5072–5129.
- Wang M, Carver JJ, Phelan V V, Sanchez LM, Garg N, Peng Y, Nguyen DD, Watrous J, Kapono CA, Luzzatto-Knaan T, Porto C, Bouslimani A, Melnik A V, Meehan MJ, Liu W-T, Crusemann M, Boudreau PD, Esquenazi E, Sandoval-Calderón M, Kersten RD, Pace LA, Quinn RA, Duncan KR, Hsu C-C, Floros DJ, Gavilan RG, Kleigrewe K, Northen T, Dutton RJ, Parrot D, Carlson EE, Aigle B, Michelsen CF, Jelsbak L, Sohlenkamp C, Pevzner P, Edlund A, McLean J, Piel J, Murphy BT, Gerwick L, Liaw C-C, Yang Y-L, Humpf H-U, Maansson M, Keyzers RA, Sims AC, Johnson AR, Sidebottom AM, Sedio BE, Klitgaard A, Larson CB, Boya P CA, Torres-Mendoza D, Gonzalez DJ, Silva DB, Marques LM, Demarque DP, Pociute E, O'Neill EC, Briand E, Helfrich EJM, Granatosky EA, Glukhov E, Ryffel F, Houson H, Mohimani H, Kharbush JJ, Zeng Y, Vorholt JA, Kurita KL, Charusanti P, McPhail KL, Nielsen KF, Vuong L, Elfeki M, Traxler MF, Engene N, Koyama N, Vining OB, Baric R, Silva RR, Mascuch SJ, Tomasi S, Jenkins S, Macherla V, Hoffman T, Agarwal V, Williams PG, Dai J, Neupane R, Gurr J, Rodríguez AMC, Lamsa A, Zhang C, Dorrestein K, Duggan BM, Almaliti J, Allard P-M, Phapale P, Nothias L-F, Alexandrov T, Litaudon M, Wolfender J-L, Kyle JE, Metz TO, Peryea T, Nguyen D-T, VanLeer D, Shinn P, Jadhav A, Müller R, Waters KM, Shi W, Liu X, Zhang L, Knight R, Jensen PR, Palsson BØ, Pogliano K, Linington RG, Gutiérrez M, Lopes NP, Gerwick WH, Moore BS, Dorrestein PC, Bandeira N (2016) Sharing and community curation of

- mass spectrometry data with Global Natural Products Social Molecular Networking. *Nature Biotechnology* 34:828–837.
- Wick J, Heine D, Lackner G, Misiek M, Tauber J, Jagusch H, Hertweck C, Hoffmeister D **(2016)** A fivefold parallelized biosynthetic process secures chlorination of *Armillaria mellea* (honey mushroom) toxins. *Applied and Environmental Microbiology* 82:1196–1204.
- World Health Organization (WHO) **(2014)** Antimicrobial resistance: global report on surveillance. <https://www.who.int/publications/i/item/9789241564748>
- Yang JS, Chen YW, Feng XZ, Yu DQ, Liang XT **(1984)** Chemical constituents of *Armillaria mellea* mycelium. I. Isolation and characterization of armillarin and armillaridin. *Planta Medica* 50:288–290.
- Yang JS, Su YL, Wang YL, Feng XZ, Yu DQ, Liang XT **(1991)** Two novel protoilludane norsesterpenoid esters, armillasin and armillatin, from *Armillaria mellea*. *Planta Medica* 57:478–480.
- Zhang L, Zhang G, Xu S, Song Y **(2021)** Recent advances of quinones as a privileged structure in drug discovery. *European Journal of Medicinal Chemistry* 223:113632.
- Zhao W-Y, Yan J-J, Liu T-T, Gao J, Huang H-L, Sun C-P, Huo X-K, Deng S, Zhang B-J, Ma X-C **(2020)** Natural sesquiterpenoid oligomers: A chemical perspective. *European Journal of Medicinal Chemistry* 203:112622.

6. Appendices: Publications of the Dissertation

Roman numerals within the text correspond to the following publications.

- I. Pathompong P†, **Pfütze S†**, Surup F, Boonpratuang T, Choeyklin R, Matasyoh JC, Decock C, Stadler M, Boonchird C (**2022**) Drimane-type sesquiterpenoids derived from the tropical Basidiomycetes *Perenniporia centrali-africana* and *Cerrena* sp. nov. *Molecules* 27(18):5968.
- II. **Pfütze S**, Khamsim A, Surup F, Decock C, Matasyoh JC, Stadler M (**2023**) Calamene-type sesqui-, mero-, and bis-sesquiterpenoids from cultures of *Heimiomyces* sp., a Basidiomycete collected in Africa. *Journal of Natural Products* 86(2):390–397.
- III. **Pfütze S**, Khamsim A, Surup F, Decock C, Matasyoh JC, Stadler M (**2023**) Heimionones A–E, new sesquiterpenoids produced by *Heimiomyces* sp., a Basidiomycete collected in Africa. *Molecules* 28(9):3723.
- IV. **Pfütze S**, Nedder DL, Surup F, Stadler M (**2023**) 5'-O-methyl-14-hydroxyarmillane, a new armillane-type sesquiterpene from cultures of *Guyanagaster necrorhiza*. *Mycological Progress* 22:70.
- V. **Pfütze S**, Charria-Girón E, Schulzke E, Toshe R, Khonsanit A, Franke R, Surup F, Brönstrup M, Stadler M (**2024**) Depicting the chemical diversity of bioactive meroterpenoids produced by the largest organism on earth. *Angewandte Chemie, International Edition* 63:e202318505.

Paper I

Drimane-Type Sesquiterpenoids Derived from the Tropical Basidiomycetes *Perenniporia centrali-africana* and *Cerrena* sp. nov

Paomephan Pathompong^{1,2,†}, **Sebastian Pfütze**^{2,3,†}, Frank Surup^{2,3}, Thitiya Boonpratang⁴, Rattaket Choeyklin^{4,5}, Josphat C. Matasyoh⁶, Cony Decock⁷, Marc Stadler^{2,3,*} and Chuenchit Boonchird^{1,*}

Molecules **2022**; 27(18):5968. DOI: <https://doi.org/10.3390/molecules27185968>

- ¹ Department of Biotechnology, Faculty of Science, Mahidol University, Bangkok 10400, Thailand
- ² Department of Microbial Drugs, Helmholtz Centre for Infection Research (HZI), German Centre for Infection Research (DZIF), Partner Site Hannover/Braunschweig, Inhoffenstrasse 7, 38124 Braunschweig, Germany
- ³ Institute of Microbiology, Technische Universität Braunschweig, Spielmannstraße 7, 38106 Braunschweig, Germany
- ⁴ National Biobank of Thailand (NBT), The National Science and Technology for Development Agency (NSTDA), Thailand Science Park, Pathum Thani 12120 Thailand
- ⁵ Biodiversity-Based Economy Development Office (Public Organization) (BEDO), the Government Complex, Building Ratthaprasasanabhakti, Bangkok 10210 Thailand
- ⁶ Department of Chemistry, Egerton University, P.O BOX 536, 20115, Njoro, Kenya
- ⁷ Mycothèque de l' Université catholique de Louvain (BCCM/MUCL), Place Croix du Sud 3, B-1348 Louvain-la-Neuve, Belgium

*Corresponding author

†These authors contributed equally to this work.

Article

Drimane-Type Sesquiterpenoids Derived from the Tropical Basidiomycetes *Perenniporia centrali-africana* and *Cerrena* sp. nov

Paomephan Pathompong ^{1,2,†}, Sebastian Pfütze ^{2,3,†}, Frank Surup ^{2,3} , Thitiya Boonpratuang ⁴ , Rattaket Choeyklin ^{4,5}, Josphat C. Matasyoh ⁶, Cony Decock ⁷, Marc Stadler ^{2,3,*}  and Chuenchit Boonchird ^{1,*}

- ¹ Department of Biotechnology, Faculty of Science, Mahidol University, Bangkok 10400, Thailand
 - ² Department of Microbial Drugs, Helmholtz Centre for Infection Research (HZI), German Centre for Infection Research (DZIF), Partner Site Hannover/Braunschweig, Inhoffenstrasse 7, 38124 Braunschweig, Germany
 - ³ Institute of Microbiology, Technische Universität Braunschweig, Spielmannstraße 7, 38106 Braunschweig, Germany
 - ⁴ National Biobank of Thailand (NBT), The National Science and Technology for Development Agency (NSTDA), Thailand Science Park, Pathum Thani 12120, Thailand
 - ⁵ Biodiversity-Based Economy Development Office (Public Organization) (BEDO), The Government Complex, Building Ratthaprasasanabhakti, Bangkok 10210, Thailand
 - ⁶ Department of Chemistry, Egerton University, P.O. Box 536, Njoro 20115, Kenya
 - ⁷ Earth and Life Institute, Mycothèque de l' Université Catholique de Louvain (BCCM/MUCL), Place Croix du Sud 3, B-1348 Louvain-la-Neuve, Belgium
- * Correspondence: marc.stadler@helmholtz-hzi.de (M.S.); chuenchit.boonchird@mahidol.ac.th (C.B.); Tel.: +49-531-6181-4240 (M.S.); +66-2-201-5304 (C.B.)
- † These authors contributed equally to this work.



Citation: Pathompong, P.; Pfütze, S.; Surup, F.; Boonpratuang, T.; Choeyklin, R.; Matasyoh, J.C.; Decock, C.; Stadler, M.; Boonchird, C. Drimane-Type Sesquiterpenoids Derived from the Tropical Basidiomycetes *Perenniporia centrali-africana* and *Cerrena* sp. nov. *Molecules* **2022**, *27*, 5968. <https://doi.org/10.3390/molecules27185968>

Academic Editors: Bruno Botta, Cinzia Ingallina, Andrea Calcaterra and Deborah Quaglio

Received: 2 September 2022

Accepted: 8 September 2022

Published: 14 September 2022

Publisher's Note: MDPI stays neutral with regard to jurisdictional claims in published maps and institutional affiliations.



Copyright: © 2022 by the authors. Licensee MDPI, Basel, Switzerland. This article is an open access article distributed under the terms and conditions of the Creative Commons Attribution (CC BY) license (<https://creativecommons.org/licenses/by/4.0/>).

Abstract: Five new drimane-type sesquiterpenoids were isolated from cultures of the tropical basidiomycetes, *Perenniporia centrali-africana* (originating from Kenya) and *Cerrena* sp. nov. (originating from Thailand). A new pereniporin A derivative (**1**), a new drimane-type sesquiterpene lactam (**2**), and the new 6,7-Dehydro-isodrimenediol (**3**) were isolated from *P. centrali-africana*. In parallel, the two new drimane-type sesquiterpene lactams **5** and **6** were isolated together with known isodrimenediol (**4**) from *Cerrena* sp. This is the first report of drimane-type sesquiterpene lactams from basidiomycetes. The structures were elucidated based on 1D and 2D nuclear magnetic resonance (NMR) spectroscopic data, in combination with high-resolution electrospray mass spectrometric (HR-ESIMS) data. The compounds were devoid of significant antimicrobial and cytotoxic activities.

Keywords: *Perenniporia centrali-africana*; *Cerrena* sp. nov.; drimane-type sesquiterpenoids

1. Introduction

Mushroom-forming fungi (mostly belonging to the division Basidiomycota) have been investigated regarding their abilities as prolific producers of structurally diverse bioactive compounds, leading to the discovery of numerous unique highly functionalized secondary metabolites [1,2]. Although the species of temperate climate zones have already been studied rather intensively, the endemic Basidiomycota of tropical countries such as Thailand have recently been found to be a good source for unprecedented metabolites [3,4]. New bioactive molecules have also been reported from Kenyan Basidiomycota that represent undescribed species [5,6].

The current study deals with the production, isolation, and characterization of further new sesquiterpenoid derivatives from two fungal species originating from Kenya and Thailand, respectively, which were examined in our ongoing projects aiming at the discovery of novel antibiotics and other beneficial molecules from Basidiomycota. These strains were selected for intensified evaluation because preliminary studies had revealed weak to moderate antimicrobial effects in the crude extracts, along with the presence of

potentially undescribed molecules, as deduced from HPLC–DAD/MS (high performance liquid chromatography coupled with diode array detection and mass spectrometry) data. Since the molecules turned out to be structurally similar, we decided to report their isolation and structure elucidation in one paper and include data on the taxonomy of the producer strain.

2. Results and Discussion

2.1. Fungal Identification and Crude Extracts

Perenniporia strain MUCL 56,028 was identified by comparison of morphological characteristics and sequencing of the 5.8S/ITS nrDNA, as described in the Experimental Section (the sequence as shown in Table S1 in the Supporting Information). *P. centrali-africana* is a common white rot, wood decay basidiomycete belonging to the family, Polyporaceae. This fungus has a dimitic or trimitic hyphal structure with clamp connections on generative hyphae. It produces ellipsoid to distinctly truncate soft and thick-walled basidiospores [7]. A BLAST search in GenBank confirmed the generic affinities of the strain to the genus *Perenniporia* in the family Polyporaceae by a closest hit (GenBank acc. no KX584430.1) (*Perenniporia centrali-africana*) with 99.85% identity (cf. Figure S1 in the Supporting Information). The crude extracts of the strain MUCL 56,028 exhibited antimicrobial activity against *Bacillus subtilis*, with a minimum inhibitory concentration (MIC) of 75 µg/mL (compared to the positive control ciprofloxacin at an MIC of 3.1 µg/mL).

Strain BCC 84,628 was identified using a comparison of morphological characteristics and sequencing of the 5.8S/ITS nrDNA region (the sequence is shown in Table S1 in the Supporting Information). The genus *Cerrena* is characterized by having a dimitic or trimitic hyphal system, nonamyloid, hyaline basidiospores, and its species are classified as white rot fungi [8]. This genus is known as an enzyme production machinery due to its decomposing capacity in biological niches [9–12]. A BLAST search in GenBank confirmed that the strain belongs to the genus *Cerrena* in the Cerrenaceae. Based on the basidiocarps and culture morphology, two of the authors (T.B. and R.C.) classified this fungus as *Cerrena* cf. *caperata*. The ITS nrDNA sequence was deposited as GenBank acc. no MW512503. Further taxonomic studies including comparisons with type specimens of related species are ongoing to characterize this strain to the species level, but it constitutes an undescribed taxon according to the data presently available. The extracts of the strain BCC 84,628 exhibited activity against *Bacillus subtilis* with an MIC of 37.5 µg/mL (compared to the positive control ciprofloxacin at an MIC of 3.1 µg/mL).

2.2. Isolation and Structure Elucidation of Metabolites from *Perenniporia centrali-africana*

Extensive chromatography of the extracts obtained from *Perenniporia centrali-africana* (MUCL 56028) led to the isolation of three previously undescribed compounds, similar to the pereniporin core structure as previously described [13]. Alongside the new 3β-Hydroxy-9-dehydroxy-pereniporin A (1), 6,7-Dihydroxy-12-deoxy-dysidealactam (2), and 6,7-Dehydro-isodrimenediol (3), the known pereniporin A and other derivatives including 6-O-acetylpereniporin A, 3β-hydroxy-6-O-acetylpereniporin A, 11α-Hydroxycinnamomolide, 6α,9α,11α-trihydroxycinnamolide, and sulphureine H were obtained from *P. centrali-africana* and were identified by comparing their NMR data (Table 1) with those reported in the literature [13–17]. The structures of 1–3 are shown in Figure 1. Furthermore, the extracts of rice standing cultures led to the isolation of the three previously described cryptoporic acids B, H, and I [18,19]. The structures of the known compounds are shown in the Supporting Information (Figure S2).

Table 1. NMR spectroscopic data (^{13}C (δ_{C}), 175 MHz and ^1H (δ_{H}), 700 MHz, methanol- d_4) for 3 β -hydroxy-9-dehydroxy-pereniporin A (1), 6,7-dihydroxy-12-deoxy-dysidealactam (2), and 6,7-dehydro-isodrimenediol (3).

| Pos | 1 | | 2 | | 3 | |
|-----|----------------------------|---|----------------------------|--|----------------------------|--|
| | δ_{C} , Type | δ_{H} (J in HZ) | δ_{C} , Type | δ_{H} (J in HZ) | δ_{C} , Type | δ_{H} (J in HZ) |
| 1 | 37.2, CH_2 | α : 1.44, m β : 1.70, m | 37.7, CH_2 | α : 1.06, m β : 2.67, m | 37.1, CH_2 | α : 1.40, m β : 1.85, dt (13.0, 3.4) |
| 2 | 26.5, CH_2 | 1.67, m | 19.6, CH_2 | α : 1.46, m β : 1.80, m | 28.3, CH_2 | 1.70, m |
| 3 | 78.2, CH | α : 3.22, dd (11.4, 4.5) | 44.3, CH_2 | α : 1.44, m β : 1.25, m | 79.4, CH | α : 3.26, m |
| 4 | 39.0, C | - | 34.2, C | - | 39.8, C | - |
| 5 | 57.0, CH | α : 1.31, d (8.9) | 50.8, CH | α : 1.48, d (1.3) | 56.2, CH | α : 1.98, br s |
| 6 | 67.4, CH | β : 4.34, br d (8.9) | 72.7, CH | α : 4.35, br s | 133.3, CH | 6.20, dd (10.1, 3.1) |
| 7 | 120.3, CH | 5.53, m | 70.9, CH | α : 4.10, br s | 129.3, CH | 5.74, br d (10.1) |
| 8 | 139.1, C | - | 149.1, C | - | 146.6, C | - |
| 9 | 60.6, CH | α : 2.25, m | 143.0, C | - | 56.9, CH | α : 2.09, br d (4.7) |
| 10 | 38.1, C | - | 36.7, C | - | 38.8, C | - |
| 11 | 98.7, CH | β : 5.17, d (4.5) | 173.4, C | - | 60.6, CH_2 | α : 3.72, dd (10.8, 7.3) β : 3.924, dd (10.8, 7.3) |
| 12 | 67.7, CH_2 | α : 4.46, m β : 4.18, m | 46.7, CH_2 | α : 3.73, dd (18.7, 2.6) β : 4.00, m | 112.6, CH_2 | 4.96, s 5.15, s |
| 13 | 15.1, CH_3 | 0.99, s | 24.1, CH_3 | 1.26, s | 16.6, CH_3 | 0.81, s |
| 14 | 29.5, CH_3 | 1.23, s | 34.1, CH_3 | 1.00, s | 28.5, CH_3 | 1.06, s |
| 15 | 14.3, CH_3 | 0.85, s | 21.3, CH_3 | 1.52, s | 15.2, CH_3 | 0.74, s |

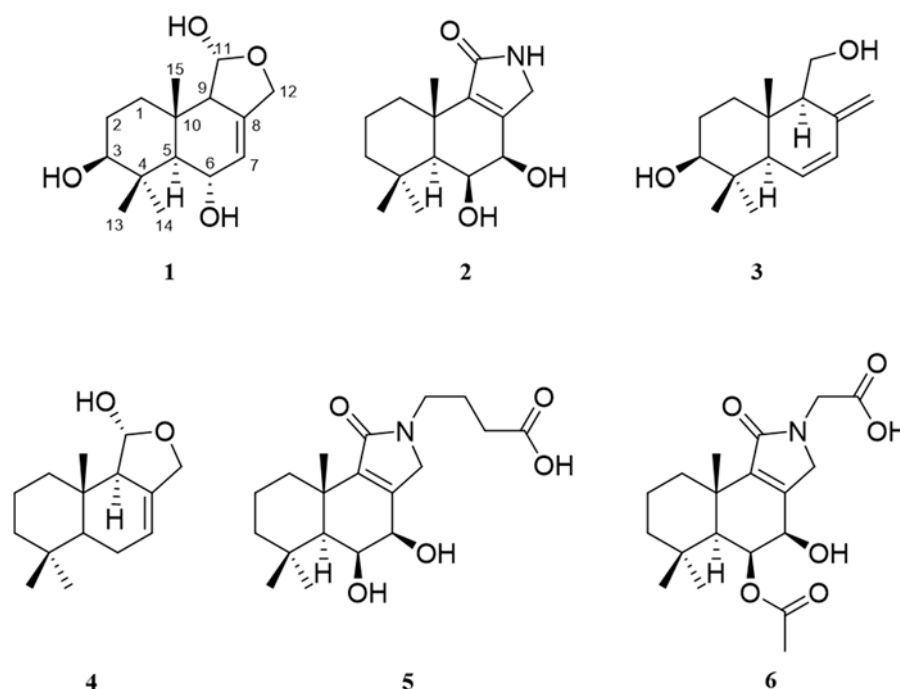


Figure 1. Chemical structures of compounds 1–3 from *Perenniporia centrali-africana* and compound 4–6 from *Cerrena* sp.

2.4. Biological Assays 3 β -hydroxy-9-dehydroxy-pereniporin A (1) was isolated as white solid from the supercritical extract, after liquid cultivation of *Perenniporia centrali-africana* on BA and medium. Its molecular formula was established from HRESIMS. Compound 1 exhibited antimicrobial activities against *Mycobacterium* and *Klebsiella* strains (MIC 1567) indicating four degrees of unsaturation. ^{13}C NMR and HSQC data (Table 1, Figure S7) led to the identification of three acetyl groups at δ 0.85 (s, H-15), 0.99 (s, H-14), and 1.23 (s, H-13) three methylenes at δ 1.44

(m, H-1 α), 1.70 (m, H-1 β), 1.67 (m, H₂-2), 4.18 (br dd, $J = 12.05, 1.08$ Hz, H-12 β), and 4.46 (m, H-12 α), two methines at δ_H 1.31 (d, $J = 8.90$ Hz, H-5) and 2.25 (m, H-9), three oxymethines at δ_H 3.22 (dd, $J = 11.4, 4.5$ Hz, H-3), 4.34 (br d, $J = 8.90$ Hz, H-12), and 5.17 (d, $J = 4.5$ Hz, H-11), and one olefinic methine at δ_H 5.53 (m, H-7). The ^{13}C and HMBC NMR data (Table 1, Figure S8) revealed the presence of 15 carbon resonances, including two sp^2 -hybridized carbons, comprising one nonprotonated carbon (δ_C 139.1, C-8) and one methine (δ_C 120.3, C-7); three oxymethines (δ_C 98.7, C-11; 78.2, C-3; 67.4, C-6); two methines (δ_C 60.6, C-9; 57.0, C-5); three methylene carbons (δ_C 37.2, C-1; 26.5, C-2; 67.7, C-12); and three methyl carbons (δ_C 29.5, C-14; 15.1, C-13; 14.3, C-15). One degree of unsaturation is given by the two sp^2 -hybridized carbons, suggesting three rings in the scaffold of 3 β -Hydroxy-9-dehydroxy-pereniporin A (**1**). Analysis of the ^1H - ^1H COSY data gave the first spin system due to correlations between H₂-1, H₂-2, and H-3. Correlations between H-5, H-6, and H-7, as well as between H-9 and H-11, led to the identification of the second and third spin system. HMBC correlations from H₃-13/H₃-14 to C-3/C-4/C-5, H₃-15 to C-1/C-5/C-9/C-10, and H-5 to C-3/C-4/C-5/C-6/C-7/C-8/C-9/C-10/C-15 revealed the presence of two six-membered rings that were fused across C-5 and C-10, carrying a hydroxyl function at C-3 and C-6, as well as one methyl group at C-10 and two methyl groups at C-4. Further HMBC correlations from H-11 to C-8/C-9/C-12 and from H₂-12 to C-7/C-8/C-9/C-11 led to the identification of a tetrahydrofuran-11-ol substructure that was fused to the molecule across C-8 and C-9. Relative configuration could be obtained by evaluation of ROE data. Due to key correlations among H-1 α /H-3 α /H-5 α /H-9 α /H-12 α /H₃-14, these protons were arbitrarily assigned to the α face of the molecule. Correlations between H-1 β /H-6 β /H-11 β /H-12 β /H₃-13/H₃-15 indicated a β orientation of these protons. Finally, the absolute configuration of **1** was determined as 3*S*,5*R*,6*S*,9*R*,10*S*,11*R*, after comparison of its ECD data to the ones of related drimane derivatives [8]. Furthermore, these compounds were isolated from the same genus (*Perenniporia*) and showed similar ROESY correlations.

6,7-Dihydroxy-12-deoxy-dysidealactam (**2**), which is closely related to **1**, was obtained as white solid. Its molecular formula was assigned as $\text{C}_{15}\text{H}_{23}\text{NO}_3$, according to the molecular ion cluster at m/z 266.1750 $[\text{M} + \text{H}]^+$ in the HRESIMS spectrum, indicating the presence of a nitrogen atom. One- and two-dimensional NMR spectra revealed the absence of the hydroxyl function at C-3, which was replaced by a methylene (δ_H 1.25, H-3 β ; 1.44, H-3 α). ^1H NMR, ^{13}C , and HSQC data indicated the presence of another oxymethine (δ_C 70.9; δ_H 4.10) at C-7, which was confirmed by HMBC correlations from H-7 α to C-5/C-6/C-8/C-9/C-12. Furthermore, a lactam functionality was placed at C-11 (δ_C 173.4), which was supported by the absence of H-11, the chemical shift of the methylene CH₂-12 (δ_C 46.7, δ_H 3.73, 4.00), and the HMBC correlations of H₂-12 to C-11. Metabolite **2** is the nitrogen derivative of deacetylugandensolide. Since **2** and deacetylugandensolide have very similar coupling constants and chemical shifts for H-5, H-6 and H-7, we propose a common relative configuration [20].

6,7-Dehydro-isodrimenediol (**3**) was isolated as white solid with a molecular formula of $\text{C}_{15}\text{H}_{24}\text{O}_2$ and showed similarities to **1**, according to its 1D and 2D NMR data. ^1H NMR and HSQC data indicated the presence of another protonated sp^2 -hybridized carbon (δ_H 6.20, H-6; δ_C 133.3, C-6) replacing oxymethine H-6 and the presence of oxymethylene and exomethylene moieties at C-11 and C-12 as key differences, respectively.

Previous reports showed that *Perenniporia* spp. generally produce drimane-type sesquiterpenoids called pereniporins, which is somewhat unfortunate because of the typo in the trivial name. Pereniporins A and B were firstly isolated in 1986 from *P. medulla-panis* [17]. Several derivatives of pereniporin A have been isolated from *P. maackiae* [13]. In this study, two further derivatives of pereniporin A were isolated from a submerged cultivation of *P. centrali-africana*. Solid cultivation of *P. centrali-africana* led to the isolation of the known cryptoporic acids B, I, and H. Cryptoporic acid B was firstly isolated from *Cryptoporus volvatus* along with cryptoporic acid A [18], while cryptoporic acid H was previously isolated from mycelial cultures of *Ganoderma neo-japonicum* and *C. volvatus*. Later, Cabrera et al.

isolated cryptoporic acid H from the culture broth of *Polyporus ciliatus* [21] (current name *Ceriporus ciliatus*).

2.3. Isolation and Structure Elucidation of Compounds 4–6 from *Cerrena* sp.

Extensive chromatography of the extracts obtained from *Cerrena* sp. (BBH 40848) led to the isolation of two previously undescribed and two known compounds called cryptoporic acid H and isodrimeniol. Isodrimeniol (**4**) was isolated as a colorless oil. The molecular formula of **4** was determined as C₁₅H₂₄O₂ by HRESIMS data. The planar structure was identified as isodrimeniol by 1D and 2D NMR data (see Table 2, Figures S27–S31 for details). Since the coupling constants of **4** are identical to those published by Rodriguez et al. [22], the stereochemistry of **4** was assigned to be identical to that of isodrimeniol, which was isolated from the bark of *Drimys winteri* Forst. The analysis of the HRESIMS spectrum of compound **5** yielded the molecular formula C₁₉H₂₉NO₅. The ¹H and ¹³C NMR data of **5** were very like those of **2**. The key differences were the presences of additional signals for three methylenes and one carboxylic moiety. Since the 2'-H₂ and 3'-H₂ showed HMBC correlations (Figure S25) to C-1' and 4'-H₂ to C-11 and C-12, the structure of **5** was assigned as the butyric acid derivative of **2**. The molecular formula of **6** was determined by HRESIMS data as C₁₉H₂₇NO₆. NMR data were highly similar to those of **2** and **5**. However, the key differences compared to **5** were an acetyl group attached to C-6 and a glyciny moiety instead of the 4-aminobutyryl residue of **5**. Consequently, **6** is the glyciny derivative of the known ugandensolide.

Table 2. NMR spectroscopic data (¹³C (δ_C), 125 MHz and ¹H (δ_H), 500 MHz) for isodrimeniol (**4**, acetone-*d*₆), the glyciny derivative of deacetylugandensolide (**5**, methanol-*d*₄), and the 4-aminobutyryl derivative of ugandensolide (**6**, acetone-*d*₆).

| Pos | 4 | | 5 | | 6 | |
|-----|-----------------------|--|-----------------------|--|-----------------------|--|
| | δ _C , Type | δ _H (J in HZ) | δ _C , Type | δ _H (J in HZ) | δ _C , Type | δ _H (J in HZ) |
| 1 | 40.0, CH ₂ | α: 1.24, m β: 1.80, dq (13.7, 2.7) | 38.2, CH ₂ | α: 2.56, br d (12.7) β: 1.13, m | 37.7, CH ₂ | α: 2.68, br d (13.2) β: 1.12, m |
| 2 | 18.7, CH ₂ | α: 1.62, qt (13.7, 3.5) β: 1.45, m | 19.9, CH ₂ | α: 1.85, m β: 1.52, m | 19.4, CH ₂ | α: 1.81, m β: 1.54, m |
| 3 | 42.7, CH ₂ | α: 1.25, m β: 1.45, m | 44.6, CH ₂ | α: 1.28, m β: 1.46, m | 44.2, CH ₂ | α: 1.29, m β: 1.49, m |
| 4 | 33.0, C | - | 34.6, C | - | 34.1, C | - |
| 5 | 50.4, CH | 1.31, dd (11.6, 5.4) | 51.2, CH | 1.45, m | 49.7, CH | 1.73, d (1.0) |
| 6 | 23.9, CH ₂ | α: 2.14, m β: 1.92, m | 72.5, CH | 4.28, br s | 73.8, CH | 5.46, m |
| 7 | 116.2, CH | 5.47, br s | 70.7, CH | 4.05, d (1.5) | 67.1, CH | 4.12, br d (1.7) |
| 8 | 138.2, C | - | 147.6, C | - | 147.0, C | - |
| 9 | 62.0, CH | 2.15, m | 144.2, C | - | 142.5, C | - |
| 10 | 33.7, C | - | 37.3, C | - | 36.8, C | - |
| 11 | 99.2, CH | 5.19, dd (4.5, 4.0) 11-OH: 5.11, br d (4.5) | 172.5, C | - | 170.4, C | - |
| 12 | 68.1, CH ₂ | α: 4.33, br d (11.3) β: 4.04, m | 52.3, CH ₂ | α: 4.09, d (19.4) β: 3.84, d (19.4) | 51.6, CH ₂ | α: 4.18, d (18.6) β: 3.92, d (18.6) |
| 13 | 21.3, CH ₃ | 0.93, s | 24.1, CH ₃ | 1.24, s | 23.5, CH ₃ | 1.04, s |
| 14 | 33.0, CH ₃ | 0.88, s | 34.2, CH ₃ | 1.03, s | 33.7, CH ₃ | 1.01, s |
| 15 | 13.8, CH ₃ | 0.81, s | 21.3, CH ₃ | 1.49, s | 21.3, CH ₃ | 1.50, s |
| 1' | - | - | 176.8, C | - | 171.2, C | - |
| 2' | - | - | 32.3, CH ₂ | 2.31, t (7.4) | 43.4, CH ₂ | 4.21, m |
| 3' | - | - | 25.2, CH ₂ | 1.88, quin (7.4) | - | - |
| 4' | - | - | 42.6, CH ₂ | 3.47, t (7.0) | - | - |
| 1'' | - | - | - | - | 170.6, C | - |
| 2'' | - | - | - | - | 21.5, CH ₃ | 2.01, s |

Previously, the cytotoxic sesquiterpenoids named cerrenins A–E were isolated from *Cerrena* sp. [23,24], which are so far the only secondary metabolites known from this genus. Interestingly, the new sesquiterpene lactams were isolated from two different families of Basidiomycota (i.e., Polyporaceae and Cerrenaceae). Sesquiterpene lactams have rarely been discovered as natural products, even though there are some reports from marine animals [25–27]. Another one was reported from the leaves of *Cinnamosma fragrans*, which revealed the first report of tyramine involved in a lactam formation from a sesquiterpene [28]. *Cerrena* produced two new sesquiterpene lactams (5, 6), which show an addition of amino acids to the lactam ring. *P. centrali-africana* also produced one sesquiterpene lactam (2), but this metabolite lacked an amino acid at the lactam ring. According to molecular phylogenetic studies, these basidiomycetes are currently classified in the residual clade (Cerrenaceae) and core polyporoid clade of the Polyporaceae [29]. The strains may possess two different biosynthesis gene clusters that contain enzymes mediating aminations that add amino acids into the lactam ring of sesquiterpenes. As recently reported, dehydrogenation is an important step of closing the ring in drimane sesquiterpenoid formation by oxidoreductases [30]. *Cerrena* should accordingly have an aminase at this step to incorporate the amine group of amino acids, to form the lactam ring instead of dehydrogenation. However, this hypothesis remains to be validated by genome sequencing and subsequent experimental work that goes far beyond to the scope of our current study.

2.4. Biological Assays

Compounds 1, 4, 5, and 6 were evaluated for antimicrobial and cytotoxic activities according to established procedures [31]. Compound 4 weakly exhibited antimicrobial activities against *Mucor hiemalis* and *Rhodoturula glutinis* (MIC 67 µg/mL), and exhibited cytotoxicity of L929 (IC₅₀ 33 µg/mL) and A549 (IC₅₀ 16 µg/mL). A detailed report on their activity is given in the Supporting Information in Tables S4 and S5. According to previous reports, the functional group at C-6 is an important factor for enabling its cytotoxicity. For the cytotoxic pereniporins, the absolute configuration at C-6 was reported to be *S* [13]. None of the sesquiterpene lactams, including compound 5 and 6, showed antimicrobial activities and cytotoxicity.

3. Materials and Methods

3.1. General Information

HPLC–DAD/MS measurements were performed using an amaZon speed ETD (electron transfer dissociation) ion trap mass spectrometer (Bruker Daltonics, Bremen, Germany) and measured in positive and negative ion modes simultaneously, with the HPLC system (column C18 Acquity UPLC BEH Waters, Eschborn, Germany); solvent A: water (H₂O), solvent B: acetonitrile (can) supplemented with 0.1% formic acid (FA), gradient conditions: 5% B for 0.5 min, increasing to 100% B for 20 min, and maintaining isocratic conditions at 100% B for 10 min, with a flow rate of 0.6 mL/min, using UV/Vis detection (200–600 nm).

HR-ESIMS (high-resolution electrospray ionization mass spectrometry) data were recorded on a MaXis ESI-TOF (electrospray ionization-time of flight) mass spectrometer (Bruker Daltonics), coupled with an Agilent 1260 series HPLC-UV system and equipped with a C18 Acquity UPLC BEH (ultraperformance liquid chromatography) (ethylene bridged hybrid) (Waters) column; DAD-UV detection at 200–600 nm; solvent A (H₂O) and solvent B (ACN) were supplemented with 0.1% FA as a modifier; a flow rate of 0.6 mL/min, at 40 °C, using a gradient elution system with the initial condition of 5% B for 0.5 min, increasing to 100% B for 19.5 min, and holding at 100% B for 5 min. Bruker Compass DataAnalysis 4.4 SR1 was used to analyze the data, including determining the molecular formula using the Smart Formula algorithm (Bruker Daltonics).

One- and two-dimensional NMR spectra were measured on a Bruker 700 MHz Avance III spectrometer, equipped with a 5 mm TCI cryoprobe (¹H: 700 MHz, ¹³C: 175 MHz), and a Bruker Avance III 500 (¹H 500 MHz, ¹³C 125 MHz) spectrometer. NMR data were referenced

to selected chemical shifts of acetone- d_6 (^1H : 2.05 ppm, ^{13}C : 29.32 ppm) and $\text{CH}_3\text{OH}-d_4$ (^1H : 3.31 ppm, ^{13}C : 49.15 ppm), respectively. Optical rotations were measured using an Anton Paar MCP-150 Polarimeter (Graz, Austria), with a 100 mm path length and a sodium D line at 589 nm. The UV spectra were measured on a Shimadzu (Kyoto, Japan) UV/Vis 2450 spectrophotometer using methanol (Uvasol, Merck, Darmstadt, Germany) as a solvent. ECD (electronic circular dichroism) spectra were measured with a J-815 spectropolarimeter (Jasco, Pfungstadt, Germany) using methanol as a solvent. The spectral data are combined in the Supplementary Information (Figures S3–S72).

3.2. Fungal Material

Perenniporia centrali-africana was collected by C. Decock and J. C. Matasyoh from wood from Mount Elgon National Reserve, located in the western part of Kenya ($1^\circ 7' 6''$ N, $34^\circ 31' 30''$ E) in April 2016. A dried specimen and the corresponding mycelial culture, which was obtained from the context of the basidome, were deposited at MUCL, Louvain-la-Neuve, Belgium, under the accession number MUCL 56028.

Cerrena sp. nov. was collected from an unnamed rotting tree trunk, isolated, and identified by T. Boonpratang, R. Choeyklin, and the team from Dong Yai Community Forest in the Plant Genetics Conservation Project, under the Royal Initiative of Her Royal Highness Maha Chakri Sirindhorn (RSPG), in Amnat Charoen Province, located in the northeastern part of Thailand, in March 2017. The voucher specimen collection was deposited in the BIOTEC Bangkok Herbarium & Fungarium, Pathum Thani, Thailand, with the designation BBH 41077, and the culture collection was deposited in the BIOTEC Culture Collection with the designation BCC 84628.

DNA was extracted from the cultures of MUCL 56028 and BBH 40848 using the EZ-10 spin column genomic DNA miniprep kit (Bio Basic Canada Inc., Markham, ON, Canada) as described previously [32]. A Precellys 24 homogenizer (Bertin Technologies, France) was used for cell disruption at a speed of 6000 rpm for 2×40 s. Standard primers ITS 1f and ITS 4r were used for the DNA region amplification by following a previously published protocol [33].

3.3. Seed Culture and Scale-Up of Fermentation

For the seed culture of *P. centrali-africana*, three 20 mm²-sized mycelium plugs of a well-grown culture on YM6.3 agar medium were transferred into a 500 mL Erlenmeyer flask, containing 200 mL of liquid YM6.3 medium. The incubation was performed on a rotary shaker at 23 °C and 140 rpm. After six days, the mycelium was homogenized with a T25 easy clean digital (S 25 N, IKA, Staufen im Breisgau, Germany) and afterwards used to inoculate twenty-five 500 mL Erlenmeyer flasks, each containing 200 mL of BAF medium. Therefore, 3 mL of the homogenized seed culture was transferred into each flask. The incubation was performed on a rotary shaker at 23 °C and 140 rpm. Every five days, the consumption of glucose was monitored regularly (using Medi-Test, Macherey Nagel, Düren, Germany).

For *Cerrena*, the fermentation was started by inoculating a plug of well-grown culture on YM agar, which was incubated at 23 ± 2 °C for up to 2 weeks until the colony covered the plate. A cork borer (diameter 6 mm) was used to plug the well-grown colony in five pieces, which were inoculated into 250 mL of liquid YM6.3 medium for 20 flasks in total, which were incubated on a rotary shaker at 27 ± 2 °C and 140 rpm. The glucose consumption was monitored every five days as mentioned above.

3.4. Harvest, Extraction, and Analytical HPLC

After 20 days of incubation, the liquid BAF cultures of *P. centrali-africana* were harvested. The mycelium and supernatant were separated by centrifugation (Sorvall RC-58 Refrigerated Superspeed Centrifuge, DuPont Instruments) at 9000 rpm for 30 min. The mycelium was extracted twice with acetone in an ultrasonic bath. The acetone and mycelium were separated by filtration and subsequently the organic solvent was removed

by evaporation (40 °C). Afterwards, the remaining aqueous phase was extracted with ethyl acetate 1:1, twice, and following this, the extract was evaporated to dryness. The supernatant was extracted with ethyl acetate 1:1, twice. After phase separation, the organic phase was collected in a round-bottom flask and the ethyl acetate was then evaporated (40 °C). Crude extracts from the mycelium and supernatant were dissolved in methanol to yield a concentration of 10 mg/mL. Solvation was aided by ultrasonication at 40 °C. Additionally, 100 µL of this solution was filtered with syringeless filters (Mini-UniPrep™, Whatman, Dassel, Germany) and 60 µL of the supernatant was analyzed by analytical HPLC–MS.

The rice standing culture of *P. centrali-africana* was harvested after 28 days of incubation. Therefore, the medium and mycelium were loosened with a spatula, covered with acetone, and finally extracted by using ultrasonification for 30 min. Afterwards, the liquid phase was separated from the solid phase by filtration to enable a second extraction of the solid phase with acetone. Following this, the organic solvent was evaporated using a rotary evaporator (40 °C) and the remaining aqueous phase was extracted with ethyl acetate (1:1) in a separatory funnel, twice. The crude extract was evaporated to dryness (40 °C) and subsequently dissolved in 5 mL of methanol. Into this solution, 50 mL of a mixture of heptane and MeOH/H₂O (1:1) was added, while the following extraction was carried out in a separatory funnel, twice, and the heptane and aqueous phase were collected separately. Finally, both fractions were evaporated to dryness (40 °C) and again dissolved in methanol to yield a concentration of 10 mg/mL. Solvation was aided by ultrasonication at 40 °C. Additionally, 100 µL of this solution was filtered with syringeless filters (Mini-UniPrep™, Whatman) and 60 µL of the supernatant was analyzed by analytical HPLC–MS.

After 35 days of cultivation, the mycelia and supernatant of the *Cerrena* cultures were separated by centrifugation. The mycelial biomass was extracted with 4 × 500 mL of acetone in an ultrasonic bath (Sonorex Digital 10 P, Bandelin Electronic GmbH & Co. KG, Berlin, Germany) for 30 min. The extracts were combined, and the solvent was evaporated by means of a rotary evaporator. The remaining water phase was suspended in 200 mL of distilled water, extracted with 3 × 500 mL of ethyl acetate, and stirred together with anhydrous sodium sulfate for 15 min. The filtered ethyl acetate extract was evaporated to dryness, leaving a brown oily solid (662 mg). The supernatant was extracted by adding 5% Amberlite XAD-16N absorbent (Rohm & Haas Deutschland GmbH, Frankfurt am Main, Germany) and stirred overnight. The Amberlite resin was then filtered and eluted with 4 × 500 mL of acetone. The resulting acetone extract was evaporated, and the remaining water phase was extracted with ethyl acetate 1:1. The organic phase was dried over anhydrous sodium sulfate and evaporated to dryness, and a brown oily extract (3.2 g) was obtained.

3.5. Isolation of the Compounds

All separations were carried out as RP-LC at a PLC 2250 system (Gilson, Middleton, WI, USA), using water as solvent A and ACN as solvent B, both containing 0.1% of formic acid.

At first, the crude extracts of the liquid BAF cultures were dissolved in methanol and filtered through a Strata X-33 µm Polymere Reversed Phase Tube (Phenomenex, Aschaffenburg, Germany) to remove nonpolar compounds and debris. To obtain a further separation, the main fractions were separated with a Gemini C18 column (250 × 50 mm, 10 µm, Phenomenex) as stationary phase with a flow rate of 60 mL/min. UV detection was carried out at 210, 220, and 250 nm.

The mycelial extract (600 mg) was separated with an elution gradient starting with isocratic conditions for 5 min at 20% of solvent B, followed by an increase to 60% B over 40 min, another increase to 100% B over 10 min, and ultimately, isocratic conditions for 10 min at 100% B. According to the observed peaks, 28 fractions were collected. In the course of the following work, fraction 1 (5.03 mg, t_R = 5.5 min) was identified as 3β-Hydroxy-9-dehydroxy-pereniporin A (1), fraction 11 (20.28 mg, t_R = 20.5 min) as 3β-Hydroxy-6-O-acetylpereniporin A, fraction 13 (20.15 mg, t_R = 23.5 min) as sulphureine

H, fraction 16 (60.56 mg, t_R = 27.5 min) as pereniporin A, fraction 17 and 18 (2.96 and 1.87 mg, t_R = 31.5–32.0 min) as 6 α ,9 α ,11 α -trihydroxycinnamolide, fraction 27 (11.48 mg, t_R = 40.5–41.0 min) as 6-O-acetylpereniporin A, and fraction 28 (2.47 mg, t_R = 43.0–44.0 min) as 11 α -Hydroxycinnamosmolide.

The extract obtained from the supernatant (720 mg, two runs) was separated by using the same gradient as described for the mycelial extract. After separation, 11 fractions were collected in the first run, whereof fraction 1 (15.51 mg, t_R = 20.5 min) was identified as 3 β -hydroxy-6-O-acetylpereniporin A, fraction 3 (12.84 mg, t_R = 23.5 min) as sulphureine H, fraction 5 (46.26 mg, t_R = 27.5 min) as pereniporin A, fraction 6 (3.32 mg, t_R = 32.0 min) as 6 α ,9 α ,11 α -trihydroxycinnamolide, and fraction 10 (2.61 mg, t_R = 44.0–44.5 min) as 11 α -Hydroxycinnamosmolide. The second run led to the isolation of 19 fractions, leading to the identification of fraction 2 (5.33 mg, t_R = 10.3 min) as 3 β -Hydroxy-9-dehydroxy-pereniporin A (**1**), fraction 10 (17.58 mg, t_R = 23.5 min) as sulphureine, and fraction 19 (1.27 mg, t_R = 43.0–43.3 min) as 11 α -Hydroxycinnamosmolide.

A second cultivation in BAF medium under the same conditions led to another supernatant crude extract (252 mg) that was purified with a Gemini C18 column (250 \times 50 mm, 10 μ m, Phenomenex) as stationary phase, a flow rate of 60 mL/min, and UV detection at 210, 220, and 250 nm. An elution gradient starting with isocratic conditions for 2 min at 25% of solvent B, followed by an increase to 55% B over 40 min, another increase to 100% B over 15 min, and ultimately, isocratic conditions for 10 min at 100% B led to the isolation of 22 fractions. Fractions 4–6 (32.96 mg, t_R = 12.0–14.5 min) were found to include 6,7-Dehydro-isodrimenediol (**3**), while fraction 7 (33.27 mg, t_R = 16.0–17.5 min) was found to contain 6,7-Hydroxy-12-deoxy-dysidealactam (**2**).

Both were submitted to RP-LC for further purification. Fraction 7 containing 6,7-Hydroxy-12-deoxy-dysidealactam (**2**) was purified with a Luna C18 column (250 \times 21.2 mm, 5 μ m, Phenomenex) as stationary phase and flow rate of 15 mL/min. An elution gradient starting with isocratic conditions for 2 min at 20% of solvent B, followed by an increase to 35% B in 30 min and another increase to 100% B in 8 min led to the isolation of nine fractions, whereof fraction 7 (1.05 mg, t_R = 25.5 min) was identified as the only pure sample of compound **2**. Fractions containing 6,7-Dehydro-isodrimenediol (**3**) were combined and purified with a Luna C18 column (250 \times 21.2 mm, 5 μ m, Phenomenex) as stationary phase and a flow rate of 20 mL/min. An elution gradient starting with isocratic conditions for 5 min at 15% of solvent B, followed by an increase to 45% B over 40 min, another increase to 55% of solvent B over 10 min, and ultimately, an increase to 100% B over 10 min led to the isolation of seven fractions, whereof fraction 5 (0.94 mg, t_R = 40.0–41.5 min) was identified as the only pure sample of compound **3**.

Furthermore, the crude extract (140 mg) of the aqueous phase obtained from rice cultures was dissolved in methanol and separation was carried out using a Nucleodur C18 column (150 \times 40 mm, 10 μ m, Macherey-Nagel) as stationary phase, with UV detection at 210, 220, and 420 nm and a flow rate of 60 mL/min. For purification, an elution gradient starting with isocratic conditions for 5 min at 30% of solvent B, followed by an increase to 70% B over 40 min, another increase to 100% B over 20 min, and ultimately, isocratic conditions for 10 min at 100% B was used. A total of eleven fractions was collected, according to the observed peaks. Analysis via HPLC–MS and NMR led to the identification of fraction 1 (2.15 mg, t_R = 15.0–15.5 min) as pereniporin A, fraction 2 (2.15 mg, t_R = 19.0–19.5 min) as cryptoporic acid I, fraction 5 (6.48 mg, t_R = 34.5–35.0 min) as cryptoporic acid B, and fraction 6 (24.44 mg, t_R = 37.0–38.0 min) as cryptoporic acid H.

The isolation of compound **4–6** from *Cerrena* started with the filtration of the crude extracts using an SPME Strata-X 33 u Polymeric RP cartridge (Phenomenex, Inc., Aschaffenburg, Germany). The fractions from the mycelial crude extracts were separated using preparative reversed-phase liquid chromatography (PLC 2020, Gilson, Middleton, WI, USA). A VP Nucleodur 100–10 C18 ec column (250 mm \times 40 mm, 7 μ m, Macherey-Nagel) was used as stationary phase. Deionized water (Milli-Q, Millipore, Schwalbach, Germany) with 0.05% trifluoroacetic acid (TFA) (solvent A) and acetonitrile with 0.05% TFA (solvent

B) were used as the mobile phase at a flow rate of 40 mL/min. The elution gradient started with 5% of solvent B isocratic for 3 min, followed by an increase to 50% of solvent B over 45 min, another increase to 100% of solvent B over 10 min and thereafter isocratic conditions at 100% of solvent B for 10 min. UV monitoring was carried out at 210, 254, and 350 nm. Fourteen fractions were collected according to the observed peaks. At this step, isodrimeniol (**4**) (2.0 mg, t_R = 57 min) was obtained from fraction 12. Reversed-phase HPLC using a VP Nucleodur 100–5C 18-ec column (150 mm × 21 mm, 7 μ m, Macherey-Nagel) as stationary phase, H₂O + 0.05% TFA as solvent A and ACN + 0.05% TFA as solvent B, at a flow rate of 20 mL/min was used to further purify the obtained fractions. A gradient starting with isocratic conditions at 20% B for 10 min, increasing to 40% B over 30 min, followed by a gradient shift from 40% to 100% B over 10 min, and maintaining isocratic conditions at 100% B for 5 min led to the isolation of **5** (3.5 mg, t_R = 16.3 min) from fraction F1. Fraction F2 was purified with a gradient starting with isocratic conditions at 20% B for 10 min, increasing to 25% B over 10 min, followed by an increase to 35% solvent B over 40 min, an increase to 100% B over 10 min, and maintaining isocratic conditions at 100% B for 5 min. This led to the isolation of the 4-Aminobutyl derivative of ugandensolide (**6**) (1.5 mg, t_R = 45.4 min). Fraction F6 was purified with a gradient starting with isocratic conditions at 20% B for 10 min, increasing to 45% B over 10 min, an increase to 55% of solvent B over 40 min, followed by a gradient shift from 55% to 100% B over 10 min, and finally maintaining isocratic conditions at 100% B for 5 min to obtain cryptoporic acid H (2.4 mg, t_R = 31.9 min). All the obtained fractions were evaporated to dryness (40 °C) and dissolved in methanol to reach a concentration of 1 mg/mL. Afterwards, 60 μ L of these solutions was transferred into 300 μ L HPLC–MS vials and submitted for analytical HPLC–MS to evaluate the purity and determine the molecular weight.

3 β -Hydroxy-9-dehydroxy-pereniporin A (**1**) white solid; $[\alpha]_D^{20}$ = +3 (c = 0.1, MeOH); UV/Vis (MeOH) λ_{max} (log ϵ) 202 (3.52) nm (c = 0.005, MeOH); ECD (c = 0.1, MeOH): λ_{max} ($\Delta\epsilon$) 208 (+1.1), 193 (−0.8) nm; NMR data (¹H: 700 MHz, ¹³C NMR 175 MHz, MeOH-*d*₄) see Table 1; ESIMS m/z 291.13 [M + Na]⁺, 267.09 [M − H][−]; HRESIMS m/z 291.1565 [M + Na]⁺ (calcd. for C₁₅H₂₄NaO₄, 291.1567); t_R = 2.3 min.

6,7-Hydroxy-12-deoxy-dysidealactam (**2**) white solid; $[\alpha]_D^{20}$ = +21 (c = 0.1, MeOH); UV/Vis (MeOH) λ_{max} (log ϵ) 206 (3.72) nm (c = 0.005, MeOH); ECD (c = 0.02, MeOH): λ_{max} ($\Delta\epsilon$) 235 (−0.8), 211 (+2.4) nm; NMR data (¹H: 700 MHz, ¹³C NMR 175 MHz, Acetone-*d*₆) see Table 1; ESIMS m/z 266.10 [M + H]⁺, 265.01 [M − H][−]; HRESIMS m/z 266.1750 [M + H]⁺ (calcd. for C₁₅H₂₄NaO₃, 266.1751); t_R = 4.6 min.

6,7-Dehydro-isodrimenediol (**3**) white solid; $[\alpha]_D^{20}$ = +10 (c = 0.04, MeOH); UV/Vis (MeOH) λ_{max} (log ϵ) 235 (3.70), 201 (3.50) nm (c = 0.0025, MeOH); ECD (c = 0.02, MeOH): λ_{max} ($\Delta\epsilon$) 234 (+1.3) nm; NMR data (¹H: 700 MHz, ¹³C NMR 175 MHz, MeOH-*d*₄) see Table 1; ESIMS m/z 219.09 [M − H₂O + H]⁺; HRESIMS m/z 219.1738 [M − H₂O + H]⁺ (calcd. for C₁₅H₂₃O, 219.1743); t_R = 6.1 min.

Isodrimeniol (**4**) yellow oil; $[\alpha]_D^{20}$ = −5 (c = 0.1, MeOH); UV/Vis (MeOH) λ_{max} (log ϵ) 201 (0.46) nm (c = 0.005, MeOH); ECD (c = 0.1, MeOH): λ_{max} ($\Delta\epsilon$) 190 (+0.9) nm; NMR data (¹H: 500 MHz, ¹³C NMR 125 MHz, Acetone-*d*₆) see Table 2; HRESIMS [M + H]⁺ m/z 219.1740, calcd. 219.1743 for C₁₅H₂₃O, [2M + H]⁺ m/z 437.3412, calcd. 437.3414 for C₃₀H₄₅O₂, [2M + Na]⁺ m/z 581.2830, calcd. 581.2833 for C₃₀H₄₂N₂NaO₈, t_R = 7.09 min, data are in good agreement with the literature [22].

Glycinyll derivative of deacetylugandensolide (**5**) light yellow oil; $[\alpha]_D^{20}$ = +36 (c = 0.1, MeOH); UV/Vis (MeOH) λ_{max} (log ϵ) 212.5 (0.545) nm (c = 0.005, MeOH); ECD (c = 0.1, MeOH): λ_{max} ($\Delta\epsilon$) 210 (+5.2) nm; NMR data (¹H: 500 MHz, ¹³C NMR 125 MHz, MeOH-*d*₄) see Table 2; HRESIMS [M + H]⁺ m/z 352.2124, calcd. 352.2118 for C₁₉H₃₀NO₅, [M + Na]⁺ m/z 374.1933, calcd. 374.1938 for C₁₉H₂₉NNaO₅, [2M + H]⁺ m/z 725.3976, calcd. 725.4008 for C₄₀H₅₇N₂O₁₀, [2M + Na]⁺ m/z 747.3802, calcd. 747.3827 for C₄₀H₅₆N₂NaO₁₀, t_R = 6.04 min.

4-Aminobutyl derivative of ugandensolide (**6**) light yellow oil; $[\alpha]_D^{20} = +31$ ($c = 0.1$, MeOH); UV/Vis (MeOH) λ_{\max} ($\log \epsilon$) 211.5 (0.681) nm ($c = 0.005$, MeOH); ECD ($c = 0.1$, MeOH): λ_{\max} ($\Delta\epsilon$) 205 (+4.9) nm; NMR data (^1H : 500 MHz, ^{13}C NMR 125 MHz, Acetone- d_6) see Table 2; HRESIMS $[\text{M} + \text{H}]^+ m/z$ 366.1915, calcd. 366.1911 for $\text{C}_{19}\text{H}_{28}\text{NO}_6$, $[\text{M} + \text{Na}]^+ m/z$ 388.1727, calcd. 388.1731 for $\text{C}_{19}\text{H}_{27}\text{NNaO}_6$, $[2\text{M} + \text{H}]^+ m/z$ 731.3747, calcd. 731.3750 for $\text{C}_{38}\text{H}_{55}\text{N}_2\text{O}_{12}$, $[2\text{M} + \text{Na}]^+ m/z$ 755.3627, calcd. 755.3608 for $\text{C}_{52}\text{H}_{48}\text{N}_2\text{NaO}_2$, $t_R = 7.64$ min.

3.6. Cytotoxicity Assay

In vitro cytotoxicity (IC_{50}) was determined as previously described [34]. In brief, the assay was performed against a mouse fibroblast cell line (L929) and HeLa (KB-3.1) to screen the cytotoxicity of all compounds. Compound **5** was tested against further cell lines including epidermoid carcinoma cells (A431), adenocarcinomic human alveolar basal epithelial cells (A549), breast cancer cells (MCF-7), prostate cancer cells (PC-3), and human ovary adenocarcinoma (SK-OV-3). All cell lines were purchased from the DSMZ collection (Braunschweig, Germany). Cell lines L929, A549, and KB-3.1 were cultured in Dulbecco's modified Eagle's medium (DMEM; Gibco; Thermo Fisher Scientific, Dreieich, Germany); MCF-7 and A431 cells were cultured in RPMI-1640 medium (Gibco) and PC-3 cells in F12K (Gibco) medium, all supplemented with 10% fetal bovine serum (FCS; Gibco) and incubated under 5% CO_2 at 37 °C. The tested compound was dissolved in methanol to yield a concentration of 1 mg/mL. A 60 μL amount of 1:1 serial dilutions of the test compounds was added to 120 μL aliquots of a cell suspension (50/mL) in 96-well microplates. After 5 days of incubation, an MTT (3-(4,5-dimethylthiazol-2-yl)-2,5-diphenyltetrazolium bromide) assay was performed. IC_{50} was reported at the concentration of the compounds that inhibited the growth of cells at 50% of the control. Methanol was used as a negative control.

3.7. Antimicrobial Assay

The minimum inhibitory concentrations (MICs) were determined according to previous reports [31]. Briefly, the MIC values were obtained using a serial dilution assay in 96-well microtiter plates. A stock solution of each compound was prepared (1 mg/mL in methanol) and 60 μL was pipetted into the first row (A) of the plate, containing 130 μL of a mixture of the test organisms (Table S2) and the culture medium. Next, 150 μL of the mixture mentioned above was pipetted to the first row and mixed gently, then 150 μL was transferred to the second row that already contained 150 μL of a mixture, and mixed by repeated pipetting before transferring to the next row until the last row (H) was reached. A 1:1 serial dilution was performed and the last 150 μL was discarded. Incubation was performed in a microplate vibrating shaker (Heidolph, Schwabach, Germany; model Titramax 1000) at 200 rpm, with an incubated temperature of 30 °C for yeast and fungi and 37 °C for bacteria, for 24–48 h. The lowest concentration of the compounds preventing visible growth of the tested microorganisms was reported as the MIC. Tested concentrations ranged from 66.7 to 0.1 $\mu\text{g/mL}$.

4. Conclusions

Five new drimane sesquiterpenoids from cultures of two tropical basidiomycetes (i.e., *Perenniporia centrali-africana*, and *Cerrena* sp. nov.), denoted as one new derivative of pereniporin A, namely 3 β -hydroxy-9-dehydroxy-pereniporin A, as well as three new drimane sesquiterpene lactams including 6,7-dihydroxy-12-deoxy-dysidealactam, glycinyl of deacetylugandensolide, and 4-aminobutyl derivative of ugandensolide, and 6,7-dehydroisodrimenediol were isolated in this study. This is the first report of the isolation of sesquiterpene lactams from tropical Basidiomycota from two different countries (i.e., Kenya and Thailand). Although both basidiomycetes belong to different families, they produce similar types of compounds, some of which were never isolated previously. None of the sesquiterpene lactams showed biological activities in this study. Studies of the metabolites on other biological activities are presently underway.

Supplementary Materials: The following supporting information can be downloaded at: <https://www.mdpi.com/article/10.3390/molecules27185968/s1>, Figure S1: BLAST comparison, Figure S2: The structure of all known compounds in the study, Figures S3–S50: ESIMS, HR-ESIMS, 1D and 2D NMR spectra. Tables S1–S5: ITS sequence and results of biological assays. Reference [31] is cited in the Supplementary Materials.

Author Contributions: Formal analysis, F.S.; Funding acquisition, C.B.; Investigation, P.P., S.P., T.B. and R.C.; Project administration, M.S.; Resources, J.C.M. and C.D. All authors have read and agreed to the published version of the manuscript.

Funding: P.P. is grateful to be supported by the Royal Golden Jubilee Ph.D. Program (RGJ-PhD) (Grant No. PHD/0039/2560) and the German Academic Exchange Service (DAAD) research grants' One-Year Grants for doctoral candidates, 2020/21 (57507870). Furthermore, C.D., J.C.M., and M.S. are grateful for the "ASAFEM" Project (grant No. IC-070), under the ERAfrica Programme. This research also benefitted from the European Union's H2020 Research and Innovation Staff Exchange program (RISE), Grant No. 101008129: MYCOBIOMICS; beneficiaries M.S. and J.C.M. Lastly, this research was also supported by Mahidol University and the CIF Grant, Faculty of Science, Mahidol University.

Institutional Review Board Statement: Not applicable.

Informed Consent Statement: Not applicable.

Data Availability Statement: The data are available in the Supporting Information of the article.

Acknowledgments: We thank Wera Collisi and Christel Kakoschke for conducting the cytotoxicity assay and NMR spectroscopic measurements, respectively. Expert technical assistance from Silke Reinecke as well as Esther Surges is appreciated. Lastly, we want to thank Kevin Becker and Clara Chepkirui for their work on the structure elucidation in the initial stage of this project. We are grateful to the Plant Genetics Conservation Project under the Royal Initiative of Her Royal Highness Maha Chakri Sirindhorn (RSPG).

Conflicts of Interest: The authors declare no conflict of interest.

Sample Availability: Samples of the compounds are not available from the authors as the material has been used up for bioassays.

References

1. Gressler, M.; Löhr, N.A.; Schäfer, T.; Lawrinowitz, S.; Seibold, P.S.; Hoffmeister, D. Mind the mushroom: Natural product biosynthetic genes and enzymes of Basidiomycota. *Nat. Prod. Rep.* **2021**, *38*, 702–722. [\[CrossRef\]](#)
2. Sandargo, B.; Chepkirui, C.; Cheng, T.; Chaverra-Muñoz, L.; Thongbai, B.; Stadler, M.; Hüttel, S. Biological and chemical diversity go hand in hand: Basidiomycota as source of new pharmaceuticals and agrochemicals. *Biotechnol. Adv.* **2019**, *37*, 107344. [\[CrossRef\]](#) [\[PubMed\]](#)
3. Sandargo, B.; Kaysan, L.; Teponno, R.B.; Richter, C.; Thongbai, B.; Surup, F.; Stadler, M. Analogs of the carotane antibiotic fulvoferuginin from submerged cultures of a Thai *Marasmius* sp. *Beilstein J. Org. Chem.* **2021**, *17*, 1385–1391. [\[CrossRef\]](#) [\[PubMed\]](#)
4. Richter, C.; Helaly, S.E.; Thongbai, B.; Hyde, K.D.; Stadler, M. Pyristriatins A and B: Pyridino-Cyathane antibiotics from the Basidiomycete *Cyathus* cf. *striatus*. *J. Nat. Prod.* **2016**, *79*, 1684–1688. [\[CrossRef\]](#)
5. Cheng, T.; Chepkirui, C.; Decock, C.; Matasyoh, J.C.; Stadler, M. Skeletocutins M–Q: Biologically active compounds from the fruiting bodies of the basidiomycete *Skeletocutis* sp. *Beilstein J. Org. Chem.* **2019**, *15*, 2782–2789. [\[CrossRef\]](#)
6. Cheng, T.; Chepkirui, C.; Decock, C.; Matasyoh, J.C.; Stadler, M. Sesquiterpenes from an Eastern African medicinal mushroom belonging to the genus *Sanghuangporus*. *J. Nat. Prod.* **2019**, *82*, 1283–1291. [\[CrossRef\]](#)
7. Zhao, C.L.; Cui, B.K.; Dai, Y.C. New species and phylogeny of *Perenniporia* based on morphological and molecular characters. *Fungal Divers.* **2013**, *58*, 47–60. [\[CrossRef\]](#)
8. Lee, J.S.; Lim, Y.W. *Cerrena aurantiopora* sp. nov. (Polyporaceae) from eastern Asia. *Mycologia* **2010**, *102*, 211–216. [\[CrossRef\]](#)
9. Winkler, E.; Moilanen, U.; Mettälä, A.; Leisola, M.; Hatakka, A. Production of lignin modifying enzymes on industrial waste material by solid-state cultivation of fungi. *Biochem. Eng. J.* **2008**, *42*, 128–132. [\[CrossRef\]](#)
10. Belova, O.V.; Lisov, A.V.; Vinokurova, N.G.; Kostenevich, A.A.; Sapunova, L.I.; Lobanok, A.G.; Leontievsky, A.A. Xylanase and cellulase of fungus *Cerrena unicolor* VKM F-3196: Production, properties, and applications for the saccharification of plant material. *Appl. Biochem. Microbiol.* **2014**, *50*, 148–153. [\[CrossRef\]](#)
11. Sulej, J.; Janusz, G.; Osirńska-Jaroszuk, M.; Rachubik, P.; Mazur, A.; Komanińska, I.; Choma, A.; Rogalski, J. Characterization of cellobiose dehydrogenase from a biotechnologically important *Cerrena unicolor* strain. *Appl. Biochem. Biotechnol.* **2015**, *176*, 1638–1658. [\[CrossRef\]](#) [\[PubMed\]](#)

12. Kachlishvili, E.; Jokharidze, T.; Kobakhidze, A.; Elisashvili, V. Enhancement of laccase production by *Cerrena unicolor* through fungal interspecies interaction and optimum conditions determination. *Arch. Microbiol.* **2021**, *203*, 3905–3917. [[CrossRef](#)] [[PubMed](#)]
13. Kwon, J.; Lee, H.; Seo, Y.H.; Yun, J.; Lee, J.; Kwon, H.C.; Guo, Y.; Kang, J.S.; Kim, J.J.; Lee, D. Cytotoxic drimane sesquiterpenoids isolated from *Perenniporia maackiae*. *J. Nat. Prod.* **2018**, *81*, 1444–1450. [[CrossRef](#)]
14. He, J.B.; Tao, J.; Miao, X.S.; Bu, W.; Zhang, S.; Dong, Z.J.; Li, Z.H.; Feng, T.; Liu, J.K. Seven new drimane-type sesquiterpenoids from cultures of fungus *Laetiporus sulphureus*. *Fitoterapia* **2015**, *102*, 1–6. [[CrossRef](#)] [[PubMed](#)]
15. Clarkson, C.; Madikane, E.V.; Hansen, S.H.; Smith, P.J.; Jaroszewski, J.W. HPLC-SPE-NMR characterization of sesquiterpenes in an antimycobacterial fraction from *Warburgia salutaris*. *Planta Med.* **2007**, *73*, 578–584. [[CrossRef](#)]
16. Madikane, V.E.; Bhakta, S.; Russell, A.J.; Campbell, W.E.; Claridge, T.D.W.; Elisha, B.G.; Davies, S.G.; Smith, P.; Sim, E. Inhibition of mycobacterial arylamine N-acetyltransferase contributes to anti-mycobacterial activity of *Warburgia salutaris*. *Bioorg. Med. Chem.* **2007**, *15*, 3579–3586. [[CrossRef](#)]
17. Kida, T.; Shibai, H.; Seto, H. Structure of new antibiotics, pereniporins A and B, from a Basidiomycete. *J. Antibiot.* **1986**, *39*, 5–24. [[CrossRef](#)]
18. Toshihiro, H.; Motoo, T.; Yasuo, M.; Yoshinori, A. Cryptoporic acids A and B, novel bitter drimane sesquiterpenoid ethers of isocitric acid, from the fungus *Cryptoporus volvatus*. *Tetrahedron Lett.* **1987**, *28*, 6303–6304.
19. Hirotani, M.; Furuya, T.; Shiro, M. Cryptoporic acids H and I, drimane sesquiterpenes from *Ganoderma neo-japonicum* and *Cryptoporus volvatus*. *Phytochemistry* **1991**, *30*, 1555–1559. [[CrossRef](#)]
20. Kioy, D.; Gray, A.I.; Waterman, P.G. A comparative study of the stem-bark drimane sesquiterpenes and leaf volatile oils of *Warburgia ugandensis* and *W. Stuhlmannii*. *Phytochemistry* **1990**, *29*, 3535–3538. [[CrossRef](#)]
21. Cabrera, G.M.; Julia Roberti, M.; Wright, J.E.; Seldes, A.M. Cryptoporic and isocryptoporic acids from the fungal cultures of *Polyporus arcularius* and *P. ciliatus*. *Phytochemistry* **2002**, *61*, 189–193. [[CrossRef](#)]
22. Rodríguez, B.; Zapata, N.; Medina, P.; Viñuela, E. A complete ¹H and ¹³C NMR data assignment for four drimane sesquiterpenoids isolated from *Drimys winterii*. *Magn. Reson. Chem.* **2005**, *43*, 82–84. [[CrossRef](#)] [[PubMed](#)]
23. Liu, H.; Tan, H.; Chen, K.; Chen, Y.; Li, S.; Li, H.; Zhang, W. Cerrenins A–C, cerapicane and isohirsutane sesquiterpenoids from the endophytic fungus *Cerrena* sp. *Fitoterapia* **2018**, *129*, 173–178. [[CrossRef](#)] [[PubMed](#)]
24. Liu, H.X.; Tan, H.B.; Chen, Y.C.; Li, S.N.; Li, H.H.; Zhang, W.M. Cytotoxic triquinane-type sesquiterpenoids from the endophytic fungus *Cerrena* sp. A593. *Nat. Prod. Res.* **2020**, *34*, 2430–2436. [[CrossRef](#)] [[PubMed](#)]
25. Khushi, S.; Salim, A.A.; Elbanna, A.H.; Nahar, L.; Bernhardt, P.V.; Capon, R.J. Dysidealactams and dysidealactones: Sesquiterpene glycinyllactams, imides, and lactones from a *Dysidea* sp. marine sponge collected in southern Australia. *J. Nat. Prod.* **2020**, *83*, 1577–1584. [[CrossRef](#)]
26. Lin, Y.C.; Abd El-Razek, M.H.; Shen, Y.C. Verticillane-type diterpenoids and an eudesmanolide-type sesquiterpene from the formosan soft coral *Cespitularia hypotentaculata*. *Helv. Chim. Acta* **2010**, *93*, 281–289. [[CrossRef](#)]
27. Lou, Y.; Zhao, F.; Wu, Z.; Peng, K.F.; Wei, X.C.; Chen, L.X.; Qiu, F. Germacrane-type sesquiterpenes from *Curcuma wenyujin*. *Helv. Chim. Acta* **2009**, *92*, 1665–1672. [[CrossRef](#)]
28. Nomoto, Y.; Harinantenaina, L.; Sugimoto, S.; Matsunami, K.; Otsuka, H. 3,4-seco-24-homo-28-nor-Cycloartane and drimane-type sesquiterpenes and their lactams from the EtOAc-soluble fraction of a leaf extract of *Cinnamosma fragrans* and their biological activity. *J. Nat. Med.* **2014**, *68*, 513–520. [[CrossRef](#)]
29. Justo, A.; Miettinen, O.; Floudas, D.; Ortiz-Santana, B.; Sjökvist, E.; Lindner, D.; Nakasone, K.; Niemelä, T.; Larsson, K.H.; Ryvarden, L.; et al. A revised family-level classification of the Polyporales (Basidiomycota). *Fungal Biol.* **2017**, *121*, 798–824. [[CrossRef](#)]
30. Huang, Y.; Hoefgen, S.; Valiante, V. Biosynthesis of fungal drimane-type sesquiterpene esters. *Angew. Chem. Int. Ed.* **2021**, *60*, 23763–23770. [[CrossRef](#)]
31. Matio Kemkuignou, B.; Treiber, L.; Zeng, H.; Schrey, H.; Schobert, R.; Stadler, M. Macrooxazoles a–d, new 2,5-disubstituted oxazole-4-carboxylic acid derivatives from the plant pathogenic fungus *Phoma macrostoma*. *Molecules* **2020**, *25*, 5497. [[CrossRef](#)] [[PubMed](#)]
32. Wendt, L.; Sir, E.B.; Kuhnert, E.; Heitkampfer, S.; Lambert, C.; Hladki, A.I.; Romero, A.I.; Luangsa-ard, J.J.; Srikritikulchai, P.; Peršoh, D.; et al. Resurrection and emendation of the Hypoxylaceae, recognised from a multigene phylogeny of the Xylariales. *Mycol. Prog.* **2018**, *17*, 115–154. [[CrossRef](#)]
33. Otto, A.; Laub, A.; Wendt, L.; Porzel, A.; Schmidt, J.; Palfner, G.; Becerra, J.; Krüger, D.; Stadler, M.; Wessjohann, L.; et al. Chilenopeptins A and B, peptaibols from the Chilean *Sepedonium* aff. *chalcipori* KSH 883. *J. Nat. Prod.* **2016**, *79*, 929–938. [[CrossRef](#)] [[PubMed](#)]
34. Hassan, K.; Matio Kemkuignou, B.; Stadler, M. Two new triterpenes from basidiomata of the medicinal and edible mushroom, *Laetiporus sulphureus*. *Molecules* **2021**, *26*, 7090. [[CrossRef](#)]

Paper II

Calamene-type Sesqui-, Mero- and Bis-sesquiterpenoids from Cultures of *Heimiomyces* sp., a Basidiomycete Collected in Africa

Sebastian Pfütze^{1,2}, Atchara Khamisim^{1,2}, Frank Surup^{1,2}, Cony Decock³, Josphat C. Matasyoh⁴, Marc Stadler^{1,2,*}

Journal of Natural Products **2023**; 86(2):390–397.

DOI: <https://doi.org/10.1021/acs.jnatprod.2c01015>

- ¹ Department of Microbial Drugs, Helmholtz Centre for Infection Research (HZI), German Centre for Infection Research (DZIF), Partner Site Hannover/Braunschweig, Inhoffenstrasse 7, 38124 Braunschweig, Germany
- ² Institute of Microbiology, Technische Universität Braunschweig, Spielmannstraße 7, 38106 Braunschweig, Germany
- ³ Mycothèque de l'Université Catholique de Louvain (BCCM/MUCL), Earth and Life Institute, Microbiology, B-1348 Louvain-la-Neuve, Belgium
- ⁴ Department of Chemistry, Egerton University, P.O BOX 536, 20115, Njoro, Kenya

*Corresponding author

Calamene-Type Sesqui-, Mero-, and Bis-sesquiterpenoids from Cultures of *Heimiomyces* sp., a Basidiomycete Collected in Africa

Sebastian Pfütz, Atchara Khamsim, Frank Surup, Cony Decock, Josphat C. Matasyoh, and Marc Stadler*



Cite This: <https://doi.org/10.1021/acs.jnatprod.2c01015>



Read Online

ACCESS |

Metrics & More

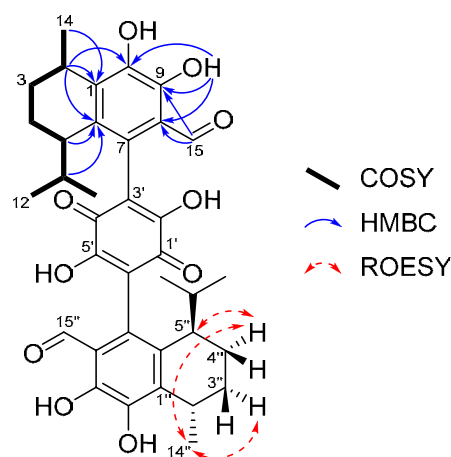
Article Recommendations

Supporting Information

ABSTRACT: New meroterpenoids bis-heimiomycons A–D (1–4) and heimiomycons D and E (5 and 6) were isolated from solid rice cultures of *Heimiomyces* sp., while new calamene-type sesquiterpenoids heimiocalamene A (7) and B (8) were isolated from shake cultures, respectively. Structures of the metabolites were elucidated by 1D and 2D NMR in addition to HRESIMS data. While relative configurations were assigned by ROESY data, absolute configurations were derived from the structurally related, previously described calamenes, which we herein name heimiocalamenes C–E (9–11). A plausible biosynthetic pathway was proposed for 1–6, with a radical reaction connecting their central *para*-benzoquinone building block to calamene-sesquiterpenoids. Based on the assumption of a common biosynthesis, we reviewed the structure of the known nitrogen-containing derivative 11, calling the validity of the originally proposed structure into question. Subsequently, the structure of 11 was revised by analysis of HMBC and ROESY NMR data. Only heimiomycon D (5) displayed cytotoxic effects against cell line KB3.1.



Basidiomycota represent the second largest phylum in the kingdom of fungi and are well known to show both a high biological diversity by comprising more than 35,000 species¹ and a high chemical diversity of their secondary metabolites, leading to the identification of many different classes of natural products and especially important bioactive molecules like strobilurins and pleuromutilins.² In particular, these species can be found in partly untapped ecosystems that have not been exhaustively explored yet. For this reason, *Heimiomyces* sp. (MUCL 56078, collected from Mount Elgon National Reserve, Kenya) was evaluated for its secondary metabolite profile, and previous studies led to the identification of several new secondary metabolites (9–14).³ In the course of this work, the presence of a vast amount of secondary metabolites was observed within the extracts, which led to further studies on this strain. Herein, we present the isolation, structure elucidation, and biological evaluation of new meroterpenoids bis-heimiomycons A–D and heimiomycons D and E (1–6) from solid rice cultures, as well as the new calamene-type sesquiterpenoids heimiocalamenes A (7) and B (8) from shaking cultures of *Heimiomyces* sp. Furthermore, known compounds heimiomycon B (13), hispidin (15), and hypholomin B (16) (Figures 2 and S4) were isolated from both liquid and solid cultures. Heimiomycon B (13) was recently published together with heimiomycons A and C, as well as three new calamene derivatives (Figure 2), which we propose to name heimiocalamenes C–E (9–11), after isolation from liquid cultures of *Heimiomyces* sp.,³ emphasizing



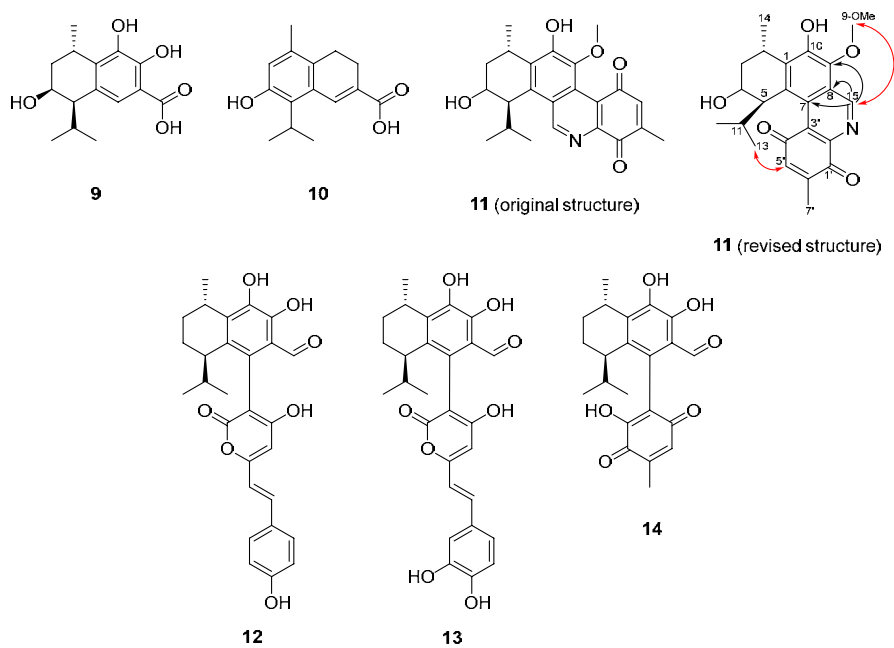


Figure 2. Compounds previously isolated from *Heimiomyces* sp. **9–11**: heimiocalamenes C–E (including originally proposed and revised structure of **11** with key HMBC (black arrows) and ROESY (red arrows) correlations); **12–14**: heimiomycins A–C.

that this species shows a very diverse secondary metabolite profile.

RESULTS AND DISCUSSION

Bis-heimiomycin A (**1**) was isolated as a red oil from extracts of solid rice cultures. Its HRESIMS data indicated the molecular formula $C_{36}H_{40}O_{10}$ according to the molecular ion cluster at m/z 633.2695 $[M + H]^+$, indicating 17 degrees of unsaturation. Based on the molecular formula together with the carbon and proton resonances a symmetry within the molecule was assumed: 1H NMR (Table 1) and HSQC data led to the identification of three methyls (H_3 -12/12", H_3 -13/13", H_3 -14/14"), four methylenes (H -3 α /3" α , H -3 β /3" β , H -4 α /4" α , H -4 β /4" β), three methines (H -2 β /2" β , H -5 α /5" α , H -11/11"), and one aldehyde function (H -15/15"). The ^{13}C (Table 1) and HMBC NMR data revealed the presence of 16 carbon resonances, comprising one carbonyl carbon (C -15/15"), seven nonprotonated sp^2 -hybridized carbons (C -1/1", C -2'/5', C -6/6", C -7/7", C -8/8", C -9/9", C -10/10"), three methines (C -2/2", C -5/5", C -11/11"), two methylene carbons (C -3/3", C -4/4"), and three methyl carbons (C -12/12", C -14/14", C -13/13"). By analyzing the COSY data a spin system between H_3 -14, H -2, H_2 -3, H_2 -4, H -5, H -11, and H_3 -12/ H_3 -13 was constructed. HMBC correlations from H_3 -14 to C -1/ C -2/ C -3, H -11 to C -4/ C -5/ C -6/ C -12/ C -13, and H_3 -12/ H_3 -13 to C -5/ C -11 revealed a 5-isopropyl-2-methylcyclohex-1-ene substructure. Further HMBC correlations from H -2 to C -1/ C -10, H -5 to C -6, 9-OH to C -8/ C -9/ C -10, and H -15 to C -8/ C -9/ C -10 led to the identification of a dihydroxybenzaldehyde substructure that was fused to the 5-isopropyl-2-methylcyclohex-1-ene substructure across C -1 and C -6. The carbonyl and sp^2 -hybridized carbons, as well as the two rings of the calamene-type substructure, accounted for 7 degrees of unsaturation, leaving 10 degrees of unsaturation to be assigned within the scaffold of bis-heimiomycin A (**1**). This led to the assumption of two calamene-type substructures being linked by a central dihydroxy-quinone moiety. Nevertheless, of the

potential dihydroxy-quinone moiety only C -2'/ C -5' could be observed in the ^{13}C spectrum, whereas signals for carbons C -1'/ C -3'/ C -4'/ C -6' were missing. To prevent rapid tautomerism, which was assumed to be the reason for the missing resonances, bis-heimiomycin A (**1**) was reacted with acetic anhydride in pyridine and positions C -15/ C -15", 2'-OH/5'-OH, 9OH/9"OH, and 10OH/10"OH were derivatized. Based on 1D and 2D NMR data (Table S5) of the resulting product **1b**, peracetylation and a ring closure at C -15/ C -15" of **1** were confirmed due to the appearance of six additional methyls (H_3 -AcC2-9/9", H_3 -AcC2-10/10", H_3 -AcC2-15/15"), six carbonyl carbons (AcC 1-9/9", AcC 1-10/10", AcC 1-15/15"), and two oxymethines (H -15/15"). Key HMBC correlations from H -15 to C -2'/ C -8/ C -9/ AcC 1-15 and H -15" to C -5'/ C -8"/ C -9"/ AcC 1-15", as well as carbons C -1'/ C -2'/ C -3'/ C -4'/ C -5'/ C -6', could be observed in the HMBC and ^{13}C spectra, leading to a confirmation of the structure previously assumed for **1**. The relative and absolute configurations were assigned as 2*S*,2'*S*,5*R*,5'*R* by comparison of ^{13}C and ROESY data, as well as ECD spectra (Figure S1), to related calamene-type derivatives described by Cheng et al.,³ which were previously isolated from the same fungal strain (*Heimiomyces* sp. MUCL 56078) and showed similar correlations.

Bis-heimiomycin B (**2**), C (**3**), and D (**4**) were isolated as closely related congeners of **1**. With the molecular formula $C_{36}H_{40}O_9$, bis-heimiomycin B (**2**) implies the loss of an oxygen in comparison to **1**. Proton NMR (Table 1) and HSQC data of **2** indicated the presence of an additional oxymethylene (H_2 -15"). HMBC correlations from H_2 -15" to C -5'/ C -6"/ C -7"/ C -8"/ C -9"/ C -10" revealed a ring closure at C -15" after elimination of an oxygen. In the 1D and 2D NMR spectra of bis-heimiomycin C (**3**) the presence of another oxymethylene group (H_2 -15) and the absence of the aldehyde H -15 occurred as a key difference in **2**. Interactions from H_2 -15 to C -7/ C -8/ C -9 obtained from HMBC data were consistent with the reduction of **3** at C -15". Finally, bis-heimiomycin D (**4**) with

Table 1. ^{13}C and ^1H NMR Spectroscopic Data of Compounds 1–4 in Acetone- d_6 (δ in ppm)

| no. | 1 ^{b,c} | | 2 ^{b,d} | | 3 ^{b,d} | | 4 ^{a,d} | |
|-------|------------------------------------|-------------------------------|----------------------------|-------------------------------|----------------------------|-------------------------------|----------------------------|-------------------------------|
| | δ_{C} , type | δ_{H} (J in Hz) | δ_{C} , type | δ_{H} (J in Hz) | δ_{C} , type | δ_{H} (J in Hz) | δ_{C} , type | δ_{H} (J in Hz) |
| 1 | 137.9, C | | 139.0, C | | 128.9, C | | 131.4, C | |
| 2 | 27.8, CH | β : 3.42, m | 28.8, CH | β : 3.41, m | 27.5, CH | 3.28, m | 28.4, CH | β : 3.35, m |
| 3 | 25.1, CH ₂ | α : 1.49, br d (13.6) | 26.1, CH ₂ | α : 1.48, m | 26.3, CH ₂ | 1.45, m | 26.8, CH ₂ | α : 1.49, m |
| | | β : 2.15, m | | β : 2.09, m | | 2.08, s | | β : 1.99, m |
| 4 | 19.6, CH ₂ | α : 1.82, m | 20.4, CH ₂ | α : 1.79, m | 19.9, CH ₂ | 1.77, m | 19.7, CH ₂ | α : 1.70, m |
| | | β : 1.89, br s | | β : 2.00, m | | 1.99, m | | β : 1.96, m |
| 5 | 40.8, CH | α : 2.48, br s | 42.0, CH | α : 2.35, br s | 41.2, CH | 2.74, m | 40.3, CH | α : 2.81, m |
| 6 | 132.6, C | | 133.6, C | | 124.6, C | | 132.5, C | |
| 7 | 132.6, C | | 124.2, C | | 118.4, C | | 117.8, C | |
| 8 | 115.9, C | | 116.4, C | | 122.2, C | | 120.3, C | |
| 9 | 147.8, C | | 148.8, C | | 142.2, C | | 145.8, C | |
| 9OH | | 11.94 | | 11.90 | | | | |
| 10 | 142.7, C | | 143.5, C | | 143.7, C | | 138.2, C | |
| 11 | 33.1, CH | 1.75, m | 33.6, CH | 1.85, m | 34.0, CH | 1.63, m | 34.6, CH | 1.70, m |
| 12 | 21.6, CH ₃ ^e | 0.82, d (6.9) | 22.2, CH ₃ | 0.84, d (6.9) | 21.8, CH ₃ | 0.65, d (6.9) | 22.0, CH ₃ | 0.64, d (6.7) |
| 13 | 20.0, CH ₃ | 0.79, d (6.9) | 21.1, CH ₃ | 0.78, d (6.9) | 20.1, CH ₃ | 0.68, d (6.9) | 20.0, CH ₃ | 0.61, d (6.7) |
| 14 | 21.6, CH ₃ ^e | 1.23, d (6.9) | 22.6, CH ₃ | 1.24, d (6.9) | 22.6, CH ₃ | 1.21, d (6.9) | 22.7, CH ₃ | 1.21, d (7.0) |
| 15 | 198.8, CH | 9.88, s | 199.5, CH | 9.79, s | 62.5, CH ₂ | 4.55, d (13.8) | 67.0, CH ₂ | 4.68, d (13.0) |
| | | | | | | 4.82, d (13.8) | | 5.64, d (13.0) |
| 1' | <i>f</i> | <i>f</i> | 180.9, C | | <i>f</i> | <i>f</i> | 178.5, C | |
| 2' | 147.5, C | | 162.4, C | | <i>f</i> | <i>f</i> | 154.2, C | |
| 3' | <i>f</i> | <i>f</i> | 114.4, C | | <i>f</i> | <i>f</i> | 125.1, C | |
| 4' | <i>f</i> | <i>f</i> | 180.7, C | | <i>f</i> | <i>f</i> | 178.5, C | |
| 5' | 147.5, C | | 157.6, C | | 157.0, C | | 154.2, C | |
| 6' | <i>f</i> | <i>f</i> | 114.4, C | | 117.2, C | | 125.1, C | |
| 1'' | 137.9, C | | 131.4, C | | 131.0, C | | 131.4, C | |
| 2'' | 27.8, CH | β : 3.42, m | 28.5, CH | β : 3.36, m | 28.1, CH | 3.36, m | 28.4, CH | β : 3.35, m |
| 3'' | 25.1, CH ₂ | α : 1.49, br d (13.6) | 26.5, CH ₂ | α : 1.48, m | 26.3, CH ₂ | 1.45, m | 26.8, CH ₂ | α : 1.49, m |
| | | β : 2.15, m | | β : 2.09, m | | 2.08, s | | β : 1.99, m |
| 4'' | 19.6, CH ₂ | α : 1.82, m | 20.2, CH ₂ | α : 1.79, m | 19.9, CH ₂ | 1.77, m | 19.7, CH ₂ | α : 1.70, m |
| | | β : 1.89, br s | | β : 2.00, m | | 1.99, m | | β : 1.96, m |
| 5'' | 40.8, CH | α : 2.48, br s | 41.5, CH | α : 2.75, m | 41.7, CH | 2.24, m | 40.3, CH | α : 2.81, m |
| 6'' | 132.6, C | | 132.6, C | | 126.7, C | | 132.5, C | |
| 7'' | 132.6, C | | 117.5, C | | 132.1, C | | 117.8, C | |
| 8'' | 115.9, C | | 119.9, C | | 119.5, C | | 120.3, C | |
| 9'' | 147.8, C | | 146.0, C | | 138.0, C | | 145.8, C | |
| 9''OH | | 11.94 | | | | | | |
| 10'' | 142.7, C | | 138.3, C | | 145.6, C | | 138.2, C | |
| 11'' | 33.1, CH | 1.75, m | 34.3, CH | 1.66, sptd (6.9) | 33.3, CH | 1.85, m | 34.6, CH | 1.70, m |
| 12'' | 21.6, CH ₃ ^e | 0.82, d (6.9) | 20.4, CH ₃ | 0.69, d (6.9) | 20.7, CH ₃ | 0.72, d (6.9) | 22.0, CH ₃ | 0.64, d (6.7) |
| 13'' | 20.0, CH ₃ | 0.79, d (6.9) | 22.2, CH ₃ | 0.67, d (6.9) | 22.2, CH ₃ | 0.83, d (6.9) | 20.0, CH ₃ | 0.61, d (6.7) |
| 14'' | 21.6, CH ₃ ^e | 1.23, d (6.9) | 23.0, CH ₃ | 1.21, d (6.9) | 22.6, CH ₃ | 1.21, d (6.9) | 22.7, CH ₃ | 1.21, d (7.0) |
| 15'' | 198.8, CH | 9.88, s | 67.2, CH ₂ | 4.73, d (12.9) | 66.9, CH ₂ | 4.73, d (13.1) | 67.0, CH ₂ | 4.68, d (13.0) |
| | | | | 5.65, d (12.9) | | 5.64, d (13.1) | | 5.64, d (13.0) |

^a ^1H 500 MHz. ^b ^1H 700 MHz. ^c ^{13}C 125 MHz. ^d ^{13}C 175 MHz. ^eOverlapped. ^f $^1\text{H}/^{13}\text{C}$ chemical shifts not shown due to the absence of corresponding signals. ^g ^{13}C chemical shifts were extracted from the HMBC NMR spectrum, since compound 3 was degraded after the measurement of the ^1H , COSY, HSQC, and HMBC NMR data.

the molecular formula $\text{C}_{36}\text{H}_{40}\text{O}_8$ implied the loss of another oxygen in comparison to **2**, affording a second ring closure at C-15, leading to a symmetric molecule as observed for **1**. This was confirmed by the replacement of the aldehyde H-15/H-15'' by an oxymethylene H₂-15/H₂-15''. Relative and absolute configurations of **2**–**4** were deduced from **1** due to comparison of ECD spectra (Figure S1), ^{13}C NMR, and ROESY data to those of **1** and other calamene-type compounds described before,³ as well as the common biological source of these compounds.

Heimiomycin D (**5**) was isolated as a red oil from extracts of solid rice cultures. It was shown to possess the molecular formula $\text{C}_{22}\text{H}_{24}\text{O}_7$ by HRESIMS data according to the molecular ion cluster at m/z 401.1593 $[\text{M} + \text{H}]^+$ requiring 11 degrees of unsaturation. The proton (Table 2) and HSQC NMR spectra of **5** were highly similar to those of heimiomycin C (**14**).³ The key difference is an additional hydroxy group at position C-5'. The relative and absolute configurations were deduced as 2*S*,5*R* from **14** by comparison of ECD spectra and ^{13}C and ROESY data (Figure S2) to those of **14**³ and due the common source of both compounds.

Table 2. ^{13}C and ^1H NMR Spectroscopic Data of Compounds 5 and 6 in Acetone- d_6 and 7 and 8 in Methanol- d_4 (δ in ppm)

| no. | $5^{b,d}$ | | $6^{a,c}$ | | $7^{a,c}$ | | $8^{a,c}$ | |
|------|--------------------------|-------------------------------|--------------------------|-------------------------------|--------------------------|-------------------------------|--------------------------|-------------------------------|
| | δ_{C} type | δ_{H} (J in Hz) | δ_{C} type | δ_{H} (J in Hz) | δ_{C} type | δ_{H} (J in Hz) | δ_{C} type | δ_{H} (J in Hz) |
| 1 | 139.0, C | | 139.2, C | | 144.8, C | | 130.6, C | |
| 2 | 28.6, CH | β : 3.39, m | 28.6, CH | 3.41, dq (6.8, 6.8) | 35.1, CH | β : 2.32, m | 121.4, C | |
| 3 | 26.4, CH_2 | α : 1.46, m | 26.3, CH_2 | α : 1.48, m | 30.7, CH_2 | α : 1.88, m | 146.8, C | |
| | | β : 2.07, m | | β : 2.08, m | | β : 1.22, m | | |
| 4 | 20.0, CH_2 | 1.80, m | 19.9, CH_2 | 1.83, m | 21.4, CH_2 | α : 1.69, m | 142.0, C | |
| | | | | | | β : 1.46, m | | |
| 5 | 40.8, CH | α : 2.51, m | 41.0, CH | α : 2.46, br s | 43.6, CH | α : 2.14, m | 132.6, C | |
| 6 | 133.4, C | | 133.3, C | | 131.3, C | | 124.0, C | |
| 7 | 126.5, C | | 124.7, C | | 138.2, CH | 7.04, d (2.4) | 136.7, CH | 7.98, s |
| 8 | 117.4, C | | 117.2, C | | 125.5, C | | 126.6, C | |
| 9 | 148.3, C | | 148.6, C | | 22.4, CH_2 | 2.56, m | 22.7, CH_2 | 2.43, br dd (8.2, 8.2) |
| 9OH | | 11.84, s | | 11.86 | | | | |
| 10 | 142.8, C | | 143.6, C | | 28.1, CH_2 | 2.18, m | 26.2, CH_2 | 2.70, br dd (8.2, 8.2) |
| 11 | 34.3, CH | 1.70, m | 34.4, CH | 1.67, sptd (6.9, 6.9) | 30.9, CH | 1.97, m | 28.5, CH | 3.53, qq (7.2, 7.2) |
| 12 | 22.2, CH_3 | 0.71, d (6.9) | 20.6, CH_3 | 0.71, d (6.9) | 21.3, CH_3 | 0.96, d (6.9) | 22.1, CH_3^e | 1.39, d (7.2) ^e |
| 13 | 20.7, CH_3 | 0.69, d (6.9) | 22.1, CH_3 | 0.75, d (6.9) | 17.7, CH_3 | 0.73, d (6.9) | 22.1, CH_3^e | 1.39, d (7.2) ^e |
| 14 | 22.4, CH_3 | 1.19, m | 22.3, CH_3 | 1.21, d (6.8) | 18.9, CH_3 | 1.01, d (7.0) | 12.1, CH_3 | 2.18, s |
| 15 | 199.6, CH | 9.76, s | 199.2, CH | 9.82, s | 168.5, C | | 171.7, C | |
| 1' | 183.6, C | | <i>f</i> | <i>f</i> | | | | |
| 2' | 146.7, C | | <i>f</i> | <i>f</i> | | | | |
| 2'OH | | 6.83, s | <i>f</i> | <i>f</i> | | | | |
| 3' | 119.6, C | | 114.0, C | | | | | |
| 4' | 183.5, C | | <i>f</i> | <i>f</i> | | | | |
| 5' | 146.7, C | | <i>f</i> | <i>f</i> | | | | |
| 5'OH | | 6.83, s | <i>f</i> | <i>f</i> | | | | |
| 6' | 112.5, C | | 104.9, CH | 6.09, s | | | | |
| 7' | 7.8, CH_3 | 1.90, s | <i>f</i> | <i>f</i> | | | | |

^a ^1H 500 MHz. ^b ^1H 700 MHz. ^c ^{13}C 125 MHz. ^d ^{13}C 175 MHz. ^eOverlapped. ^f $^1\text{H}/^{13}\text{C}$ chemical shifts not shown due to the absence of signals.

For heimiomycin E (6) a molecular formula of $\text{C}_{21}\text{H}_{22}\text{O}_7$ was identified by HRESIMS data, indicating the formal loss of a CH_2 fragment in comparison to 5. Highly similar NMR spectra showed the absence of methyl group C-7', leaving an sp^2 -hybridized methine (H-6') as the difference between both. In contrast to 5, the signals for C-1', C-2', C-4', and C-5' were not visible, most likely due to tautomerism.

New calamene-type sesquiterpenoids heimioalamenes A (7) and B (8) were isolated from the mycelial extracts of liquid cultures. The molecular formula of 7 was assigned as $\text{C}_{15}\text{H}_{22}\text{O}_2$ according to the molecular ion cluster at m/z 235.1689 [$\text{M} + \text{H}$]⁺ in the HRESIMS spectrum. The NMR spectra of 7 were highly similar to those of 9. Key differences are the loss of the hydroxy group at C-4, resulting in a methylene (H_2 -4) and the replacement of the oxygenated sp^2 -hybridized carbons at C-9 and C-10 by two methylenes (H_2 -9 and H_2 -10). The relative and absolute configurations were deduced as 2*S*,5*R* by analogy to assignments for 9,³ as these compounds were isolated from the same biological source (*Heimiomyces* sp. MUCL 56078) and showed similar ROESY correlations. Heimioalamenes B (8) was identified as the 3-hydroxy derivative of 10 due to close similarities of their NMR data. ^{13}C (Table 2) and HMBC data revealed the presence of the oxygenated sp^2 -hybridized carbon at position C-3. We propose to name compounds 9–11 as heimioalamenes C–E, because they have been isolated from the same biological source and show structural similarities to 7 and 8.

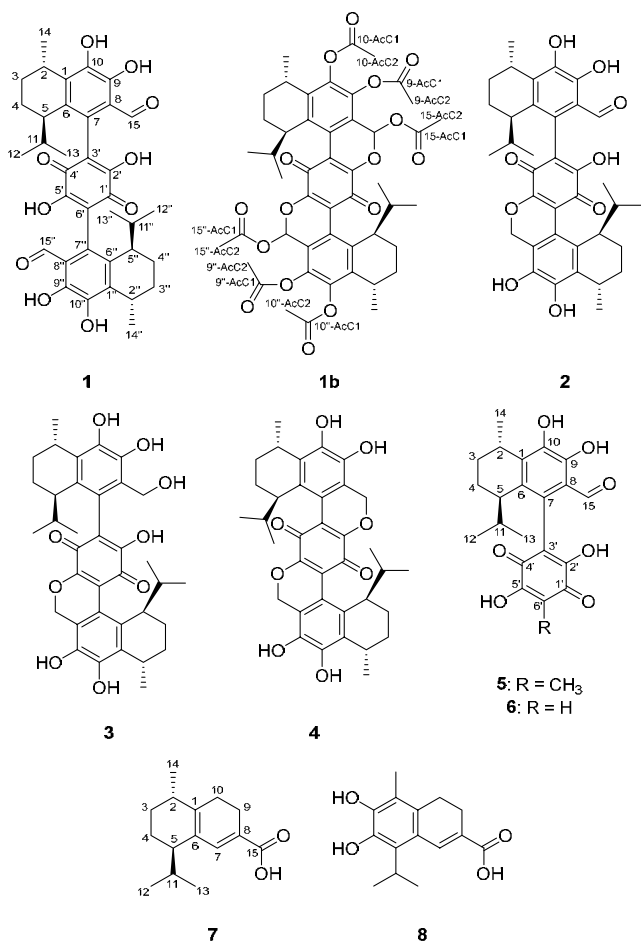
Minor isomers were observed in the HPLC-MS and NMR data for compounds 1 and 2. After purification via preparative HPLC, results from the analytical HPLC of compound 1

showed the presence of two peaks with the same molecular mass (Figure S5) in a ratio of 9:1. Since this ratio adjusted spontaneously, it is most likely caused by interconversion of 1 between two different forms of the compound. The presence of two peaks with the same molecular mass was also observed in the HPLC-MS data of compound 2 (Figure S6). This is also reflected in the ^1H and ^{13}C spectra of both 1 and 2, where additional weak signals of the minor isomers can be observed (Tables S4 and S6). However, two possible explanations to cause the presence of these minor isomers can be taken into account. On the one hand, the quinone substructure of 1–6 could possess a *para*- or *ortho*-orientation, while both would show similar features, and on the other hand, there is the possibility of atropisomerism within the molecules that would lead to different stereoisomers.

Compounds 1–6 were described to possess a *para*-quinone substructure due to comparison of their UV spectra (Figure S7) and ^{13}C data (Tables S4–10) to the ones of structurally related *para*- and *ortho*-quinones previously described in the literature.⁴ Especially, absorption maxima at lower wavelengths (maxima with strongest intensity at $\lambda_{\text{max}} = 240$ –300 nm and with medium intensity at $\lambda_{\text{max}} = 285$ –440 nm), characteristic for *para*-quinones, were observed, while the absorption maximum at 500–580 nm, characteristic for *ortho*-quinones, was not observed. However, UV spectra of 1b and 4 slightly differed from the ones of the other compounds. Therefore, IR spectra of compounds 1b and 4 (Figures S8 and S9) were measured and compared to the ones of similar quinones described in the literature to support the structural assignment of the *para*-quinone, since for *ortho*-quinones a characteristic

and well-separated carbonyl band around 1680–1700 cm^{-1} was not observed.⁴

For compounds 1–6 there is the possibility of hindered rotation around the C-3'/C-7 and C-6'/C-7" bonds. In the case of bis-heimiomycin A (1) and heimiomycins D and E (5 and 6) a tautomerism within the *p*-benzoquinone substructure is preventing atropisomerism, while compounds 2–4 did not show any effects in their ECD data that indicate the presence of atropisomers. The rapid conversion of possible atropisomers can be rationalized by low rotational barriers of the C-7/C-3' and C-6'/C-7" bonds. An effective radius of only 1.53 pm and rotational barrier of 27.1 kJ/mol had been determined by Bott et al. for the hydroxy group.⁵ Thus, we assume the keto and hydroxy substituents to be small enough for allowing rotation of the C-7/C-3' and C-6'/C-7" bonds.



Additionally, the previously described compounds heimiomycin B (13),³ hispidin (15),⁶ and hypholomin B⁷ (16) were observed in both liquid and solid cultures (Figures 2 and S4). Hispidin and its derivatives, including hypholomin B, are reported to show antioxidant effects.^{8–10}

The variety of secondary metabolites produced by *Heimiomyces* sp. MUCL 56078 can be explained by the combination of calamene-type sesquiterpenoid precursors with various oxidized building blocks. In the case of 1–4, the resulting intermediate undergoes another linkage reaction to a second calamene-type sesquiterpenoid precursor. These reactions might follow a radical mechanism, similar to the biosynthesis of the bibenzoquinone oosporein,¹¹ or an electrophilic aromatic substitution mechanism (Figure S5).

Both proposed mechanisms are expected to leave the configurations of carbon centers C-2 and C-5 unaffected. Nevertheless, two sesquiterpenoids being linked via a *p*-benzoquinone is an uncommon feature for natural products.¹² So far only a few similar compounds, like popolohuanones F–H^{13,14} and nakijiquinone E,¹⁵ have been described in the literature.

However, the structure of the nitrogen-containing derivative 11, isolated in the preceding study, did not match this logic. In particular, the biogenetic origin of the Schiff base carbon C-15 could not be mechanistically derived from the parental calamene scaffold. Therefore, we carefully reviewed the NMR data of 11 (Table S13) and observed HMBC correlations from H-15 to C-7, C-8, and C-9. By contrast, a correlation from H-15 to C-6 was not observed, which would have been expected for the structure proposed in our earlier study. In addition, ROESY correlations were observed between H-15/9-OMe and H₃-13/H-5', respectively, indicating that the linkages of C-15 and C-8 to the calamene moiety have to be exchanged (Figure 2). This assignment does explain the addition of an amino-*p*-benzoquinone to a calamene precursor as a possible biosynthetic pathway to 11.

All isolated compounds were evaluated for their antimicrobial activities in a serial dilution assay against several Gram positive and Gram negative bacteria as well as fungal strains, but were mostly inactive (Table S1). Furthermore, they were tested for cytotoxicity against the human cervical cancer cell line KB3.1 and the murine fibroblast cell line L929,¹⁶ where only heimiomycin D (5) showed cytotoxic effects against KB3.1 with an IC₅₀ of 6.3 μM (Table S2) and therefore was tested against further cell lines (Table S3), resulting in effects on breast cancer cell line MCF-7 (IC₅₀ of 2.5 μM), ovarian cancer cell line SKOV-3 (IC₅₀ of 3 μM), and skin cancer cell line A431 (IC₅₀ of 4.25 μM). Quinone derivatives have been reported to be an important class of molecules, showing a number of various biological activities, presumably due to their ability to undergo nucleophilic attacks and electron reductions.^{17,18} For this reason, compounds 1–6 should be considered as candidates for various other targets, such as antiviral or antioxidant assays.

In summary, cultivation of a *Heimiomyces* sp. led to the isolation and identification of new meroterpenoids (1–6) and two new calamene-type sesquiterpenoids (7 and 8), as well as the previously described hispidin (15), hypholomin B (16), and heimiomycin B (13), from shaking and solid rice cultures. Together with the compounds isolated in the preceding study (9–14),³ this *Heimiomyces* sp. showed a vast chemical diversity of its secondary metabolite profile, which emphasizes that Basidiomycota, especially unexplored species from the tropics, should be explored as potentially rich sources of novel natural products in the ongoing search for new drug leads.

EXPERIMENTAL SECTION

General Experimental Procedures. Measurements of the optical rotation were performed using a PerkinElmer 241 polarimeter. UV spectra were obtained using a Shimadzu UV–vis spectrophotometer UV-2450, and ECD spectra were measured using a Jasco J-815 spectropolarimeter. Measurements of the IR spectra were performed using a PerkinElmer FT-IR spectrometer Spectrum 100. NMR spectra were recorded using a Bruker Avance III 500 MHz spectrometer equipped with a BBFO (Plus) SmartProbe (¹H 500 MHz, ¹³C 125 MHz) and a Bruker Avance III 700 MHz spectrometer equipped with a 5 mm TCI cryoprobe (¹H 700 MHz, ¹³C 175 MHz), and NMR data were referenced to selected chemical shifts of acetone-

d_6 (^1H : 2.05 ppm, ^{13}C : 29.32 ppm) and $\text{MeOH-}d_4$ (^1H : 3.31 ppm, ^{13}C : 49.15 ppm), respectively. HRESIMS mass spectra were measured using the Agilent 1200 series HPLC-UV system in combination with an ESI-TOF-MS (Maxis, Bruker). Measurements were performed with a 2.1×50 mm, $1.7 \mu\text{m}$, C18 Acquity UPLC BEH (Waters) column, using Milli-Q H_2O + 0.1% formic acid as solvent A and MeCN + 0.1% formic acid as solvent B (gradient: 5% B for 0.5 min increasing to 100% B in 19.5 min and maintaining 100% B for 5 min, flow rate: 0.6 mL/min, UV detection: 200–600 nm).

Fungal Material. *Heimiomyces* sp. (MUCL 56078) was collected from Mount Elgon National Reserve ($1^\circ 7' 6''$ N, $34^\circ 31' 30''$ E) in Kenya by C. Decock and J. C. Matasyoh. Identification of the genus and deposition of a dried specimen were carried out as described by Cheng et al.³

Fermentation and Extraction. Cultures of *Heimiomyces* sp. were maintained on YM6.3 agar plates.

For the seed cultures, three 50 mm² sized pieces of well-grown mycelium from YM6.3 agar plates were transferred into a 500 mL Erlenmeyer shape culture flask containing 200 mL of YM6.3 medium (10 g/L malt extract, 4 g/L D-glucose, 4 g/L yeast extract, pH 6.3). The incubation was performed at 23 °C and 140 min^{−1} on a rotary shaker. After 23 days of cultivation the culture broth was homogenized with an Ultra-Turrax (T25 easy clean digital, IKA), equipped with a S 25 N – 25 F dispersing tool, at 8000 rpm for 10–20 s.

Solid Rice Cultures. The inoculum (8 mL per flask) was transferred into four 500 mL Erlenmeyer shape culture flasks containing BRFT medium (1 g/L yeast extract, 0.5 g/L sodium tartrate, 0.5 g/L K_2HPO_4 , 100 mL of the solution added to 28 g of brown rice). Afterward, the medium was loosened with a spatula to make it accessible for oxygen and homogeneously distribute the inoculum. The incubation was performed at 23 °C in an incubator. After 72 days the fermentation process was stopped. At first, the medium and the mycelium were covered with acetone. Following this, the medium was loosened with a spatula and mixed with the acetone. Extraction was carried out by using ultrasonication for 30 min. Liquid and solid phase were separated by filtration. This procedure was repeated, followed by evaporation (40 °C) of the organic solvent with a rotary evaporator. The remaining aqueous phase was extracted with EtOAc (1:1) in a separatory funnel, twice. The organic phase was evaporated to dryness (40 °C). Furthermore, the extract was dissolved in 5 mL of MeOH. Afterward, 50 mL of a 1:1 mixture of heptane and MeOH/ H_2O (1:1) was added. Extraction was carried out in a separatory funnel twice, and the heptane and aqueous phases were collected separately. Finally, both were evaporated to dryness (40 °C). This led to the isolation of 476 mg of aqueous extract and 206 mg of heptane extract. A second fermentation of six solid rice cultures was performed using the same conditions, leading to the isolation of 1071 mg of aqueous extract (no heptane extraction).

Liquid Cultures. The inoculum (3 mL per flask) was transferred into 21 500 mL Erlenmeyer shape culture flasks containing 200 mL of YM6.3 medium and five 500 mL Erlenmeyer shape culture flasks containing 200 mL of MOF medium (75 g/L mannitol, 16.2 g/L MES, 15 g/L oat flour, 5 g/L yeast extract, 4 g/L L-glutamic acid, pH 6.0). The incubation was performed at 23 °C and 140 min^{−1} on a rotary shaker. Glucose consumption was monitored using test strips (Medi-Test Glucose, Macherey-Nagel). The fermentation process was stopped 2 days after the culture broth tested negative for glucose (33 days in total for YM6.3 cultures and 27 days in total for MOF cultures). Mycelium and supernatant were separated by centrifugation at 5100 min^{−1} for 15 min (lab centrifuge 4-16KS, Sigma Laborzentrifugen GmbH). The mycelium was overlaid with acetone and afterward extracted in an ultrasonic bath for 30 min, twice. Solid and liquid phases were separated by filtration, followed by evaporation (40 °C) of the organic solvent with a rotary evaporator. The remaining aqueous phase was diluted with H_2O and extracted against EtOAc. Following this, the organic phase was evaporated to dryness (40 °C). The supernatant was extracted with EtOAc (1:1) twice in a separatory funnel. The organic phase was kept and evaporated to dryness (40 °C). This led to the isolation of 567 mg of extract from

the mycelium and 651 mg of extract from the supernatant of YM6.3 cultures, as well as 211 mg of extract from the mycelium and 339 mg of crude extract from the supernatant of MOF cultures. Filtration of the extracts was performed by using an SPME Strata-X 33 μm Polymeric RP cartridge (Phenomenex, Inc.).

Analytical HPLC. The obtained extracts were dissolved in acetone to yield a concentration of 10 mg/mL. Solvation was aided by ultrasonication at 40 °C for 10 min. Samples were analyzed by an analytical HPLC device (Dionex UltiMate 3000 series) coupled to an ion trap mass spectrometer (amazon speed by Bruker) to conduct the measurements. HPLC grade H_2O and HPLC grade MeCN supplemented by 0.1% formic acid were used as mobile phase. With a flow rate of 600 $\mu\text{L}/\text{min}$, 2 μL of the injected samples was separated over an ACQUITY-UPLC BEH C18 column (50 \times 2.1 mm; particle size: 1.7 μm) by Waters. Starting with 5% of MeCN, the amount was increased to 100% in 20 min and retained for 5 min at 100%. The obtained chromatograms were evaluated with the appropriate Bruker analysis software (Data Analysis 4.4).

Isolation of Compounds 1–8. After evaluation of the analytical data, the extracts were separated via RP HPLC using a Gilson PLC 2250 purification system.

Solid Rice Cultures (BRFT). The extract obtained from the aqueous phase of the solid rice cultures of the first fermentation was purified using a Gemini LC column 250 \times 50 mm, 110 Å, 10 μm (Phenomenex); solvent A: Milli-Q H_2O + 0.1% formic acid, solvent B: MeCN + 0.1% formic acid, flow rate: 60 mL/min, gradient: 5 min B at 25%, increasing to 80% B in 55 min, increasing to 100% B in 10 min, maintaining 100% B for 10 min. The fraction at 60.5–61.5 min led to 2.76 mg of 3, the fraction at 63.5–64.5 min led to 6.8 mg of compound 4, and the fraction at 65.5–66.5 min led to 2.8 mg of compound 2. The extract obtained from the solid rice cultures of the second fermentation was purified using a Synergi Polar RP 250 \times 50 mm, 80 Å, 10 μm (Phenomenex) column; solvent A: Milli-Q H_2O + 0.1% formic acid, solvent B: MeCN + 0.1% formic acid, flow rate: 60 mL/min, gradient: 5 min B at 20%, increasing to 40% B in 5 min, increasing to 85% B in 50 min, increasing to 100% B in 5 min, maintaining 100% B for 10 min. The fraction at 29.5–30.5 min led to 7.4 mg of 6, the fraction at 37.0–37.75 min led to 4.5 mg of compound 5, and the fraction at 48.0–48.75 min led to 43.2 mg of compound 1.

Liquid Cultures (YM6.3). The extract obtained from the supernatant was purified using a Gemini LC column 250 \times 50 mm, 110 Å, 10 μm (Phenomenex); solvent A: Milli-Q H_2O + 0.1% formic acid, solvent B: MeCN + 0.1% formic acid, flow rate: 60 mL/min, gradient: 5 min B at 20%, increasing to 65% B in 50 min, increasing to 100% B in 20 min, maintaining 100% B for 10 min. The fraction at 36.5–37.5 min led to 4.2 mg of 8.

Liquid Cultures (MOF). The extract obtained from the mycelium of the culture broth was purified using a Gemini LC column 250 \times 50 mm, 110 Å, 10 μm (Phenomenex); solvent A: Milli-Q H_2O + 0.1% formic acid, solvent B: MeCN + 0.1% formic acid, flow rate: 50 mL/min, gradient: 5 min B at 30%, increasing to 50% B in 10 min, increasing to 100% B in 50 min, maintaining 100% B for 10 min. The fraction at 48.0–49.0 min led to 2.5 mg of 7.

Acetylation of 1. Acetylation was performed as previously described by Duncan et al.;¹⁹ 16 mg of 1 was dissolved in 4.8 mL of pyridine, and afterward 2.4 mL of acetic anhydride (resulting in a 2:1 mixture) was added. The solution was left at room temperature for 3–4 h. Following this, the reagents were removed by evaporation (40 °C) with a rotary evaporator. The product was dissolved in acetone and analyzed by HPLC/MS. Due to side product formation, a purification was performed via RP HPLC using a Gilson PLC 2050 purification system. The sample was purified using an XBridge Prep C18 column, 19 \times 250 mm, 5 μm (Waters); solvent A: Milli-Q H_2O + 0.1% formic acid, solvent B: MeCN + 0.1% formic acid, flow rate: 20 mL/min, gradient: 5 min B at 70%, increasing to 90% B in 35 min, increasing to 100% B in 5 min, maintaining 100% B for 5 min. The fraction at 20.5–21.5 min led to 3.3 mg of compound 1b.

Bis-heimiomycin A (1): red oil; $[\alpha]_D^{25} + 16$ (c 0.01, acetone); UV/vis (0.01 mg/mL, MeCN) λ_{max} (log ϵ) 372 (3.89), 283 (4.55), 245

(4.45) nm; ECD (0.2 mg/mL, MeOH) λ ($\Delta\epsilon$) 297 (+32.5), 261 (−34.0), 240 (+39.9), 204 (−29.5) nm, Figure S1; ^1H and ^{13}C NMR data (acetone- d_6), Table 1; ESIMS m/z 633.30 $[\text{M} + \text{H}]^+$, 631.11 $[\text{M} - \text{H}]^-$; HRESIMS m/z 633.2695 $[\text{M} + \text{H}]^+$ (calcd for $\text{C}_{36}\text{H}_{41}\text{O}_{10}$, 633.2694); t_R = 13.3 min (analytical HPLC).

Bis-heimiomycin B (2): red oil; $[\alpha]_D^{25}$ +150 (c 0.01, MeOH); UV/vis (0.01 mg/mL, MeOH) λ_{max} (log ϵ) 378 (3.78), 287 (4.14), 208 (4.40) nm; ECD (0.2 mg/mL, MeOH) λ ($\Delta\epsilon$) 342 (+6.0), 315 (+1.3), 295 (+20.8), 245 (−2.3), 223 (+17.0), 200 (−11.6), 194 (+2.5) nm, Figure S1; ^1H and ^{13}C NMR data (acetone- d_6), Table 1; ESIMS m/z 617.31 $[\text{M} + \text{H}]^+$, 615.37 $[\text{M} - \text{H}]^-$; HRESIMS m/z 617.2749 $[\text{M} + \text{H}]^+$ (calcd for $\text{C}_{36}\text{H}_{41}\text{O}_9$, 617.2745); t_R = 13.3 min (analytical HPLC).

Bis-heimiomycin C (3): red oil; $[\alpha]_D^{25}$ +130 (c 0.01, MeOH); UV/vis (0.01 mg/mL, MeOH) λ_{max} (log ϵ) 373 (3.93), 293 (4.16), 205 (4.54) nm; ECD (0.2 mg/mL, MeOH) λ ($\Delta\epsilon$) 315 (+2.8), 293 (+9.9), 264 (+3.7), 242 (+8.2), 230 (+2.1) nm, Figure S1; ^1H and ^{13}C NMR data (acetone- d_6), Table 1; ESIMS m/z 601.32 $[\text{M} - \text{H}_2\text{O} + \text{H}]^+$, 617.36 $[\text{M} - \text{H}]^-$; HRESIMS m/z 641.2720 $[\text{M} + \text{Na}]^+$ (calcd for $\text{C}_{36}\text{H}_{42}\text{NaO}_9$, 641.2721); t_R = 12.5 min (analytical HPLC).

Bis-heimiomycin D (4): red oil; $[\alpha]_D^{25}$ −290 (c 0.01, MeOH); UV/vis (0.01 mg/mL, MeOH) λ_{max} (log ϵ) 372 (3.86), 327 (4.17), 303 (4.15), 204 (4.59) nm; ECD (0.2 mg/mL, MeOH) λ ($\Delta\epsilon$) 387 (+6.7), 328 (−5.5), 293 (+17.8), 267 (+10.0), 261 (+10.4), 251 (+6.8), 240 (+15.0), 233 (+11.9), 218 (+29.8), 200 (−17.1) nm, Figure S1; ^1H and ^{13}C NMR data (acetone- d_6), Table 1; ESIMS m/z 601.31 $[\text{M} + \text{H}]^+$, 599.35 $[\text{M} - \text{H}]^-$; HRESIMS m/z 601.2797 $[\text{M} + \text{H}]^+$ (calcd for $\text{C}_{36}\text{H}_{41}\text{O}_8$, 601.2796); t_R = 12.9 min (analytical HPLC).

Heimiomycin D (5): red oil; $[\alpha]_D^{25}$ +27 (c 0.01, acetone); UV/vis (0.01 mg/mL, MeCN) λ_{max} (log ϵ) 305 (3.86) nm; ECD (0.2 mg/mL, MeCN) λ ($\Delta\epsilon$) 299 (+16.7), 259 (−1.1), 223 (+13.8) nm, Figure S2; ^1H and ^{13}C NMR data (acetone- d_6), Table 2; ESIMS m/z 401.16 $[\text{M} + \text{H}]^+$, 398.94 $[\text{M} - \text{H}]^-$; HRESIMS m/z 401.1593 $[\text{M} + \text{H}]^+$ (calcd for $\text{C}_{22}\text{H}_{25}\text{O}_7$, 401.1595); t_R = 9.8 min (analytical HPLC).

Heimiomycin E (6): red oil; $[\alpha]_D^{25}$ +170 (c 0.01, MeCN); UV/vis (0.01 mg/mL, MeCN) λ_{max} (log ϵ) 369 (3.73), 283 (4.33), 240 (4.18) nm; ECD (0.2 mg/mL, MeCN) λ ($\Delta\epsilon$) 295 (+36.9), 275 (−9.1), 255 (−1.3), 246 (−4.0), 204 (+5.1) nm, Figure S2; ^1H and ^{13}C NMR data (acetone- d_6), Table 2; ESIMS m/z 387.14 $[\text{M} + \text{H}]^+$, 384.93 $[\text{M} - \text{H}]^-$; HRESIMS m/z 387.1437 $[\text{M} + \text{H}]^+$ (calcd for $\text{C}_{21}\text{H}_{23}\text{O}_7$, 387.1438); t_R = 8.4 min (analytical HPLC).

Heimiocalamene A (7): yellow oil; $[\alpha]_D^{25}$ +53 (c 0.01, acetone); UV/vis (0.01 mg/mL, MeCN) λ_{max} (log ϵ) 305 (3.86) nm; ECD (0.2 mg/mL, MeOH) λ ($\Delta\epsilon$) 307 (−2.1), 254 (+1.0), 235 (+0.4), 202 (+2.5), 194 (−0.03) nm, Figure S3; ^1H and ^{13}C NMR data (acetone- d_6), Table 2; ESIMS m/z 235.10 $[\text{M} + \text{H}]^+$, 232.90 $[\text{M} - \text{H}]^-$; HRESIMS m/z 235.1689 $[\text{M} + \text{H}]^+$ (calcd for $\text{C}_{15}\text{H}_{23}\text{O}_2$, 235.1693); t_R = 11.7 min (analytical HPLC).

Heimiocalamene B (8): yellow oil; $[\alpha]_D^{25}$ +70 (c 0.01, MeOH); UV/vis (0.01 mg/mL, MeOH) λ_{max} (log ϵ) 310 (3.59), 246 (3.75), 198 (4.47) nm; ^1H and ^{13}C NMR data (MeOH- d_4), Table S2; ESIMS m/z 263.05 $[\text{M} + \text{H}]^+$, 260.82 $[\text{M} - \text{H}]^-$; HRESIMS m/z 263.1275 $[\text{M} + \text{H}]^+$ (calcd for $\text{C}_{15}\text{H}_{19}\text{O}_4$, 263.1275); t_R = 6.1 min (analytical HPLC).

■ ASSOCIATED CONTENT

SI Supporting Information

The Supporting Information is available free of charge at <https://pubs.acs.org/doi/10.1021/acs.jnatprod.2c01015>.

ECD spectra of compounds 1–7; protocol: antimicrobial and cytotoxicity assay, Tables S1–S3; structures of compounds 15 and 16, Figure S4; ^{13}C and ^1H NMR data of compound 1b, Table S5; 1D and 2D NMR data of compounds 1–8 and 11, Tables S4–S13; 1D and 2D NMR spectra of compounds 1–8 and 11 (PDF)

■ AUTHOR INFORMATION

Corresponding Author

Marc Stadler – Department of Microbial Drugs, Helmholtz Centre for Infection Research GmbH (HZI) and German Centre for Infection Research (DZIF), Partner Site Hannover-Braunschweig, 38124 Braunschweig, Germany; Institute of Microbiology, Technische Universität Braunschweig, 38106 Braunschweig, Germany; orcid.org/0000-0002-7284-8671; Phone: +49 531 6181-4240; Email: marc.stadler@helmholtz-hzi.de; Fax: +49 531 6181 9499

Authors

Sebastian Pfützte – Department of Microbial Drugs, Helmholtz Centre for Infection Research GmbH (HZI) and German Centre for Infection Research (DZIF), Partner Site Hannover-Braunschweig, 38124 Braunschweig, Germany; Institute of Microbiology, Technische Universität Braunschweig, 38106 Braunschweig, Germany

Atchara Khamsim – Department of Microbial Drugs, Helmholtz Centre for Infection Research GmbH (HZI) and German Centre for Infection Research (DZIF), Partner Site Hannover-Braunschweig, 38124 Braunschweig, Germany; Institute of Microbiology, Technische Universität Braunschweig, 38106 Braunschweig, Germany

Frank Surup – Department of Microbial Drugs, Helmholtz Centre for Infection Research GmbH (HZI) and German Centre for Infection Research (DZIF), Partner Site Hannover-Braunschweig, 38124 Braunschweig, Germany; Institute of Microbiology, Technische Universität Braunschweig, 38106 Braunschweig, Germany; orcid.org/0000-0001-5234-8525

Cony Decock – MycOTHèque de l'Université Catholique de Louvain (BCCM/MUCL), Earth and Life Institute, Microbiology, B-1348 Louvain-la-Neuve, Belgium

Josphat C. Matasyoh – Department of Chemistry, Egerton University, Njoro 20115, Kenya

Complete contact information is available at:

<https://pubs.acs.org/doi/10.1021/acs.jnatprod.2c01015>

Notes

The authors declare no competing financial interest.

■ ACKNOWLEDGMENTS

S.P. is grateful for a grant from the Life Science-Stiftung zur Förderung von Wissenschaft und Forschung (LSS). The authors thank T. Cheng and C. Chepkirui for providing supporting data and biological material of their previous experiments. J.-P. Wennrich, K. Becker, and C. Lambert are thanked for their expert advisory assistance. C. Kakoschke and W. Collisi are thanked for their expert technical assistance. Lastly, the authors want to acknowledge the “ASAFEM” Project (Grant No. IC-070) under the ERAfrica Programme of the European Commission to J.C.M., C.D., and M.S. for financial support. This research also benefitted from the European Union's H2020 Research and Innovation Staff Exchange program (RISE), Grant No. 101008129: MYCO-BIOMICS; beneficiaries M.S. and J.C.M.

■ REFERENCES

- (1) Sandargo, B.; Chepkirui, C.; Cheng, T.; Chaverra-Muñoz, L.; Thongbai, B.; Stadler, M.; Hüttel, S. *Biotechnol. Adv.* **2019**, *37* (6), 107344.

- (2) Mapook, A.; Hyde, K. D.; Hassan, K.; Matio Kemkuignou, B.; Čmoková, A.; Surup, F.; Kuhnert, E.; Paomephan, P.; Cheng, T.; de Hoog, S.; Song, Y.; Jayawardena, R. S.; Al-Hatmi, A. M. S.; Mahmoudi, T.; Ponts, N.; Studt-Reinhold, L.; Richard-Forget, F.; Chethana, K. W. T.; Harishchandra, D. L.; Mortimer, P. E.; Li, H.; Lumyong, S.; Aduang, W.; Kumla, J.; Suwannarach, N.; Bhunjun, C. S.; Yu, F.-M.; Zhao, Q.; Schaefer, D.; Stadler, M. *Fungal Divers.* **2022**, *116* (1), 547–614.
- (3) Cheng, T.; Chepkirui, C.; Decock, C.; Matasyoh, J. C.; Stadler, M. *J. Nat. Prod.* **2020**, *83* (8), 2501–2507.
- (4) Berger, S.; Rieker, A. In *Quinonoid Compounds (1974)*; PATAI'S Chemistry of Functional Groups; 1974; pp 163–229.
- (5) Bott, G.; Field, L. D.; Sternhell, S. *J. Am. Chem. Soc.* **1980**, *102* (17), 5618–5626.
- (6) Edwards, R. L.; Lewis, D. G.; Wilson, D. V. *J. Chem. Soc.* **1961**, No. 0, 4995–5002.
- (7) Fiasson, J.-L.; Gluchoff-Fiasson, K.; Steglich, W. *Chem. Ber.* **1977**, *110* (3), 1047–1057.
- (8) Park, I.-H.; Chung, S.-K.; Lee, K.-B.; Yoo, Y.-C.; Kim, S.-K.; Kim, G.-S.; Song, K.-S. *Arch. Pharm. Res.* **2004**, *27* (6), 615–618.
- (9) Lee, I.-K.; Seok, S.-J.; Kim, W.-K.; Yun, B.-S. *J. Nat. Prod.* **2006**, *69* (2), 299–301.
- (10) Jung, J.-Y.; Lee, I.-K.; Seok, S.-J.; Lee, H.-J.; Kim, Y.-H.; Yun, B.-S. *J. Appl. Microbiol.* **2008**, *104* (6), 1824–1832.
- (11) Feng, P.; Shang, Y.; Cen, K.; Wang, C. *Proc. Natl. Acad. Sci. U. S. A.* **2015**, *112* (36), 11365–11370.
- (12) Zhao, W.-Y.; Yan, J.-J.; Liu, T.-T.; Gao, J.; Huang, H.-L.; Sun, C.-P.; Huo, X.-K.; Deng, S.; Zhang, B.-J.; Ma, X.-C. *Eur. J. Med. Chem.* **2020**, *203*, 112622.
- (13) Li, J.; Wu, W.; Yang, F.; Liu, L.; Wang, S.-P.; Jiao, W.-H.; Xu, S.-H.; Lin, H.-W. *Chem. Biodivers.* **2018**, *15* (6), e1800078.
- (14) Utkina, N. K.; Denisenko, V. A.; Krasokhin, V. B. *J. Nat. Prod.* **2010**, *73* (4), 788–791.
- (15) Takahashi, Y.; Kubota, T.; Kobayashi, J. *Bioorg. Med. Chem.* **2009**, *17* (6), 2185–2188.
- (16) Harms, K.; Surup, F.; Stadler, M.; Stchigel, A. M.; Marin-Felix, Y. *Microorganisms.* **2021**, *9*, 1191.
- (17) El-Najjar, N.; Gali-Muhtasib, H.; Ketola, R. A.; Vuorela, P.; Urtti, A.; Vuorela, H. *Phytochem. Rev.* **2011**, *10* (3), 353.
- (18) Zhang, L.; Zhang, G.; Xu, S.; Song, Y. *Eur. J. Med. Chem.* **2021**, *223*, 113632.
- (19) Duncan, S. J.; Grischow, S.; Williams, D. H.; McNicholas, C.; Purewal, R.; Hajek, M.; Gerlitz, M.; Martin, S.; Wrigley, S. K.; Moore, M. *J. Am. Chem. Soc.* **2001**, *123* (4), 554–560.

Paper III**Heimionones A-E, New Sesquiterpenoids Produced by
Heimiomyces sp., a Basidiomycete Collected in Africa**

Sebastian Pfütze^{1,2}, Atchara Khamsim^{1,2}, Frank Surup^{1,2}, Cony Decock³, Josphat C. Matasyoh⁴, Marc Stadler^{1,2,*}

Molecules **2023**; 28(9):3723. DOI: <https://doi.org/10.3390/molecules28093723>

- ¹ Department of Microbial Drugs, Helmholtz Centre for Infection Research (HZI), German Centre for Infection Research (DZIF), Partner Site Hannover/Braunschweig, Inhoffenstrasse 7, 38124 Braunschweig, Germany
- ² Institute of Microbiology, Technische Universität Braunschweig, Spielmannstraße 7, 38106 Braunschweig, Germany
- ³ Mycothèque de l'Université Catholique de Louvain (BCCM/MUCL), Earth and Life Institute, Microbiology, B-1348 Louvain-la-Neuve, Belgium
- ⁴ Department of Chemistry, Egerton University, P.O BOX 536, 20115, Njoro, Kenya

*Corresponding author

Article

Heimionones A–E, New Sesquiterpenoids Produced by *Heimiomyces* sp., a Basidiomycete Collected in Africa

Sebastian Pfütze ^{1,2}, Atchara Khamsim ^{1,2}, Frank Surup ^{1,2} , Cony Decock ³ , Josphat C. Matasyoh ⁴  and Marc Stadler ^{1,2,*} 

¹ Department of Microbial Drugs, Helmholtz Center for Infection Research (HZI), German Center for Infection Research (DZIF), Partner Site Hannover/Braunschweig, Inhoffenstrasse 7, 38124 Braunschweig, Germany; sebastian.pfuetze@helmholtz-hzi.de (S.P.); frank.surup@helmholtz-hzi.de (F.S.)

² Institute of Microbiology, Technische Universität Braunschweig, Spielmannstraße 7, 38106 Braunschweig, Germany

³ Earth and Life Institute, Mycothèque de l' Université Catholique de Louvain (BCCM/MUCL), Place Croix du Sud 3, B-1348 Louvain-la-Neuve, Belgium; cony.decock@uclouvain.be

⁴ Department of Chemistry, Egerton University, P.O. Box 536, Njoro 20115, Kenya

* Correspondence: marc.stadler@helmholtz-hzi.de; Tel.: +49-531-6181-4240

Abstract: With heimionones A–E (1–5), five new terpenoids were isolated from submerged cultures of *Heimiomyces* sp. in addition to the previously described compounds hispidin, hypholomin B, and heimiomycins A and B. Planar structures of the metabolites were elucidated by 1D and 2D NMR in addition to HRESIMS data. While ROESY data assigned relative configurations, absolute configurations were determined by the synthesis of MTPA esters of 1, 3, and 5. The [6.3.0] undecane core structure of compounds 3–5 is of the asteriscane-type, however, the scaffold of 1 and 2 with their bicyclo [5.3.0] decane core and germinal methyl substitution is, to our knowledge, unprecedented. Together with several new compounds that were previously isolated from solid cultures of this strain, *Heimiomyces* sp. showed an exceptionally high chemical diversity of its secondary metabolite profile.

Keywords: *Heimiomyces* sp.; heimionone; chemical diversity



Citation: Pfütze, S.; Khamsim, A.; Surup, F.; Decock, C.; Matasyoh, J.C.; Stadler, M. Heimionones A–E, New Sesquiterpenoids Produced by *Heimiomyces* sp., a Basidiomycete Collected in Africa. *Molecules* **2023**, *28*, 3723. <https://doi.org/10.3390/molecules28093723>

Academic Editor: Kemal Husnu Can Baser

Received: 4 April 2023

Revised: 19 April 2023

Accepted: 24 April 2023

Published: 26 April 2023



Copyright: © 2023 by the authors. Licensee MDPI, Basel, Switzerland. This article is an open access article distributed under the terms and conditions of the Creative Commons Attribution (CC BY) license (<https://creativecommons.org/licenses/by/4.0/>).

1. Introduction

In the ever-growing effort to isolate, identify, and characterize novel natural products, the kingdom of Fungi serves as a well-known, reliable, and nearly inexhaustible source. Ongoing developments in numerous modern techniques significantly support the identification of hitherto unknown secondary metabolites, leading to a continuously rising number of newly discovered molecules. With regard to the ca. 35.000 species comprising [1] and therefore the second-largest phylum of the kingdom Fungi, the Basidiomycota have proven to produce chemically very diverse secondary-metabolite profiles next to their biological diversity [2]. While there are Basidiomycota that mainly produce several congeners of the same compound family, such as members of the genus *Armillaria*, which are known for their large amount of structurally closely related sesquiterpenoids aryl esters [3], there are also genera that show a high chemical diversity within their secondary metabolite profile concerning the presence of different core structures. *Heimiomyces* sp. (MUCL 56078) is an example of the latter since our previous studies already led to the isolation and identification of heimiocalamenes C–E (8–10) and heimiomycins A–C (11–13) [4], as well as bis-heimiomycins A–D (14–17), heimiomycins D–E (18–19) and heimiocalamenes A–B (20–21) [5], showing the enormous potential of this specimen to produce chemically very diverse secondary metabolites. Intriguingly, the secondary metabolite pattern of *Heimiomyces* sp. even changed drastically after switching the cultivation conditions from solid rice cultures to submerged cultures.

We herein present the isolation, structural elucidation, and biological evaluation of the new terpenoids heimionones A–E (1–5) with uncommon bicyclo [5.3.0] decane and

[6.3.0] undecane core structures, respectively, that were isolated from submerged cultures of *Heimiomyces* sp. alongside the previously described heimiomycins A–B (11–12) [4], as well as hispidin and hypholomin B (6–7) [6,7].

2. Results and Discussion

2.1. Isolation and Structure Elucidation of Metabolites from *Heimiomyces* sp. (Figures 1–3)

Heimionone A (1) was isolated as a yellow oil from the mycelial extracts of liquid cultures. Based on an HRESIMS analysis, its molecular formula was assigned as $C_{22}H_{28}O_5$ according to the molecular ion cluster at m/z 373.2012 $[M + H]^+$ (calcd. for $C_{22}H_{29}O_5$ 373.2023) indicating nine degrees of unsaturation. 1H NMR and HSQC data (Table S6) led to the identification of six methyls at δ_H 1.02 (s, H₃-12), 1.13 (s, H₃-11), 1.40 (d, $J = 6.3$ Hz, H₃-15), 1.77 (s, H₃-7'), 1.82 (d, $J = 7.0$ Hz, H₃-6'), and 2.31 (s, H₃-13), three oxymethines at δ_H 4.70 (q, H-14), 5.14 (s, H-9), and 6.12 (s, H-1), and five olefinic methines at δ_H 5.81 (d, $J = 15.7$ Hz, H-2'), 6.07 (q, H-5'), 7.35 (d, $J = 15.7$ Hz, H-3'), 7.56 (d, $J = 9.8$ Hz, H-4), and 7.69 (d, $J = 9.8$ Hz, H-5). The ^{13}C and HMBC NMR data (Table S6) revealed the presence of 22 carbon resonances, including two carbonyl carbons (δ_C 187.5, C-7; 168.6, C-1'); ten sp^2 -hybridized carbons, comprising five nonprotonated carbons (δ_C 153.0, C-2; 152.4, C-3; 151.7, C-6; 146.1, C-8; 135.3, C-4') and five methines (δ_C 152.6, C-3'; 139.2, C-5'; 138.6, C-5; 131.8, C-4; 115.1, C-1'); one quaternary carbon (δ_C 45.5, C-10); three methines (δ_C 84.2, C-9; 83.5, C-1; 67.8, C-14); and six methyl carbons (δ_C 26.1, C-15; 22.3, C-13; 20.7, C-12; 20.5, C-11; 14.8, C-6'; 11.9 C-7'). The carbonyl and sp^2 -hybridized carbons accounted for seven degrees of unsaturation, suggesting two rings in the scaffold of heimionone A (1). By analyzing the 1H - 1H COSY data, the first spin system was given due to correlations between H₃-13, H-5, H-4, H-14, and H₃-15. Correlations between H₃-11/H₃-12, H₂-9, and H-1 led to the identification of the second spin system. HMBC correlations from H₃-13 to C-4/C-5/C-6/C-7/C-8 and H-4 to C-2/C-3/C-5/C-6/C-7/C-8 revealed a cyclohepta-3,5,8-triene-7-one ring. The 14-hydroxyethyl moiety was deduced from the HMBC correlations of H₃-15 to C-3/C-14. Further HMBC correlations from H₃-11 and H₃-12 to C-1/C-9/C-10, from H-9 to C-2/C-8/C-10/C-11, and from H-1 to C-2/C-8/C-9/C-10/C-11 led to the identification of a dimethylcyclopentane substructure that was fused to the cyclohepta-3,5,8-triene-7-one ring across C-2 and C-8. HMBC correlations from H₃-6' to C-3'/C-4'/C-5'/C-7' and from H-3' to C-1'/C-2'/C-4'/C-5'/C-7' revealed the presence of a 4'-methylhexa-2',4'-dienoic acid partial structure that was fused to C-1 according to an HMBC correlation from H-1 to C-1'. The E $\Delta^{2',3'}$ configuration was assigned according to the large coupling constants ($J = 15.7$ Hz) between the olefinic methines H-2' and H-3', while the $\Delta^{4',5'}$ configuration was assigned as E due to the ROESY correlation between H-3' and H-5'. Furthermore, this structural elucidation was supported by the comparison of the 1H and ^{13}C data to the ones of daldinin F (Figure S17 and Table S11), which was reported to carry the same side chain as heimionone A [8]. The relative configuration of the bicyclic core was obtained by the evaluation of ROE data. Due to the key correlation between H-1 and H₃-12, these protons were arbitrarily assigned to the α face of the molecule. A correlation between H-9 β /H-11 indicated an β orientation of these protons. Finally, the absolute configuration was determined by Mosher's method. The derivatization of heimionone A (1) to its corresponding *R*- and *S*-MTPA esters at position C-9 and C-14 was done with *S*- and *R*-MTPA chloride. The pattern of $\Delta\delta^{S,R}$ chemical shifts (see Figure 3) with positive values of H-4, H-5, H₃-11, and H₃-12, and negative ones of H₃-13 and H₃-15 determined the 1*S*,9*R*,14*S* absolute configuration.

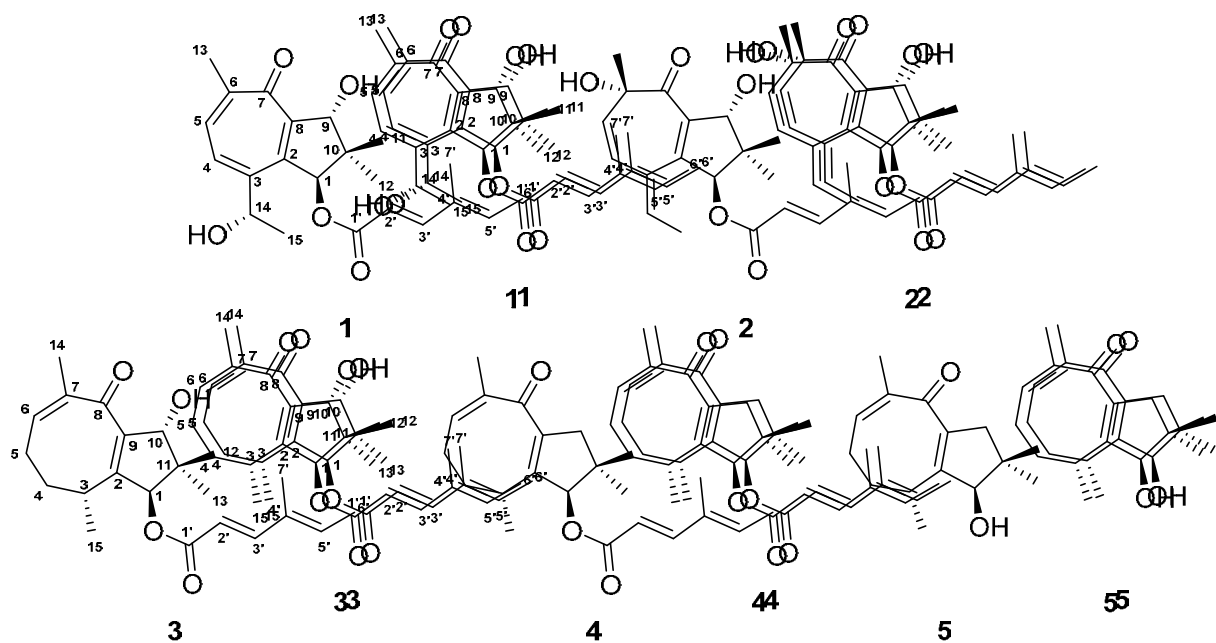


Figure 1. Chemical structures of heimonone A–E (1–5) isolated from liquid cultures of *Heimiomyces* sp.

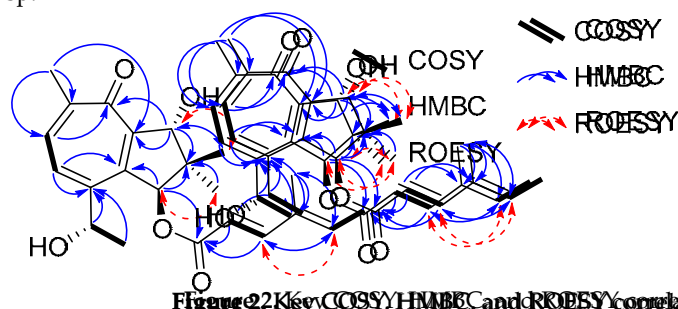


Figure 2. Key COSY, HMBC, and ROESY correlations of heimonone A (1).

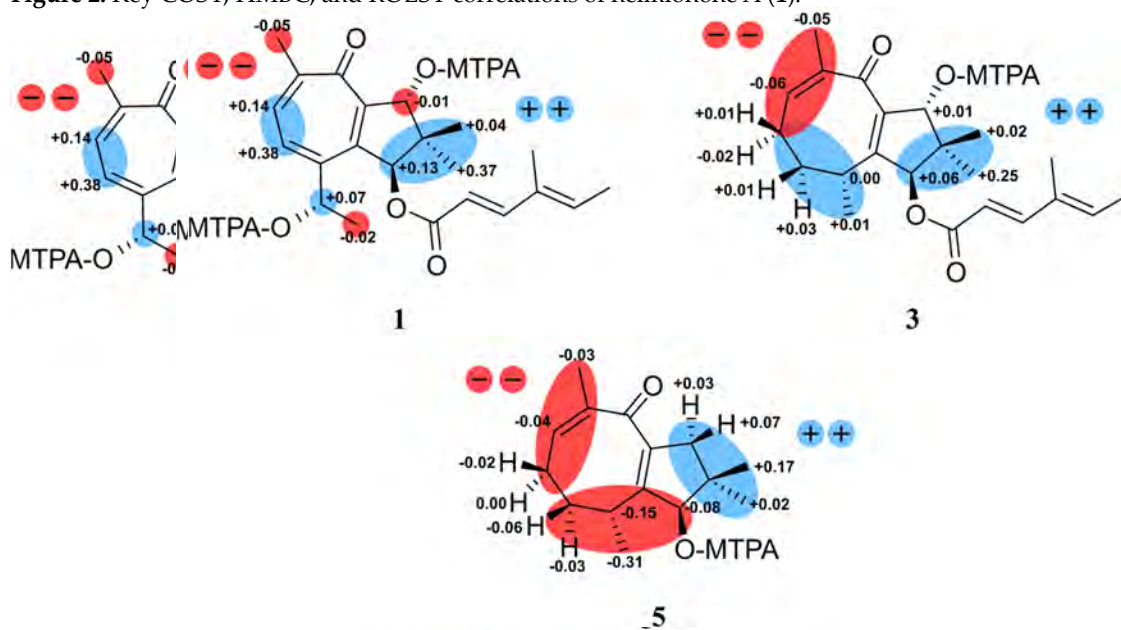


Figure 3. The $\Delta\delta^R$ values of (S)/(R) MTPA-esters obtained from heimonone A (1) diagnostic for 1S,9R,14S; heimonone C (3) diagnostic for 1S,3R,10R and heimonone E (5) diagnostic for 1R,3R,15,9R,14S; heimonone C (3) diagnostic for 1S,3R,10R and heimonone E (5) diagnostic for 1R,3R.

Heimonone B (2), which is closely related to 1, was obtained as a yellow oil from the supernatant extracts of liquid cultures. Its HRESIMS data indicated the same molecular

formula ($C_{22}H_{28}O_5$) as obtained for **1**. 1H and ^{13}C data showed high similarities to **1**. They differ by the relocation of the hydroxy function from C-14 for **1** to C-6 (δ_C 78.7) for **2**, whereas the oxymethine at C-14 was replaced by an olefinic methine (δ_H 6.16, δ_C 141.6). The cyclohepta-4,8-diene-7-one scaffold was confirmed by HMBC correlations of H_3 -13 to C-5/C-6/C-7 and H-4 to C-2/C-3/C-6. Relative configuration was assigned according to the ROE correlations. In particular, interactions between H-9 β and H_3 -11 and between H-1 α and H_3 -12 implied the same configuration as **1**. Additionally, correlations among H-9 α /H-11/H-13 defined the 6*R* configuration. The absolute configuration of **2** was confirmed by comparison to heimionone A (**1**) as 1*S*,9*R*,6*R*.

The yellow oil heimionone C (**3**) was isolated from the mycelial extracts of liquid cultures with a molecular formula of $C_{22}H_{30}O_4$, implying eight degrees of unsaturation. Analysis of the 1H and ^{13}C spectra showed similarities to those of **1** and **2**. HMBC and COSY interactions confirmed the presence of the previously described dimethylcyclopentane substructure carrying a 4'-methylhexa-2',4'-dienoc acid partial structure that was fused to C-1. A spin system was given based on 1H - 1H COSY correlations among H_3 -14, H-6, H_2 -5, H_2 -4, H-3, and H_3 -15. Furthermore, HMBC correlations from H_3 -14 to C-6/C-7/C-8, H_2 -4 to C-3/C-5, and H_3 -15 to C-2/C-3/C-4 led to the identification of the 3,7-dimethylcycloocta-6,9-dien-8-one ring that was fused to the dimethylcyclopentane ring across C-2 and C-9 according to correlations from H-1/H-3/ H_3 -15 to C-2 and from H-1/H-10/ H_3 -12 to C-9. The relative configuration was deduced by an analysis of ROE data. Due to the key correlations among H-1 α /H-4 α /H-5 α / H_3 -13/ H_3 -15, these protons were arbitrarily assigned to the α face of the molecule. Correlations between H-3 β /H-4 β /H-5 β and between H-10 β / H_3 -12 indicated a β orientation of these protons. Finally, the absolute configuration was determined after heimionone C (**3**) was derivatized to its corresponding S- and R-MTPA esters at position C-10 in the course of Mosher's method. The $\Delta\delta^{SR}$ chemical shift pattern (see Figure 3) indicated R-configuration of C-10 and thus a 1*S*,3*R*,10*R* absolute configuration.

Heimionone D (**4**) was obtained as a yellow oil from the mycelial extracts of liquid cultures with a molecular formula of $C_{22}H_{30}O_3$. The 1D and 2D NMR data of **4** suggested a high similarity to **3**. They only differ in the absence of a hydroxy function, which was replaced by a methylene (δ_H 2.30 H-10 α ; 2.77, H-10 β). This was confirmed by the HMBC correlations from H-1, H_3 -12, and H_3 -13 to C-10 (δ_C 47.8). The ROESY correlations among H-1 α /H-4 α /H-5 α /H-10 α / H_3 -13/ H_3 -15 implied **4** has the same configuration as heimionone C (**3**).

Heimionone E (**5**) was isolated as a yellow oil from the mycelial extracts of liquid cultures. Its NMR spectroscopic data were highly similar to the ones of heimionone D (**4**). They only differ in the absence of the 4'-methylhexa-2',4'-dienoc acid moiety that was replaced by the hydroxy function at position C-1. Finally, the absolute configuration was determined as 1*R*,3*S**R* after heimionone E (**5**) was derivatized to its corresponding S- and R-MTPA esters at position C-1 using Mosher's method with both R- and S-MTPA chloride.

Compounds **3**–**5** can be assigned to the asteriscanes according to their characteristic four methyl groups on the five-eight-membered ring system [9].

Although the bicyclo [5.3.0] decane scaffold of **1** and **2** is part of daucane-, isodaucane, aromadendrane, lactarane-, africane, gualane-, nor-guaiane and pseudoguaiane-type sesquiterpenoids, the methyl pattern of **1** and **2** with its germinal demethylation of C-10 is different from those [10]. Thus, the carbon backbone of **1** and **2** can be regarded as a new scaffold. Nevertheless, nardoguaianone E-I with similar structures were previously described after isolation from *Nardostachys chinensis* [11]. Interestingly, asteriscane-type sesquiterpenoids have been isolated from the soft coral *Simularia capillosa* [12].

Furthermore, hispidin (**6**) [6] and hypholomin B (**7**) [7], both of which have been described to show antioxidant effects [13,14], were isolated from the submerged cultures of *Heimiomyces* sp., together with heimiomycins A (**11**) and B (**12**), which were previously published from fermentations of the same fungal strain under different conditions [4].

Interestingly, the secondary metabolite profile of *Heimiomyces* sp. mainly changed after the cultivation conditions were switched from solid to liquid media. While our previous

experiments led to the isolation and identification of bis-heimiomycins A–D (14–17) and heimiomycins D–E (18–19) [5] from cultures on a solid rice medium, other compounds such as heimiocalamenes C–E (8–10), heimiomycins A–C (11–13) and heimiocalamenes A–B (20–21) [4,5], as well as the herein described heimionones A–E (1–5), were isolated after cultivation of *Heimiomyces* sp. in liquid YM6.3 and an MOF medium, respectively. Up to this point, this strain has already shown impressive chemical diversity. Since several other, yet unidentified, minor peaks were observed in the UV/Vis- and MS-spectra of its extracts, there is a potential even to find more exciting and new secondary metabolites if their production in more significant amounts can be triggered, for example by another change in the cultivation conditions.

2.2. Biological Assays

To evaluate the antimicrobial activity of compounds 1–5 a serial-dilution assay against several Gram-positive and Gram-negative bacteria as well as fungal strains was carried out, though no outstanding activities were observed (Table S4). Furthermore, all compounds were tested for their cytotoxicity against the human cervical cancer cell line KB3.1 and the mouse fibroblast cell line L929 where heimionone A (1) and heimionone C (3) showed weak cytotoxic effects (Table S5).

3. Materials and Methods

3.1. General Experimental Procedures

Optical rotations were measured using the 241 polarimeter (PerkinElmer, Waltham, MA, USA). Measurements of the UV spectra were carried out using the UV-Vis spectrophotometer UV-2450 (Shimadzu, Kyōto, Japan) and measurements of the ECD spectra were carried out using a J-815 spectropolarimeter (Jasco, Pfungstadt, Germany). NMR spectra were obtained using the Avance III 500 MHz spectrometer equipped with a BBFO (plus) SmartProbe (^1H 500 MHz, ^{13}C 125 MHz) and the Avance III 700 MHz spectrometer equipped with a 5 mm TCI cryoprobe (^1H 700 MHz, ^{13}C 175 MHz) (both Bruker, Billerica, MA, USA). NMR data were referenced to selected chemical shifts of acetonitrile- d_3 (^1H : 1.94 ppm, ^{13}C : 1.4 ppm), methanol- d_4 (^1H : 3.31 ppm, ^{13}C : 49.2 ppm), and pyridine- d_5 (^1H : 7.22 ppm), respectively. HRESIMS mass spectra were recorded with a 1200 series HPLC-UV system (Agilent, Santa Clara, CA, USA) in combination with an ESI-TOF-MS (Maxis, Bruker). Performance of the measurements was conducted with a 2.1×50 mm, $1.7 \mu\text{m}$, C18 Acquity UPLC BEH (Waters, Milford, MA, USA) column, using MilliQ H_2O + 0.1% formic acid as solvent A and MeCN + 0.1% formic acid as solvent B (gradient: 5% B for 0.5 min increasing to 100% B in 19.5 min and maintaining 100% B for 5 min, flow rate: 0.6 mL/min, UV detection: 200–600 nm).

3.2. Fungal Material

Heimiomyces sp. (MUCL 56078) was collected by C. Decock and J. C. Matasyoh from Mount Elgon National Reserve in Kenya ($1^\circ 7' 6''$ N, $34^\circ 31' 30''$ E). The genus was identified, and a dried specimen was deposited, as previously described by Cheng et al. [4].

3.3. Seed Culture and Fermentation of *Heimiomyces* sp.

The maintenance of *Heimiomyces* sp. cultures was carried out on YM6.3 agar plates. A 500 mL Erlenmeyer shape culture flask containing 200 mL of YM6.3 medium (10 g/L malt extract, 4 g/L D-glucose, 4 g/L yeast extract, pH 6.3) was used for inoculation with three 50 mm^2 sized pieces of well-grown mycelium from YM6.3 agar plates. The seed culture was incubated at 23°C and 140 min^{-1} on a rotary shaker for 23 days. For the following homogenization an Ultra-Turrax® (T25 easy clean digital, IKA, Staufen im Breisgau, Germany), equipped with an S 25 N–25 F dispersing tool was used at 8000 rpm for 10–20 s. The homogenized culture broth was utilized as inoculum by transferring 3 mL per flask into 15 500 mL Erlenmeyer shape culture flasks containing 200 mL of YM6.3 medium and subsequently, the incubation was performed at 23°C and 140 min^{-1} on a

rotary shaker. Consumption of the glucose was monitored using test strips (Medi-Test Glucose, Macherey-Nagel, Düren, Germany) leading to a termination of the fermentation process two days after the culture broth tested negative for glucose.

3.4. Harvest and Extraction

Separation of the mycelium and supernatant was carried out by centrifugation at 5100 min^{-1} for 15 min (lab centrifuge 4-16KS, Sigma Laborzentrifugen GmbH, Osterode am Harz, Germany). Extraction of the mycelium was performed with acetone in an ultrasonic bath for 30 min, twice. The liquid phase was evaporated at $40\text{ }^{\circ}\text{C}$ after separation from the solid phase by filtration, leading to a remaining aqueous phase that was subsequently diluted with water and extracted against ethyl acetate. Afterward, the organic phase was evaporated to dryness ($40\text{ }^{\circ}\text{C}$) and led to 607 mg of extract from the mycelium. Extraction of the supernatant was carried out with ethyl acetate (1:1) in a separatory funnel, twice. Evaporation of the organic phase at $40\text{ }^{\circ}\text{C}$ led to 251 mg extract from the supernatant of YM6.3 cultures. Both extracts were filtered using the SPME StrataTM-X 33 μm Polymeric RP cartridge (Phenomenex, Aschaffenburg, Germany).

3.5. Analytical HPLC

The extracts obtained from liquid cultures of *Heimiomyces* sp. were dissolved in acetone to yield a concentration of 10 mg/mL. Analysis of the samples was performed with an analytical HPLC device (Dionex UltiMate 3000 series, Sunnyvale, CA, USA) coupled to an ion trap mass spectrometer (amazon speedTM by Bruker). As mobile phase HPLC grade water and MeCN, both containing 0.1% of formic acid, were used. After injection of 2 μL of the samples, the separation was carried out over an ACQUITY-UPLC[®] BEH C18 column ($50 \times 2.1\text{ mm}$; particle size: 1.7 μm) (Waters) with a flow rate of 600 $\mu\text{L}/\text{min}$. The gradient started at 5% of MeCN, then increased to 100% MeCN in 20 min and remained for 5 min at 100%. To evaluate the obtained chromatograms, the appropriate analysis software (Data Analysis, version 4.4 by Bruker) was used.

3.6. Isolation of Compounds 1–5 via Reversed-Phase Liquid Chromatography

After evaluation of the analytical data, the extracts were separated via RP HPLC using a Gilson PLC 2250 Purification System (Limburg, Germany). The extract obtained from the supernatant of the culture broth was purified using the SynergiTM Polar RP $250 \times 50\text{ mm}$, 80 \AA , 10 μm (Phenomenex); solvent A: MilliQ water + 0.1% formic acid, solvent B: acetonitrile + 0.1% formic acid, flow rate: 50 mL/min, gradient: 5 min B at 20%, increasing to 100% B in 80 min, maintaining 100% B for 10 min. This yielded compound 5 (3.83 mg, $t_R = 44.0\text{--}44.75\text{ min}$), compound 2 (2.46 mg, $t_R = 47.5\text{--}48.5\text{ min}$), compound 1 (3.5 mg, $t_R = 49.5\text{--}50.5\text{ min}$) and compound 3 (1.26 mg, $t_R = 65.0\text{--}66.0\text{ min}$). The extract obtained from the mycelium of the culture broth was purified using the same equipment and conditions. This yielded compound 1 (1.77 mg, $t_R = 49.5\text{--}50.5\text{ min}$), compound 3 (1.87 mg, $t_R = 58.5\text{--}59.5\text{ min}$), and compound 4 (2.31 mg, $t_R = 68.0\text{--}68.5\text{ min}$).

3.7. Spectral Data of Compounds 1–5

Heimionone A (1): yellow oil; $[\alpha]_D^{25} +250$ (c 0.50, MeOH); UV/vis (0.01 mg/mL, MeOH) $\lambda_{\text{max}}(\log \epsilon)$: 325 (3.99), 268 (4.48), 247 (4.48), 202 (3.82) nm; ECD (0.2 mg/mL, MeOH) $\lambda(\Delta \epsilon)$: 265 (+19.8), 243 (−18.0), 220 (−1.2), 202 (−7.6) nm, Figure S1; ^1H and ^{13}C NMR data (MeOH- d_4), Table 1 and Table S6; ESIMS m/z 373.19 $[\text{M} + \text{H}]^+$, 371.24 $[\text{M} - \text{H}]^-$; HRESIMS m/z 373.2012 $[\text{M} + \text{H}]^+$ (calcd. for $\text{C}_{22}\text{H}_{29}\text{O}_5$, 373.2023); $t_R = 9.2\text{ min}$ (analytical HPLC).

Table 1. ^1H and ^{13}C spectroscopic data of compounds **1**, **2**, and **5** in methanol- d_4 and **3–4** in acetonitrile- d_3 (δ in ppm).

| 1 ^{b,d} | | | 2 ^{b,d} | | 3 ^{a,c} | | 4 ^{b,d} | | 5 ^{b,d} | |
|-------------------------|----------------------------|-------------------------------|----------------------------|-------------------------------|----------------------------|---|----------------------------|---|----------------------------|---|
| No. | δ_{C} , Type | δ_{H} (J in Hz) | δ_{C} , Type | δ_{H} (J in Hz) | δ_{C} , Type | δ_{H} (J in Hz) | δ_{C} , Type | δ_{H} (J in Hz) | δ_{C} , Type | δ_{H} (J in Hz) |
| 1 | 83.5, CH | α : 6.12, s | 86.1, CH | α : 6.32, m | 83.1, CH | α : 5.62, s | 85.6, CH | α : 5.58, s | 85.3, CH | α : 4.13, s |
| 2 | 153.0, C | | 146.2, C | | 150.3, C | | 150.3, C | | 156.5, C | |
| 3 | 152.4, C | | 133.5, C | | 31.2, CH | β : 2.86, dqd (12.8, 6.9, 6.0) | 31.2, CH | β : 2.96, m | 31.9, CH | β : 2.98, dqd (12.5, 6.9, 5.0) |
| 4 | 131.8, CH | 7.56, d (9.8) | 134.8, C | 6.26, d (11.8) | 37.1, CH ₂ | α : 1.57, m β : 1.78, m | 37.3, CH ₂ | α : 1.53, m β : 1.74, m | 38.3, CH ₂ | α : 1.82, m β : 1.51, m |
| 5 | 138.6, CH | 7.69, dd (9.8, 0.9) | 130.5, CH | 5.53, d (11.8) | 26.3, CH ₂ | α : 2.46, m β : 2.11, m | 26.3, CH ₂ | α : 2.07, m β : 2.32, m | 26.7, CH ₂ | α : 2.30, m β : 2.08, m |
| 6 | 151.7, C | | 78.7, C | | 140.9, CH | 6.47, m | 139.1, CH | 6.35, ddd (9.7, 8.4, 1.4) | 139.4, CH | 6.36, ddd (9.8, 8.4, 1.4) |
| 7 | 187.5, C | | 199.3, C | | 142.0, C | | 141.5, C | | 142.1, C | |
| 8 | 146.1, C | | 142.2, C | | 194.2, C | | 194.3, C | | 196.3, C | |
| 9 | 84.2, CH | β : 5.14, s | 83.4, CH | β : 4.61, s | 148.9, C | | 146.9, C | | 144.7, C | |
| 10 | 45.5, C | | 47.2, C | | 83.3, CH | β : 4.89, s | 47.8, CH ₂ | α : 2.30, d (16.4) β : 2.77, d (16.4) | 47.2, CH ₂ | α : 2.21, d (16.1) β : 2.76, d (16.1) |
| 11 | 20.5, CH ₃ | 1.13, s | 22.0, CH ₃ | 0.98, m | 44.2, C | | 39.4, C | | 39.6, C | |
| 12 | 20.7, CH ₃ | 1.02, s | 21.7, CH ₃ | 1.18, m | 20.4, CH ₃ | 1.01, s | 22.2, CH ₃ | 0.99, s | 22.5, CH ₃ | 1.13, s |
| 13 | 22.3, CH ₃ | 2.31, br s | 27.2, CH ₃ | 1.45, m | 21.4, CH ₃ | 0.98, s | 28.0, CH ₃ | 1.06, s | 28.3, CH ₃ | 0.96, s |
| 14 | 67.8, CH | β : 4.70, q (6.3) | 141.6, CH | 6.16, q (7.7) | 20.1, CH ₃ | 1.89, s | 20.3, CH ₃ | 1.88, s | 20.3, CH ₃ | 1.90, s |
| 15 | 26.1, CH ₃ | 1.40, d (6.3) | 16.9, CH ₃ | 1.90, d (7.7) | 16.7, CH ₃ | 0.95, d (6.9) | 17.0, CH ₃ | 0.97, d (6.9) | 18.0, CH ₃ | 1.26, d (6.9) |
| 1' | 168.6, C | | 168.7, C | | 167.7, C | | 167.6, C | | | |
| 2' | 115.1, CH | 5.81, d (15.7) | 115.3, CH | 5.81, d (15.7) | 115.7, CH | 5.79, d (15.7) | 115.9, CH | 5.81, d (15.7) | | |
| 3' | 152.6, CH | 7.35, d (15.7) | 152.2, CH | 7.33, d (15.7) | 150.9, CH | 7.30, d (15.7) | 150.8, CH | 7.31, d (15.7) | | |
| 4' | 135.3, C | | 135.3, C | | 134.9, C | | 134.9, C | | | |
| 5' | 139.2, CH | 6.07, q (7.0) | 139.0, CH | 6.06, q (7.1) | 138.4, CH | 6.06, q (7.0) | 138.2, CH | 6.06, q (6.9) | | |
| 6' | 14.8, CH ₃ | 1.82, d (7.0) | 14.8, CH ₃ | 1.84, d (7.1) | 14.8, CH ₃ | 1.80, d (7.0) | 14.8, CH ₃ | 1.80, d (6.9) | | |
| 7' | 11.9, CH ₃ | 1.77, m | 11.9, CH ₃ | 1.79, m | 12.0, CH ₃ | 1.77, s | 12.0, CH ₃ | 1.77, br s | | |

^a ^1H 500 MHz, ^b ^1H 700 MHz; ^c ^{13}C 125 MHz, ^d ^{13}C 175 MHz.

Heimionone B (**2**): yellow oil; $[\alpha]_D^{25} +230$ (c 0.10, MeOH); UV/vis (0.01 mg/mL, MeOH) $\lambda_{\max}(\log \epsilon)$: 329 (3.70), 267 (4.23), 248 (4.22), 198 (4.73) nm; ECD (0.2 mg/mL, MeOH) $\lambda(\Delta \epsilon)$: 266 (+10.2), 241 (−7.7), 222 (+0.1) nm, Figure S1; ^1H and ^{13}C NMR data (MeOH- d_4), Tables 1 and S7; ESIMS m/z 373.21 $[\text{M} + \text{H}]^+$, 371.04 $[\text{M} - \text{H}]^-$; HRESIMS m/z 373.2011 $[\text{M} + \text{H}]^+$ (calcd. for $\text{C}_{22}\text{H}_{29}\text{O}_5$, 373.2010); $t_R = 9.3$ min (analytical HPLC).

Heimionone C (**3**): yellow oil; $[\alpha]_D^{25} +156$ (c 0.50, MeOH); UV/vis (0.01 mg/mL, MeOH) $\lambda_{\max}(\log \epsilon)$: 376 (3.18), 269 (4.35), 198 (4.41) nm; ECD (0.2 mg/mL, MeOH) $\lambda(\Delta \epsilon)$: 270 (+8.9), 241 (−0.6), 219 (+0.2), 205 (−10.8) nm, Figure S2; ^1H and ^{13}C NMR data (acetonitrile- d_3), Tables 1 and S8; ESIMS m/z 341.25 $[\text{M} - \text{H}_2\text{O} + \text{H}]^+$, 375.28 $[\text{M} - \text{H} + \text{H}_2\text{O}]^-$; HRESIMS m/z 381.2034 $[\text{M} + \text{Na}]^+$ (calcd. for $\text{C}_{22}\text{H}_{30}\text{NaO}_4$, 381.2036); $t_R = 11.9$ min (analytical HPLC).

Heimionone D (**4**): yellow oil; $[\alpha]_D^{25} +72$ (c 1.00, MeOH); UV/vis (0.01 mg/mL, MeOH) $\lambda_{\max}(\log \epsilon)$: 268 (3.68), 198 (4.50) nm; ECD (0.4 mg/mL, MeOH) $\lambda(\Delta \epsilon)$: 270 (+1.9), 247 (−0.7), 218 (+0.6), 200 (−3.7) nm, Figure S2; ^1H and ^{13}C NMR data (acetonitrile- d_3) Tables 1 and S9; ESIMS m/z 365.20 $[\text{M} + \text{Na}]^+$; HRESIMS m/z 365.2086 $[\text{M} + \text{Na}]^+$ (calcd. for $\text{C}_{22}\text{H}_{30}\text{NaO}_3$, 365.2087); $t_R = 14.1$ min (analytical HPLC).

Heimionone E (**5**): yellow oil; $[\alpha]_D^{25} +20$ (c 0.25, MeOH); UV/vis (0.05 mg/mL, MeOH) $\lambda_{\max}(\log \epsilon)$: 266 (3.83), 202 (3.82) nm; ECD (1.0 mg/mL, MeOH) $\lambda(\Delta \epsilon)$: 404 (+0.2), 361 (−1.0), 319 (+0.2), 255 (−2.0), 225 (+1.0), 204 (−6.8) nm, Figure S2; ^1H and ^{13}C NMR data (methanol- d_4), Tables 1 and S10; ESIMS m/z 235.07 $[\text{M} + \text{H}]^+$, 251.06 $[\text{M} - \text{H} + \text{H}_2\text{O}]^-$; HRESIMS m/z 235.1694 $[\text{M} + \text{H}]^+$ (calcd. for $\text{C}_{15}\text{H}_{23}\text{O}_2$, 235.1693); $t_R = 8.1$ min (analytical HPLC).

3.8. Preparation of the (R)- and (S)-MTPA Ester Derivatives of **1**, **3**, and **5**

The 0.5 mg of each compound were dissolved in 300 μL deuterated pyridine. Afterward, 2 μL of (R)-(-)- α -methoxy- α -(trifluoromethyl)phenylacetyl chloride were added into the solution and left for 15 min at room temperature. The reaction was monitored by analytical HPLC/MS. Another 2 μL of R-MTPA were added if the compounds were not completely converted into the corresponding Mosher-ester. Immediately after Mosher esterification, the samples were transferred into 3.0 mm NMR tubes. This was followed by measurements of ^1H NMR (Tables S1–S3), ^1H , ^1H -COSY NMR, ^1H , ^{13}C -HSQC NMR, and ^1H , ^{13}C -HMBC NMR spectra. The same procedure was repeated with another 0.5 mg of each compound using (S)-(+)- α -methoxy- α -(trifluoromethyl)phenylacetyl chloride. Evaluation of the obtained $\Delta\delta^{\text{SR}}$ values was conducted as described by Hoyer et al. [15].

3.9. Antimicrobial Assay

Antimicrobial activities of all isolated compounds were assessed by performing a serial-dilution assay resulting in the determination of their minimum inhibitory concentration (MIC) against several yeast, fungal, and bacterial strains (Table S4). The assay was carried out in 96-well microtiter plates, as previously described by Harms et al. [16].

3.10. Cytotoxicity Assay

The in vitro cytotoxicity of compounds **1–5** against the mouse fibroblast cell line L929 and the cervix carcinoma cell line KB3.1 (Table S5) was assessed in 96-well plates, as previously published by Harms et al. [15].

4. Conclusions

Five new terpenoids, namely heimionones A–E (**1–5**), with uncommon bicyclo [5.3.0] decane and [6.3.0] undecane core structures, respectively, were isolated from submerged cultures of *Heimiomyces* sp. (MUCL 56078). In association with the previously described hispidin (**6**), hypholomin B (**7**), heimiocalamenes C–E (**8–10**), and heimiomycins A–C (**11–13**), as well as bis-heimiomycins A–D (**14–17**), heimiomycins D–E (**18–19**), and heimiocalamenes A–B (**20–21**), it becomes clear that *Heimiomyces* sp. is capable of producing a chemically very diverse spectrum of secondary metabolites. On top of that, a high number of as yet unidentified minor peaks were observed in the UV/Vis- and MS-spectra of the extracts obtained from *Heimiomyces* sp., therefore especially this strain should be considered for further

analysis of its secondary metabolism, particularly for cultivation in more different media. Since all isolated compounds did not show outstanding activities in the antimicrobial and cytotoxicity assays, they can be considered for other assays with different targets. However, our findings once again show the importance of examining unexplored species from the tropics for their secondary metabolism during the search for novel natural products.

Supplementary Materials: The following supporting information can be downloaded at: <https://www.mdpi.com/article/10.3390/molecules28093723/s1>, Figure S1. ECD spectra of **1** and **2**; Figure S2. ECD spectra of **3–5**; Figure S3. ^1H NMR spectrum (700 MHz, pyridine- d_5) of the *S*-MTPA ester of heimionone A (**1**); Figure S4. COSY NMR spectrum (700 MHz, pyridine- d_5) of the *S*-MTPA ester of heimionone A (**1**); Figure S5. ^1H NMR spectrum (700 MHz, pyridine- d_5) of the *R*-MTPA ester of heimionone A (**1**); Figure S6. COSY NMR spectrum (700 MHz, pyridine- d_5) of the *R*-MTPA ester of heimionone A (**1**); Figure S7. ^1H NMR spectrum (700 MHz, pyridine- d_5) of the *S*-MTPA ester of heimionone C (**3**); Figure S8. COSY NMR spectrum (700 MHz, pyridine- d_5) of the *S*-MTPA ester of heimionone C (**3**); Figure S9. ^1H NMR spectrum (700 MHz, pyridine- d_5) of the *R*-MTPA ester of heimionone C (**3**); Figure S10. COSY NMR spectrum (700 MHz, pyridine- d_5) of the *R*-MTPA ester of heimionone C (**3**); Figure S11. ^1H NMR spectrum (700 MHz, pyridine- d_5) of the *S*-MTPA ester of heimionone E (**5**); Figure S12. ^1H NMR spectrum (700 MHz, pyridine- d_5) of the *R*-MTPA ester of heimionone E (**5**); Figure S13. COSY NMR spectrum (700 MHz, pyridine- d_5) of the *R*-MTPA ester of heimionone E (**5**); Figure S14. Previously described compounds that were observed in submerged cultures of *Heimiomyces* sp.: **6**: hispidin, **7**: hypholomin B.; Figure S15. Compounds previously isolated from *Heimiomyces* sp.: **8–10**: heimiocalamenes C–E (including originally proposed and revised structure of **10**), **11–13**: heimiomycins A–C; Figure S16. Compounds previously isolated from *Heimiomyces* sp.: **14–17**: bis-heimiomycins A–D, **18–19**: heimiomycins D–E, **20–21**: heimiocalamenes A–B; Figure S17. Chemical structures of heimionone A (**1**) and daldinin F [**8**]; Figures S18–S47: NMR spectra. Table S1. ^1H NMR data (700 MHz, Pyridine- d_5 , δ in ppm) of (*S*)/(*R*) MTPA esters obtained from heimionone A (**1**); Table S2. ^1H NMR data (700 MHz, Pyridine- d_5 , δ in ppm) of (*S*)/(*R*) MTPA esters obtained from heimionone C (**3**); Table S3. ^1H NMR data (700 MHz, Pyridine- d_5 , δ in ppm) of (*S*)/(*R*) MTPA esters obtained from heimionone E (**5**); Table S4. Minimum inhibitory concentration (MIC in $\mu\text{g/mL}$) for bacterial and fungal strains; Table S5. Half inhibitory concentration (IC_{50} in μM); Table S6. NMR spectroscopic data (^{13}C (δC), 175 MHz and ^1H (δH), 500 MHz, methanol- d_4) for heimionone A (**1**); Table S7. NMR spectroscopic data (^{13}C (δC), 175 MHz and ^1H (δH), 700 MHz, methanol- d_4) for heimionone B (**2**); Table S8. NMR spectroscopic data (^{13}C (δC), 125 MHz and ^1H (δH), 500 MHz, acetonitrile- d_3) for heimionone C (**3**); Table S9. NMR spectroscopic data (^{13}C (δC), 175 MHz and ^1H (δH), 700 MHz, acetonitrile- d_3) for heimionone D (**4**); Table S10. NMR spectroscopic data (^{13}C (δC), 175 MHz and ^1H (δH), 700 MHz, methanol- d_4) for heimionone E (**5**); Table S11. Comparison of the NMR spectroscopic data for the 4-methylhexa-2,4-dienoic acid partial structure of heimionone A (**1**) (^{13}C (δC), 175 MHz and ^1H (δH), 500 MHz, methanol- d_4) and daldinin F (^{13}C (δC), 150 MHz and ^1H (δH), 600 MHz, chloroform- d_1) [**8**].

Author Contributions: Formal analysis, F.S.; investigation, S.P. and A.K.; resources, J.C.M. and C.D.; writing—original draft preparation, S.P.; writing—review and editing, F.S. and M.S.; project administration, M.S.; funding acquisition, M.S. All authors have read and agreed to the published version of the manuscript.

Funding: S.P. is grateful for a grant from the Life Science-Stiftung zur Förderung von Wissenschaft und Forschung (LSS). Furthermore, this research benefitted from the financial support of the “ASAFEM” Project (Grant No. IC-070) under the ERAfrica Programme of the European Commission; beneficiaries J.C.M., C.D., and M.S. Finally, the authors want to acknowledge the European Union’s H2020 Research and Innovation Staff Exchange program (H2020-MSCA-RISE), Grant No. 101008129: MYCOBIOMICS.

Institutional Review Board Statement: Not applicable.

Informed Consent Statement: Not applicable.

Data Availability Statement: The data are available in the Supporting Information of the article.

Acknowledgments: The authors thank W. Collisi and C. Kakoschke for performing the bioassays and NMR spectroscopic measurements, respectively. T. Cheng and C. Chepkirui are thanked for providing supporting data and biological material from their previous experiments. At last, S. Pfütze

wants to thank E. Charria, J-P. Wennrich, K. Becker, S. Reinecke, E. Surges, and C. Lambert for their expert advisory assistance.

Conflicts of Interest: The authors declare no conflict of interest.

Sample Availability: Samples of the isolated compounds are not available from the authors, due to consumption for structure elucidation and bioassays.

References

1. Kirk, P.M.; Cannon, P.F.; David, J.C.; Stalpers, J.A. *Ainsworth and Bisby's Dictionary of the Fungi*; CABI: Wallingford, UK, 2008.
2. Sandargo, B.; Chepkirui, C.; Cheng, T.; Chaverra-Muñoz, L.; Thongbai, B.; Stadler, M.; Hüttel, S. Biological and chemical diversity go hand in hand: Basidiomycota as source of new pharmaceuticals and agrochemicals. *Biotechnol. Adv.* **2019**, *37*, 107344. [[CrossRef](#)] [[PubMed](#)]
3. Dörfer, M.; Gressler, M.; Hoffmeister, D. Diversity and bioactivity of *Armillaria* sesquiterpene aryl ester natural products. *Mycol. Prog.* **2019**, *18*, 1027–1037. [[CrossRef](#)]
4. Cheng, T.; Chepkirui, C.; Decock, C.; Matasyoh, J.C.; Stadler, M. Heimiomycins A–C and calamenens from the African basidiomycete *Heimiomycetes* sp. *J. Nat. Prod.* **2020**, *83*, 2501–2507. [[CrossRef](#)] [[PubMed](#)]
5. Pfütze, S.; Khamsim, A.; Surup, F.; Decock, C.; Matasyoh, J.C.; Stadler, M. Calamene-type sesqui-, mero-, and bis-sesquiterpenoids from cultures of *Heimiomycetes* sp., a basidiomycete collected in Africa. *J. Nat. Prod.* **2023**, *86*, 390–397. [[CrossRef](#)] [[PubMed](#)]
6. Edwards, R.L.; Lewis, D.G.; Wilson, D.V. 983. Constituents of the Higher Fungi. Part I. Hispidin, a new 4-hydroxy-6-styryl-2-pyrone from *Polyporus hispidus* (Bull.) Fr. *J. Chem. Soc.* **1961**, 4995–5002. [[CrossRef](#)]
7. Fiasson, J.-L.; Gluchoff-Fiasson, K.; Steglich, W. Über die Farb- und Fluoreszenzstoffe des Grünblättrigen Schwefelkopfes (*Hypholoma fasciculare*, Agaricales). *Chem. Ber.* **1977**, *110*, 1047–1057. [[CrossRef](#)]
8. Quang, D.N.; Hashimoto, T.; Tanaka, M.; Stadler, M.; Asakawa, Y. Cyclic azaphilones daldinins E and F from the ascomycete fungus *Hypoxylon fuscum* (Xylariaceae). *Phytochemistry* **2004**, *65*, 469–473. [[CrossRef](#)] [[PubMed](#)]
9. Qin, G.-F.; Liang, H.-B.; Liu, W.-X.; Zhu, F.; Li, P.-L.; Li, G.-Q.; Yao, J.-C. Bicyclo [6.3.0] undecane sesquiterpenoids: Structures, biological activities, and syntheses. *Molecules* **2019**, *24*, 3912. [[CrossRef](#)] [[PubMed](#)]
10. Foley, D.A.; Maguire, A.R. Synthetic approaches to bicyclo [5.3.0]decane sesquiterpenes. *Tetrahedron* **2010**, *66*, 1131–1175. [[CrossRef](#)]
11. Takaya, Y.; Akasaka, M.; Takeuji, Y.; Tanitsu, M.; Niwa, M.; Oshima, Y. Novel guaianoids, nardoguaianone E–I, from *Nardostachys chinensis* Roots. *Tetrahedron* **2000**, *56*, 7679–7683. [[CrossRef](#)]
12. Chen, D.; Chen, W.; Liu, D.; van Ofwegen, L.; Proksch, P.; Lin, W. Asteriscane-type sesquiterpenoids from the soft coral *Simularia capillosa*. *J. Nat. Prod.* **2013**, *76*, 1753–1763. [[CrossRef](#)] [[PubMed](#)]
13. Park, I.-H.; Chung, S.-K.; Lee, K.-B.; Yoo, Y.-C.; Kim, S.-K.; Kim, G.-S.; Song, K.-S. An antioxidant hispidin from the mycelial cultures of *Phellinus linteus*. *Arch. Pharm. Res.* **2004**, *27*, 615–618. [[CrossRef](#)] [[PubMed](#)]
14. Jung, J.-Y.; Lee, I.-K.; Seok, S.-J.; Lee, H.-J.; Kim, Y.-H.; Yun, B.-S. Antioxidant polyphenols from the mycelial culture of the medicinal fungi *Inonotus xeranticus* and *Phellinus linteus*. *J. Appl. Microbiol.* **2008**, *104*, 1824–1832. [[CrossRef](#)] [[PubMed](#)]
15. Hoye, T.R.; Jeffrey, C.S.; Shao, F. Mosher Ester analysis for the determination of absolute configuration of stereogenic (chiral) carbinol carbons. *Nat. Protoc.* **2007**, *2*, 2451–2458. [[CrossRef](#)] [[PubMed](#)]
16. Harms, K.; Surup, F.; Stadler, M.; Stchigel, A.M.; Marin-Felix, Y. Morinagadepsin, a depsipeptide from the fungus *Morinagamycetes vermicularis* gen. et comb. nov. *Microorganisms* **2021**, *9*, 1191. [[CrossRef](#)] [[PubMed](#)]

Disclaimer/Publisher's Note: The statements, opinions and data contained in all publications are solely those of the individual author(s) and contributor(s) and not of MDPI and/or the editor(s). MDPI and/or the editor(s) disclaim responsibility for any injury to people or property resulting from any ideas, methods, instructions or products referred to in the content.

Paper IV

5'-O-methyl-14-hydroxyarmillane, a new armillane-type sesquiterpene from cultures of *Guyanagaster necrorhiza*

Sebastian Pfütze^{1,2}, Dana Nedder^{1,2}, Frank Surup^{1,2}, Marc Stadler^{1,2,*}

Mycological Progress **2023**; 22:70. DOI: <https://doi.org/10.1007/s11557-023-01920-6>

¹ Department of Microbial Drugs, Helmholtz Centre for Infection Research (HZI), German Centre for Infection Research (DZIF), Partner Site Hannover/Braunschweig, Inhoffenstrasse 7, 38124 Braunschweig, Germany

² Institute of Microbiology, Technische Universität Braunschweig, Spielmannstraße 7, 38106 Braunschweig, Germany

*Corresponding author



ORIGINAL ARTICLE

5'-O-methyl-14-hydroxyarmillane, a new armillane-type sesquiterpene from cultures of *Guyanagaster necrorhiza*

Sebastian Pfütze^{1,2} · Dana Leoni Nedder^{1,2} · Frank Surup^{1,2} · Marc Stadler^{1,2}

Received: 25 June 2023 / Revised: 28 August 2023 / Accepted: 29 August 2023
© The Author(s) 2023

Abstract

Protoilludene-type sesquiterpene aryl esters are a unique and very diverse compound class that were exclusively isolated from members of the genus *Armillaria* (*Agaricomycetes*, *Physalacriaceae*) up to this point. Herein, we describe the isolation and structural characterization of 5'-O-methyl-14-hydroxyarmillane (**1**), a new armillane-type derivative, that was obtained from submerged cultures of *Guyanagaster necrorhiza* (CBS 138623) together with the known congeners melleolide G (**2**), melleolide B (**3**), and 10-dehydroxy-melleolide B (**4**). ROESY data and coupling constants assigned the relative configurations of **1**, while common absolute configurations were confirmed from comparison of its ECD spectrum to the one of 10-hydroxy-5'-methoxy-6'-chloroarmillane (**5**). Additionally, the configuration of melleolide G (**2**) was revised based on observed ROESY correlations. It is the first time that protoilludene-type sesquiterpene aryl esters were isolated from another genus, namely, *Guyanagaster*, that is closely related to *Armillaria*. **1–4** were evaluated for their biological activities in a serial dilution assay against several yeast, fungi, and bacteria, as well as in a cytotoxicity assay against different cell lines. Compound **4** was moderately active against *Bacillus subtilis*, *Staphylococcus aureus*, and *Mucor hiemalis*. Furthermore, **1**, **3**, and **4** showed weak cytotoxic effects against the mouse fibroblast cell line L929 and the cervix carcinoma cell line KB3.1.

Keywords *Guyanagaster necrorhiza* · Protoilludene · Sesquiterpene · Armillane

Introduction

The protoilludene-type sesquiterpene aryl esters are a chemically very diverse class of compounds among the natural products that can be obtained from fungal sources. Up to this point, more than 70 congeners of this compound class were discovered and described in literature (Dörfer et al. 2019). Often casually summarized as melleolides, strictly speaking protoilludene-type aryl esters have to be divided into three groups according to the localization of the double bond within the protoilludene backbone. Melleolides

are Δ^{2-3} -unsaturated and armillyl orsellinates are Δ^{2-4} -unsaturated, while armillanes are characterized by the absence of the double bond within the 6-membered ring (Engels et al. 2021). Alongside their chemical diversity, several members of the protoilludene-type aryl esters show a wide range of bioactivities, including antibacterial, antifungal, and cytotoxic effects (Dörfer et al. 2019). Interestingly, this class of natural products was exclusively isolated from cultures of the genus *Armillaria* (*Agaricomycetes*, *Physalacriaceae*) until now. *Armillaria* spp. are well-known and globally distributed parasitic fungi that affect a broad range of different hosts in timber and agronomic systems, where they play a critical role as root pathogens and decomposers (Baumgartner et al. 2011; Coetzee et al. 2018). In 2010, a gasteroid fungus that is closely related to *Armillaria* was described as *Guyanagaster necrorhiza* (Henkel et al. 2010) and together with *Desarmillaria*, these genera were later assigned to the Armillarioid clade (Koch et al. 2017; Kedves et al. 2021). Phylogenetic reconstruction showed that *Guyanagaster* species are extant taxa that diverged from early members of the Armillarioid clade when this lineage evolved in Eurasia about 51 million years ago (Koch et al. 2017).

Section Editor: Ji-Kai Liu

✉ Marc Stadler
marc.stadler@helmholtz-hzi.de

¹ Department Microbial Drugs, Helmholtz Centre for Infection Research (HZI), German Centre for Infection Research (DZIF), Partner Site Hannover-Braunschweig, Inhoffenstrasse 7, 38124 Braunschweig, Germany

² Institute of Microbiology, Technische Universität Braunschweig, Spielmannstraße 7, 38106 Braunschweig, Germany

During this process, the mushroom ancestor of *Guyanagaster* underwent a process referred to as gasteromycation leading to the gasteroid species that were only found in the Guiana Shield region (Guyana) up to this point (Henkel et al. 2010; Koch et al. 2017). The close taxonomic relationship of the genera *Armillaria* and *Guyanagaster* led to the endeavor to investigate the secondary metabolism of *Guyanagaster* species for the production of protoilludene-type sesquiterpene aryl esters. Herein, we describe the isolation and structural characterization of 5'-O-methyl-14-hydroxyarmillane (**1**), a new armillane-type derivative, that was obtained from submerged cultures of *G. necrorrhiza* (CBS 138623) together with the known congeners melleolide G (**2**), whose configuration we revise, melleolide B (**3**), and 10-dehydroxymelleolide B (**4**).

Results and discussion

Guyanagaster necrorrhiza was cultivated in liquid YM6.3 medium. Extraction of the harvested mycelium and culture broth led to extracts that were purified by preparative

HPLC. This resulted in the isolation and characterization of the new meroterpenoid 5'-O-methyl-14-hydroxyarmillane (**1**) that showed a molecular ion cluster at m/z 451.2333 $[M+H]^+$ (calcd. for $C_{24}H_{35}O_8$, 451.2326) in the HRESIMS spectrum revealing the molecular formula $C_{24}H_{34}O_8$. Its 1H and ^{13}C NMR (Table 1) data were highly similar to those of armillane (Donnelly and Hutchinson 1990). The key difference is the methylation of the hydroxy group at C-5' and the presence of an additional hydroxy group at C-14 for **1**. The relative configuration was confirmed by coupling constants and ROESY data: the large coupling constants $J_{H_2,H_3} = J_{H_3,H_{13}} = 11.0$ Hz, observed in the triplet of H-3, indicate that all of these three protons are in axial position on alternating sides of the ring structure. ROESY correlations between H_3 -15/ H -9 and H_3 -15/ H -13, as well as between H_2 -14 and H-3, H-10 α , H-12 α confirm an unchanged configuration compared to **5**. The absolute configuration was assigned as 2*R*,3*S*,4*R*,5*R*,7*R*,9*S*,11*R*,13*R*, which is characteristic for melleoid sesquiterpenoids, since the ECD spectra of 5'-O-methyl-14-hydroxyarmillane (**1**) and the one of 10-hydroxy-5'-methoxy-6'-chloroarmillane (**5**) (Mándi and Kurtán 2019) are very similar. Due to the absence of the

Table 1 ^{13}C (175 MHz) and 1H (700 MHz) NMR spectroscopic data of compound **1** in acetone- d_6 (δ in ppm)

| No. | δ_C , type | δ_H (J in Hz) | COSY | C to H HMBC | N/ROESY |
|-----|-----------------------|---|---|---------------------------------------|--|
| 1 | 63.0, CH ₂ | 3.86, dd (10.9, 5.1) 4.00, dd (10.9, 3.4) | 2 β , 1 2 β , 1 | 2, 3, 4 3, 4 | |
| 2 | 46.4, CH | β : 2.09, m | 3 α , 1, 1 | 1, 5, 4 | |
| 3 | 68.7, CH | α : 3.74, t (11.0) | 13 β , 2 β | 12, 7, 2, 1 | 10 α , 14 |
| 4 | 81.6, C | | | | |
| 5 | 76.8, CH | α : 5.41, t (8.5) | 6 α | 6, 2, 4, 1' | 8, 6 α |
| 6 | 34.4, CH ₂ | α : 1.94, d (2.4) β : 1.88, m | 5 α 8 | 8, 7, 4 8, 7, 9, 5 | 5 α |
| 7 | 39.0, C | | | | |
| 8 | 22.5, CH ₃ | 1.18, s | 6 β | 6, 7, 9, 4 | 5 α |
| 9 | 47.5, CH | β : 2.17, m | 10 β , 10 α | 6, 7, 10, 4 | 15 |
| 10 | 39.7, CH ₂ | α : 1.57, m β : 1.34, m | 10 β , 9 β 10 α , 9 β | 15, 7, 11, 9, 14 12, 13 | 14, 3 α 15 |
| 11 | 42.9, C | | | | |
| 12 | 38.6, CH ₂ | α : 2.11, m β : 1.34, m | 12 β 12 α , 13 β | 15, 10, 11, 9, 3, 14 15, 11, 3, 14 | 14 15 |
| 13 | 47.3, CH | β : 2.02, m | 12 β , 3 α | 10, 11, 3 | |
| 14 | 72.6, CH ₂ | 3.34, m | | 15, 12, 10, 11 | 10 α , 12 α , 3 α |
| 15 | 27.5, CH ₃ | 1.01, s | | 12, 10, 11, 14 | 10 β , 12 β , 9 β , 13 β |
| 1' | 172.4, C | | | | |
| 2' | 106.1, C | | | | |
| 3' | 166.7, C | | | | |
| 4' | 99.7, CH | 6.33, d (2.4) | | 2', 6', 5' | |
| 5' | 165.2, C | | | | |
| 6' | 111.7, CH | 6.36, d (2.4) | | 8', 4' | |
| 7' | 144.2, C | | | | |
| 8' | 24.7, CH ₃ | 2.57, s | | 4', 2', 6', 7' | |
| 9' | 55.9, CH ₃ | 3.82, s | | 5' | |

double bond in the 6-membered ring of the protoilludene backbone, **1** can be assigned to the armillane-type sesquiterpene aryl esters.

Furthermore, with melleolide G (**2**), melleolide B (**3**), and 10-dehydroxy-melleolide B (**4**) three known congeners, previously described from *Armillaria* spp. in the literature, were isolated from the same batch of submerged *G. necrorhiza* cultures. While **2** and **3** were reported from cultures of *A. mellea* (Arnone et al. 1986; Arnone et al. 1988), **4** was obtained from an undefined species *Armillaria* sp. (Yin et al. 2012). As their names already imply, **2–4** belong to the subclass of melleolides, due to their characteristic double bond localization (Δ^{2-3} -unsaturated). Although our ^{13}C data of **2** is virtually identical to those of Arnone et al. (1988), the assignment of C-2 and C-3 has to be exchanged based on HMBC data (Table S1, Figure S10). More importantly, the published confirmation of **2** is not consistent with the ROESY correlations we observed: while methyl H₃-15 shows ROESY correlations to both methines H-9 and H-13, oxymethylene H₂-14 has correlations with H-10 α , H-12 α , and H₃-8 (Table S1, Figure S11). Therefore, the stereoconfigurational assignment of C-11 has to be revised, with the oxymethylene (CH₂-14) pointing below the main molecular plane.

Protoilludene-type sesquiterpene aryl esters are well known for their broad spectrum of biological activities and several derivatives were reported as antibacterial, antifungal, or cytotoxic (Dörfer et al. 2019). Therefore, the potential bioactivities of compounds **1–4** were evaluated in a serial dilution assay against several yeast, fungi, and bacteria, as well as in a cytotoxicity assay against different cell lines. In the serial dilution assay, only **4** showed moderate activities against *B. subtilis*,

S. aureus, and *M. hiemalis* (Table 2). The relationship between structures and biological activities of this compound class has not been systematically investigated yet; thus, no conclusions to explain the activities of **4** can be made. Solely the weak or missing cytotoxic effects of **1–4** (Table 3) can be associated with the hydroxylation of C-1, since especially derivatives with an aldehyde function at this position are reported to be the ones with the highest potential for cytotoxicity (Dörfer et al. 2019).

For the first time, protoilludene-type sesquiterpene aryl esters are reported from another genus than *Armillaria*. Our data confirm previous results describing the genus *Guyanagaster* as closely related to *Armillaria* (Henkel et al. 2010; Koch et al. 2017; Kedves et al. 2021).

Table 3 Half inhibitory concentration (IC₅₀ in μM) of compounds **1–4** isolated from *Guyanagaster necrorhiza* (CBS 138623) to assess the cytotoxicities

| Compound | KB3.1 | L929 |
|--|----------------------|----------------------|
| 1 (5'-O-methyl-14-hydroxyarmillane) | 37.8 | 10.9 |
| 2 (melleolide G) | – | – |
| 3 (melleolide B) | 16.2 | 46.3 |
| 4 (10-dehydroxy-melleolide B) | 13.7 | 18.3 |
| Epo B (positive control) | 3.8×10^{-5} | 1.1×10^{-3} |

The assay was performed with stock solutions of **1–4** (1 mg/mL in acetone). Epothilone B was used as positive control, while acetone (20 μL) was used as negative control and did not show inhibitory effects

IC₅₀ in μM ; – no activity

Table 2 Minimum inhibitory concentrations (MIC in $\mu\text{g/mL}$) of compounds **1–4** isolated from *Guyanagaster necrorhiza* (CBS 138623) to assess the antimicrobial activities

| Compound | <i>Bacillus subtilis</i> DSM 10 | <i>Staphylococcus aureus</i> DSM 346 | <i>Mycobacterium smegmatis</i> ATCC 700084 | <i>Schizosaccharomyces pombe</i> DSM 70572 | <i>Pichia anomala</i> DSM 6766 | <i>Mucor hiemalis</i> DSM 2656 | <i>Rhodotorula glutinis</i> DSM 10134 |
|--|---------------------------------|--------------------------------------|--|--|--------------------------------|--------------------------------|---------------------------------------|
| 1 (5'-O-methyl-14-hydroxyarmillane) | 33.3 | – | – | – | – | – | – |
| 2 (melleolide G) | 66.6 | – | – | – | – | – | – |
| 3 (melleolide B) | 66.6 | 33.3 | – | 33.3 | 66.7 | 33.3 | 33.3 |
| 4 (10-dehydroxy-melleolide B) | 16.6 | 16.6 | 66.6 | 33.3 | – | 16.6 | 66.6 |
| Positive control | 16.6 [O] | 0.21 [G] | 1.7 [K] | 4.2 [N] | 4.2 [N] | 1.0 [N] | 1.0 [N] |

Stock solutions of **1–4** were used to perform the serial dilution assay (1 mg/mL in acetone). As positive controls, the antimicrobials [O] oxytetracycline, [G] gentamycin, and [K] kanamycin were used for bacteria and [N] nystatin was used for filamentous fungi and yeast. Acetone (20 μL) was used as negative control and did not show inhibitory effects. All tested compounds did not show activities against *Candida albicans* (DSM 1665), *Escherichia coli* (DSM 1116), *Pseudomonas aeruginosa* (DSM PA14), and *Chromobacterium violaceum* (DSM 30191)

IC₅₀ in $\mu\text{g/mL}$; – no activity

Material and methods

General experimental procedures

A PerkinElmer 241 polarimeter was used to measure the optical rotation. To record the UV spectra, a Shimadzu UV-Vis spectrophotometer UV-2450 (Duisburg, Germany) was used. NMR spectra were measured with the Bruker Avance III 500-MHz spectrometer (Bremen, Germany) equipped with a BBFO (plus) SmartProbe (^1H 500 MHz, ^{13}C 125 MHz) and the Bruker Avance III 700-MHz spectrometer (Bremen, Germany) equipped with a 5-mm TCI cryoprobe (^1H 700 MHz, ^{13}C 175 MHz). Selected chemical shifts of acetone- d_6 (^1H : 2.05 ppm, ^{13}C : 29.92 ppm) were used to reference the NMR data. The Agilent 1200 series HPLC-UV system (Santa Clara, CA, USA) in combination with an ESI-TOF-MS (Maxis, Bruker, Bremen, Germany) was used to record HRESIMS data. These measurements were performed with the 2.1×50 mm, $1.7 \mu\text{m}$, C18 Acquity UPLC BEH (Waters, Milford, MA, USA) column, using MilliQ water + 0.1% formic acid as solvent A and acetonitrile + 0.1% formic acid as solvent B (gradient: 5% B for 0.5 min increasing to 100% B in 19.5 min and maintaining 100% B for 5 min, flow rate: 0.6 mL/min, UV/Vis detection: 200–600 nm).

Fungal material

The culture of *G. necrorhiza* we studied (original code MCA 3950) was kindly provided by M. Cathie Aime, who also deposited the strain at the Westerdijk Fungal Biodiversity Institute (Utrecht, Netherlands) under the accession number CBS 138623. The strain was previously used in the study by Koch and Aime (2018).

Fermentation of *G. necrorhiza* and extraction

Forty 500-mL Erlenmeyer shape culture flasks, each of them containing 200 mL of YM6.3 medium (10 g/L malt extract, 4 g/L D-glucose, 4 g/L yeast extract, pH 6.3), were inoculated with three 50-mm² sized pieces of well-grown mycelium from YM6.3 agar plates per flask. The cultures were incubated on a rotary shaker at 23 °C and 140 min⁻¹. To monitor the consumption of the glucose, test strips (Medi-Test Glucose, Macherey-Nagel, Düren, Germany) were used. After 24 days, the culture broth was tested negative for glucose and 2 days later the cultures were harvested (26 days in total). Mycelium and supernatant were separated by centrifugation at 5100 rpm for 30 min. The mycelium was extracted with acetone in an ultrasonic bath for 30 min, twice. Subsequently, the mycelium was separated from the

liquid phase by filtration and the organic solvent was evaporated at 40 °C on a rotary evaporator. Dilution of the remaining aqueous phase with H₂O was followed by an extraction against EtOAc (1:1, twice). The obtained organic phase was evaporated to dryness on a rotary evaporator at 40 °C leading to 126 mg mycelial extract. Extraction of the supernatant was carried out against EtOAc (1:1) in a separatory funnel, twice. After phase separation, the organic phase was kept and evaporated to dryness (40 °C) leading to 360 mg of supernatant extract.

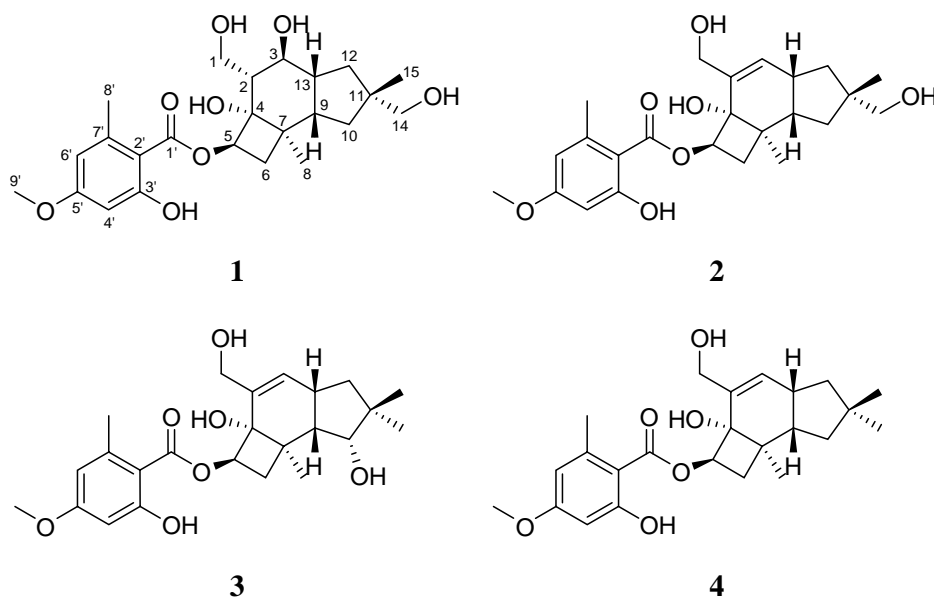
Analytical HPLC

The extracts that were obtained from the mycelium and supernatant of *G. necrorhiza* were dissolved with acetone to yield a concentration of 10 mg/mL. This was followed by a filtration of 100 μL of the solution with Whatman Mini-UniPrepTM syringeless filter devices (cytiva, Marlborough, MA, USA). All samples were analyzed using an analytical HPLC device (Dionex UltiMate 3000 series) coupled to an ion trap mass spectrometer (amazon speed by Bruker). After injection of 2 μL of the samples, the separation was carried out with an ACQUITY-UPLC BEH C18 column (50×2.1 mm; particle size: $1.7 \mu\text{m}$) by Waters. As mobile phase HPLC grade H₂O and MeCN with 0.1% formic acid were used at a flow rate of 600 $\mu\text{L}/\text{min}$. The gradient started at 5% of MeCN, continued with an increase to 100% MeCN in 20 min, and remained at 100% MeCN for 5 min. All obtained chromatograms were analyzed with the software Data Analysis 4.4 (Bruker).

Isolation of compounds 1–4 via reversed phase liquid chromatography

Purification of the obtained extracts was carried out using a Gilson PLC 2250 purification system coupled to a Gemini LC column 250×50 mm, 110 \AA , $10 \mu\text{m}$ (Phenomenex, Torrance, CA, USA). HPLC grade H₂O + 0.1% formic acid (solvent A) and MeCN + 0.1% formic acid (solvent B) were used as mobile phase at a flow rate of 50 mL/min. The gradient for the purification of the supernatant extract started with isocratic conditions at 15% B for 5 min, followed by an increase to 80% B in 60 min, another increase to 100% B in 5 min and remained at 100% B for 10 min. The fraction at 37.8–38.5 min led to 2.6 mg of **1**, the fraction at 45.5–46.5 min led to 1.5 mg of **2**, the fraction at 52.0–53.0 min led to 1.1 mg of **3**, and the fraction at 60.3–61.0 min led to 0.2 mg of **4**. The gradient for the purification of the mycelial extract started with isocratic conditions at 25% B for 5 min, followed by an increase to 100% B in 75 min and remained at 100% B for 10 min. The fraction at 35.0–36.5 min led to 0.5 mg of **2**, the fraction at 39.5–41.0 min led to 0.5 mg of **3**, and the fraction at 71.0–72.5 min led to 0.5 mg of **4** (Fig. 1).

Fig. 1 Protoilludene-type sesquiterpene aryl esters isolated from cultures of *G. necrorhiza*. **1**: 5'-O-methyl-14-hydroxyarmillane; **2**: melleolide G; **3**: melleolide B; **4**: 10-dehydroxy-melleolide B



Spectral data

5'-O-methyl-14-hydroxyarmillane (**1**): colorless oil; $[\alpha]_D^{20} = -13$ (c 0.1, MeOH); UV/Vis (0.01 mg/mL, MeOH) $\lambda_{\max}(\log \epsilon)$: 301 (4.30), 265 (4.01), 212 (3.59) nm; ECD (0.25 mg/mL, MeOH) $\lambda(\Delta \epsilon)$ 302 (1.1), 263 (−1.1), 238 (0.0), 219 (−0.7), 198 (1.8) nm, Fig. 2; ^1H and ^{13}C NMR data (acetone- d_6), Table 1; ESIMS m/z 451.25 $[\text{M}+\text{H}]^+$, 449.30 $[\text{M}-\text{H}]^-$; HRESIMS m/z 451.2333 $[\text{M}+\text{H}]^+$ (calcd. for $\text{C}_{24}\text{H}_{35}\text{O}_8$, 451.2326); $t_R = 9.2$ min (analytical HPLC).

Evaluation of antimicrobial activity

To determine minimum inhibitory concentrations (MICs) against several yeast, fungi, and bacteria, serial dilution assays in 96-well microtiter plates were performed as described by Harms et al. (2021). Compounds **1–4** were tested against *Bacillus subtilis*, *Staphylococcus aureus*, *Mycobacterium smegmatis*, *Escherichia coli*, *Pseudomonas aeruginosa*, *Chromobacterium violaceum*, *Schizosaccharomyces pombe*, *Candida albicans*, *Pichia anomala*, *Mucor hiemalis*, and *Rhodotorula glutinis*.

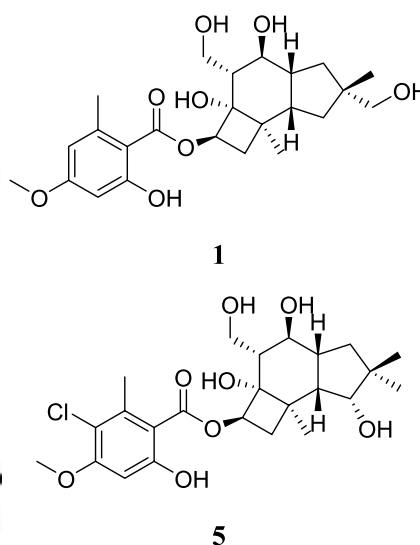
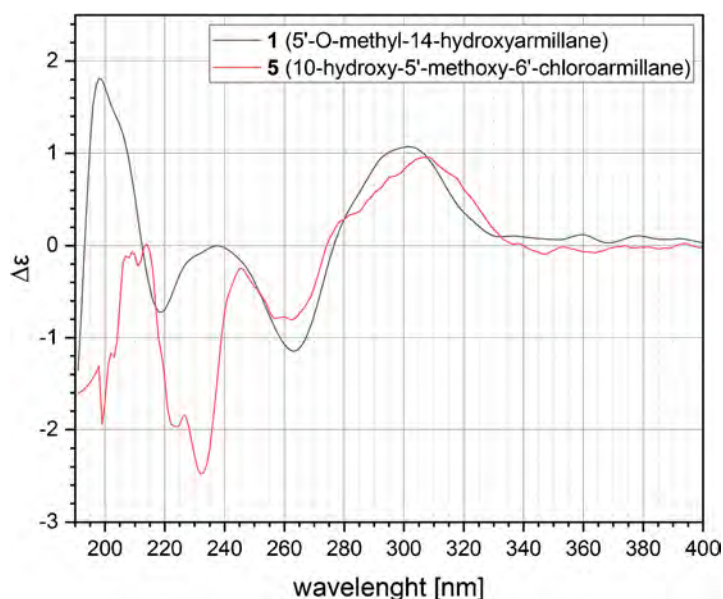


Fig. 2 ECD spectrum of 5'-O-methyl-14-hydroxyarmillane (**1**) in comparison to the one of 10-hydroxy-5'-methoxy-6'-chloroarmillane (**5**) that was previously isolated from cultures of *Armillaria ostoyae* (DSM 115711)

Evaluation of cytotoxicity

The cytotoxicities of compounds **1–4** were assessed by in vitro assays in 96-well plates as described by Harms et al. (2021). They were tested against the mouse fibroblast cell line L929 and the cervix carcinoma cell line KB3.1.

Conclusions

With 5'-*O*-methyl-14-hydroxyarmillane (**1**), a new armillane-type derivative, and the known congeners melleolide G (**2**), melleolide B (**3**), and 10-dehydroxy-melleolide B (**4**), four protoilludene-type sesquiterpene aryl esters were obtained from submerged cultures of *G. necrorhiza* (CBS 138623). It is the first time that members of this compound class were isolated from cultures of another genus than *Armillaria*. These results confirmed the close relationship between *Armillaria* and *Guyanagaster* leading to the assumption that more congeners, including new derivatives, can be found during further investigations on the secondary metabolism of *Guyanagaster* species. Therefore, *G. necrorhiza* (CBS 138623) can be cultivated under different conditions or other specimen can be investigated for their secondary metabolite production.

Supplementary Information The online version contains supplementary material available at <https://doi.org/10.1007/s11557-023-01920-6>.

Acknowledgements The authors are grateful for the help of C. Kakschke and E. Surges by measuring the NMR spectra, as well as for Wera Collisi by performing the bioassays. Furthermore, we wish to thank Aileen Gollasch for recording the HRESIMS spectra. S. Pfütz is grateful for the expert advisory assistance and support of E. Charria, J.-P. Wennrich, A. Skiba, and S. Reinecke.

Author contribution The study including cultivation, extraction, and compound isolation was conducted by D. Nedder with support from S. Pfütz. Analysis and structure elucidation was conducted by S. Pfütz. The first draft of the manuscript was written by S. Pfütz and revised by F. Surup and M. Stadler. All authors approved the final version.

Funding Open Access funding enabled and organized by Projekt DEAL. S. Pfütz is thankful for a grant from the Life Science-Stiftung zur Förderung von Wissenschaft und Forschung (LSS).

Declarations

Ethics approval Not applicable.

Consent to participate Not applicable.

Consent for publication Not applicable.

Conflict of interest The authors declare no competing interests.

Open Access This article is licensed under a Creative Commons Attribution 4.0 International License, which permits use, sharing, adaptation, distribution and reproduction in any medium or format, as long

as you give appropriate credit to the original author(s) and the source, provide a link to the Creative Commons licence, and indicate if changes were made. The images or other third party material in this article are included in the article's Creative Commons licence, unless indicated otherwise in a credit line to the material. If material is not included in the article's Creative Commons licence and your intended use is not permitted by statutory regulation or exceeds the permitted use, you will need to obtain permission directly from the copyright holder. To view a copy of this licence, visit <http://creativecommons.org/licenses/by/4.0/>.

References

- Arnone A, Cardillo R, Modugno VD, Nasini G (1988) Secondary mould metabolites. XXII. Isolation and structure elucidation of melleolids D and E and melleolids E-H, novel sesquiterpenoid aryl esters from *Clitocybe elegans* and *Armillaria mellea*. Gazz Chim Ital 118:517–521
- Arnone A, Cardillo R, Nasini G (1986) Structures of melleolids B-D, three antibacterial sesquiterpenoids from *Armillaria mellea*. Phytochemistry 25(2):471–474
- Baumgartner K, Coetzee MPA, Hoffmeister D (2011) Secrets of the subterranean pathosystem of *Armillaria*. Mol Plant Pathol 12:515–534. <https://doi.org/10.1111/j.1364-3703.2010.00693.x>
- Coetzee MPA, Wingfield BD, Wingfield MJ (2018) *Armillaria* root-rot pathogens: species boundaries and global distribution. Pathogens 7:83. <https://doi.org/10.3390/pathogens7040083>
- Donnelly DMX, Hutchinson RM (1990) Armillane, a saturated sesquiterpene ester from *Armillaria mellea*. Phytochemistry 29:179–182. [https://doi.org/10.1016/0031-9422\(90\)89033-6](https://doi.org/10.1016/0031-9422(90)89033-6)
- Dörfer M, Gressler M, Hoffmeister D (2019) Diversity and bioactivity of *Armillaria* sesquiterpene aryl ester natural products. Mycol Prog 18:1027–1037. <https://doi.org/10.1007/s11557-019-01508-z>
- Engels B, Heinig U, McElroy C et al (2021) Isolation of a gene cluster from *Armillaria gallica* for the synthesis of armillyl orsellinate-type sesquiterpenoids. Appl Microbiol Biotechnol 105:211–224. <https://doi.org/10.1007/s00253-020-11006-y>
- Harms K, Surup F, Stadler M et al (2021) Morinagadepsin, a depsipeptide from the fungus *Morinagamyces vermicularis* gen. et comb. nov. Microorganisms 9:1191
- Henkel TW, Smith ME, Aime MC (2010) *Guyanagaster*, a new wood-decaying sequestrate fungal genus related to *Armillaria* (Physalaciaceae, Agaricales, Basidiomycota). Am J Bot 97:1474–1484. <https://doi.org/10.3732/ajb.1000097>
- Kedves O, Shahab D, Champramary S et al (2021) Epidemiology, biotic interactions and biological control of armillarioids in the Northern Hemisphere. Pathogens 10:76. <https://doi.org/10.3390/pathogens10010076>
- Koch RA, Aime MC (2018) Population structure of *Guyanagaster necrorhizus* supports termite dispersal for this enigmatic fungus. Mol Ecol 27:2667–2679. <https://doi.org/10.1111/mec.14710>
- Koch RA, Wilson AW, Séné O et al (2017) Resolved phylogeny and biogeography of the root pathogen *Armillaria* and its gasteroid relative, *Guyanagaster*. BMC Evol Biol 17:33. <https://doi.org/10.1186/s12862-017-0877-3>
- Mándi A, Kurtán T (2019) Applications of OR/ECD/VCD to the structure elucidation of natural products. Nat Prod Rep 36:889–918. <https://doi.org/10.1039/C9NP00002J>
- Yin X, Feng T, Liu J-K (2012) Structures and cytotoxicities of three new sesquiterpenes from cultures of *Armillaria* sp. Nat Prod Bioprospect 2:245–248. <https://doi.org/10.1007/s13659-012-0077-1>

Publisher's note Springer Nature remains neutral with regard to jurisdictional claims in published maps and institutional affiliations.

Paper V

Depicting the Chemical Diversity of Bioactive Meroterpenoids Produced by the Largest Organism on Earth

Sebastian Pfütze^{1,2,†}, Esteban Charria-Girón^{1,2,†}, Frank Surup^{1,2}, Esther Schulzke^{1,2}, Rita Toshe^{1,3}, Artit Khonsanit⁴, Raimo Franke⁵, Frank Surup^{1,2}, Mark Brönstrup⁵, Marc Stadler^{1,2,*}

Angewandte Chemie, International Edition **2024**; 63:e202318505.

DOI: <https://doi.org/10.1002/anie.202318505>

- ¹ Department of Microbial Drugs, Helmholtz Centre for Infection Research (HZI), German Centre for Infection Research (DZIF), Partner Site Hannover/Braunschweig, Inhoffenstrasse 7, 38124 Braunschweig, Germany
- ² Institute of Microbiology, Technische Universität Braunschweig, Spielmannstraße 7, 38106 Braunschweig, Germany
- ³ Institute of Pharmaceutical Biology Pharm. Biotechnology, Universität des Saarlandes, Campus C2 3, 66123 Saarbrücken, Germany
- ⁴ BIOTEC, National Science and Technology Development, Agency (NSTDA), 111 Thailand Science Park, Phahonyothin Road, Khlong Nueng, Khlong Luang 12120, Pathum Thani, Thailand
- ⁵ Department Chemical Biology, Helmholtz Centre for Infection Research (HZI), and German Center for Infection Research (DZIF), Partner Site Hannover-Braunschweig, Inhoffenstrasse 7, 38124 Braunschweig, Germany

*Corresponding author

†These authors contributed equally to this work.

Natural Products

Depicting the Chemical Diversity of Bioactive Meroterpenoids Produced by the Largest Organism on Earth

Sebastian Pfütze⁺, Esteban Charria-Girón⁺, Esther Schulzke, Rita Toshe, Artit Khonsanit, Raimo Franke, Frank Surup, Mark Brönstrup, and Marc Stadler*

Abstract: In this investigation, we explored the diversity of melleolide-type meroterpenoids produced by *Armillaria ostoyae*, one of the largest and oldest organisms on Earth, using extracts from liquid and solid fermentation media. The study unveiled three unprecedented dimeric bismelleolides and three novel fatty-acid-substituted congeners, along with 11 new and 21 known derivatives. The structures were elucidated by 1D and 2D NMR spectroscopy and HRESI-MS, and ROESY spectral analysis for relative configurations. Absolute configurations were determined from crystal structures and through ECD spectra comparison. A compound library of melleolide-type meroterpenoids facilitated metabolomics-wide associations, revealing production patterns under different culture conditions. The library enabled assessments of antimicrobial and cytotoxic activities, revealing that the $\Delta^{2,4}$ double bond is not crucial for antifungal activity. Cytotoxicity was linked to the presence of an aldehyde at C1, but lost with hydroxylation at C13. Chemoinformatic analyses demonstrated the intricate interplay of chemical modifications on biological properties. This study marks the first systematic exploration of *Armillaria* spp. meroterpenoid diversity by MS-based untargeted metabolomics, offering insight into structure–activity relationships through innovative chemoinformatics.

Introduction

The phylum Basidiomycota comprises ca. 40,000 species and represents the second largest division within the Eumycota after the Ascomycota.^[1] Taxa belonging to this phylum are well known as creative producers of bioactive natural products.^[2] Even though most of the fungal natural product-derived drugs on the market were originally isolated from species of the Ascomycota, some of them were obtained from Basidiomycota.^[3] For instance, the pleuromutilins are a family of sesquiterpenoid antibiotics produced by *Clitopilus* spp. (Agaricales, Basidiomycota) that are the most recent antibacterial drug class to make it to the market.^[4]

An important representative of the Basidiomycota is *Armillaria* (Physalacriaceae—also known as honey mushrooms), a globally distributed genus of plant pathogens whose species infect trees by causing butt and root diseases that can lead to entire forest diebacks.^[5,6] In particular, the ability to form thickened mycelium strands (rhizomorphs), that allow *Armillaria* spp. to exploit large areas in the search for essential nutrients, is of great importance for their pathogenicity. *Armillaria bulbosa* and *A. ostoyae* have become famous for being among the largest and oldest organisms on Earth. This is owing to the facts that *i)* genetic studies on their occurrence in some large forests of Northeastern North America revealed that the same mycelium can cover up to several thousands of square km and, *ii)* extrapolating their growth speed, these fungal mycelia are estimated to have reached an age of several thousand years.^[7,8]

[*] S. Pfütze,⁺ E. Charria-Girón,⁺ E. Schulzke, R. Toshe, Dr. F. Surup, Prof. M. Stadler
Department Microbial Drugs
Helmholtz Centre for Infection Research (HZI), and German Centre for Infection Research (DZIF), Partner Site Hannover-Braunschweig
Inhoffenstrasse 7, 38124 Braunschweig, Germany
E-mail: marc.stadler@helmholtz-hzi.de
S. Pfütze,⁺ E. Charria-Girón,⁺ E. Schulzke, Dr. F. Surup, Prof. M. Stadler
Institute of Microbiology
Technische Universität Braunschweig
Spielmannstraße 7, 38106 Braunschweig, Germany
R. Toshe
Institute of Pharmaceutical Biology Pharm. Biotechnology
Universität des Saarlandes
Campus C2 3, 66123 Saarbrücken, Germany

A. Khonsanit
BIOTEC, National Science and Technology Development, Agency (NSTDA), 111 Thailand Science Park, Phahonyothin Road, Khlong Nueng, Khlong Luang 12120, Pathum Thani, Thailand
Dr. R. Franke, Prof. M. Brönstrup
Department Chemical Biology
Helmholtz Centre for Infection Research (HZI), and German Center for Infection Research (DZIF), Partner Site Hannover-Braunschweig
Inhoffenstrasse 7, 38124 Braunschweig, Germany

[†] These authors contributed equally

© 2024 The Authors. Angewandte Chemie International Edition published by Wiley-VCH GmbH. This is an open access article under the terms of the Creative Commons Attribution License, which permits use, distribution and reproduction in any medium, provided the original work is properly cited.

Melleolides are composed of a sesquiterpene protoilludene backbone that is esterified with an orsellinic acid moiety. They are the largest subclass of protoilludanes, which seem to be exclusively produced by the honey mushrooms and their relatives.^[9] Orsellinic acid production, on the other hand, is not restricted to Basidiomycota, although the orsellinic acid polyketide synthases (oaPKS) encoding the biosynthesis of this simple tetraketide are evolutionarily unrelated to ascomycetes or bacterial oaPKS.^[10] The biosynthesis of melleolides involves the non-reducing polyketide synthase (nrPKS) Mld15 (formerly ArmB), which catalyzes the formation of orsellinic acid and the subsequent intermolecular transesterification to the terpenoid core structure, resulting in this unique class of meroterpenoids (Figure 1).^[11,12] In addition, several melleolides contain chlorinated orsellinic acids, which apparently originate from an uncommon, coordinated 5-fold parallelized biosynthetic step.^[13] In parallel, the biosynthesis of the terpenoid core structure begins with the formation of Δ^6 -protoilludene, which is derived from farnesyl diphosphate (FPP) by the sesquiterpene cyclase Mld5 (formerly Pro1).^[12,14] This is followed by a combination of several enzymatic modifications including hydroxylation, a stereochemical inversion, transesterification of the orsellinic acid residue and the isomerization of the olefin bond position, enabling the diversification of this compound class.^[12]

To date, over 70 different melleolide-type compounds have been reported exclusively from *Armillaria* species,^[15] but recently this compound class was also encountered in the phylogenetically closely related tropical genus

Guyanagaster.^[16] This exceptional chemical diversity is likewise accompanied by a wide range of biological activities. Amongst others, these meroterpenoids exert antibiotic, phytotoxic, and cytotoxic activities.^[6] Moreover, the melleolides might play a role in the activation of host defense responses, since they induce caspase-3 activation and consequently apoptosis in human cancer cells, as well as in interspecific communication or competition with other wood-decaying fungi.^[6] It has also already been attempted to establish preliminary structure–activity relationships (SAR) for the antifungal and cytotoxic properties of melleolides. Based on a limited number of compounds, it was concluded that the $\Delta^{2,3}$ double bond in the protoilludene backbone was instrumental for the observed bioactivities.^[17]

For a systematic study of the secondary metabolome by means of conventional chemical screening combined with untargeted metabolomics, we chose the strain *Armillaria ostoyae* (DSM 115711), since it was identified as the same species that represents the largest organism on Earth. Among *ca.* 40 cultures belonging to 10 species of *Armillaria*, the strain showed relatively rapid growth as compared to other strains and also produced a fair diversity of melleolides upon preliminary screening (data not shown here but included in some Bachelor and Master theses that were performed in our lab beforehand).

Herein, we report the isolation and identification of seventeen new melleolide derivatives **1–17** as well as twenty one previously known congeners **18–38**. In parallel, the antimicrobial and cytotoxic activities of the isolated metabolites were assessed under consistent laboratory conditions, enabling structure–activity relationships (SAR) of these compounds to be determined using chemoinformatic approaches.

Results and Discussion

Isolation and Structure Elucidation of Sesquiterpene Aryl Esters from *A. ostoyae* (DSM 115711)

After cultivation of *A. ostoyae* in liquid (YMWB) and on solid (rice) media, a large number of different melleolides were detected by HR-ESI-MS analysis and their distinctive UV/Vis absorption at λ_{\max} 220, 260, and 300 nm. Unexpectedly, congeners with higher molecular weights (> 800 Da) with similar UV/Vis spectra were found alongside the typical melleolide-type compounds (382–490 Da). Consequently, the extracts were fractionated by preparative HPLC, which finally led to the isolation of seventeen new derivatives (**1–17**; Figures 2–4), as well as the previously known melleolides **18–38** (Figures S6–S7).

All melleolide-type metabolites follow the same absolute configuration as established by X-ray analysis of melleolide, armillarin, 4-*O*-methylmelleolide, melledonal C, melleolide L and armillarivin,^[18–23] confirmed by electronic circular dichroism (ECD) comparison (Figure S1–S5) to structurally closely related derivatives for the new compounds described herein.

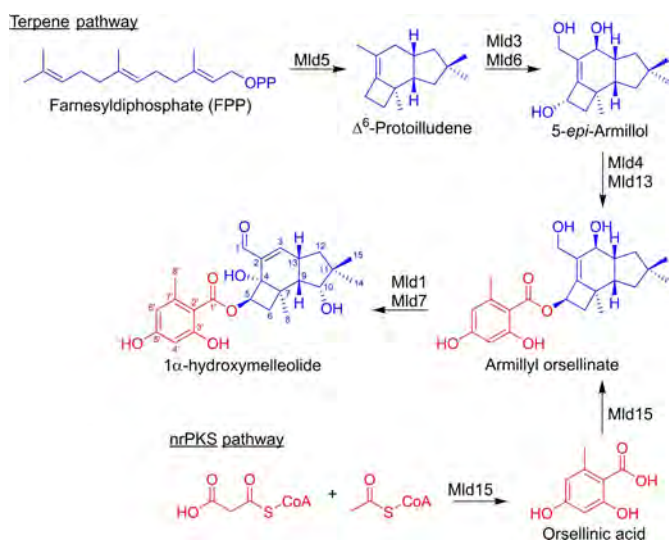


Figure 1. Biosynthetic pathway for 1 α -hydroxymelleolide as proposed by Fukaya et al.,^[12] which involves the cyclization of the universal sesquiterpene precursor farnesyl diphosphate into Δ^6 -protoilludene (Mld5), followed by cytochrome P450 monooxygenase-catalyzed hydroxylations (Mld3, Mld6) and a stereochemical inversion at position C5 (Mld4, Mld13), before the orsellinic acid moiety is esterified to that position (Mld15). Finally, further hydroxylations and the multistep isomerization of the double bond in the protoilludene backbone (Mld7) lead to 1 α -hydroxymelleolide.

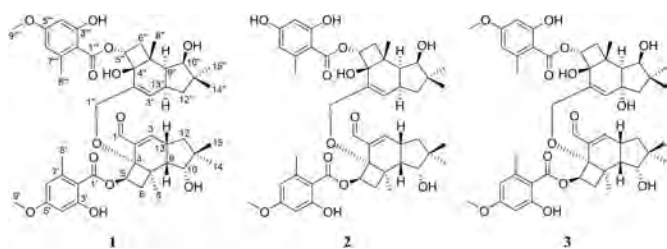


Figure 2. Melleolide dimers isolated from cultures of *A. ostoyae*: 1: bismelleolide BH; 2: bismelleolide EH; 3: bismelleolide CH.

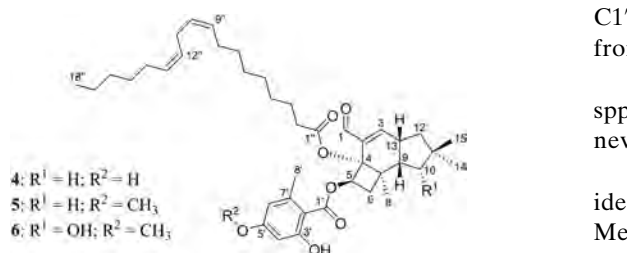


Figure 3. Melleolides with a fatty acid side chain isolated from cultures of *A. ostoyae*: melleolide linoleate (4); armillarine linoleate (5); melleolide H linoleate (6).

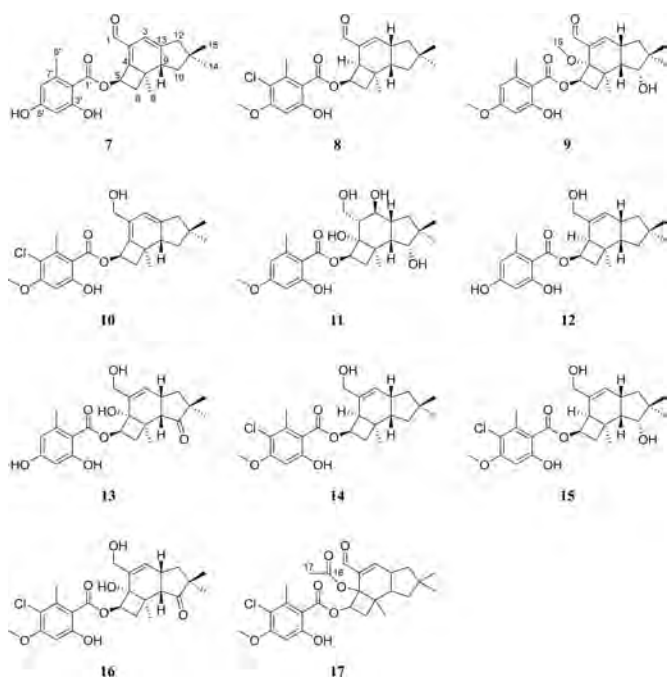


Figure 4. Melleolides isolated from cultures of *A. ostoyae*: 5'-*O*-desmethyllumillaribin (7); 4-dehydroxyarmillaridin (8); 4-methoxymelleolide H (9); 1-hydroxyarmillaricin (10); 10-hydroxy-5'-*O*-methyllumillarane (11); 4-dehydroxymelleolide F (12); 10-ketomelleolide E (13); 4,10-dehydroxymelleolide I (14); 4-dehydroxymelleolide I (15); 10-ketomelleolide I (16); 4-acetyllumillaridin (17).

Bismelleolide BH (1) was shown to have the molecular formula $C_{48}H_{60}O_{13}$ by HR-ESI-MS data. Its NMR spectroscopic data implied the presence of the melleolides B and

H moieties being linked to each other over an ether bridge between C4 and C1'.^[24,25] This assignment was confirmed by an HMBC correlation from $H_{2-1''}$ to C4.

HR-ESI-MS data determined the molecular formula of bismelleolide EH (2) as $C_{47}H_{58}O_{13}$ and its 1H and ^{13}C NMR data implied melleolides E and H substructures being linked to each other via an ether bridge between C4 and C1'.^[25]

Analysis of bismelleolide CH (3) revealed a molecular formula of $C_{48}H_{60}O_{14}$ and its 1H and ^{13}C NMR data indicated the presence of melleolides C and H units being linked to each other over an ether bridge between C4 and C1'.^[24,25] This was confirmed by an HMBC correlation from $H_{2-1''}$ to C4.

Even though the secondary metabolism of *Armillaria* spp. has been studied thoroughly, melleolide dimers were never reported before.

HR-ESI-MS data of melleolide linoleate (4) led to the identification of its molecular formula as $C_{41}H_{58}O_7$. Melleolide was identified as a substructure of 4 by analyzing the 1D and 2D NMR spectra.^[18] Furthermore, a fatty acid side chain was identified that is esterified to C4. The chemical shift of $11''-H_2$ (δ_H 2.80) indicated that a methylene unit is located between two olefins. To determine the positions of the double bonds, 4 was degraded to its fatty acid methyl ester (4-FAME) and analyzed by GC, subsequently. Comparison of the retention times with authentic standards (Figure S6) led to the identification of a $C_{18}:2\omega 6,9$ fatty acid (linoleic acid). The *cis* (Z)/*cis* (Z) 1,4-diene configuration of $\Delta^{9'',10''}$ and $\Delta^{12'',13''}$ was assigned due to the characteristic chemical shifts of C8'' and C14'' (Table S6).^[26]

For armillarine linoleate (5) the molecular formula $C_{42}H_{60}O_7$ was derived from its HR-ESI-MS data. Analysis of the 1H and ^{13}C NMR spectra revealed armillarine as substructure of 5 with a fatty acid side chain connected to C4, which was identified analogously to 4 as linoleic acid.^[19]

Melleolide H linoleate (6) was analyzed by HR-ESI-MS to yield a molecular formula of $C_{42}H_{60}O_8$. Further analysis of the 1H and ^{13}C NMR spectra revealed melleolide H as substructure of 6 with a linoleic acid side chain connected to C4.^[25] The presence of a linoleic acid side chain, esterified to the protoilludene core structure of the sesquiterpene aryl esters, is a very uncommon structural feature among members of this compound class.^[15] To date, armillatin is the only other congener known to carry a fatty acid side chain.^[27]

5'-*O*-Desmethyllumillaribin (7) was isolated from extracts of solid rice cultures. According to the molecular ion cluster at m/z 383.1851 $[M+H]^+$ its HR-ESI-MS data indicated the molecular formula $C_{23}H_{26}O_5$ (calcd for $C_{23}H_{27}O_5$ 383.1853). 1H and ^{13}C NMR data revealed a structure that is highly similar to the one of armillaribin.^[28] The key difference is the demethylation at $H_{3-9'}$ resulting in a hydroxy group at C5'.

For 4-dehydroxyarmillaridin (8) the molecular formula $C_{24}H_{29}ClO_5$ was identified by HR-ESI-MS data. Its 1H and ^{13}C NMR data were highly similar to those of armillaridin

and the absence of the hydroxyl group at C4 was identified as key difference between both.^[19]

As shown by its HR-ESI-MS data, 4-methoxymelleolide H (**9**) has the molecular formula $C_{25}H_{32}O_7$ and its 1H and ^{13}C NMR data showed similarities to melleolide H.^[25] An additional methoxy-group at position C4 of **9** was identified as the key difference (Figure 4).

1-hydroarmillaricin (**10**) was shown to have the molecular formula $C_{24}H_{29}ClO_5$ by HR-ESI-MS data. Its 1D and 2D NMR spectra implied the replacement of the C1 aldehyde by an oxymethylene compared to the known derivative armillaricin.^[28,29]

The molecular formula of 10-hydroxy-5'-*O*-methyllumillane (**11**) was determined from its HR-ESI-MS data as $C_{24}H_{34}O_8$. The analysis of its NMR data revealed that its structure is highly similar to the one of armillane with the appearance of an additional methoxyl group at position C5' of **11** as key difference between both.^[30]

4-Dehydroxymelleolide F (**12**) was isolated from extracts of solid rice cultures and was shown to have the molecular formula $C_{23}H_{30}O_5$ by HR-ESI-MS data. Its 1H and ^{13}C NMR data were highly similar to those of melleolide F, but they differed by the absence of the hydroxy group at position C4 for **12**.^[25,31]

10-Ketomelleolide E (**13**) showed a molecular ion cluster at m/z 417.1911 $[M+H]^+$ (calcd for $C_{23}H_{29}O_7$ 417.1908) in the HR-ESI-MS spectrum, which revealed the molecular formula $C_{23}H_{28}O_7$. In comparison to the previously described melleolide E,^[25,31] 1D and 2D NMR spectra of **13** showed the presence of an additional ketone at position C10 instead of the methylene.

Analysis of 4,10-dehydroxymelleolide I (**14**) revealed its molecular formula to be $C_{24}H_{31}ClO_5$, and the evaluation of its NMR spectra led to the identification of a molecule that is highly similar to melleolide I.^[32] However, the loss of the hydroxy functions at C4 and C10 for **14** was established as key differences between the two compounds.

4-Dehydroxymelleolide I (**15**) was shown to possess the molecular formula $C_{24}H_{31}ClO_6$ as revealed from its HR-ESI-MS data. The structure resembled that of melleolide I,^[32] except that the hydroxyl function at C4 was not detected.

10-Ketomelleolide I (**16**) has the molecular formula $C_{24}H_{29}ClO_7$, as shown by its HR-ESI-MS data. 1H and ^{13}C NMR data for **16**, which contains an additional ketone at C10, revealed a structure highly similar to that of melleolide I.^[32]

4-Acetylarmillaridin (**17**) was isolated with a molecular formula of $C_{26}H_{31}ClO_7$. Its planar structure was derived from analysis of the 1H , COSY, HSQC and HMBC data. HMBC correlations from H_{3-17} to C4 and C16, as well as detailed comparative analysis of HR-ESI-MS/MS data revealed **17** as the 4-acetyl derivative of armillaridin (Figure S10).^[19]

Metabolomics Evaluation of Melleolide Production under Different Cultivation Conditions

The discovery of unprecedented bismelleolides (**1–3**) and uncommon linoleate-type melleolides (**4–6**), alongside thirty-two other congeners (**7–38**), collectively account for more than 40 % of all previously known sesquiterpene aryl esters. To comprehensively explore the chemical diversity generated by this fungus under various cultivation conditions, MS-based untargeted metabolomics were used. For this purpose, *A. ostoyae* was cultured in two different liquid media (YM 6.3 and Q6 $1/2$) and one solid medium (BRFT) and its secondary metabolite production was evaluated using different metabolomic analyses. The liquid cultures were harvested 3 days after glucose depletion, and the solid cultures 15 days post-inoculation according to previous work on the cultivation of basidiomycetes.^[16,33] Both, the supernatant and mycelia were extracted with ethyl acetate, and the obtained crude extracts were analyzed by ultrahigh performance liquid chromatography coupled to diode array detection and ion mobility tandem mass spectrometry (UHPLC-DAD-IM-MS/MS). To obtain an overall picture of the metabolomes observed in each extract, a principal component analysis (PCA) was performed, enabling a representation of the similarity between samples in a two-dimensional scores plot (Figure 5A). Three main clusters were evidently observed by the PCA, the first one contained the BRFT extracts, while the second cluster included both, the extracts obtained from the supernatant and mycelia of the YM liquid cultures. Similarly, the third cluster was represented by the supernatant and mycelial extracts of the Q6 liquid cultures. Thus, the different cultivation and extraction procedures led to distinct metabolomes (Figure 5B). We decided to further explore the differential production of melleolide-type metabolites using Feature Based Molecular Networking (FBMN) analysis.^[34]

MS/MS fragmentation patterns of the isolated melleolides were evaluated from the crude extracts obtained after the cultivation of *A. ostoyae* in different media. We observed that these metabolites give rise to a distinctive MS/MS fragmentation pattern (Figure 6A). Despite the variations in their structures, melleolides present a set of characteristic neutral losses corresponding to the loss of the substituted orsellinic acid moiety. For instance, arnamial (**27**) and 6'-dechloroarnamial, which only differ by a chloride substitution in the orsellinic acid moiety, generated both a main fragment ion at m/z 273.1456 Da corresponding to the 6-protoilludene backbone. In addition, both compounds generated fragment ions at m/z 220.9961 and 187.0369 Da. This mass difference can be attributed to the chloride substitution in the orsellinic acid moiety. Similarly, the same structural motif is identified in both mass spectra as a neutral loss. The *O*-methylation in several melleolides could be recognized in their MS/MS spectra by a mass difference of 14 Da in the fragment ions representing the orsellinic acid when compared to their hydroxy congeners. The different hydroxylation patterns typically observed within this compound class can be

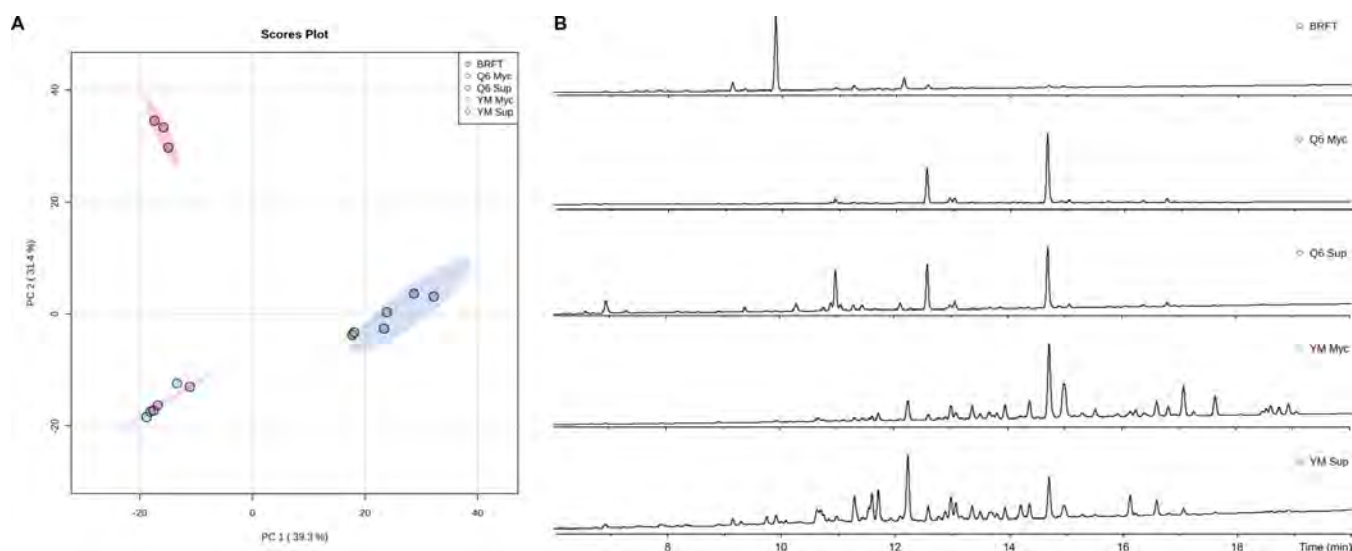


Figure 5. A) PCA scores plot of the secondary metabolomes of *A. ostoyae* after its cultivation in different media (YM 6.3, Q6 $\frac{1}{2}$, and BRFT, $n = 3$, 95 % confidence interval of normalized m/z intensities from the features detected at MS1 level, positive ionization mode). B) HPLC-UV/Vis chromatograms (210 nm) of the different crude extracts.

inferred from MS/MS experiments; however, the position of the modification cannot be discerned based on our analyses. In a similar way, when melleolides are substituted with a fatty acid side chain, they also present a distinct neutral loss attributed to the orsellinic acid moiety. For example, melleolide linoleate (**4**) presents a main fragment ion at m/z 535.3763 Da attributed to the loss of this moiety in the molecule (Figure 6A). In the case of the dimeric melleolides, the loss of each orsellinic acid moiety from the respective monomers can be observed as well as their corresponding substitutions, as represented in melleolide BH (**1**) by fragment ions at m/z 704.3490 Da and 539.3058 Da (Figure 6A).

For the FBMN analyses, the obtained UHPLC-DAD-IM-MS/MS raw data from the different crude extracts were pre-processed using the MetaboScape software and the obtained feature table was dereplicated based on accurate m/z , MS/MS spectra, retention times, and UV/Vis spectra using the reference data obtained from the herein isolated metabolites. From 4269 features detected at the MS level, 1838 detected in the media blanks were removed for further analyses. From the remaining 2431 features, 2227 features were detected at the MS2 level and afterwards organized into 156 molecular families (MFs) with at least two clustered nodes and 1339 singletons (Figure 6B). A total of 22 MFs encompassing 277 features were found to belong to the melleolide compound class by the propagation of annotations from reference spectra obtained from the herein isolated metabolites (Table S20). The two major MFs included melleolide B, 5'-methoxyarmillarizin, 4'-methoxymelleolide H, 4-dehydroxymelleolide I, 10-hydroxy-5'-O-methylarmillane, and bismelleolide EH, respectively. To our surprise the bismelleolide EH cluster represented the second biggest MF (85 nodes) with compounds with parent masses ranging from 820.3770 Da to 969.3803 Da,

however the bismelleolides BH and CH were clustered in a separate MF including only 19 nodes. In metabolomics analyses, a common challenge arises from structurally similar metabolites exhibiting distinct MS/MS spectra due to minor chemical modifications. For a comprehensive understanding of this phenomenon, a meticulous examination and the accessibility of pure standards are imperative.^[35] On the other hand, the melleolide linoleate MF was represented by only three nodes, suggesting that the number of dimeric melleolides is much higher than the one of analogs with a substituted fatty acid chain. To show the effect of cultivation under different media on metabolite abundance, compounds **1–5**, **6–9**, **11–16**, and 6'-dechloroarnamial annotated within the FBMN were grouped by hierarchical clustering, as shown by the heat map in Figure 6C. In contrast to the PCA scores plot, which clustered crude extracts obtained from the supernatant and mycelia in separate groups regardless of the medium (Figure 5A), the heat map showed a clear distinction between the Q6 $\frac{1}{2}$ mycelial extract and the other crude extracts. Compounds significantly induced in this extract corresponded to bismelleolide BH (**1**), bismelleolide EH (**2**), melleolide linoleate (**4**), armillarine linoleate (**5**), 5'-O-desmethyarmillaribin (**7**), 4-methoxymelleolide H (**9**), 4-dehydroxymelleolide F (**12**), and 10-ketomelleolide E (**13**). The other major clade corresponded to the crude extracts obtained from the supernatant of Q6 $\frac{1}{2}$ and YM 6.3, as well as the mycelial extract from the latter and the crude extract obtained from BRFT solid cultivation. From this group the mycelial extract from YM 6.3 appeared in a separate clade, explained by the significant presence of 4-dehydroxyarmillaridin (**8**), 4,10-dehydroxymelleolide I (**14**), 4-dehydroxymelleolide I (**15**), 10-ketomelleolide I (**16**), and 6'-dechloroarnamial. The supernatant extract from Q6 $\frac{1}{2}$ presented a similar profile to its mycelial extract, but bismelleolide CH (**3**)

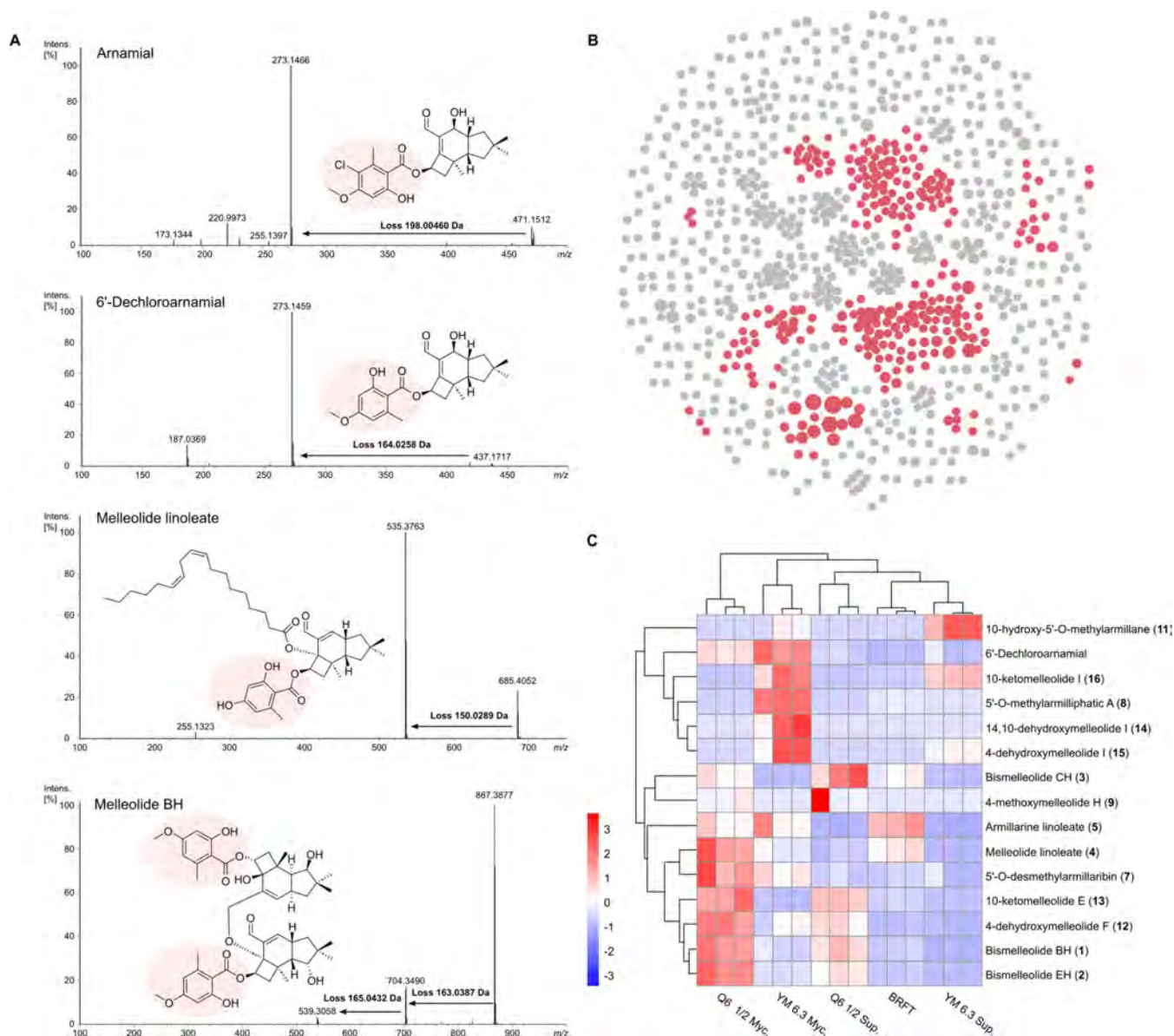


Figure 6. A) Reference MS/MS spectra of melleolide BH, arnamimal, 6'-dechloroarnamial, and melleolide linoleate, isolated in this study. B) Feature based molecular network for the crude extracts obtained from the cultivation of *A. ostoyae* in different media (YM 6.3, Q6 1/2, and BRFT) with annotated melleolide molecular families based on the comparison of their MS/MS spectra with the isolated metabolites (hexagons in red represents melleolide derivatives, while gray ones represents unknown features, node size indicates the abundance of the compound). C) Heatmap following a hierarchical clustering of compounds 1–5, 6–9, 11–16, and 6'-dechloroarnamial annotated in the FBMN. Heatmap displays compound abundance values with hierarchical clustering of compounds and crude extracts obtained from different media, each extract is represented by three columns as three biological replicates. Scaled abundance is color-coded from red (high abundance) to dark blue (low abundance). The heatmap with dendrograms was generated by the R package pheatmap.

and 4-methoxymelleolide H (9) were highly induced under this condition. In the case of the BRFT solid cultivation it can be observed that the melleolide linoleate (4) and armillarine linoleate (5) were more abundant than in the nearest clustering extracts, even though these compounds were also present in the mycelial extracts from the liquid cultures. Likewise, 10-hydroxy-5'-O-methylarmillane (11) and 10-ketomelleolide I (16) were induced in the supernatant extract of YM 6.3.

Insight into the Structure–Activity Relationships of Melleolide-Type Meroterpenoids

Over the course of time, a variety of melleolide-type meroterpenoids described in literature were evaluated for their antimicrobial and cytotoxic potential. Various non-systematic assays against different strains and cell lines led to many different statements and assumptions about possible structure activity relationships. Our study represents the first attempt to test a large number of these

chemically diverse secondary metabolites under constant laboratory conditions to deduce structural motifs that are responsible for the observed effects.

Results from preliminary evaluations of antibacterial activity testing led to the assumption that hydroxylations at C4, C10 and C13 increase bacterial growth inhibition, primarily against Gram-positive bacteria.^[15] In contrast, we obtained an opposing result with 5'-O-desmethyllumillaribin (**7**), 4-dehydroxymelleolide F (**12**), arnamial (**26**) and A52a (**36**) as the most active antibacterial congeners (4.2 µg/mL against *B. subtilis* and *S. aureus*, Table S1), of which only **36** shows a hydroxylation at C4 (Figure S9). Since no activity against Gram-negative bacteria was observed, our findings only confirm that this compound class mainly inhibits the growth of Gram-positive bacteria. A further comparison of bioactivity and chemical data did not result in the identification of certain structural features that are responsible for the antibacterial effects.

Furthermore, previous efforts have stated that the presence of the $\Delta^{2,4}$ double bond in the protoilludene moiety is a necessary feature for the antifungal activity against *Aspergillus flavus*, *A. nidulans*, and *Penicillium notatum*, while $\Delta^{2,3}$ -melleolides did not exhibit any antifungal property against these fungal strains.^[17] Following this hypothesis, we tested 35 different melleolide-type meroterpenoids (Figure S9) against *Schizosaccharomyces pombe*, *Wickerhamomyces anomalus*, *Mucor hiemalis*, and *Rhodotorula glutinis*. To identify distinct patterns in the observed antifungal activities, the compounds were clustered according to their obtained MIC (minimal inhibitory concentration) values (µg/mL) in a hierarchical clustering approach (Figure 7A). Three major clusters could be identified by this approach, which exhibited no, or very limited antifungal activity, selective antifungal activity against *S. pombe*, *M. hiemalis*, and/or *R. glutinis*, as well as broad antifungal activity against all tested fungi (Figure 7B). Out of 35 tested compounds, 11 exhibited

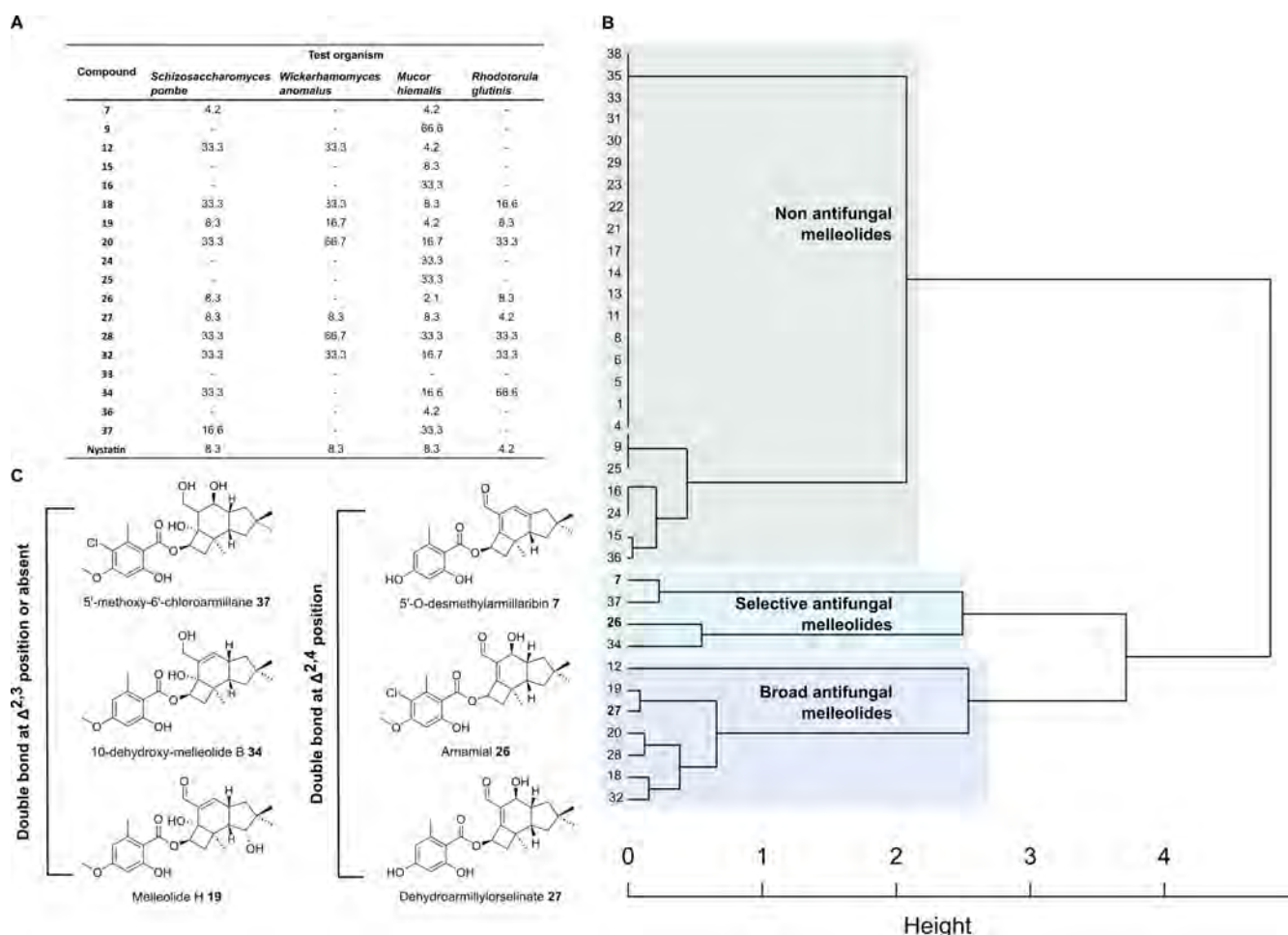


Figure 7. Analysis of antifungal activities exhibited by melleolide-type meroterpenoids against *S. pombe*, *W. anomalus*, *M. hiemalis*, and *R. glutinis*. A) MIC values (µg/mL) against selected fungal test organisms. Inactive compounds are not shown, but the complete dataset can be found in Table S1. B) Dendrogram resulting from hierarchical clustering of antifungal activities of the evaluated melleolide-type meroterpenoids, with the three major clusters denoted with colored boxes, and compounds numbers presenting a $\Delta^{2,4}$ double bond in the protoilludene moiety underlined. C) Chemical structures of melleolide-type meroterpenoids exhibiting significant antifungal activity and presenting a $\Delta^{2,3}$ double bond or no terpene double bond in the protoilludene moiety (left), as well as presenting a $\Delta^{2,4}$ double bond in the terpene backbone (right).

significant antifungal activities, from which only 5'-*O*-desmethylarmillaribin (**7**), arnamial (**26**), and dehydroarmillyorselinate (**27**) have a $\Delta^{2,4}$ double bond in the protoilludene backbone. Notably, melleolide H (**19**) and 10-dehydroxy-melleolide B (**34**), which contain a $\Delta^{2,3}$ double bond in the protoilludene backbone, and 5'-methoxy-6'-chloroarmillane (**37**), which is devoid of a terpene double bond, also exhibited significant antifungal properties.

On the contrary, it has been assumed that the cytotoxicity of melleolides is not significantly influenced by the double bond position in the protoilludene backbone, while the presence of an aldehyde at C-1 was identified as key feature for a higher cytotoxicity.^[17,36] Based on these assumptions, 35 different melleolide-type meroterpenoids (Figure S9) were tested against L929 (mouse fibroblast) and KB3.1 (cervix carcinoma) cell lines (Table S2). In addition, compounds with the highest cytotoxicities against the L929 and KB3.1 cell lines were selected for further testing against five additional mammalian cell lines as shown in Table S2.

By using a hierarchical clustering approach based on their IC₅₀ values (μ M), two major clusters were identified (Figure 8A). One cluster contains compounds without

cytotoxic properties against the tested cell lines, whereas the other cluster presents those compounds active against both cell lines. Within the latter group, 12 compounds displayed significant cytotoxicity and were clustered together in a single clade. Thereby, already one structural feature stands out in relation to high cytotoxic effects. All compounds, except **12**, within this clade carry an aldehyde at position C1, confirming that this feature is the main driver of the cytotoxic activities. Subsequently, we conducted a comparative analysis of this clade with the dendrogram generated from hierarchical clustering of their respective chemical structures using circular fingerprints and a Tanimoto similarity score (Figure 8B and C). In this way, we observed that most clades or compound subtypes did not follow similar clustering based on their IC₅₀ values, except for the bismelleolide BH (**1**), as well as for melleolide H (**19**) and armillarin (**25**). Compounds **19** (2.2 μ M against KB3.1 and 3.7 μ M against L929) and **25** (1.7 μ M against KB3.1 and 3.9 μ M against L929) only differ by the hydroxylation at C-10, which does not seem to influence their cytotoxicity. However, for melleolide J (**20**; 5.8 μ M against KB3.1 and 13.8 μ M against L929) and armillaridin (**24**; 2.1 μ M against KB3.1 and 5.1 μ M against L929), which represent the same pair as **19** and **25**, but

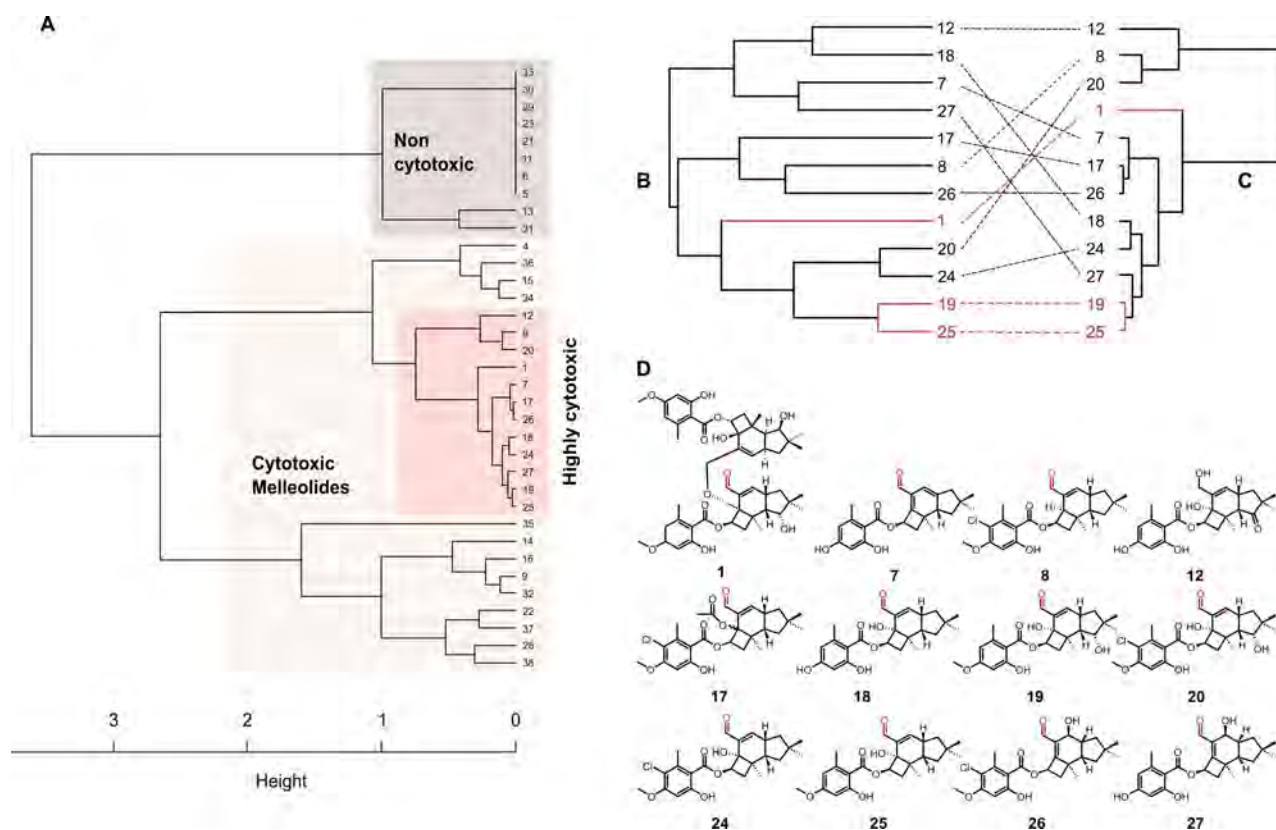


Figure 8. Analysis of cytotoxic properties exhibited by melleolide-type meroterpenoids against the mouse fibroblast cell line L929 and the cervix carcinoma cell line KB3.1. A) Dendrogram resulting from hierarchical clustering of cytotoxic activities of the evaluated melleolide-type meroterpenoids, with major groups denoted with colored boxes. Comparison of dendrograms resulting from hierarchical clustering of chemical structures from the compounds exhibiting significant cytotoxicity using circular fingerprints and Tanimoto similarity (B) and of their corresponding cytotoxic activities (C); where common clades are highlighted in dark orange. D) Chemical structures of melleolide-type meroterpenoids exhibiting significant cytotoxic properties against L929 and KB3.1 cell lines, with the aldehyde group in the protoilludene moiety highlighted in red.

with a chloride substitution in the orsellinic acid moiety, the hydroxylation at C-10 results in an almost threefold decrease of cytotoxicity. This suggests that the hydroxylation at C-10 might play an important role in the cytotoxicity of these molecules in an antagonistic manner with the chlorination at the orsellinic acid. The group containing compounds **8** (3.7 μM against KB3.1 and 14.6 μM against L929), **17** (1.3 μM against KB3.1 and 2.7 μM against L929), and **26** (1.7 μM against KB3.1 and 2.9 μM against L929) also have chlorinated rings, but in this case all of them lack a hydroxyl group at C-10. 4-dehydroxyarmillaridin (**8**) and arnamial (**26**) differ by the change of the double bond position and the hydroxylation at C-3, which results in an increased cytotoxicity for the latter. In addition, the presence of an acetoxyl group at position C-4 of compound **8** results in a higher cytotoxicity as observed for compound **17**. In the case of the upper group, which is divided in two clades, it can be observed that the compounds belonging to it do not have any substitution in the orsellinic acid moiety. In the clade that contained compound **7** (1.9 μM against KB3.1 and 1.9 μM against L929) and **27** (3.0 μM against KB3.1 and 4.3 μM against L929), we observed that the hydroxylation at C-3 resulted in a decreased cytotoxicity. However, in the clade that contained compound **12** (2.9 μM against KB3.1 and 19.2 μM against L929) and **18** (1.3 μM against KB3.1 and 5.8 μM against L929), it became evident that the absence of the aldehyde and the presence of an alcohol instead in combination with the keto group at C-10 negatively affect the cytotoxicity of these compounds. The most distinct correlation between chemical structure and cytotoxicity is the total loss of activity for sesquiterpene aryl esters carrying a hydroxylation at position C13. For instance, melleolide H (**19**) and melleolide J (**20**) are among the most cytotoxic compounds tested in this survey, while their C13 hydroxy derivatives 5'-*O*-methylmelledonal (**23**) and melledonal C (**22**), respectively, did not show any cytotoxicity. Furthermore, melledonal A (**21**), melleolide D (**30**) and melledonal (**33**), which show the same hydroxylation pattern at positions C10 and C13, were tested negative for cytotoxicity as well.

Conclusion

Our exploration of the chemical space of *Armillaria ostoyae* unveiled the production of unprecedented melleolide-type dimers (**1–3**) and uncommon fatty acid side chain carrying melleolides (**4–6**). Even though the monomers have been reported in the literature before, a dimerization of two melleolide-type meroterpenoids or the attachment of a linoleic acid side chain has not been observed and described up to now. Additionally, we also isolated 11 new (**7–17**) and 21 known (**18–38**) sesquiterpene aryl esters. Notably, metabolites isolated from *A. ostoyae* constitute nearly the half of all known melleolide-type meroterpenoids to date. Furthermore, our metabolomics analyses shed lights on the vast diversity of these compounds, encompassing a total of 22 molecular families

with 277 features, a number which exceeds by far the repertoire of known sesquiterpene aryl esters from this class. Remarkably, the tandem MS analysis implies that a very high number of dimeric analogs exists, although those have remained unnoticed so far. In parallel, our heatmap analysis following a hierarchical clustering approach, revealed distinct metabolomics-wide associations oppositely to the principal component analysis. These patterns support our understanding of the media-dependent production of different melleolide-type meroterpenoids.

A systematic study of the biological activities of these sesquiterpene aryl esters under consistent laboratory conditions has so far not been carried out. For this reason, we evaluated the antimicrobial and cytotoxic activities of thirty-five melleolide-type compounds concurrently and employed a range of chemoinformatic approaches to study their structure–activity relationships. Contrary to previous assumptions, our results suggest that the presence of the $\Delta^{2,4}$ double bond in the protoilludene moiety is not essential for antifungal activity. Evaluation against *Schizosaccharomyces pombe*, *Wickerhamomyces anomalus*, *Mucor hiemalis*, and *Rhodotorula glutinis* revealed potent antifungal effects for compounds with and without a $\Delta^{2,4}$ double bond, broadening the spectrum of active metabolites.

Our study further confirmed the importance of the aldehyde at C1 in conferring high cytotoxicity to melleolides,^[15] whereas the presence of a hydroxyl group at position C13 lead to a loss of this activity. Notably, our cheminformatics approach unveiled the intricate interplay of multiple chemical modifications on the biological properties of these compounds. For example, we observed that hydroxylation at C10 had different effects on the activity of melleolides, depending on the presence of a chlorine substitution in the orsellinic acid moiety as compared to their dechlorinated counterparts.

Our pilot study not only represents the first systematic investigation of a class of unique fungal meroterpenoids on such a scale. It also provides a strategy on how to combine and analyze the large amount of chemical and biological data available by using different methodologies. For instance, our metabolomics analyses provided insight into the vast diversity of these sesquiterpene aryl esters, with the detected number melleolide-type features surpassing by far the one of previously reported compounds from this class. Future endeavors must ensure the reassessment of additional species of this genus using our proposed methodology to gain a broader overview of the production of these metabolites. Likewise, such approaches might enable the targeted search for melleolides harboring structural motifs that are presumed to be related to a specific biological activity. Hence, a comprehensive understanding of the SAR of these intriguing fungal metabolites can be driven by cheminformatics. These approaches can be useful for medicinal chemistry by helping to suggest specific structural motifs that improve the properties of the bioactive compounds. At the same time, the untargeted metabolomics approach

may prove useful in future studies, using multi-OMICS techniques to elucidate the ecological role of the melleolides in Nature, as well as for a chemotaxonomic study on the genus *Armillaria*, in order to complement the existing morphological and molecular phylogenetic data.

Acknowledgements

This research benefitted from funding by the European Union's Horizon 2020 Research Innovation and Staff Exchange program (RISE) under the Marie Skłodowska-Curie grant agreement No. 101008129, project acronym "Mycobiomics". S. Pfütze is grateful for a grant from the Life Science-Stiftung zur Förderung von Wissenschaft und Forschung (LSS). E. Charria-Girón was supported by the HZI POF IV Cooperativity and Creativity Project Call granted to F. Surup. R. Toshe is thankful for a grant from Die Bischöfliche Studienförderung Cusanuswerk. C. Koschke and E. Surges are thanked for recording the NMR spectra. We thank W. Collisi for the performance of the bioassays and B. Karbowy-Thongbai for her work on the identification of the strain. Furthermore, we are grateful for measurements of the HR-ESI-MS spectra by A. Gollasch. We also thank U. Beutling for the UHPLC-DAD-IM-MS/MS measurements and R. J. Cox for valuable suggestions to improve the wording. Open Access funding enabled and organized by Projekt DEAL.

Conflict of Interest

The authors declare no conflict of interest.

Data Availability Statement

The data that support the findings of this study are available in the supplementary material of this article.

Keywords: *Armillaria* • melleolides • metabolomics • meroterpenoids • structure–activity relationships

- [1] M.-Q. He, R.-L. Zhao, D.-M. Liu, T. T. Denchev, D. Begerow, A. Yurkov, M. Kemler, A. M. Millanes, M. Wedin, A. R. McTaggart, R. G. Shivas, B. Buyck, J. Chen, A. Vizzini, V. Papp, I. V. Zmitrovich, N. Davoodian, K. D. Hyde, *Fungal Divers.* **2022**, *114*, 281–325.
- [2] B. Sandargo, C. Chepkirui, T. Cheng, L. Chaverra-Muñoz, B. Thongbai, M. Stadler, S. Hüttel, *Biotechnol. Adv.* **2019**, *37*, 107344.
- [3] A. G. T. Niego, C. Lambert, P. Mortimer, N. Thongklang, S. Rapior, M. Grosse, H. Schrey, E. Charria-Girón, A. Walker, K. D. Hyde, M. Stadler, *Fungal Divers.* **2023**, *121*, 95–137.
- [4] A. Mapook, K. D. Hyde, K. Hassan, B. M. Kemkuignou, A. Čmoková, F. Surup, E. Kuhnert, P. Paomephan, T. Cheng, S. de Hoog, Y. Song, R. S. Jayawardena, A. M. S. Al-Hatmi, T. Mahmoudi, N. Ponts, L. Studt-Reinhold, F. Richard-Forget, K. W. T. Chethana, D. L. Harishchandra, P. E. Mortimer, H. Li, S. Lumyong, W. Aiduang, J. Kumla, N. Suwannarach, C. S. Bhunjun, F.-M. Yu, Q. Zhao, D. Schaefer, M. Stadler, *Fungal Divers.* **2022**, *116*, 547–614.
- [5] M. P. A. Coetzee, B. D. Wingfield, M. J. Wingfield, *Pathog. (Basel, Switzerland)* **2018**, *7*, 83.
- [6] K. Baumgartner, M. P. A. Coetzee, D. Hoffmeister, *Mol. Plant Pathol.* **2011**, *12*, 515–534.
- [7] M. L. Smith, J. N. Bruhn, J. B. Anderson, *Nature* **1992**, *356*, 428–431.
- [8] B. A. Ferguson, T. A. Dreisbach, C. G. Parks, G. M. Filip, C. L. Schmitt, *Can. J. For. Res.* **2003**, *33*, 612–623.
- [9] M. M. Cadelis, B. R. Copp, S. Wiles, *Antibiotics (Basel, Switzerland)* **2020**, *9*, 928.
- [10] M. Gressler, N. A. Löhr, T. Schäfer, S. Lawrinowitz, P. S. Seibold, D. Hoffmeister, *Nat. Prod. Rep.* **2021**, *38*, 702–722.
- [11] B. Engels, U. Heinig, C. McElroy, R. Meusinger, T. Grothe, M. Stadler, S. Jennewein, *Appl. Microbiol. Biotechnol.* **2021**, *105*, 211–224.
- [12] M. Fukaya, S. Nagamine, T. Ozaki, Y. Liu, M. Ozeki, T. Matsuyama, K. Miyamoto, H. Kawagishi, M. Uchiyama, H. Oikawa, A. Minami, *Angew. Chem. Int. Ed.* **2023**, *62*, e202308881.
- [13] J. Wick, D. Heine, G. Lackner, M. Misiek, J. Tauber, H. Jagusch, C. Hertweck, D. Hoffmeister, *Appl. Environ. Microbiol.* **2016**, *82*, 1196–1204.
- [14] B. Engels, U. Heinig, T. Grothe, M. Stadler, S. Jennewein, *J. Biol. Chem.* **2011**, *286*, 6871–6878.
- [15] M. Dörfer, M. Gressler, D. Hoffmeister, *Mycol. Prog.* **2019**, *18*, 1027–1037.
- [16] S. Pfütze, D. L. Nedder, F. Surup, M. Stadler, *Mycol. Prog.* **2023**, *22*, 70.
- [17] M. Bohnert, H.-W. Nützmann, V. Schroeckh, F. Horn, H.-M. Dahse, A. A. Brakhage, D. Hoffmeister, *Phytochemistry* **2014**, *105*, 101–108.
- [18] S. L. Midland, R. R. Izac, R. M. Wing, A. I. Zaki, D. E. Munnecke, J. J. Sims, *Tetrahedron Lett.* **1982**, *23*, 2515–2518.
- [19] J. S. Yang, Y. W. Chen, X. Z. Feng, D. Q. Yu, X. T. Liang, *Planta Med.* **1984**, *50*, 288–290.
- [20] D. M. X. Donnelly, F. Abe, D. Coveney, N. Fukuda, J. O'Reilly, J. Polonsky, T. Prangé, *J. Nat. Prod.* **1985**, *48*, 10–16.
- [21] A. Arnone, R. Cardillo, G. Nasini, S. V. Meille, *J. Chem. Soc. Perkin Trans. 1* **1988**, 503–510.
- [22] I. Momose, R. Sekizawa, N. Hosokawa, H. Iinuma, S. Matsui, H. Nakamura, H. Naganawa, M. Hamada, T. Takeuchi, *J. Antibiot. (Tokyo)* **2000**, *53*, 137–143.
- [23] B. D. Schwartz, E. Matoušová, R. White, M. G. Banwell, A. C. Willis, *Org. Lett.* **2013**, *15*, 1934–1937.
- [24] A. Arnone, R. Cardillo, G. Nasini, *Phytochemistry* **1986**, *25*, 471–474.
- [25] A. Arnone, G. Nasini, V. Di Modugno, R. Cardillo, *Gazz. Chim. Ital.* **1988**, *118*, 517–521.
- [26] E. Alexandri, R. Ahmed, H. Siddiqui, M. I. Choudhary, C. G. Tsiafoulis, I. P. Gerothanassis, *Molecules* **2017**, *22*, 1663.
- [27] J. S. Yang, Y. L. Su, Y. L. Wang, X. Z. Feng, D. Q. Yu, X. T. Liang, *Planta Med.* **1991**, *57*, 478–480.
- [28] J. S. Yang, P. Z. Cong, *Acta Chim. Sin.* **1988**, *46*, 1093–1100.
- [29] J. S. Yang, Y. W. Chen, X. Z. Feng, D. Q. Yu, C. H. He, Q. T. Zheng, J. Yang, X. T. Liang, *Planta Med.* **1989**, *55*, 564–565.
- [30] D. M. X. Donnelly, R. M. Hutchinson, *Phytochemistry* **1990**, *29*, 179–182.
- [31] D. M. X. Donnelly, T. Konishi, O. Dunne, P. Cremin, *Phytochemistry* **1997**, *44*, 1473–1478.
- [32] A. Arnone, R. Cardillo, G. Nasini *Gazz. Chim. Ital.* **1988**, *118*, 523–527.
- [33] S. Pfütze, A. Khamsim, F. Surup, C. Decock, J. C. Matasyoh, M. Stadler, *J. Nat. Prod.* **2023**, *86*, 390–397.

- [34] L.-F. Nothias, D. Petras, R. Schmid, K. Dührkop, J. Rainer, A. Sarvepalli, I. Protsyuk, M. Ernst, H. Tsugawa, M. Fleischauer, F. Aicheler, A. A. Aksenov, O. Alka, P.-M. Allard, A. Barsch, X. Cachet, A. M. Caraballo-Rodriguez, R. R. Da Silva, T. Dang, N. Garg, J. M. Gauglitz, A. Gurevich, G. Isaac, A. K. Jarmusch, Z. Kameník, K. Bin Kang, N. Kessler, I. Koester, A. Korf, A. Le Gouellec, M. Ludwig, C. Martin, H. L.-I. McCall, J. McSayles, S. W. Meyer, H. Mohimani, M. Morsy, O. Moyne, S. Neumann, H. Neuweiger, N. H. Nguyen, M. Nothias-Espósito, J. Paolini, V. V. Phelan, T. Pluskal, R. A. Quinn, S. Rogers, B. Shrestha, A. Tripathi, J. J. J. van der Hooft, F. Vargas, K. C. Weldon, M. Witting, H. Yang, Z. Zhang, F. Zubeil, O. Kohlbacher, S. Böcker, T. Alexandrov, N. Bandeira, M. Wang, P. C. Dorrestein, *Nat. Methods* **2020**, *17*, 905–908.
- [35] E. Charria-Girón, Y. Marin-Felix, U. Beutling, R. Franke, M. Brönstrup, A. M. Vasco-Palacios, N. H. Caicedo, F. Surup, *Microbiol. Spectr.* **2023**, *11*(6):e0274323. doi:10.1128/spectrum.02743-23.
- [36] M. Bohnert, S. Miethbauer, H.-M. Dahse, J. Ziemer, M. Nett, D. Hoffmeister, *Bioorg. Med. Chem. Lett.* **2011**, *21*, 2003–2006.

Manuscript received: December 3, 2023

Accepted manuscript online: February 23, 2024

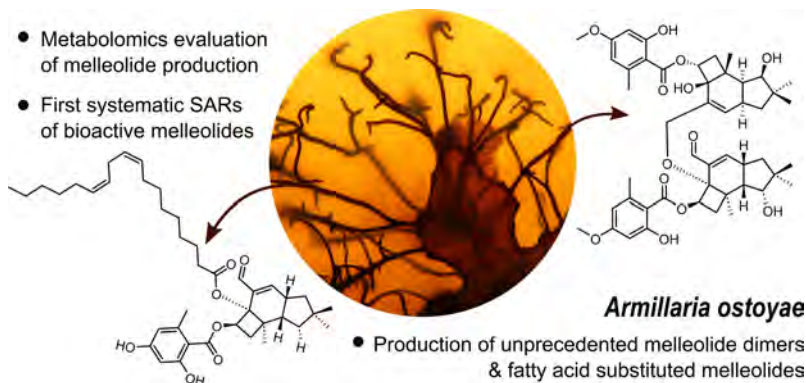
Version of record online: February 23, 2024

Research Articles

Natural Products

S. Pfütze, E. Charria-Girón, E. Schulzke, R. Toshe, A. Khonsanit, R. Franke, F. Surup, M. Brönstrup, M. Stadler* — **e202318505**

Depicting the Chemical Diversity of Bioactive Meroterpenoids Produced by the Largest Organism on Earth



Exploring melleolide-type meroterpenoids from *Armillaria ostoyae* in liquid and solid fermentations yielded 17 new and 21 known derivatives. A compound library enabled metabolomics, unveiling

production patterns under varied culture conditions. Assessment of antimicrobial and cytotoxic activities, aided by innovative chemoinformatics, offered insight into structure–activity relationships.

Sebastian Pfütze

Personal information

Address: Ludwigstraße 36
38106 Braunschweig
Phone number: +49163 / 8713970
Email address: spf17@helmholtz-hzi.de
Date/Place of Birth: 14.09.1992 / Schönebeck (Elbe)

Work experience

06/2019 – Present **Research associate**
Helmholtz Centre for Infection Research

03/2017 – 07/2018 **Student assistant**
Helmholtz Centre for Infection Research

Education

06/2019 – Present **PhD candidate**
Helmholtz Centre for Infection Research
Doctoral thesis: “Exploring the Secondary Metabolism of Basidiomycota: Unveiling Novel Bioactive and Chemically Diverse Compounds”

08/2015 – 06/2019 **Master of Science Biotechnology**
Technische Universität Braunschweig
Grade: 1.5
Master thesis: Studies on the secondary metabolism of Hypoxylaceae (Xylariales, Ascomycota)

10/2011 – 08/2015 **Bachelor of Science Biotechnology**
Technische Universität Braunschweig
Grade: 2.0
Bachelor thesis: Produktion der Sekundärmetabolite Obionin A und C durch *Microcyclospora malicola* und Screening weiterer Rußfleck- und Fliegendreckpilze

08/2003 – 06/2011 **Abitur**
Friedrich-Schiller-Gymnasium Calbe/Saale
Grade: 1.7

Publications

Pfütze S, Charria-Girón E, Schulzke E, Toshe R, Khonsanit A, Franke R, Surup F, Brönstrup M, Stadler M (2024) Depicting the chemical diversity of bioactive meroterpenoids produced by the largest organism on earth. *Angewandte Chemie, International Edition* 63:e202318505.

Pfütze S, Nedder DL, Surup F, Stadler M (2023) 5'-O-methyl-14-hydroxyarmillane, a new armillane-type sesquiterpene from cultures of *Guyanagaster necrorhiza*. *Mycological Progress* 22:70.

- Pfütze S**, Khamsim A, Surup F, Decock C, Matasyoh JC, Stadler M (2023) Heimionones A–E, new sesquiterpenoids produced by *Heimiomyces* sp., a Basidiomycete collected in Africa. *Molecules* 28(9):3723.
- Pfütze S**, Khamsim A, Surup F, Decock C, Matasyoh JC, Stadler M (2023) Calamene-type sesqui-, mero-, and bis-sesquiterpenoids from cultures of *Heimiomyces* sp., a Basidiomycete collected in Africa. *Journal of Natural Products* 86(2):390–397.
- Pathompong P†, **Pfütze S†**, Surup F, Boonpratuang T, Choeyklin R, Matasyoh JC, Decock C, Stadler M, Boonchird C (2022) Drimane-type sesquiterpenoids derived from the tropical Basidiomycetes *Perenniporia centrali-africana* and *Cerrena* sp. nov. *Molecules* 27(18):5968.
- Becker K, **Pfütze S**, Kuhnert E, Cox RJ, Stadler M, Surup F (2021) Hybridorubins A–D: azaphilone heterodimers from stromata of *Hypoxylon fragiforme* and insights into the biosynthetic machinery for azaphilone diversification. *Chemistry – A European Journal* 27:1438–1450.
- Surup F, Minh Thi Tran T, **Pfütze S**, Budde J, Moussa-Ayoub TE, Rohn S, Jerz G (2021) Opuntisines, 14-membered cyclopeptide alkaloids from fruits of *Opuntia stricta* var. *dillenii* isolated by high-performance countercurrent chromatography. *Food Chemistry* 334:127552.
- Surup F, Hennicke F, Sella N, Stroot M, Bernecker S, **Pfütze S**, Stadler M, Rühl M (2019) New terpenoids from the fermentation broth of the edible mushroom *Cyclocybe aegerita*. *Beilstein Journal of Organic Chemistry* 15:1000–1007.
- Wang C, Becker K, **Pfütze S**, Kuhnert E, Stadler M, Cox RJ, Skellam E (2019) Investigating the function of cryptic cytochalasan cytochrome P450 monooxygenases using combinatorial biosynthesis. *Organic Letters* 21(21):8756–8760.
- Surup F, Narmani A, Wendt L, **Pfütze S**, Kretz R, Becker K, Menbrivès C, Giosa A, Elliott M, Petit C, Rohde M, Stadler M (2018) Identification of fungal fossils and novel azaphilone pigments in ancient carbonised specimens of *Hypoxylon fragiforme* from forest soils of Châtillon-sur-Seine (Burgundy). *Fungal Diversity* 92:345–356.
- † these authors contributed equally to this work
-

Presentations and Conferences

- | | |
|---------|--|
| 10/2023 | Talk Title: Chemical Diversity and Bioactivity of Natural Products Isolated from Basidiomycota Asian Mycological Congress (AMC) in Busan, Republic of Korea |
| 05/2023 | Poster Title: Chemical diversity of Sesquiterpenoids produced by <i>Heimiomyces</i> sp. International Helmholtz Drug Discovery Conference (HDDC) in Braunschweig, Germany |
| 05/2023 | Poster Title: Chemical diversity of Sesquiterpenoids produced by <i>Heimiomyces</i> sp. Assembly for HZI and UoS Doctoral Researchers in Saarbrücken, Germany |
| 07/2022 | Poster Title: Chemical diversity of Sesquiterpenoids produced by <i>Heimiomyces</i> sp. American Society of Pharmacognosy (ASP) in Charleston, SC, USA |
| 03/2022 | Poster Title: Chemical diversity of Sesquiterpenoids produced by <i>Heimiomyces</i> sp. TTU Novel Antibiotics Strategic Meeting in Braunschweig, Germany |
-

- This research benefitted from funding by the European Union's Horizon 2020 research and innovation program (RISE) under the Marie Skłodowska-Curie grant agreement No. 101008129, project acronym "Mycobiomics".



**Funded by
the European Union**

